



**Australian Government**  
**Department of Agriculture  
and Water Resources**



# **Anaerobic pond sludge profiling and trigger point determination**

**Final Report**  
**APL Project 2016/085**

**May 2019**

**Department of Agriculture and Fisheries**

Alan Skerman

PO Box 102, 203 Tor Street

Toowoomba QLD 4350

**Advanced Water Management Centre, The University of Queensland**

Prof. Damien Batstone, Dr. Mohammad Shakil Ahmmed and Mr. Sahadev

Somasundaram

Level 6, Gehrman Bldg (60)

St. Lucia, QLD 4072

## **Acknowledgements**

This project was supported by funding provided by Australian Pork Limited, the Department of Agriculture and Water Resources, the Department of Agriculture and Fisheries (Queensland) and the University of Queensland. The authors are also grateful for the support and cooperation received from the owners and employees of the various commercial piggeries where the sludge profiling and sampling was undertaken.

## Executive Summary

The accumulation of sludge in anaerobic effluent treatment ponds used at the majority of Australian piggeries has proved to be a difficult issue to manage effectively for several decades. While the sludge has a significant value as an organic fertiliser and soil amendment, in many instances, producers have delayed removing sludge from their anaerobic ponds, resulting in the accumulation of large volumes of highly dense sludge deposits which have proven to be extremely difficult and expensive to remove; particularly from large, deep ponds. As the sludge progressively accumulates over time, the treatment capacity of an anaerobic pond decreases. This potentially results in; increased odour emission, ineffective treatment of piggery effluent, and carryover of solids into secondary effluent storage ponds. Furthermore, the solids content and viscosity of the sludge increase with storage time and depth within the sludge profile. Consequently, desludging ponds, which have not had any sludge removed for periods over five years, can prove to be very difficult, time consuming and expensive.

Several factors have constrained producers from effectively managing sludge. These include; the lack of reliable Australian data on sludge accumulation rates, pond designs which have not adequately considered the need for periodic desludging, lack of relatively simple and inexpensive technology for effectively monitoring sludge levels in anaerobic ponds, lack of reliable information and knowledge regarding effective desludging methods, lack of guidance on the most appropriate timing of desludging for ease of removal, without significantly reducing the energy potential of sludge stored in covered anaerobic ponds (CAPs), lack of experienced desludging contractors with suitable machinery in some regional/rural areas, and the significant costs involved in employing desludging contractors and/or labour costs to carry out desludging operations. The major objectives of this project were to address the constraining factors outlined above.

Sludge profiling was carried out by Premise Agriculture (formerly FSA Consulting) on eleven primary anaerobic ponds and four secondary effluent storage ponds operating at ten commercial piggeries located on the Darling Downs in southern Queensland. The sludge profiling method involved using a sonar fish finder and GPS unit mounted in a human-operated aluminium punt which was propelled in a grid pattern over the pond surface. The resulting sludge depth and position data were used to generate a digital terrain model (DTM) of the sludge surface using specialised computer software. Sludge volumes were determined from the sludge DTMs and the original design or as-constructed survey data for the various ponds. Future developments for pond sludge profiling could include developing a remote-controlled raft to convey the sonar and GPS units over the pond surface, to further improve the safety and convenience of sludge profiling operations.

The PigBal 4 model (Skerman et al., 2013) was used by DAF to estimate the total solids (TS) loading rates which had contributed to the sludge volumes measured in each of the ponds. This modelling used historical pig herd, feed consumption and pond management data provided by the piggery operators. The resulting TS loading rates, estimated by the PigBal modelling, were used in conjunction with the sludge volumes determined by the sludge profiling survey, and the available pond desludging history, to estimate sludge accumulation rates for each of the surveyed ponds.

The estimated sludge accumulation rates ranged from 0.00054 to 0.00324 m<sup>3</sup>/kg TS, with a mean value of 0.00228 ± 0.00053 m<sup>3</sup>/kg TS (95% confidence intervals). This mean value is approximately equal to the mean of the previous design standard 0.00303 m<sup>3</sup>/kg TS (Barth, 1995) and the current design standard 0.00137 m<sup>3</sup>/kg TS (ASABE, 2011). The variability in the sludge accumulation rate estimates reflects the variation in pond design characteristics, uncertainty regarding pond desludging dates and

volumes of sludge removed. Furthermore, there is the possibility of unreported changes in pig herd, diet and management practices, particularly as the ownership of some of the piggeries has changed over long operational periods. The results demonstrate that the current design standard is within the measured range of sludge accumulation rates and that there is insufficient evidence to suggest any major changes to this standard.

A procedure developed by DAF was used to obtain several samples of the pond sludge and supernatant from three uncovered anaerobic ponds. A further sludge sample was obtained from a covered anaerobic pond (CAP) undergoing desludging. These samples were analysed at the DAF Toowoomba and UQ AWMC laboratories.

The final component of this project involved the development of computational models to predict hydrodynamics and sludge behaviour within four selected ponds surveyed during previous stages. This work was carried out by researchers based at the Advanced Water Management Centre (AWMC) at the University of Queensland (UQ). The modelling method involved several components, each of which simulated particular aspects of the system to provide a complete picture of pond performance when used in combination. Firstly, a hydrodynamics or computational fluid dynamics (CFD) simulation platform, used a custom hydrodynamic physics and solver implementation to predict the liquid, solid and combined liquid-solid dynamics occurring within the ponds. This gave greater understanding of the hydraulic flow and solids settling and sludge accumulation behaviour.

The four ponds were modelled in the hydrodynamics platform under three different bases: A two-dimensional (2D) system, in which fluid only travels across a horizontal plane depicted as a top-down view; a three-dimensional (3D) system, in which the fluid travelled through all spatial dimensions but was still modelled as a sole liquid; and a three-dimensional, two-phase system, in which solids were included in the framework and a more realistic representation of concentrated sludge ponds was produced. Previous work in large scale systems has not included a solid phase. A compartmental based hydraulic model used a simplified pond geometry and parameter optimisation to further assess hydraulic flow (and, to some extent, solids and sludge behaviour). This compartmental model was then applied to a biochemical model, to provide long-term predictions of sludge behaviour, overall pond performance and achievement of the original objectives.

The hydrodynamic model was generally effective at predicting flow patterns and early-operation sludge behaviour but was not suitable for predicting long-term pond performance. The compartmental based model and biochemical model both performed as expected, identifying process kinetic behaviour, sludge accumulation behaviour, and long-term pond performance. To the best of our knowledge, this is the first reported hydrodynamic model of large-scale ponds to include a solids phase in the framework. Furthermore, this also appears to be the first study of sludge accumulation through an extensive hydrodynamic-biochemical simulation approach.

Each pond showed non-ideal mixing hydrodynamic behaviour. Solids settled rapidly in sloped wall ponds, forming a variable depth bed which occupied a substantial fraction of the pond. Shallow ponds were dominated by substantial surface recirculation dynamics, and were susceptible to solids accumulation, while deep ponds allowed the formation of a well-developed settled fraction. The very long HRT pond had an increased bypass, though this may also be due to a shallow depth.

The optimal pond design as determined by the model-based assessment is 150d HRT, which balances pond lifetime, capital cost, and performance. This will have a lifetime in the order of 3-5 years without in-situ desludging, assuming kinetics from methane potential tests. Lifetime will be longer based on the higher extent observed from the sampling campaign. A deep pond (6m+) is preferred to a shallow pond in order to (a) increase sludge holding capacity, (b) decrease the hydrodynamic impacts of sludge accumulation, (c) minimise internal recycles and bypass flows, and (d) enable in-situ desludging. Sloped sidewalls are important to minimise dead zones and allow the sludge to accumulate in a desludging zone. Desludging events should be at relatively long term intervals (100 days) to minimise the methane potential of the resulting product (and maximise the in-pond performance).

## Table of Contents

Acknowledgements .....	2
Executive Summary .....	3
1. Background to Research.....	14
2. Objectives of the Research Project .....	16
3. Introductory Technical Information.....	17
3.1 Previous Australian research.....	17
3.2 Sludge profiling.....	17
3.3 Sludge accumulation rates .....	18
3.4 Sludge distribution.....	18
4. Research Methodology.....	20
4.1 Sludge profiling.....	20
4.1.1 Hydro Survey.....	20
4.1.2 Ground truth survey (RTK-GPS).....	21
4.1.3 Post processing.....	21
4.2 PigBal modelling .....	21
4.3 Sludge accumulation rate estimation .....	21
4.4 Sludge, supernatant and effluent sampling .....	22
4.5 Sample analysis .....	24
4.6 Data analysis .....	26
4.7 Hydrodynamic-biochemical model development .....	27
4.7.1 Problem Statement.....	27
4.7.2 Mechanisms .....	27
4.7.3 Model Description.....	29
5. Results .....	34
5.1 Sludge profiling.....	34
5.1.1 Pond 1, Piggery A (Primary pond: 1000 sows farrow to finish unit – 11,350 SPU).....	34
5.1.2 Pond 2, Piggery A (Primary pond: 980 gilts - 1,679 SPU) .....	35
5.1.3 Pond 3, Piggery A (Primary pond: 5000 sow breeder unit - 14,705 SPU).....	36
5.1.4 Pond 4, Piggery A (Secondary pond: grower / finisher unit - 48,064 SPU) .....	37
5.1.5 Pond 5, Piggery B (Primary pond: grower / finisher unit - 6,350 SPU).....	38
5.1.6 Pond 6, Piggery C (Primary pond: nursery / weaner unit - 3,387 SPU).....	39
5.1.7 Pond 7, Piggery D (Primary pond: 1,500 sow farrow to finish unit - 16,000 SPU).....	40
5.1.8 Pond 8, Piggery D (Secondary Pond: 1,500 sow farrow to finish unit - 16,000 SPU).....	41
5.1.9 Pond 9, Piggery E (Primary Pond: 3,600 sow breeder unit - 7,241 SPU) .....	42
5.1.10 Pond 10, Piggery E (Secondary Pond: 3,600 sow breeder unit - 7,241 SPU) .....	43
5.1.11 Pond 11, Piggery F (Primary Pond: 1200 sow farrow to finish unit - 12,054 SPU) .....	44
5.1.12 Pond 12, Piggery G (Primary pond: 600 sow breeder unit - 1,245 SPU) .....	45
5.1.13 Pond 13, Piggery H (Secondary pond: 3100 sow breeder and grower unit - 18,546 SPU) .....	46
5.1.14 Pond 14, Piggery I (Primary pond: 2,600 sow breeder unit - 5,195 SPU) .....	47

5.1.15	Pond 15, Piggery J (Primary pond: grower-finisher unit - 21,168 SPU).....	48
5.2	Sludge accumulation rate estimation.....	50
5.3	Sampled sludge, supernatant and effluent analysis results.....	55
5.4	Hydrodynamic modelling results.....	70
5.4.1	2D Flow Simulation.....	70
5.4.2	3D Single-Phase Flow Simulation.....	71
5.4.3	3D Two-Phase Flow Simulation.....	73
5.4.4	Solids Behaviour.....	76
5.4.5	Compartmental Based Model Simulation.....	79
5.4.6	Biochemical Model Simulation.....	81
6.	Discussion.....	84
6.1	Sludge profiling.....	84
6.2	Sludge accumulation rate.....	84
6.3	Hydrodynamic modelling.....	84
6.3.1	Model Performance.....	84
6.3.2	Pond design considerations.....	86
6.3.3	Operational considerations.....	87
7.	Implications & Recommendations.....	89
8.	Intellectual Property.....	91
9.	Literature cited.....	92
10.	Publications Arising.....	95
Appendix A - Pond cross-sections produced by the Premise Agriculture sludge surveys.....		96
A1.	Piggery A, Pond 1.....	96
A2.	Piggery A, Pond 2.....	100
A3.	Piggery A, Pond 3.....	104
A4.	Piggery A, Pond 4.....	106
A5.	Piggery B, Pond 5.....	108
A6.	Piggery C, Pond 6.....	110
A7.	Piggery D, Pond 7.....	113
A8.	Piggery D, Pond 8.....	115
A9.	Piggery E, Pond 9.....	117
A10.	Piggery E, Pond 10.....	119
A11.	Piggery F, Pond 11.....	121
A12.	Piggery G, Pond 12.....	124
A13.	Piggery H, Pond 13.....	127
A14.	Piggery I, Pond 14.....	130
A15.	Piggery J, Pond 15.....	133
Appendix B.....		136
Standard Operating Procedure (SOP).....		136

Sampling sludge from uncovered effluent ponds, Version: [2].....	136
B1. Purpose.....	136
B2. Application/scope.....	136
B3. Resources.....	136
B4. Warnings.....	136
B5. Abbreviations, acronyms and definitions.....	137
B6. Procedure.....	137
B7. Responsibilities and accountabilities.....	138
B8. Related and reference documents.....	138
B9. Appendices.....	139



## List of Tables

Table 1 Masses of sludge (substrate) and distilled water added to the reactor bottles used in the AMPTS II analyses. ....	26
Table 2 Pond parameters used for initial compartmental based model design .....	32
Table 3 Summary of piggery pond characteristics including the total solids (TS) loading rates and sludge accumulation times used to estimate the sludge accumulation rates. ....	53
Table 4 Summary of piggery pond characteristics including volatile solids (VS) loading rates and hydraulic retention times. ....	54
Table 5 Mean $B_o$ and $k_{hyd}$ values and 95% confidence intervals determined by fitting curves to the BMP analysis results. ....	69
Table 6 Compartmental based model optimised parameters.....	80
Table 7 Summary of results from biochemical model simulations. ....	82

## List of Figures

Figure 1 Premise Agriculture employee carrying out the hydro-survey to determine sludge profiles in secondary pond 4 at piggery A on 4 April 2017. ....	20
Figure 2 Sampling sludge from pond 5 (piggery B) on 21 February 2018. ....	22
Figure 3 Aerial photos showing pond sludge sampling sites (a) Pond 5, piggery B, (b) Pond 2, piggery A and (c) Pond 7, piggery D.....	23
Figure 4 Aerial photograph (Google Earth) showing the effluent inlet and outlet and sludge sampling locations on the covered anaerobic pond operating at a large commercial piggery in southern New South Wales.....	24
Figure 5 Schematic representation of four ponds under study. ....	31
Figure 6 Compartmental based model configuration.....	32
Figure 7 Aerial photograph of Piggery A, Pond 1. ....	34
Figure 8 Sludge contour plan for Piggery A, Pond 1. ....	34
Figure 9 Aerial photograph of Piggery A, Pond 2. ....	35
Figure 10 Sludge contour plan for Piggery A, Pond 2. ....	35
Figure 11 Aerial photograph of Piggery A, Pond 3.....	36
Figure 12 Sludge contour plan for Piggery A, Pond 3.....	36
Figure 13 Aerial photograph of Piggery A, Pond 4.....	37
Figure 14 Sludge contour plan for Piggery A, Pond 4.....	37
Figure 15 Aerial photograph of Piggery B, Pond 5. ....	38
Figure 16 Sludge contour plan for Piggery B, Pond 5.....	38
Figure 17 Aerial photograph of Piggery C, Pond 6.....	39
Figure 18 Sludge contour plan for Piggery C, Pond 6.....	39
Figure 19 Aerial photograph of Piggery D, Pond 7.....	40
Figure 20 Sludge contour plan for Piggery D, Pond 7.....	40
Figure 21 Aerial photograph of Piggery D, Pond 8.....	41
Figure 22 Sludge contour plan for Piggery D, Pond 8.....	41
Figure 23 Aerial photograph of Piggery E, Pond 9.....	42
Figure 24 Sludge contour plan for Piggery E, Pond 9.....	42
Figure 25 Aerial photograph of Piggery E, Pond 10. ....	43
Figure 26 Sludge contour plan for Piggery E, Pond 10.....	43
Figure 27 Aerial photograph of Piggery F, Pond 11.....	44
Figure 28 Sludge contour plan for Piggery F, Pond 11.....	44

Figure 29 Aerial photograph of Piggery G, Pond 12. ....	45
Figure 30 Sludge contour plan for Piggery G, Pond 12. ....	45
Figure 31 Aerial photograph of Piggery H, Pond 13. ....	46
Figure 32 Sludge contour plan for Piggery H, Pond 13. ....	46
Figure 33 Aerial photograph of Piggery I, Pond 14.....	47
Figure 34 Sludge contour plan for Piggery I, Pond 14.....	47
Figure 35 Aerial photograph of Piggery J, Pond 15.....	48
Figure 36 Sludge contour plan for Piggery J, Pond 15.....	48
Figure 37 Estimated sludge accumulation rates in the eleven primary anaerobic ponds surveyed in this study. The mean and 95% confidence limits are shown on the graph along with the previous (Barth, 1985) and current (ASABE, 2011) standard values.....	50
Figure 38 Pond 2 (Piggery A) showing the pontoon mounted pump used to transfer effluent to a secondary pond.....	51
Figure 39 Sludge TS, VS and tCOD analysis results. ....	55
Figure 40 Supernatant and effluent TS, VS and tCOD analysis results.....	56
Figure 41 Sludge VS/TS and COD/VS analysis results. ....	57
Figure 42 Supernatant and effluent VS/TS and COD/VS analysis results. (The COD/VS result for '2 In' (14%) appears to be an anomaly and has been omitted from the mean and CI calculations).....	58
Figure 43 Sludge TKN and NH <sub>4</sub> -N analyses results. ....	59
Figure 44 Supernatant and effluent TKN and NH <sub>4</sub> -N analyses results.....	60
Figure 45 Sludge TKP, TP (ICP) and PO <sub>4</sub> -P analysis results. ....	61
Figure 46 Supernatant and effluent TKP, TP (ICP) and PO <sub>4</sub> -P analysis results.....	62
Figure 47 Sludge K (ICP) analysis results. ....	63
Figure 48 Supernatant and effluent K (ICP) analysis results.....	64
Figure 49 Stacked bar graph showing the concentrations of the eleven most abundant cations determined by ICP analysis for the sludge samples.....	65
Figure 50 Stacked bar graph showing the concentrations of the eleven most abundant cations in the supernatant and effluent samples, determined by ICP analysis.....	66
Figure 51 Stacked bar graph showing concentrations of various VFAs in the sludge samples. The bar representing sample '7A' has been truncated for scaling reasons (Total VFAs = 12,320 mg/L). .	67
Figure 52 Stacked bar graph showing concentrations of various VFAs in the supernatant and effluent samples. The bar for sample '7 In' has been truncated for scaling reasons (Total VFAs = 2173 mg/L).....	68
Figure 53 Cumulative CH <sub>4</sub> production data plotted against time, derived from the triplicate AMPTS II analyses carried out on sludge samples collected from sampling location F on pond 2.....	69
Figure 54 Top-view (i.e. x-y plane) of the streamlines for 2D single-phase models of Pond (a) 2, (b) 5, (c) 7 and (d) 16. Note that the unit of the x and y axis' are in m.....	70

Figure 55 Non-dimensional velocity contours for 2D single-phase models of Pond (a) 2, (b) 5, (c) 7 and (d) 16. Note that the unit of the velocity magnitude is in m/s whereas the x- and y-axis are in m. ....	71
Figure 56 Top-view (i.e. x-y plane) of the streamlines for 3D single-phase models of Pond (a) 2, (b) 5, (c) 7 and (d) 16. Note that the origin of the axis, $x = y = z = 0$ , is taken at the bottom of the ponds. Here, x-y planes correspond to the top-surfaces of the ponds.....	72
Figure 57 Top-view (i.e. x-y plane) of the non-dimensional velocity contours for 3D single-phase models of Pond (a) 2, (b) 5, (c) 7 and (d) 16. Note that the origin of the axis, $x = y = z = 0$ , is taken at the bottom of the ponds. Here, x-y plane corresponds to the top-surfaces of the ponds.....	72
Figure 58 Side-view (i.e. x-z plane) of the non-dimensional velocity contours for 3D single-phase models of Pond (a) 2, (b) 5, (c) 7 and (d) 16. Note that the sections are taken through the stream-wise directions, i.e. through the inlet, of the ponds. Here, the legends of the velocity contours are same as the previous figures, i.e. Figure 57, and the arrows represent the glyph of the velocity vectors.....	73
Figure 60 Top-view (i.e. x-y plane) of the non-dimensional velocity contours for 3D two-phase models of Pond (a) 2, (b) 5, (c) 7 and (d) 16. Note that the origin of the axis, $x = y = z = 0$ , is taken at the bottom of the ponds. Here, x-y plane corresponds to the top-surfaces of the ponds.....	75
Figure 61 Side-view (i.e. x-z plane) of the non-dimensional velocity contours for 3D two-phase models of Pond (a) 2, (b) 5, (c) 7 and (d) 16. Note that the sections are taken through the stream-wise directions, i.e. through the inlet, of the ponds. ....	75
Figure 62 Side view (i.e. x-z plane) of concentration contours for 3D two-phase models of Pond (a) 2, (b) 5, (c) 7 and (d) 16. Note that the sections are taken through the stream-wise directions, i.e. through the inlet, of the ponds.....	77
Figure 63 Orthographic view (i.e. longitudinal axis is parallel with inlet-outlet plane) of concentration contours for 3D two-phase models of Pond (a) 2, (b) 5, (c) 7 and (d) 16. Here, the black-dotted rectangle represents the enlarged section of the inlet plume.....	78
Figure 64 Concentration profiles for 3D two-phase models of Pond (a) 2, (b) 5, (c) 7 and (d) 16. ....	78
Figure 65 Residence time distribution curves of 3D single-phase models of Pond (a) 2, (b) 5, (c) 7 and (d) 16. Note that the concentration and the times are non-dimensionalised using the widely used relations as $C/C_0$ , and $t/T_H$ , respectively. Here, $C$ is the concentration $C(t)$ , $C_0$ is the initial concentration, which is inlet concentration during the pulse-width in this case, $t$ is the time, and $T_H$ is the theoretical retention time of the ponds. ....	79
Figure 66 Comparison of residence time distribution between models of Pond (a) 2, (b) 5, (c) 7 and (d) 16. Optimised compartmental based model is shown in blue, and the CFD model is shown in red. ....	81
Figure 67 Comparison of occupied volume over the pond life.....	82
Figure 68 Sludge vs. fraction (indicating stability) over time for Pond 2.....	83
Figure 69 Outlet solids concentration from Pond 2.....	83
Figure B1 Sampling pole.....	139
Figure B2 Slot in sampling pole.....	139
Figure B3 Sampling pole handles used to open and close the slot. ....	140

Figure B4	DAF 3.0 m flat-bottomed punt identification plate. ....	140
Figure B5	Punt mid-hull sampling port. ....	141

## **I. Background to Research**

The accumulation of sludge in anaerobic effluent treatment ponds used at the majority of Australian piggeries has proved to be a difficult issue to manage effectively over several decades. While the sludge has a significant value as an organic fertiliser and soil amendment, in many instances, producers have delayed removing sludge from their anaerobic ponds, resulting in the accumulation of large volumes of highly dense sludge deposits which have proven to be extremely difficult and expensive to remove, particularly from large, deep ponds. In some cases, sludge-filled anaerobic ponds have been abandoned, requiring the construction of new ponds at sites where there is sufficient land area available. At other sites where there is insufficient land available for the construction of a new pond, producers have employed contractors to remove part or all of the sludge using long-reach excavators, vacuum tankers and agitators, various types of solids handling pumps and floating dredges. As the sludge progressively accumulates over time, the treatment capacity of an anaerobic pond decreases. This potentially results in increased odour emission, ineffective treatment of piggery effluent, and carryover of solids into secondary effluent storage ponds. Furthermore, the solids content and viscosity of the sludge generally increase with storage time and depth within the sludge profile. Consequently, desludging ponds, which have not had any sludge removed for periods over five years can prove to be difficult, time consuming and expensive.

The following factors have constrained producers from effectively managing sludge:

- Lack of reliable Australian data on sludge accumulation rates.
- Pond designs which have not adequately considered the need for periodic desludging.
- Lack of relatively simple technology for effectively monitoring sludge levels in anaerobic ponds.
- Lack of guidance on the most appropriate timing of desludging for ease of removal without significantly reducing the energy potential of sludge stored in covered anaerobic ponds (CAPs).
- Lack of reliable information and knowledge regarding effective desludging technologies.
- Lack of experienced desludging contractors with suitable machinery in some regional/rural areas.
- Significant costs involved in employing desludging contractors and/or labour costs for piggery employees to carry out desludging operations.

Following the installation of several CAPs over the past decade, combined heat and power (CHP) systems are being used to generate electrical power and heat from the collected biogas. Consequently, it is becoming increasingly more important to select pond desludging intervals (triggers) to avoid excessive premature export of volatile solids which could potentially contribute significantly to valuable biogas yields. Some of the recently constructed CAPs have included sludge extraction pipes installed at regular intervals along the length of the pond. However, there is currently minimal monitoring data available to assist with the selection of appropriate extraction pipe spacing and diameter to enable effective pond desludging.

Several new mixed hybrid CAPs, fitted with stirring and heating systems, are currently being planned and installed at Australian piggeries (RCM International). It is currently unknown how the addition of stirring / sludge circulation systems will affect sludge profiles and the subsequent management of sludge removal from these ponds.

Notwithstanding the recent interest in CAPs, sludge management remains as a major issue faced by the majority of pig producers throughout Australia who continue to use conventional uncovered anaerobic ponds for primary treatment of piggery manure. The outcomes from this project will assist in the design of new anaerobic ponds by providing reliable Australian data on sludge accumulation rates and the formation of sludge profiles, over extended time periods, for a range of different pond configurations, loading rates and management practices.

Two key issues make the study and understanding of sludge behaviour in ponds difficult;

- the sludge behaviour is intimately linked to biological processes and hydrodynamic flow conditions, both of which are influenced by the pond geometry, design loading rate and real-time sludge inventory;
- ponds are non-steady state systems and so undergo progressive change between desludging events, making interpretation of grab sampling data difficult.

The latter is influenced by the age and history of the pond, and hence, sampling of specific ponds over a usual project period of 2-3 years, only gives a snap-shot of progressively changing conditions. To address this limitation, this report details the development of a series of models and model-based analyses at the Advanced Water Management Centre (AWMC) providing additional predictions of hydrodynamic and sludge behaviour within the ponds investigated in the profiling, sampling and analysis components of the project. Hydrodynamic models are used to simulate the fluid flow, solid dynamics and settling behaviour. A compartmental model is used to validate the results of the hydrodynamic modelling and provide simplified flow behaviour for use with a biochemical model. A biochemical model is used to replicate the physicochemical and biochemical reactions occurring and provide continuous information on the compositional and physical state of components within the pond.

## **2. Objectives of the Research Project**

As outlined in the project agreement, the objectives of this project were:

1. To develop and trial methods for effectively monitoring sludge profiles and accumulation rates and collecting sludge samples from uncovered anaerobic effluent ponds.
2. To determine sludge profiles in approximately 15 existing anaerobic effluent ponds at southern Queensland piggeries.
3. To estimate the sludge accumulation rates in each of the ponds, based on site-specific data relating to the pond loading rate (pig herd, diet and production performance), the original pond dimensions and desludging history.
4. To collect several sludge samples from selected ponds (included one covered anaerobic pond) to determine the solids and nutrient contents and the biochemical methane potential of sludge sampled at various depths and locations within the ponds.
5. To further develop (including calibration) and use an integrated hydrodynamic-biochemical model to provide predictions of sludge behaviour.
6. To determine optimal desludging intervals for ease of pumping while avoiding significant losses of methane potential.
7. To provide recommendations for the design of anaerobic ponds to enhance the ease of desludging.



### 3. Introductory Technical Information

#### 3.1 Previous Australian research

The following Australian research projects have some relevance to the present study. The majority of these projects were carried out with funding assistance from the Australian pork industry:

- APL Project No. 2012/1029 - Sludge Handling and Management. <https://australianpork.infoservices.com.au/items/2012-1029-REPORT>
- APL Project No. 2108 - Improved piggery effluent management systems incorporating highly loaded primary ponds. <https://australianpork.infoservices.com.au/items/2006-2108-REPORT>
- RIRDC Project No. PRJ-005672 - Methane recovery and use at Grantham piggery. <https://www.agrifutures.com.au/product/methane-recovery-and-use-at-grantham-piggery/>
- APL Project No 2009/2295 - Sludge Management for a Covered Anaerobic Pond at Bears Lagoon Piggery. <https://australianpork.infoservices.com.au/items/2009-2295-REPORT>
- Pork CRC Project 4C-109 - Enhanced methane production from pig manure in covered ponds and digesters. <http://porkcrc.com.au/research/program-4/program-4-projects/>
- Linking biological processes to solids behaviour & performance in anaerobic ponds, a developing collaborative project between UQ and Melbourne Water. <http://www.awmc.uq.edu.au/linking-biological-processes-solids-behaviour-performance-anaerobic-lagoons>

#### 3.2 Sludge profiling

Sludge profiling has generally been carried out by manually using a probe or T-bar from a boat to detect the top of the sludge layer in a piggery effluent pond. Sludge surveys were generally carried out in a grid pattern, over the pond surface. This practice was labour and time intensive and subjected the operators to a degree of risk. Detecting the indistinct top of the sludge layer was also quite subjective due to the fluid nature of the top layer. Physical limitations on the length of probe or T-bar also restricted the use of this method in deep ponds.

More recently, sonar and GPS have been used to more rapidly and objectively measure sludge accumulation (e.g. Duperouzel, 2005, Singh et al., 2007 and Westerman, 2008). Sonar (fish finder) units determine the depth to the sludge by measuring the time lapse between the transmitted and reflected signals from the sonar transducer. Duperouzel (2005) found that sonar methods can rapidly measure the depth to sludge in piggery effluent ponds. This technique was also used by Skerman et al. (2008) for the measurement of sludge accumulation in a highly loaded piggery effluent pond near Dalby (Queensland). This study indicated that the accuracy of the sonar method was comparable to that of light reflectance (nephelometer) methods. Singh et al., (2007) and Westerman (2008) reported on the development of remote controlled rafts which used GPS-enabled sonar equipment to map sludge profiles without deploying people in a boat on the effluent pond. This was considered to be safer and less time consuming compared to traditional manual methods.

### **3.3 Sludge accumulation rates**

O'Keefe et al. (2013) (APL Project No. 2012/1029) reviewed the physical and rheological properties of pond sludge and the methods used to pump, remove, dewater and manage the wet sludge. This work has assisted in the selection of pumps for use in pond desludging. They also provided a comprehensive overview of studies which identified sludge accumulation rates in piggery effluent ponds.

Until relatively recently, sludge storage allowances used in the design of piggery effluent ponds in Australia were generally based on the linear Rational Design Standard (RDS) recommendation of 0.00303 m<sup>3</sup>/kg TS (Barth, 1985). This rate of sludge accumulation, which was the average value reported by Barth and Kroes (1985) for six piggery lagoons in the US, was later adopted in the ASAE standards (2004). Chastain (2006) proposed a new sludge accumulation model using a basic treatment and mass balance approach. This publication led to the adoption of updated ASABE standards (2011) which suggested a substantially lower sludge accumulation rate of 0.00137 m<sup>3</sup>/kg TS.

Hamilton (2010) monitored sludge accumulation in two anaerobic / facultative ponds treating the wastewater from breeder piggeries over a nine-year period. They found that sludge accumulated more rapidly in the second unit where some sludge was removed by effluent irrigation, compared to the first unit which was left undisturbed. This suggested that the regular removal of sludge also removed some of the micro-organisms which were responsible for breaking down the wastewater, resulting in incomplete digestion of the incoming waste. The results of this study suggested that the standard sludge accumulation rate could be lowered to 0.00120 m<sup>3</sup>/kg TS for ponds where the sludge is undisturbed during operation and the storage period is longer than ten years. The sludge accumulation rate also escalated when sludge accumulation approached 30% of the pond drawdown volume and following encroachment within 1.00 and 1.25 m from the maximum drawdown level.

Examples of Australian studies include Birchall (2010) who determined a sludge accumulation rate of 0.00094 m<sup>3</sup>/kg TS in a covered anaerobic pond at a commercial piggery near Bendigo (Victoria) over a five-year operating period. Skerman et al. (2008) identified a sludge accumulation rate of less than 0.00100 m<sup>3</sup>/kg TS after 22 months of operating a highly loaded pond.

A study carried out at a municipal wastewater pond in Greece (Papadopoulos et al., 2003) suggested that three distinctly different zones formed within the anaerobic pond: The first zone, which formed at the base of the pond, consisted of inert, high-density sludge. The second zone, which formed above this, contained a high concentration of volatile (easily biodegradable) sludge. The third upper zone (supernatant), was a liquid layer having a low suspended solids concentration. Local climate conditions are known to affect sludge distributions throughout the year. In this pond, sludge accumulation followed an annual sinusoidal pattern, with higher rates reported during winter, and lower rates during summer, due to the increased anaerobic digestion activity.

### **3.4 Sludge distribution**

The design and management of anaerobic ponds and sludge removal systems requires an understanding of the distribution of sludge across the base and batters of the pond. Previous studies have shown that this distribution is highly uneven (O'Keefe et al., 2013).

For a primary pond treating municipal wastewater in of Mèze (France), the depth of sludge at the entrance of the first pond was greater than 1 m, rapidly decreasing to less than 0.6 m at a distance of 50 m from the inlet. Greater accumulation of sludge was also observed in the corners of the pond. Gaseous products of the anaerobic decomposition process apparently convey solids to the pond surface where they are blown into the corners by wind action (Picot et al., 2005). Similar findings were reported by Gratziou and Chalatsi (2015). Ponds with steep sides were found to provide favourable conditions for uniform distribution of sludge (Papadopoulos et al., 2003).

Sludge accumulation effectively reduces the pond hydraulic retention time (HRT), potentially adversely affecting treatment efficiency. Nelson et al. (2004) suggested that effective hydraulic retention times (HRTs) in the facultative ponds may be even further reduced by the formation of preferential flow paths and dead zones. Their research supported previous findings which indicated that the majority of sludge accumulates directly in front of the inlet in facultative ponds with single inlets. Alternative inlet configurations, such as installing additional inlet pipes and/or increasing the inlet velocity or direction, may be more effective in distributing sludge more uniformly over a wider area.

Abis and Mara (2005) suggested that regular, elongated pond shapes may have encouraged a regular distribution of the sludge solids in three pilot-scale facultative ponds treating municipal wastewater in the UK.

The previous research suggests that there are clear interactions between sludge distribution and pond hydrodynamics. These processes are poorly understood and have not been well studied for anaerobic ponds, particularly under Australian conditions.

## 4. Research Methodology

### 4.1 Sludge profiling

Sludge profiling was carried out by Premise Agriculture (formerly FSA Consulting) on eleven primary anaerobic ponds and four secondary effluent storage ponds operating at ten commercial piggeries located on the Darling Downs in southern Queensland. Details regarding the piggeries and pond capacities are provided in Table 2. The secondary ponds were included in the profiling schedule after observing that three of the secondary ponds were receiving effluent discharged from primary ponds, which were storing high levels of sludge, while pond 4 was receiving effluent discharged from a heated, mixed, in-ground, hybrid digester. It was concluded that surveying these secondary ponds may provide valuable data on the carryover of sludge from different primary pond configurations.

The sludge profile monitoring method used in this project was developed based on the experience of Premise Agriculture and DAF employees working in this area over the past 20 years, and included the three stages described below:

#### 4.1.1 Hydro Survey

A Lowrance HDS 5 echo sounder was attached to the transom of Premise Agriculture's aluminium punt, just below the waterline. The sounder was connected to a Trimble Yuma which logged the position and depth data into HydroSurvey software. The punt was propelled by an outboard electric motor, in a grid pattern, over the pond surface to collect depth data to the top of the sludge. The sludge depths were confirmed using DAF's 6 m long aluminium tee-pole to physically feel the depth of sludge and to confirm whether the physically derived depth corresponded with the depth indicated on the sounder readout. The physical sludge pole measurements consistently confirmed the sounder readings throughout the hydro survey process. For total pond depths less than 6 m, the sludge pole was pushed through the sludge until it reached a solid base to confirm the original (as-constructed) depth of the pond.

Figures 1(a) and 1(b) are photographs showing the hydro-surveying procedure being carried out on pond 4 (piggery A).



Figure 1 Premise Agriculture employee carrying out the hydro-survey to determine sludge profiles in secondary pond 4 at piggery A on 4 April 2017.

#### 4.1.2 *Ground truth survey (RTK-GPS)*

A Topcon GR-5 RTK-GPS multi-constellation high performance receiver was used to survey accurate GPS points around the pond sites. The receiver was coupled with a Panasonic Tough Book (CF-U1) running Magnet Field to control the GR-5 RTK-GPS unit. A base station was established to correct the GPS locations picked up by the rover unit, via a radio link between the two units. The rover unit was used in conjunction with a 2 m survey staff to pick up individual survey points. Benchmarks were established at all piggery sites so that any future surveys can be compared with the previous surveys. Survey points were taken of the effluent storage level, bank crest level and the pond inlets and outlets. Additional survey points were taken in certain locations to ensure an accurate representation of the size of the pond and the effluent storage level. For example, extra points were taken on curved embankment profiles to ensure that the shape of the pond was accurately captured.

#### 4.1.3 *Post processing*

The survey data was initially opened in Microsoft Excel to convert the format for import into Topcon Magnet software. The 'as constructed' or 'as designed' pond data was imported into Magnet and a digital terrain model (DTM) was created for each pond. The ground and hydro surveys were imported and a DTM created of the hydro survey data, with the outer boundary being the crest of the pond embankment.

A volume report was created for each pond using the 'design' DTM from the crest to the base, typically in 0.1 m horizontal slices. This produced a report that defined the pond volumes in 0.1 m depth increments. A similar report was then generated using the hydro survey data for the sludge height, in similar 0.1 m slices. This effectively gave the pond storage volume above the sludge level recorded during the hydro survey. The pond volumes from the original (as-built) base and the sludge surface were determined up to the effluent storage elevation, confirmed by the ground truth surveys. The difference between these volumes gave the sludge volume on the day of the hydro survey. Aerial photographs and sludge contour plans produced by Premise Agriculture for the 15 ponds surveyed for this project are provided in Section 5.1 of this report. Cross sections were taken across the ponds to produce a visual representation of the original design and sludge levels. These cross sections and pond outline and inlet/outlet information were exported into Autodesk AutoCAD to produce the figures provided in Appendix B.

## 4.2 *PigBal modelling*

The PigBal 4 model (Skerman et al., 2013) was used by DAF to estimate the total solids (TS) loading rates contributing to the sludge volumes measured for each of the ponds (Table 3). This modelling used historical pig herd, feed consumption and pond management data obtained from the piggery operators. In instances when reliable, site-specific model input data was not available, assumptions were made based on normal industry practices. The PigBal modelling also provided estimates of volatile solids (VS) loading and hydraulic retention time for each of the ponds, as reported in Table 4.

## 4.3 *Sludge accumulation rate estimation*

The sludge volumes determined by the sludge profiling survey were used along with the TS loading rates estimated by the PigBal modelling and the pond desludging history, to estimate sludge accumulation rates which are generally expressed in terms of the volume of sludge deposited on the

base of the pond per unit mass of TS entering the pond in the shed effluent stream. In some instances, there were limited reliable records available regarding pond desludging history. Also, for ponds that had previously been desludged, piggery operators were generally unable to provide accurate estimates of the volume of sludge removed. This lack of reliable data may have affected the accuracy of the sludge accumulation rate estimates for some of the ponds. The assumed sludge accumulation periods for each pond are shown in Table 3.

#### **4.4 Sludge, supernatant and effluent sampling**

DAF developed a Standard Operating Procedure (SOP) for safely and effectively sampling sludge from uncovered effluent ponds. The procedure involved using a 3.0 m long, flat-bottomed, aluminium punt fitted with an outboard electric motor and a sludge sampling pole, developed by DAF for use in previous projects. This SOP is included in Appendix B of this report. A photograph of the sludge sampling operation is provided in Figure 2.



*Figure 2 Sampling sludge from pond 5 (piggery B) on 21 February 2018.*

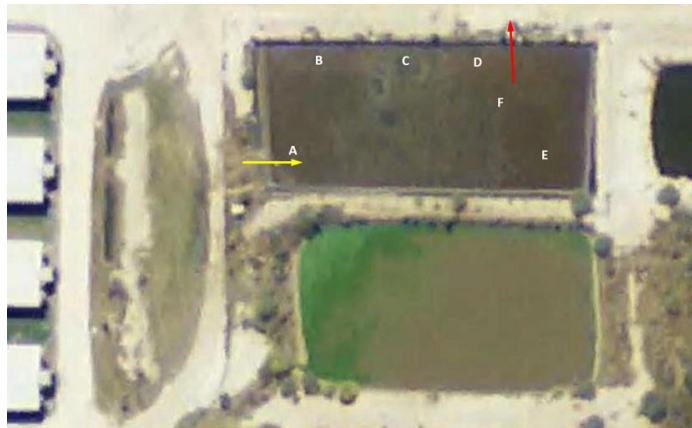
Following consultation with the University of Queensland (UQ) researchers carrying out the modelling component of this project, it was decided to collect the following samples from ponds 5, 2 and 7:

- Six sludge samples (A-F), generally along the assumed flow path between the pond inlet and outlet.
- Three supernatant samples, from near the pond inlet, the centre of the assumed flow path and near the pond outlet.
- One sample of the treated effluent discharged from the pond gravity overflow.

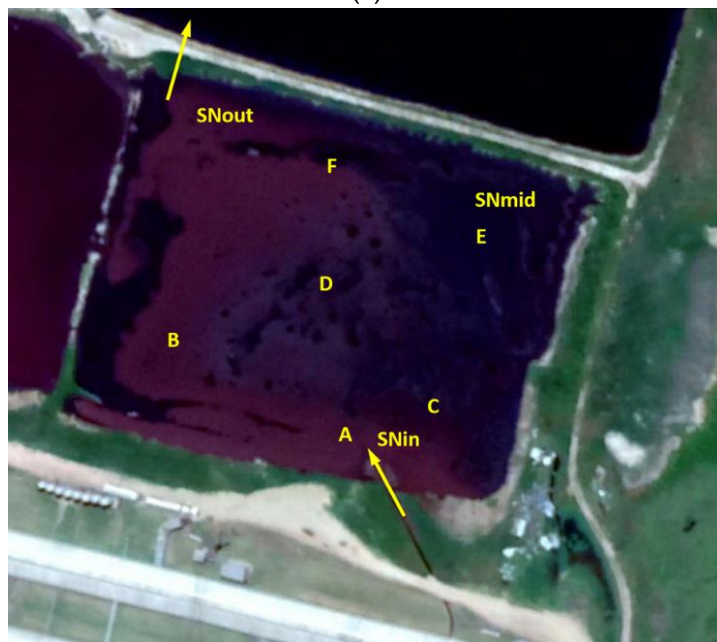
The above samples were subsequently collected by DAF from ponds 5, 2 and 7, on 21 February, 27 February and 8 March 2018, respectively. These ponds were selected for sampling, partly because of the physical limitations of sampling sludge using a 3 m long sampling pole and also to ensure that they were representative of the range of pond sizes, loading rates and operating practices adopted by industry. The sludge sampling locations (A-F) on ponds 5, 2 and 7 are shown in Figures 3(a), (b) and (c), respectively. The yellow arrows on these figures indicate pond effluent entry and discharge locations.



(a)



(b)



(c)

Figure 3 Aerial photos showing pond sludge sampling sites (a) Pond 5, piggery B, (b) Pond 2, piggery A and (c) Pond 7, piggery D.

All sludge, supernatant and effluent samples were placed on ice in polystyrene cooler boxes for transport to the DAF and UQ laboratories. On arrival at the laboratories, the samples were refrigerated at approximately 4°C prior to analysis.

In addition to the above samples collected from uncovered anaerobic ponds, a further sludge sample was obtained on 15 May 2018 from a covered anaerobic pond (CAP) operating at a large commercial breeder unit located in southern New South Wales. This sample was collected during an ongoing desludging operation being carried out using a cover mounted desludging pump, as shown on the aerial photograph below (Figure 4).



Figure 4 Aerial photograph (Google Earth) showing the effluent inlet and outlet and sludge sampling locations on the covered anaerobic pond operating at a large commercial piggery in southern New South Wales.

#### 4.5 Sample analysis

Two sets of each of the pond sludge, supernatant and effluent samples were collected for the various analyses carried out independently at the DAF Toowoomba laboratory and the AWMC laboratory at UQ St Lucia campus.

The following analyses were carried out at the DAF Toowoomba laboratory:

- Total solids (TS), volatile solids (VS) and fixed solids (FS) or ash for all sludge, supernatant and effluent samples.
- Biochemical methane potential (BMP) for selected sludge samples.

The following analyses were carried out at the UQ AWMC laboratory on all of the sludge, supernatant and effluent samples:

- Total chemical oxygen demand (tCOD), Soluble chemical oxygen demand (sCOD), Ammonium nitrogen ( $\text{NH}_4\text{-N}$ ), Phosphate phosphorus ( $\text{PO}_4\text{-P}$ ), Total volatile fatty acids (tVFA), Total Kjeldahl nitrogen (TKN), Total Kjeldahl phosphorus (TKP).



- Various individual volatile fatty acids (VFA).
- Various trace elements and nutrients.

The TS and VS concentrations were measured in triplicate using a modified version of the method recommended by Greenberg et al. (1992). In the modified method, the samples were dried at 60°C for 48 hours to avoid losses of volatile compounds which are suspected to occur at the higher drying temperatures (105°C) typically used in standard laboratory methods. After weighing the dried sample to determine the TS concentrations, the samples were ashed in a muffle furnace at 550°C for two hours, prior to cooling in a desiccating cabinet and reweighing to determine the FS and VS concentrations. The TS and VS analyses were commenced on the day following the sample collection.

The concentrations of various trace elements and nutrients were determined by inductively coupled plasma optical emission spectroscopy (ICP-OES, Perkin Elmer Optima 7300DV, Waltham, MA, USA). This involved digesting the media samples with a 6:2:2 ratio of HCl, HNO<sub>3</sub> and HF, respectively, using a Milestone Ethos-I microwave digester, prior to analysis using a Varian Vista Pro ICP-OES instrument. The samples analysed for P and K were solubilised using acid digestion, followed by microwave digestion, before being analysed using ICP-OES.

For the TKN analyses, samples were diluted directly for measurement. Then 0.5 to 20 mL of homogenous sample was digested with sulphuric acid, potassium sulphate and copper sulphate catalyst in a block digester (Lachat BD-46). After the evaporation of the water, the digestion was run for 3.5 hours at 380°C. The digested samples were analysed on a Lachat QuikChem8000 Flow Injection Analyser (FIA), using QuikChem method 10-115-01-1-D for TKP (analysis of phosphate) and 10-107-06-2-D for TKN (analysis of ammonia).

The samples analysed for NH<sub>4</sub>-N were centrifuged at 2500g and the supernatant filtered through a syringe filter (0.4 mm PES membrane). The solutions were further diluted with Milli-Q water such that the concentrations of the samples were within the range of the standards. The diluted samples were then analysed on a Flow Injection Analyser (Lachat QuikChem8000, Lachat Instruments, Loveland, CO, USA) using the QuikChem method.

The biochemical methane potential (BMP) analyses were carried out using the automatic methane potential test system (AMPTS II) at the DAF Toowoomba laboratory. The analysis method is described in the manufacturer's operating manual (Bioprocess Control, 2016). The system has capacity for 15 x 500 mL glass reactor bottles and is therefore capable of testing up to five triplicate samples (or four samples and one blank containing inoculum only) per batch. The AMPTS II analyses of the eleven selected sludge samples were carried out in three batches, commencing as soon as possible after the pond sampling was completed.

Once the results of the TS and VS analyses were available, the contents of the reactor bottles were prepared for the anaerobic digestion process by adding calculated masses of the substrate (sludge) and distilled water to each reactor bottle to give consistent total solids concentrations for each batch of samples. As shown in Table 1, each bottle contained a total mass of 400 g (substrate + distilled water), with total solids concentrations of 5%, 4% and 5% for batches 1, 2 and 3, respectively. No inoculum was added to the reactor bottles for these analyses, as each of the sludge samples were collected from active anaerobic ponds. The glass reactor bottles were immersed in a water bath maintained at a

constant temperature of 37°C. The contents of the reactor bottles were continuously stirred throughout the digestion period, which ranged from 15 to 50 days.

*Table 1 Masses of sludge (substrate) and distilled water added to the reactor bottles used in the AMPTS II analyses.*

<b>Batch</b>	1	1	1	1	1	2	2	2	2	3
<b>Pond/Sample</b>	5A	5D	5F	2A	2D	2F	7A	7D	7F	11
<b>Reactor TS conc (%)</b>	5	5	5	5	5	4	4	4	4	5
<b>Substrate TS mass (g)</b>	20	20	20	20	20	16	16	16	16	20
<b>Substrate water mass (g)</b>	42	118	98	104	87	139	27	268	264	184
<b>Total substrate mass(g)</b>	62	138	118	124	107	155	43	284	280	204
<b>Distilled water mass (g)</b>	338	262	282	276	293	245	357	116	120	196
<b>Total mass (g)</b>	400	400	400	400	400	400	400	400	400	400

In the AMPTS II CO<sub>2</sub>-absorbing unit, the biogas produced in each reactor bottle passes through an individual 100 mL vial containing an alkaline solution (3M NaOH). Several acid gas fractions, such as CO<sub>2</sub> and H<sub>2</sub>S, are retained by chemical interaction with the NaOH, only allowing CH<sub>4</sub> to pass through to the CH<sub>4</sub> gas volume measuring device. A pH indicator (thymolphthalein) is added to each vial for monitoring the acid binding capacity of the solution. In the gas volume measuring device, the volume of CH<sub>4</sub> released from the CO<sub>2</sub>-absorbing unit is measured using a wet gas flow measuring device with a multi-flow cell arrangement. This measuring device works according to the principle of liquid displacement & buoyancy and can monitor ultra-low gas flows; a digital pulse is generated when a defined volume of gas flows through the device. An integrated embedded data acquisition system is used to record, display and analyse the results (Bioprocess Control, 2016). Fifteen minute, hourly and daily CH<sub>4</sub> production data were downloaded at regular intervals from the PC connected to the data acquisition system. The analyses were continued until no further CH<sub>4</sub> production was recorded over consecutive time periods.

#### **4.6 Data analysis**

Mean values and 95% confidence intervals were calculated for each set of chemical analysis data.

The cumulative CH<sub>4</sub> production data derived from the AMPTS II analyses were further analysed by performing a non-linear least-squares fit of a simple first-order kinetic model (Eq. 5) to the measured cumulative methane produced ( $B_t$ ) at incubation time ( $t$ ) (Jensen et al., 2011) for each of the ten sets of triplicate sludge samples analysed using the AMPTS II system:

$$B_t = B_0(1 - e^{-k_{hyd} \cdot t}) \quad (1)$$

Where  $B_0$  = degradation extent or degradability (L CH<sub>4</sub>. kg VS<sub>fed</sub><sup>-1</sup>);  $k_{hyd}$  = fitted first-order kinetic rate coefficient (day<sup>-1</sup>) and  $t$  = time (days).

## 4.7 Hydrodynamic-biochemical model development

### 4.7.1 Problem Statement

In conjunction with the project objectives defined earlier, the model development was driven by the following questions:

- What are the mechanisms occurring within the pond that affect the solids settling, sedimentation and sludge accumulation?
- How can we accurately represent these mechanisms using modelling and simulation and predict the sludge behaviour?
- What does the model reveal regarding pond and sludge behaviour, and how can we implement this to optimise production and minimise operational expenditure for current and future ponds?

### 4.7.2 Mechanisms

#### Hydrodynamics

The sludge and solids behaviour is mostly controlled by the dynamics of the bulk fluid. The specific mechanisms governing solids transport are advection and vertical flux driven by gravity. The latter can include compressive effects, often simulated through solids diffusion. Advection refers to the carried transport of solids by the greater motion of the bulk fluid, and diffusive motion occurs as the solids relocate to even out concentration gradients in compressive zones. Understanding the flow mechanics of the fluid and their specific effects on the sludge is crucial to capturing overall sludge behaviour.

To effectively represent multiple hydrodynamic interactions, the current model adopts a two-phase system, in which solids are represented as suspended particles subject to settling forces (i.e. the dispersed phase). The model is developed by adding phase models successively with continuous validation (i.e. application of continuity and momentum equations), all under an Eulerian frame of reference (i.e. phases are represented by dispersed control volumes rather than individual particles). Firstly, the rudimentary single fluid phase is modelled, and standard continuity and momentum equations applied to the fluid domain. Secondly, the solid phase is added with an additional transport equation, which is correlated to the rheological and turbulent effects. At this stage, the solid-liquid phase flow is described through a drift-flux framework, in which momentum compression arises due to interfacial slip between phases, and an additional continuity equation is added for the solid phase. The continuity and momentum equations for two-phase systems may be summarised by the following equations:

$$\frac{\partial(\rho U)}{\partial t} + \nabla \cdot (\rho U) = 0; \quad (2)$$

$$\frac{\partial(\rho U)}{\partial t} + \nabla \cdot (\rho U U) = -\nabla P + \nabla \cdot (\tau + \tau^t) + \rho g - \nabla \cdot \left( \frac{\alpha_s \rho_s \rho_l}{1 - \alpha_l} v v \right) + M_\phi; \quad (3)$$

and the dispersed phase (solid) continuity equation is:

$$\frac{\partial \alpha_s}{\partial t} + \nabla \cdot (\alpha_s U) = -\nabla \cdot \left( \frac{\alpha_s \rho_l}{\rho} v \right) + \nabla \cdot (\gamma \alpha_s) \quad (4)$$

where:  $U$  is the velocity,  $\rho$  is the density,  $\alpha$  is the phase fraction,  $P$  is the pressure,  $\tau$  is the stress tensor,  $\tau^t$  is the time,  $M_\phi$  is the interphase momentum transfer,  $v$  is the solids settling velocity, and  $\gamma$  is a diffusion coefficient. The subscripts  $s$  and  $l$  denote solids or liquids, respectively.

### *Settling & Sedimentation*

Settling refers to the natural settling and compression of solids, resulting in sinking to the pond base and the accumulation of sludge. In the case of ponds, settling of particles is considered as an aggregate process primarily driven by gravity, and the counteraction is driven by forces such as drag, buoyancy, and displacement of liquid volume. An empirical settling velocity function is considered which represents non-ideal (hindered) settling.

The present model incorporates the double-exponential settling equation (Takács, Patry, and Nolasco, 1991) into the hydrodynamic model; the double-exponential settling equation is widely used for wastewater settling tanks. The double-exponential model uses two exponential functions to more accurately represent the disordered relationship between solids settling velocity and concentration, as well as the distribution of particle settling velocities in practical settings. The double exponential equation is:

$$v=v_0e^{-r_hX_j^*}-v_0e^{-r_pX_j^*};\text{with} \quad (5)$$

$$X_j^*=X_j-X_{\min} \quad (6)$$

where:  $v_0$  is the maximum settling velocity;  $X_j$  and  $X_{\min}$  are the actual and minimum settling solids concentrations, respectively; and  $r_h$  and  $r_p$  are coefficients for hindered settling and low concentration zones, respectively. The two terms of equation (5) separately represent the velocities of the flocculated section and the smaller, slowly settling section. In this study, typical values of coefficients  $r_h$  and  $r_p$  were used as derived from previous work on modelling clarifiers (Gernaey, Vanrolleghem and Lessard, 2001).

The double-exponential settling model is also based on existing work in which settling is assumed to occur sequentially as a series of one-dimensional layers. A limiting-solids-flux-type behaviour is applied in which the gravity flux and bulk fluid flux are the sole drivers of the downwards flux of the solids. The velocity profiles are then derived by applying mass balances to each layer.

### *Turbulence*

Turbulence, or chaotic patterns in fluid flow directions and velocities, is usually associated with mixing of the fluid, which is a necessary component for anaerobic treatment systems. Turbulence is typically modelled through a system of equations based on the kinetic energy ( $\kappa$ ) and dissipation rate ( $\epsilon$ ), also known as the  $\kappa$ - $\epsilon$  model. The  $\kappa$ - $\epsilon$  model is widely used in industrial practice and has better numerical stability than counterpart models such as the  $\kappa$ - $\omega$  and shear stress transport (SST) models (Moukalled et al., 2016). In the case of solid settling, buoyancy is expected to have a large influence and must be taken into account. Specifically, buoyancy is caused by an interaction between turbulent energy and potential energy, and it causes disruptions to the average flow pattern.

The  $\kappa$ - $\epsilon$  model, taking into account the effect of buoyancy, can be expressed as a series of equations (Moukalled et al., 2016; Brennen and Brennen, 2005; Brennan, 2001) which are excluded from this report for concision.

### *Rheology*

The rheology defines viscous characteristics of a fluid, which relate the deformation behaviour of a particle to its internal structure. Modelling the rheology is essential for the current ponds given the

high concentrations of sludge. Under the typical methods of rheological modelling, fluids are categorised into one of two types: Newtonian or Non-Newtonian. Under Newtonian behaviour, fluids exhibit a linear relationship between shear rate and shear stress, and the viscosity remains independent of shear rate. Conversely, Non-Newtonian fluids exhibit a dependent relationship between viscosity and shear rate. The Bingham and Herschel-Bulkley models of rheology are perhaps the most widely used for modelling of fluid behaviour (Brennan, 2001; Yang et al., 2009; Weiss et al., 2007; Eshtiaghi et al., 2013). The Bingham model is expressed by the equation (Lakehal et al., 1999):

$$\mu = \frac{\tau_0}{\dot{\gamma}} + \mu_p \quad (7)$$

While the Herschel-Bulkley model is expressed by the equation (Craig, Nieuwoudt and Niemand, 2013):

$$\mu = \frac{\tau_0}{\dot{\gamma}} + K\dot{\gamma}^{n-1} \quad (8)$$

Where:  $\mu$  is the dynamic viscosity,  $\tau_0$  is the yield stress,  $\mu_p$  is the plastic viscosity,  $K$  is the consistency index,  $n$  is the power law exponent, and  $\dot{\gamma}$  is the shear rate.

#### *Biochemical Reactions*

The solids travelling through the pond are subject to a number of chemical reactions through interaction with other reactants within the pond. Being primarily organic matter, a large portion of the solids are biological in nature. These biochemical reactions change the structure and phase of the solids, which largely affect the behaviour and amount of sludge. Additionally, biochemical reactions are the primary mechanism driving methane production and other gaseous emissions, which are primary operational outcomes.

#### *4.7.3 Model Description*

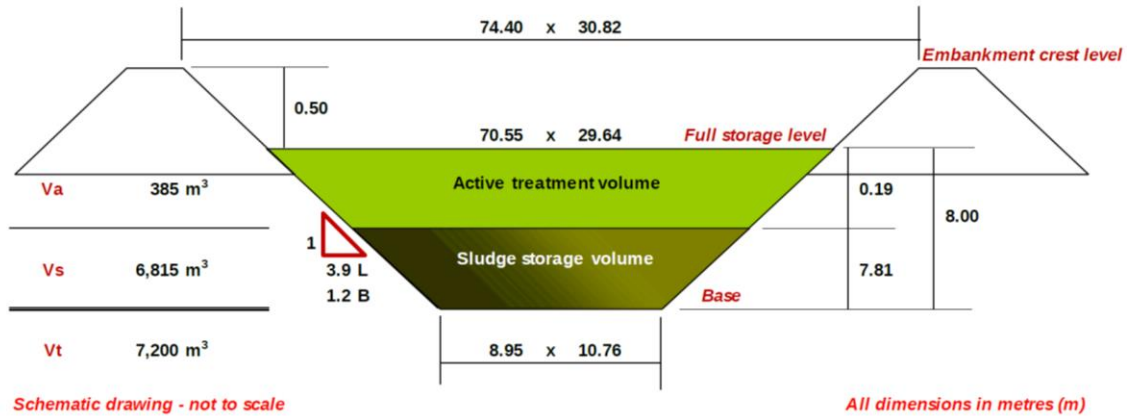
##### *Hydrodynamic and Settling Model*

Computational Fluid Dynamics (CFD) has experienced significant development in recent years due to the rapid expansion of processing power in common computing, and has since proven itself as an invaluable technique for pond design and management (Passos, Dias and von Sperling, 2016; Ho, Van Echelpoel and Goethals, 2017; Peterson, Harris and Wadhwa, 2000). CFD modelling is a technique by which a series of complex numerical equations governing fluid dynamics in a given system are computationally solved to derive specific outcomes and parameters. It is noted that various degrees of complexity can be applied to modelling (2-3D, 1-3 phases), and that we have proposed a 3D, 2 phase (solid and liquid approach), with the state of the art in pond modelling being generally single phase (Passos, Dias and von Sperling, 2016; Ho, Van Echelpoel and Goethals, 2017; Peterson, Harris and Wadhwa, 2000). Previous work in large scale systems has not included incorporation of the solids. After defining certain properties of the system, such as the geometry of the pond, velocities under certain constant conditions (e.g. inlet and outlet) and the behaviour of the fluid at the boundaries and within the domain, the numerical system is solved through computational iteration and the resulting solution can be visually or textually analysed to explain the hydrodynamic behaviour.

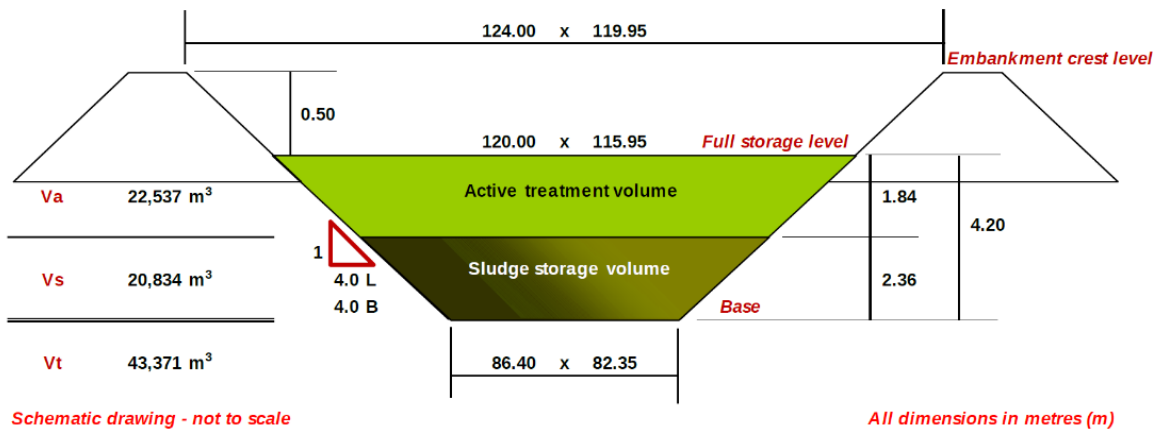
The implementations here required custom physics and solvers, and due to its ability to modify the physics engine (and share model codes), the open-sourced CFD software OpenFOAM (v5.0) was used

as the platform. For the single-phase fluid models, the fluid is assumed to be incompressible and Newtonian with a density of  $998 \text{ kg m}^{-3}$  and a dynamic viscosity of  $1.003 \times 10^{-3} \text{ kg m}^{-1} \text{ s}^{-1}$ . All model dimensions are based on their respective actual pond designs as depicted in Figure 5. All results presented are based on simulations performed for 24 hours unless otherwise stated.

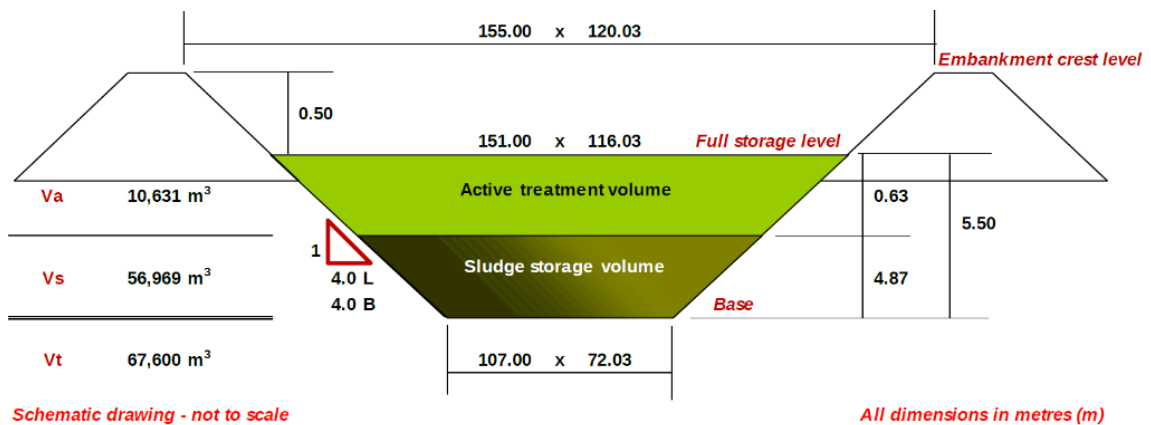
### Pond 2 - Piggery A



### Pond 5 - Piggery B



### Pond 7 - Piggery D



## Pond 16 - Piggery K (Covered anaerobic pond)

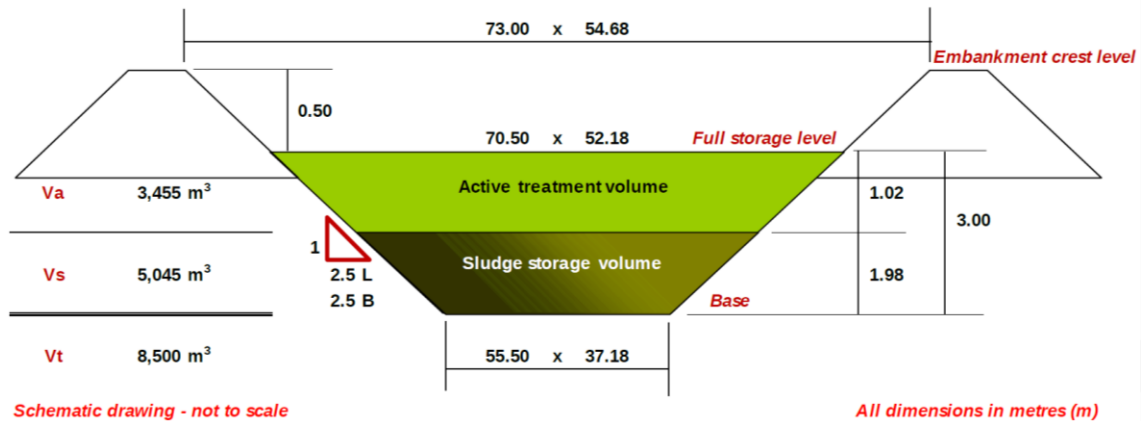


Figure 5 Schematic representation of four ponds under study.

Four ponds were selected for model analysis in this report – Ponds 2, 5, 7 and 16, mainly due to availability of geometric information and validation data. Based on preliminary findings from the DAF report, Ponds 2, 5 and 7 were selected based on their exemplary pond geometries and sludge accumulation behaviour and likeliness to reveal outcomes applicable to most other ponds. Pond 2 and 7 were comparable in HRT (~200d), but with deep and shallow geometries respectively, while Pond 5 was a very long HRT system. Pond 16, a covered anaerobic pond, was selected for modelling as it is the only covered pond and has a very short HRT. Hydrodynamics in each pond were simulated under 2D, single-phase 3D and two-phase (liquid-solid) 3D models as described above. After simulations, the post-processed images were generated from simulations under steady-state flow. Flow behaviours are depicted through post-processed images of the dominant flow streamline patterns and colour-coded velocity and sludge concentration contours. All distances are given in m, velocities in m/s and concentrations in kg / m<sup>3</sup> (g / L) unless otherwise stated. Inlet and outlet locations were varied throughout each model to identify positional effects.

### Compartmental Based Model

A recent approach within wastewater modelling research involves using a compartmental-based model (CBM) to couple biochemical models with preliminary results from a simplified hydrodynamic model. The CBM approach involves modelling the pond as a collection of smaller, more manageable pond volumes (compartments). This allows for more specific and precise biochemical modelling, as simulations can be performed for each compartment. This approach has been shown to produce specific and more precise outcomes while drastically reducing the heavy computational demands of a model consisting entirely in CFD (Alvarado, Vedantam, et al., 2012; Bellandi et al., 2019).

A virtual tracer test is first simulated in the CFD platform to determine residence time distributions (RTD) within each case. Then, the pond geometry is divided into discrete compartments such that a second tracer simulation based on these compartments produces similar RTD behaviour. The compartmental tracer tests are modelled in Aquasim 2.1d, which allows for direct comparison with the RTD of the previous simulation, as well as parameter and sensitivity estimation for pertinent variables such as compartment volume, recycle or bypass volume or (HRT). Once the compartment configuration is assessed to be a good fit, biochemical modelling can be performed on each compartment.

The main objectives of the CBM are to identify:

- The degree to which a simplified model can replicate the more complex CFD model of the pond.
- Characteristic features of the four cases assessed, including apparent bypass and inactive volumes.
- Suitable hydraulic models for biochemical modelling.

The initial virtual tracer tests were performed in the hydrodynamic platform described in section 2.3.1. The dimensions and parameters of each pond are given in Table 2. The feed is simulated as a pulse injection at 1 mg/L over 1000 seconds (0.01 days), increased to 0.1 days to avoid numerical issues caused by long HRTs.

Table 2 Pond parameters used for initial compartmental based model design

Case	length (m)	width (m)	depth (m)
Pond 2	71	30	8
Pond 5	120	116	4
Pond 7	151	116	6
Pond 16	71	52	3

The CBM consists of two main compartments in series, two bypass compartments in series, a recycle compartment, and an outlet compartment. The configuration is shown below in Figure 6. This geometry is based on general characteristic response (particularly from Ponds 2 and 7). The recycle enables oscillatory behaviour, while the bypass allows for a high initial peak. A variable inactive zone was also added. Volumes for the 1<sup>st</sup> and 2<sup>nd</sup> main compartments and recycle were fitted individually. The total bypass volume was fitted, split equally between both zones. Flows were individually fitted. A delay was also included, simulating mainly movement of the fluid in the inlet works prior to entering the main pond. The data was resampled to 500 evenly spaced points throughout for Ponds 2, 5 and 7. For Pond 16, a higher sampling count was used to accurately represent the high frequency oscillations seen in the initial tracer tests.

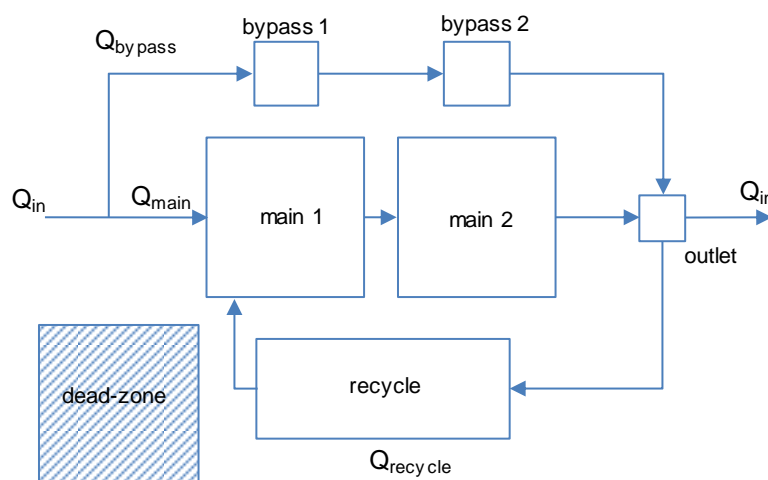


Figure 6 Compartmental based model configuration



### Biochemical Model

To predict long-term performance, a biochemical model was implemented using the optimal hydraulic configuration identified in the previous section. To simplify the model, and allow long-term simulations over the course of years, the influent was fractionated into mineral solids ( $X_{MSS}$ ), degradable organics ( $X_d$ ), and non-degradable organics ( $X_{nd}$ ). A degradable fraction (of total organic solids) of 60% (BMP of 340 mL CH<sub>4</sub>/g VS) was applied in accordance with Skerman et al. (2017). An option (particularly for covered ponds) would be to expand this to an advanced model such as the IWA ADMI (Batstone et al., 2002), but this is mainly used for prediction of acid-base effects and chemistry, which are not controlling mechanisms here. Degradable organics are assumed to break down according to a first order hydrolysis:

$$r_{x,hyd} = -k_{hyd}X_d \quad (9)$$

The hydrolysis coefficient ( $k_{hyd}$ ) was set to 0.1 d<sup>-1</sup> (Skerman et al., 2017), accounting for a decrease from 0.3 d<sup>-1</sup> based on the decreased ambient temperature (20°C).

Within the main compartments of main 1, main 2, and recycle, a fraction of the solids ( $f_{ns}$ ) is assumed to pass through to the effluent in each pass. This is estimated based on the observed effluent solids from the measured data and the results from the CFD analysis, to be 10%. The hydraulic volume occupied by the solids is calculated based on the observed sludge concentration from the sampling campaign. No loss in degradation activity was applied to settled solids.

The delay was excluded from the biochemical model, given it is likely mainly due to inlet effects.

In order to compare the ponds on the same basis, the inputs and main parameters were set consistently based on the observed sludge profiling results (Section 5.1). These were an input solids concentration of 3%, with 80% VS fraction, and a settled sludge concentration of 10% (TS).

## 5. Results

### 5.1 Sludge profiling

Aerial photographs and sludge contour plans, showing the depths to the sludge surface from the pond full storage level, are provided in the following sections. Cross-sections showing the original as-built pond base and the sludge level at the time of the survey are provided in Appendix A.

#### 5.1.1 Pond 1, Piggery A (Primary pond: 1000 sows farrow to finish unit – 11,350 SPU)



Figure 7 Aerial photograph of Piggery A, Pond 1.

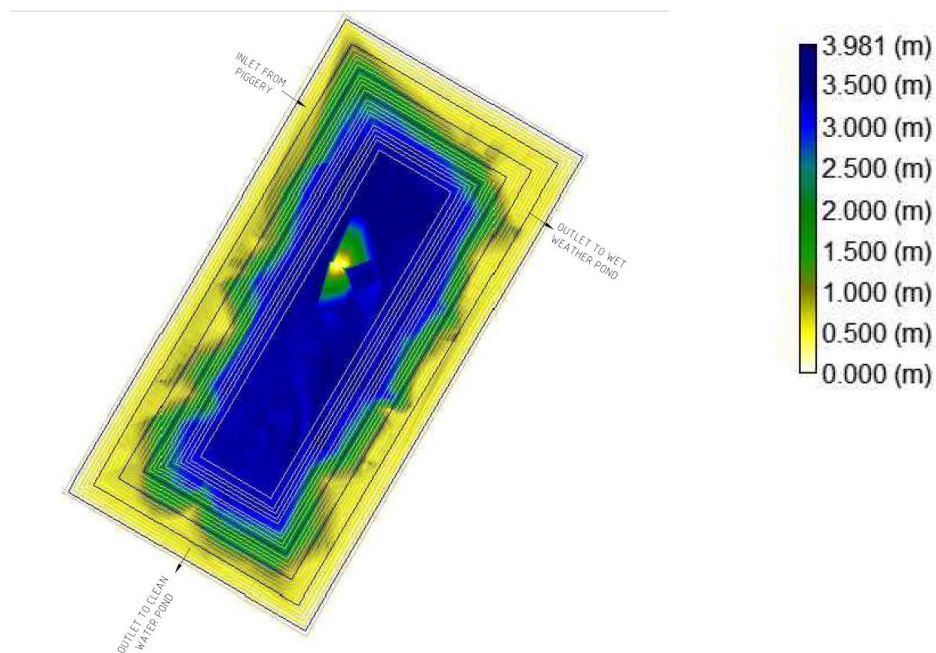


Figure 8 Sludge contour plan for Piggery A, Pond 1.

5.1.2 Pond 2, Piggery A (Primary pond: 980 gilts - 1,679 SPU)

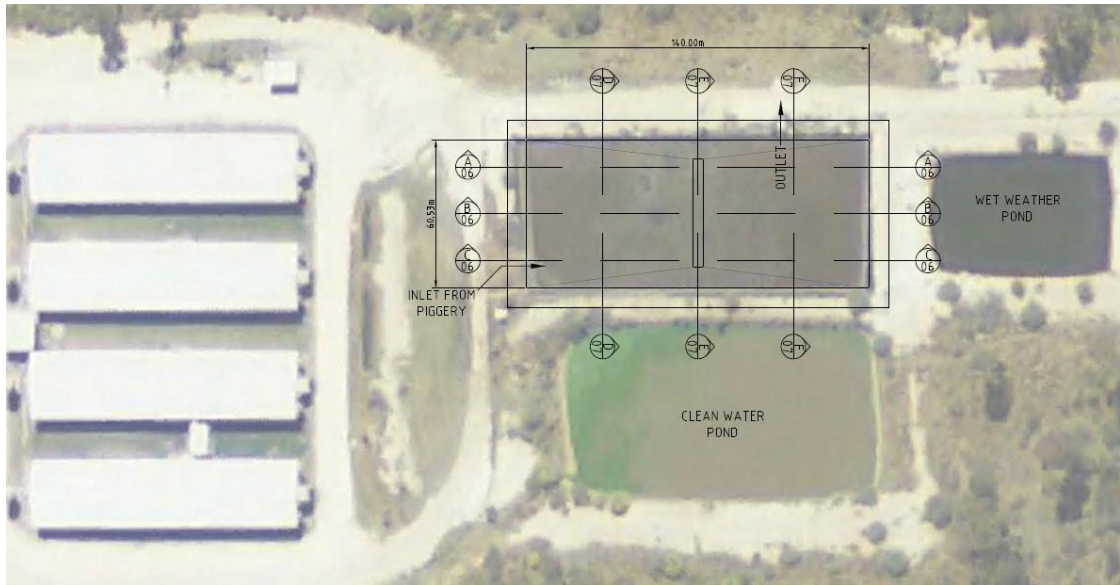


Figure 9 Aerial photograph of Piggery A, Pond 2.

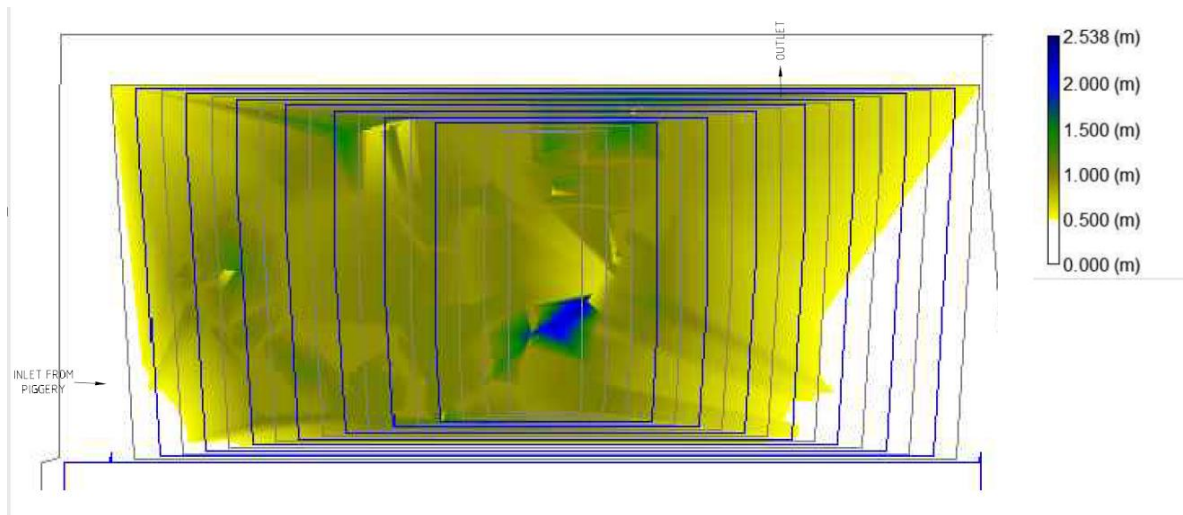


Figure 10 Sludge contour plan for Piggery A, Pond 2.

5.1.3 Pond 3, Piggery A (Primary pond: 5000 sow breeder unit - 14,705 SPU)

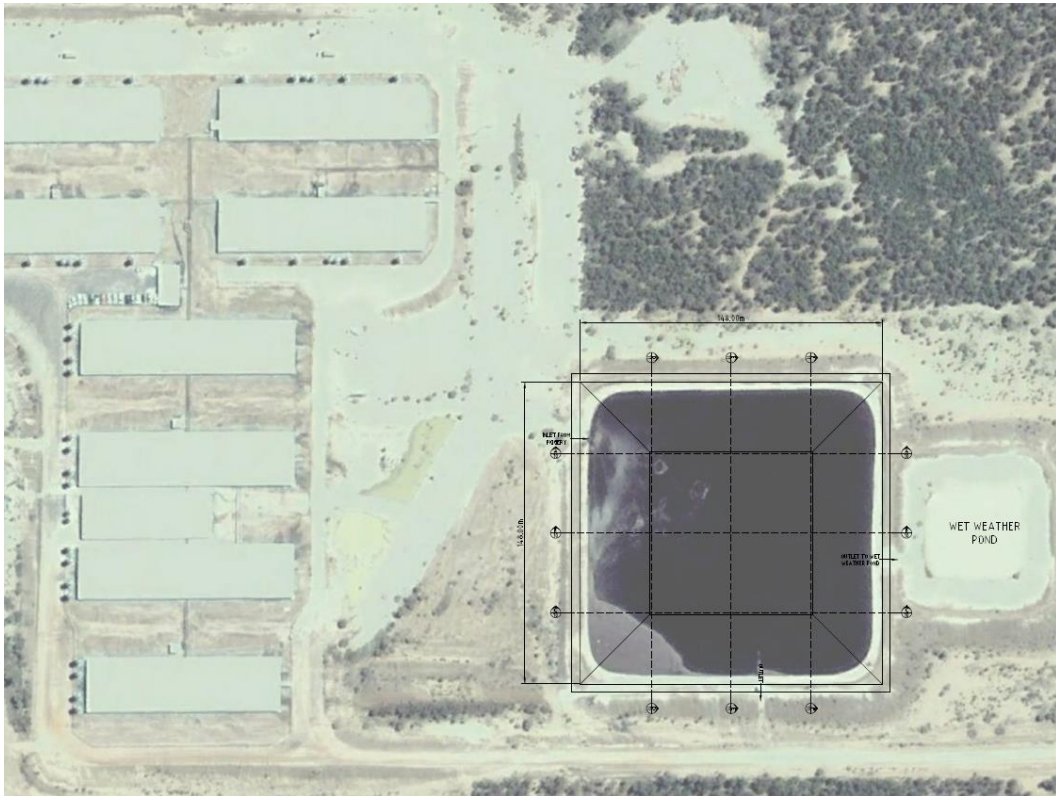


Figure 11 Aerial photograph of Piggery A, Pond 3.

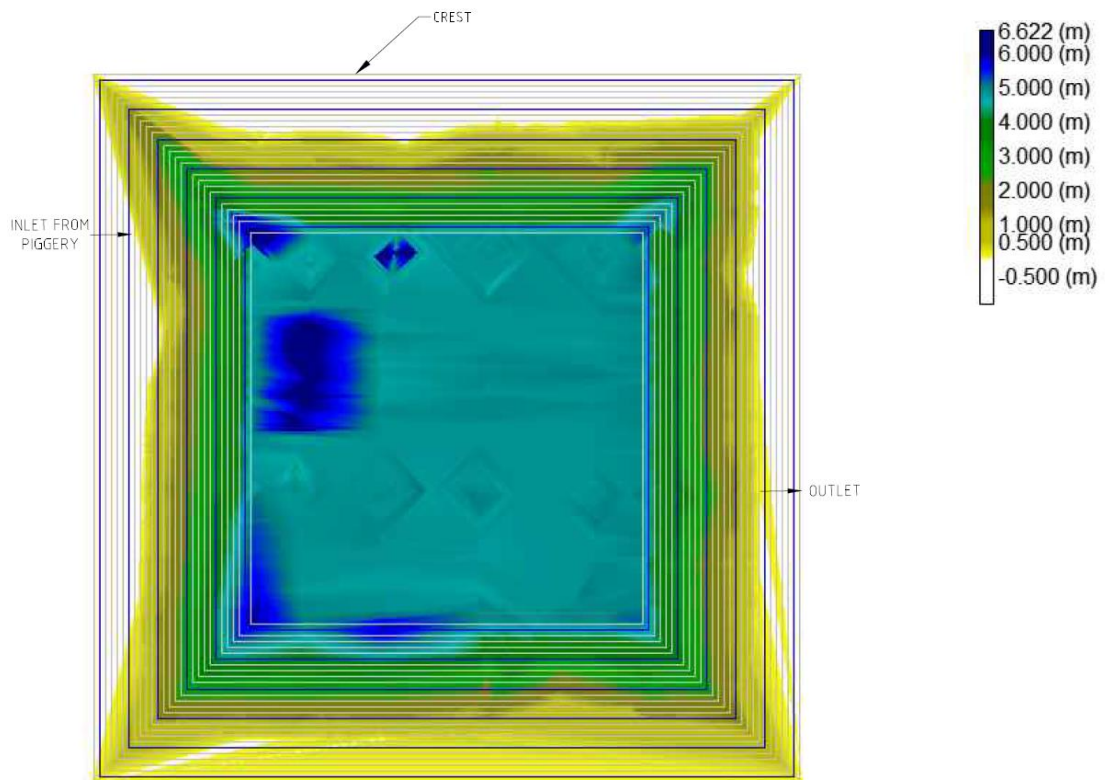


Figure 12 Sludge contour plan for Piggery A, Pond 3.

5.1.4 Pond 4, Piggery A (Secondary pond: grower / finisher unit - 48,064 SPU)

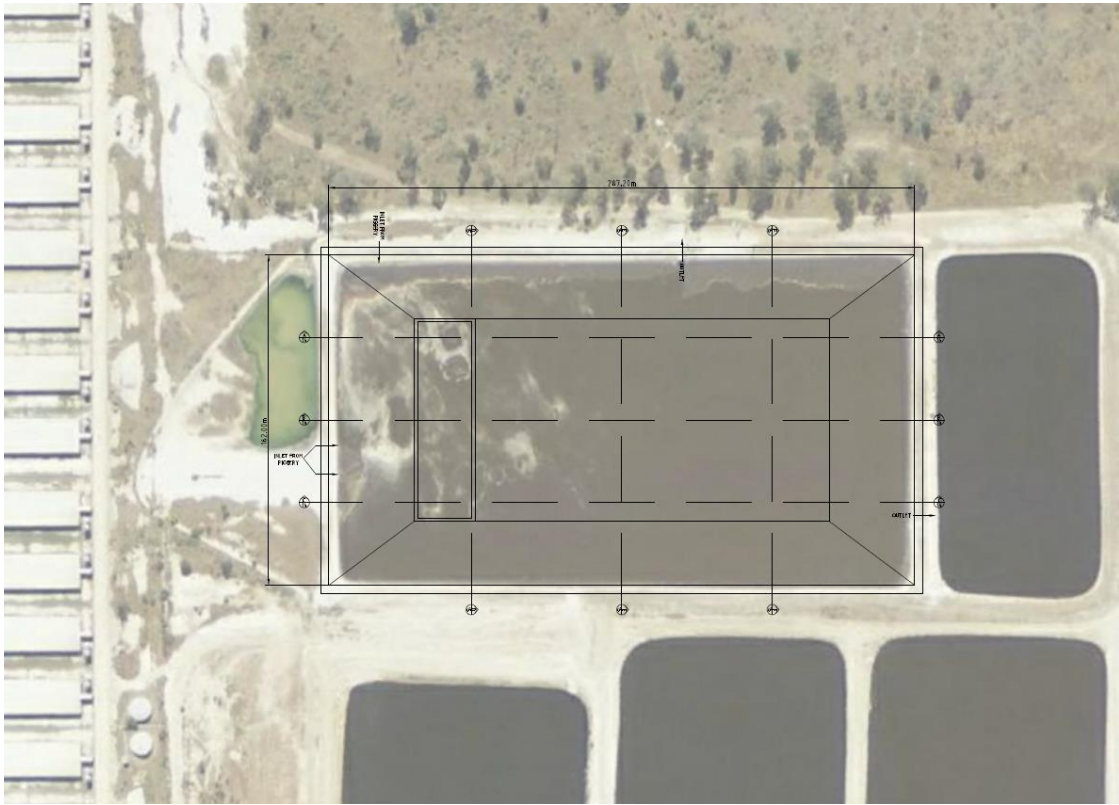


Figure 13 Aerial photograph of Piggery A, Pond 4.

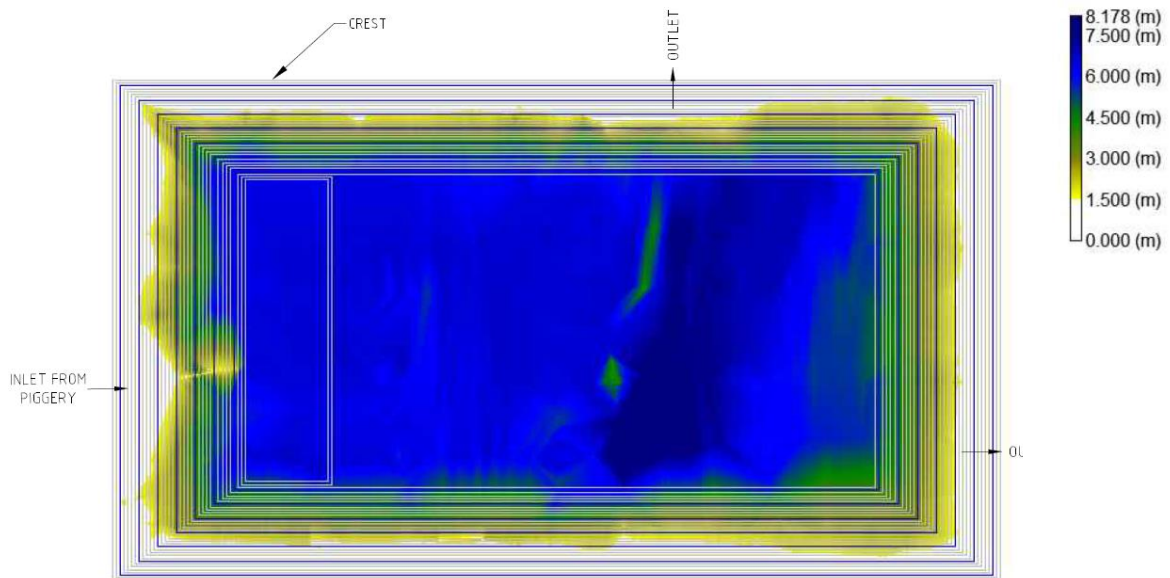


Figure 14 Sludge contour plan for Piggery A, Pond 4.

5.1.5 Pond 5, Piggery B (Primary pond: grower / finisher unit - 6,350 SPU)



Figure 15 Aerial photograph of Piggery B, Pond 5.

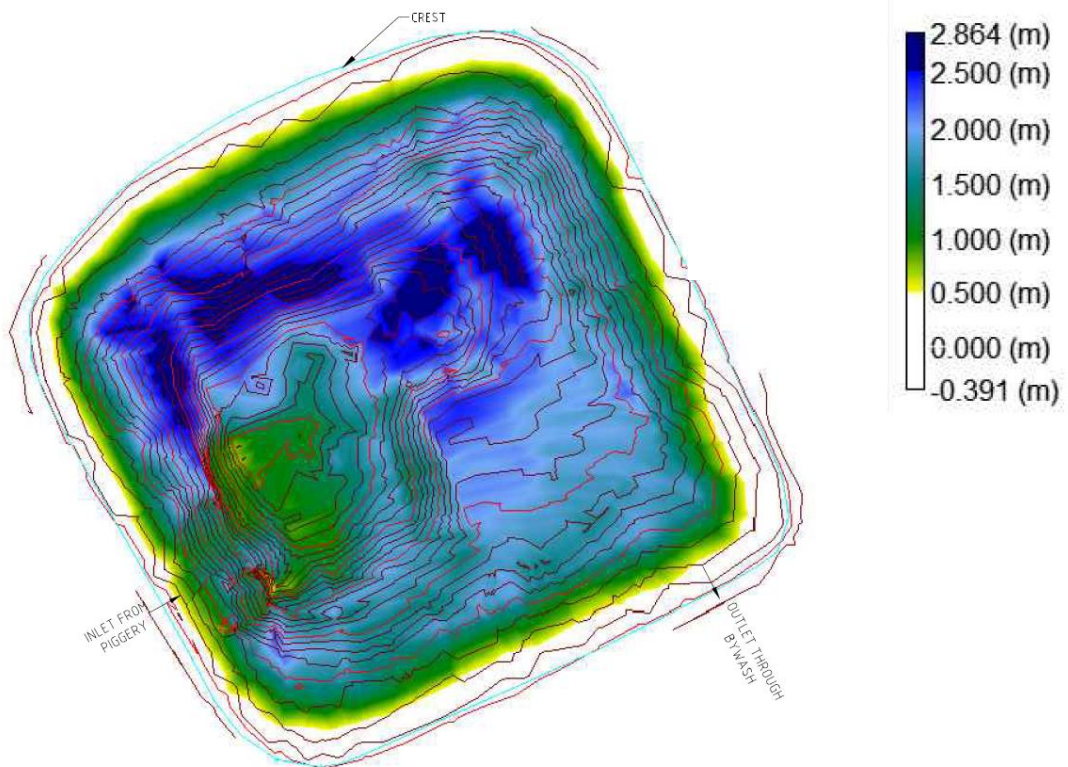


Figure 16 Sludge contour plan for Piggery B, Pond 5.

5.1.6 Pond 6, Piggery C (Primary pond: nursery / weaner unit - 3,387 SPU)



Figure 17 Aerial photograph of Piggery C, Pond 6.

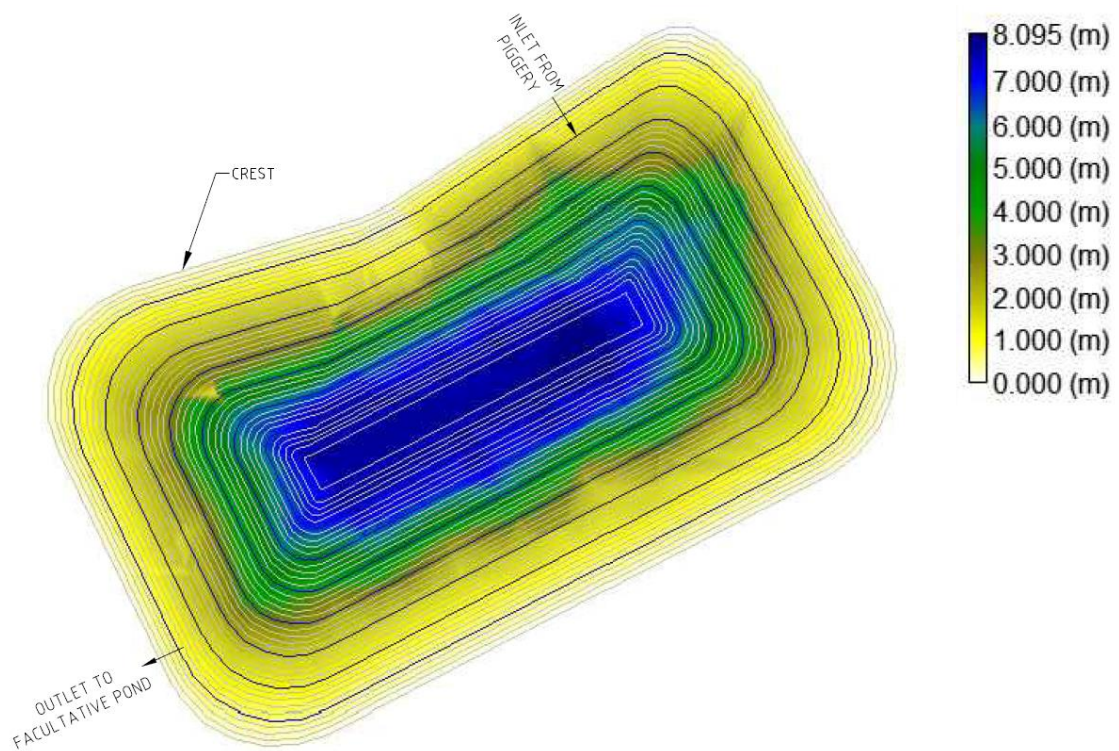


Figure 18 Sludge contour plan for Piggery C, Pond 6.

5.1.7 Pond 7, Piggery D (Primary pond: 1,500 sow farrow to finish unit - 16,000 SPU)

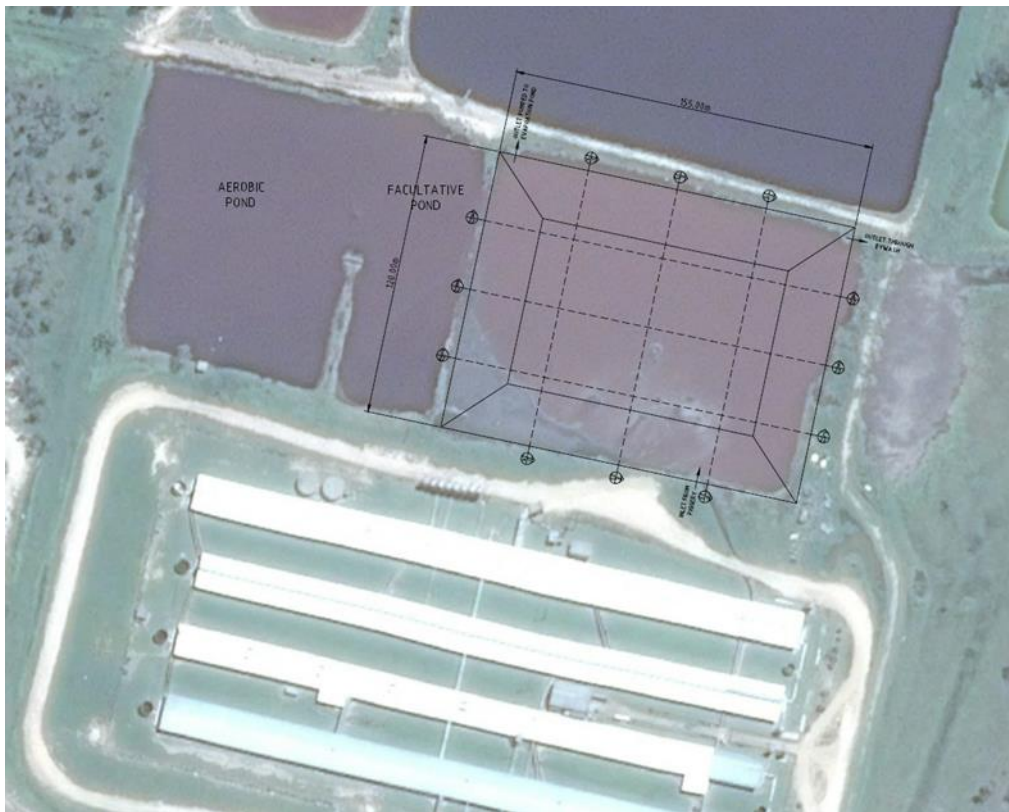


Figure 19 Aerial photograph of Piggery D, Pond 7.

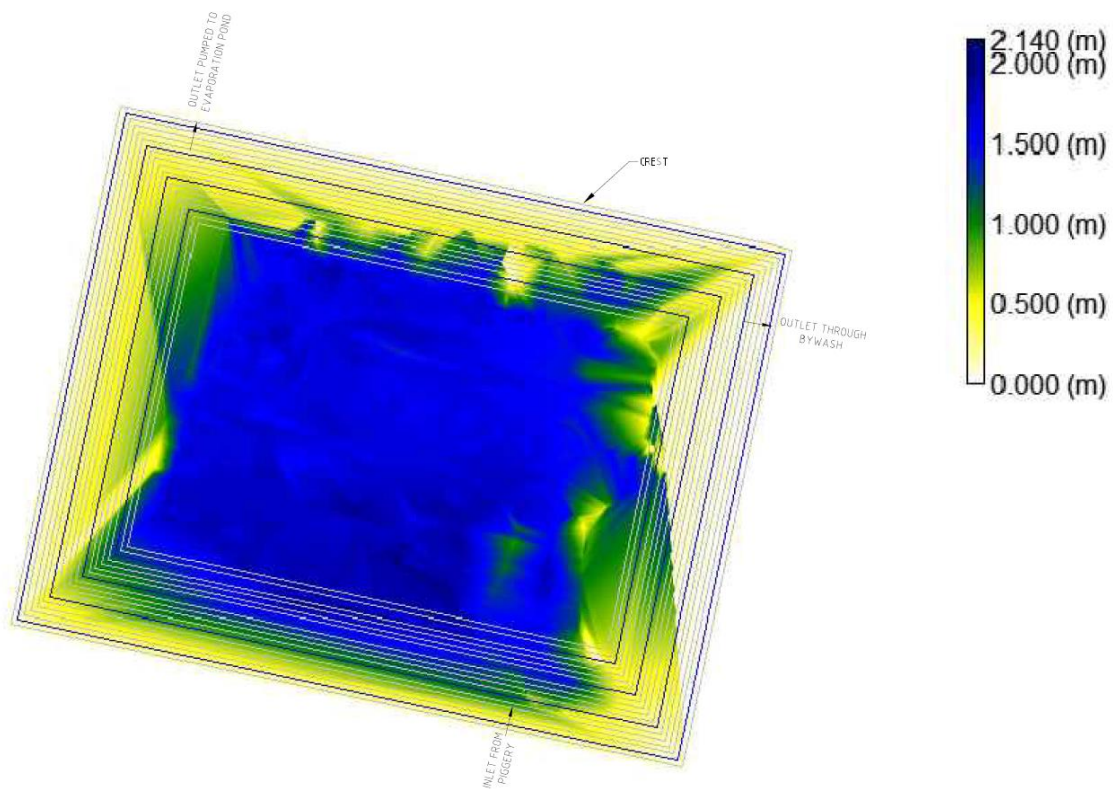


Figure 20 Sludge contour plan for Piggery D, Pond 7.



5.1.8 Pond 8, Piggery D (Secondary Pond: 1,500 sow farrow to finish unit - 16,000 SPU)

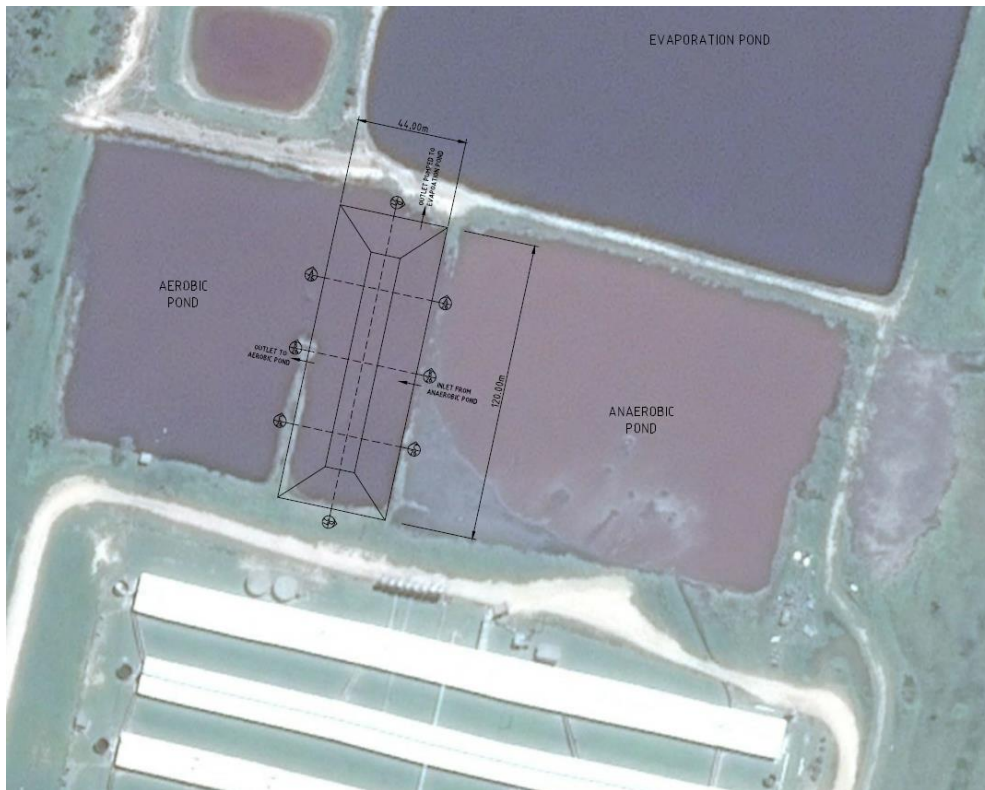


Figure 21 Aerial photograph of Piggery D, Pond 8.

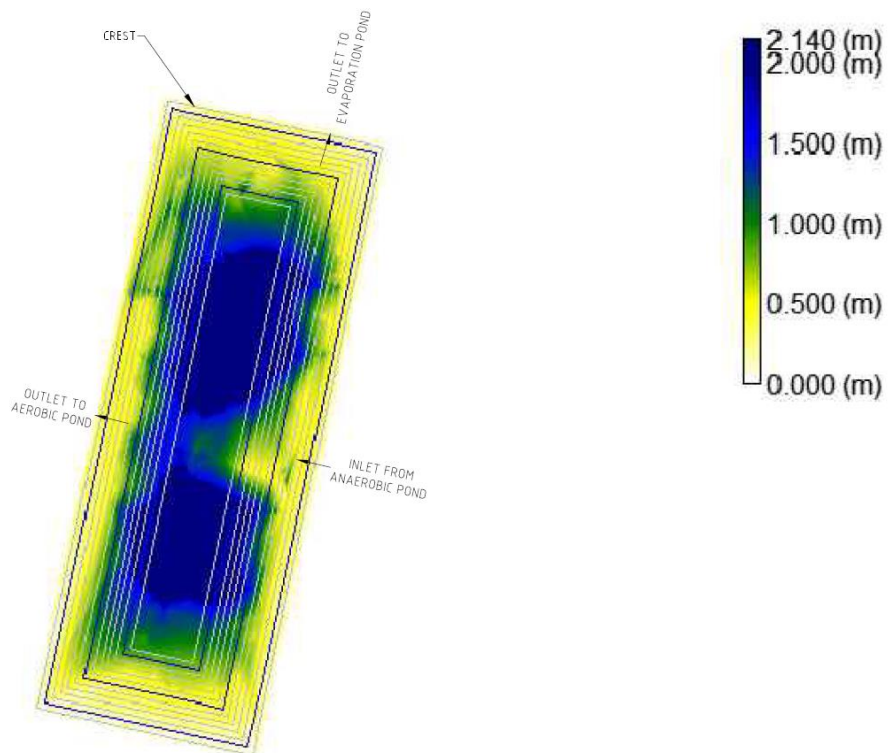


Figure 22 Sludge contour plan for Piggery D, Pond 8.

5.1.9 Pond 9, Piggery E (Primary Pond: 3,600 sow breeder unit - 7,241 SPU)



Figure 23 Aerial photograph of Piggery E, Pond 9.

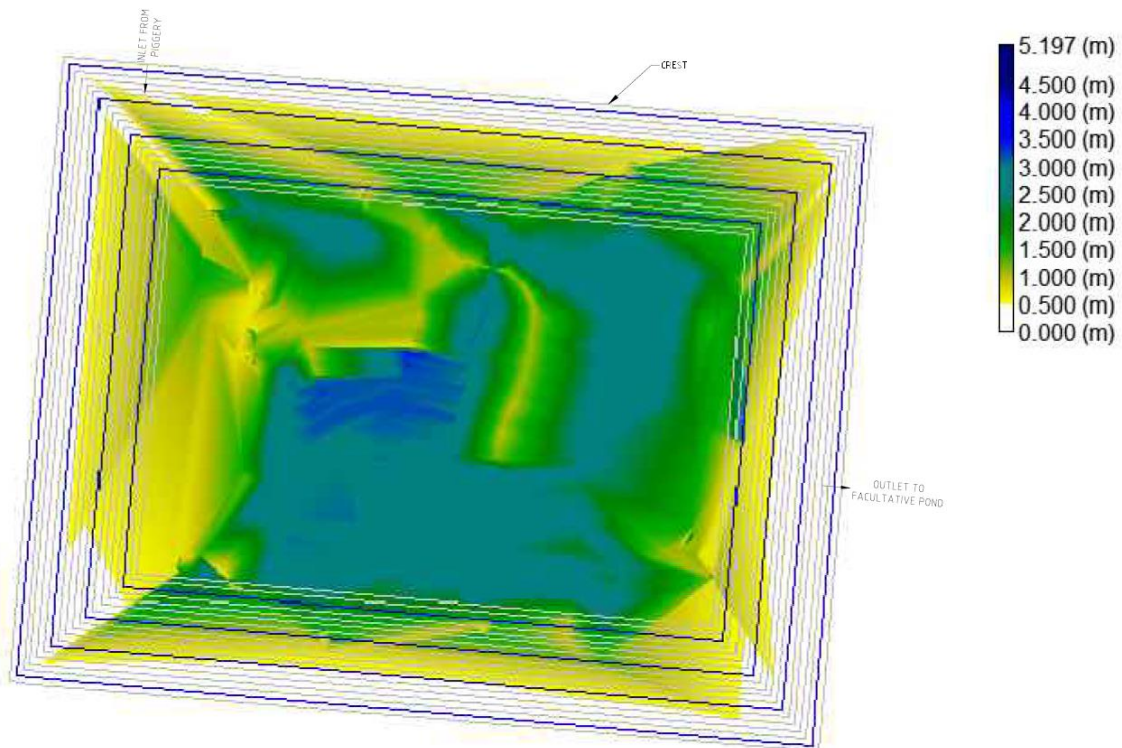


Figure 24 Sludge contour plan for Piggery E, Pond 9.

5.1.10 Pond 10, Piggery E (Secondary Pond: 3,600 sow breeder unit - 7,241 SPU)



Figure 25 Aerial photograph of Piggery E, Pond 10.

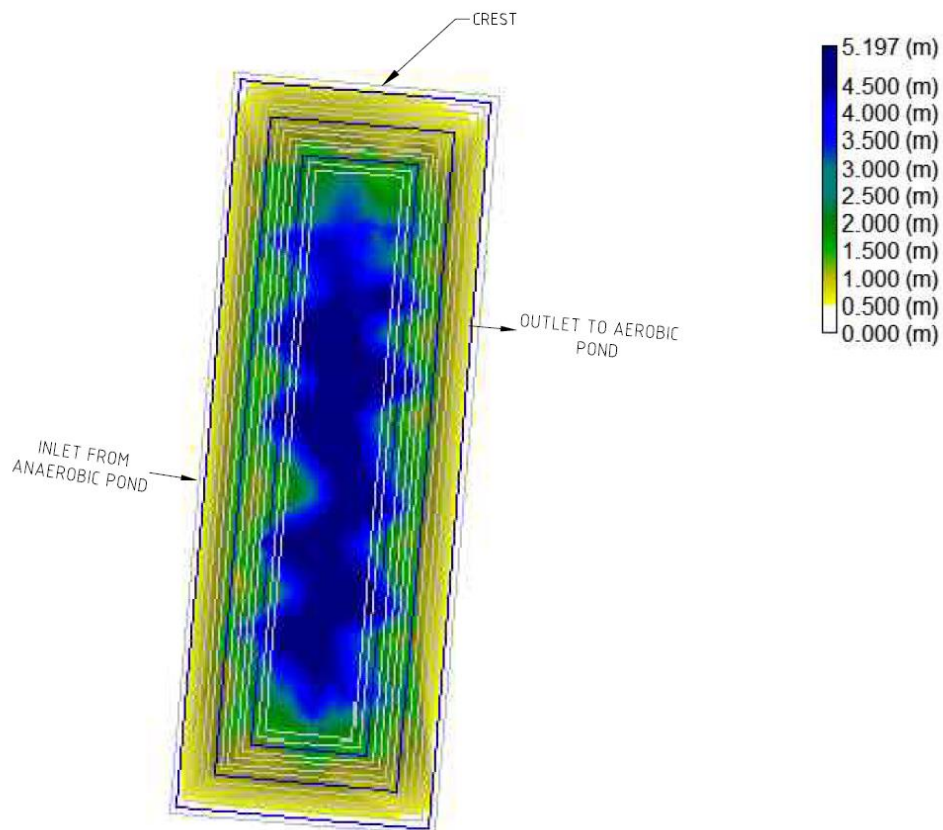


Figure 26 Sludge contour plan for Piggery E, Pond 10.

5.1.11 Pond 11, Piggery F (Primary Pond: 1200 sow farrow to finish unit - 12,054 SPU)



Figure 27 Aerial photograph of Piggery F, Pond 11.

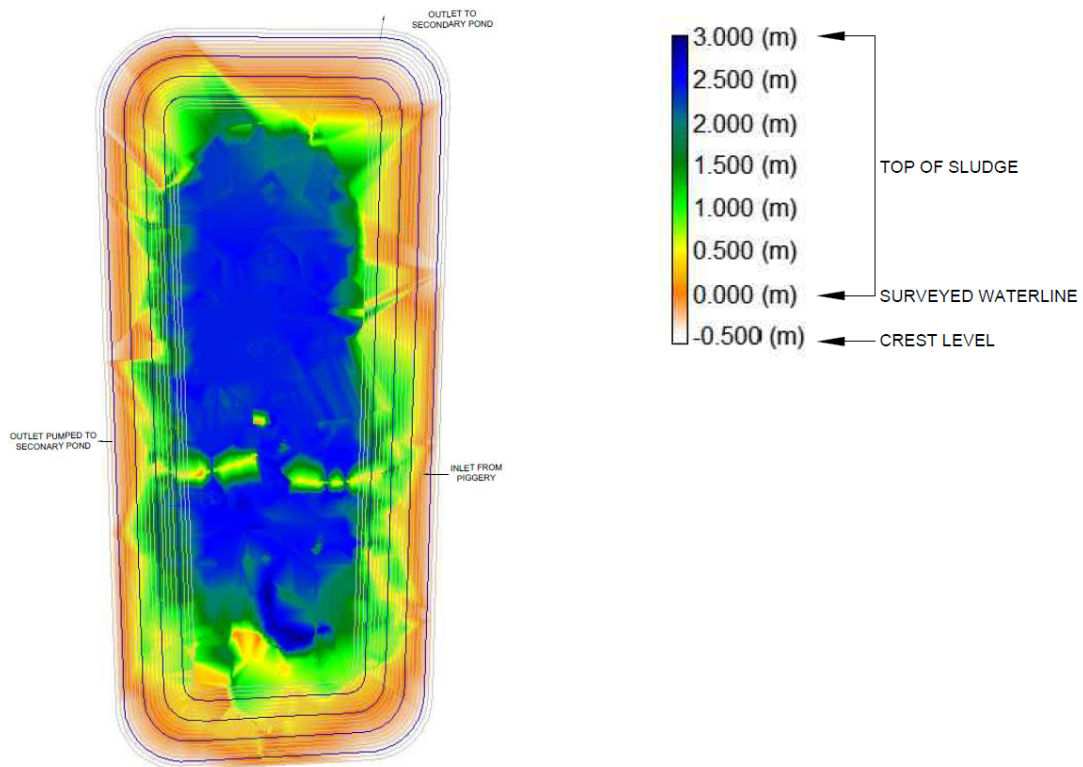


Figure 28 Sludge contour plan for Piggery F, Pond 11.

5.1.12 Pond 12, Piggery G (Primary pond: 600 sow breeder unit - 1,245 SPU)



Figure 29 Aerial photograph of Piggery G, Pond 12.

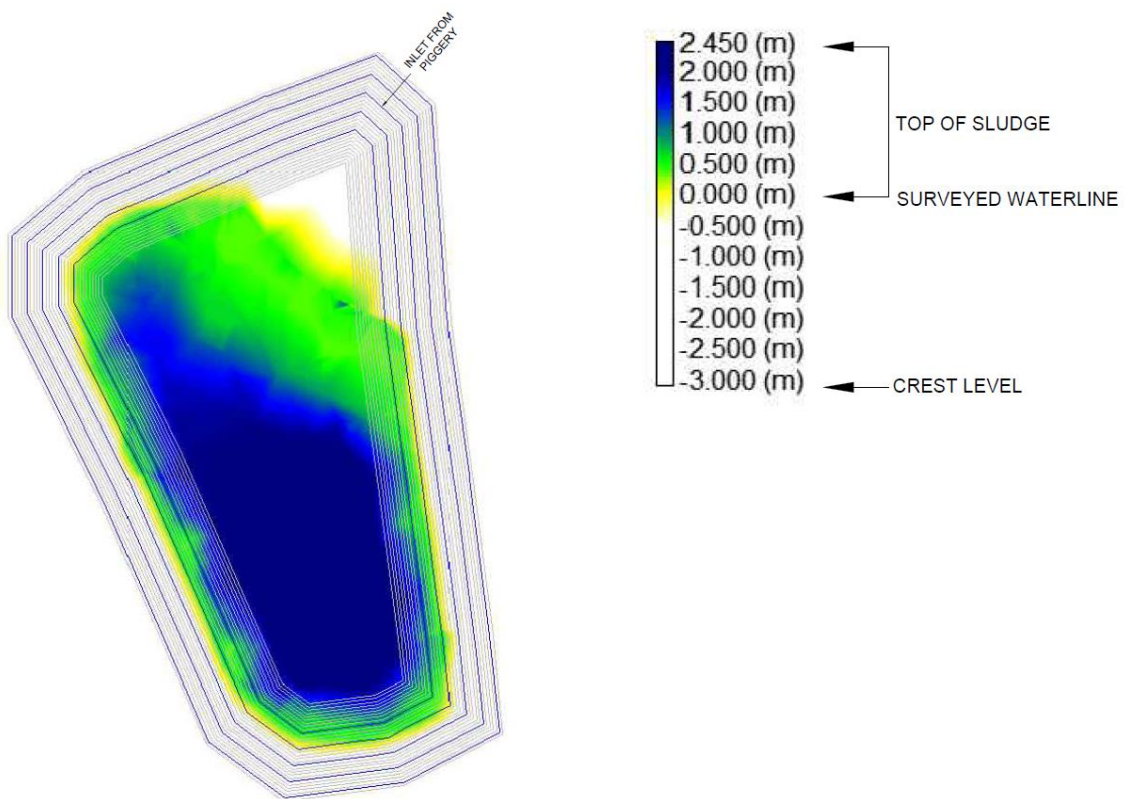


Figure 30 Sludge contour plan for Piggery G, Pond 12.

5.1.13 Pond 13, Piggery H (Secondary pond: 3100 sow breeder and grower unit - 18,546 SPU)



Figure 31 Aerial photograph of Piggery H, Pond 13.

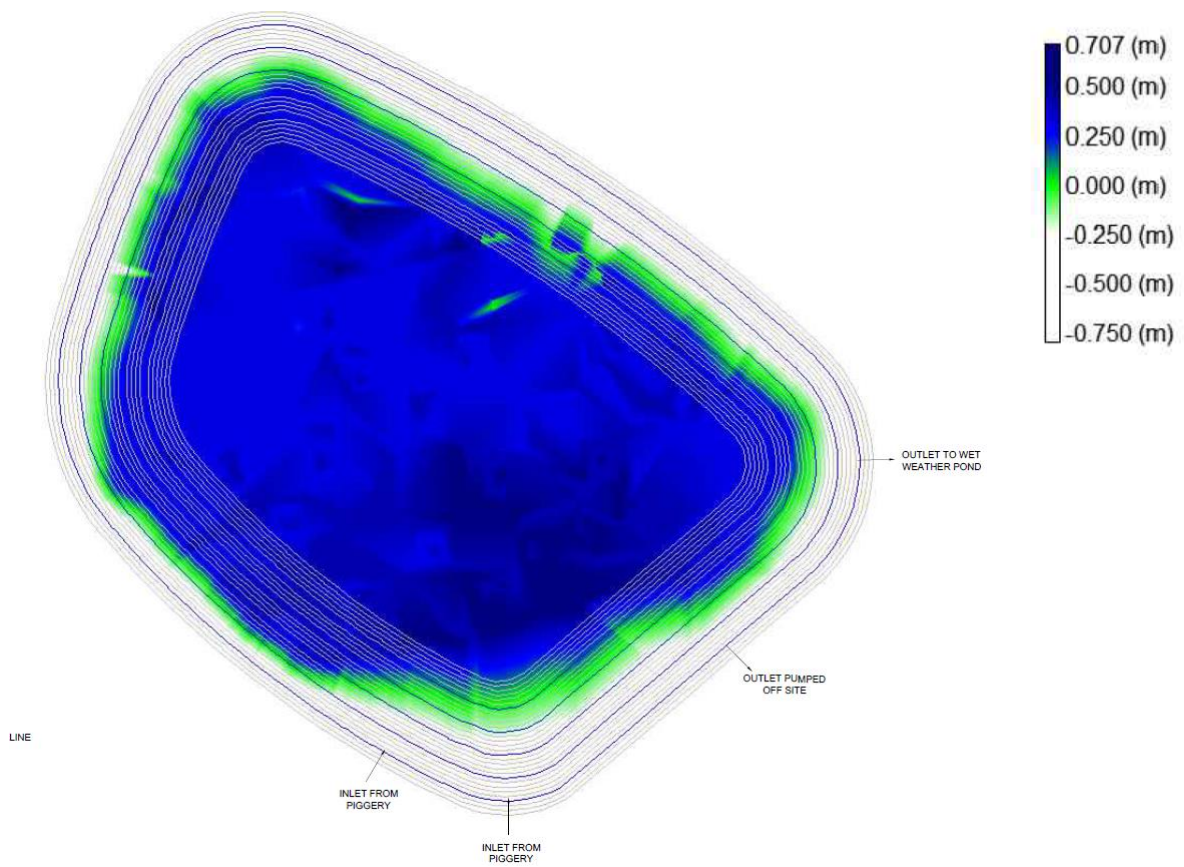


Figure 32 Sludge contour plan for Piggery H, Pond 13.

5.1.14 Pond 14, Piggery I (Primary pond: 2,600 sow breeder unit - 5,195 SPU)

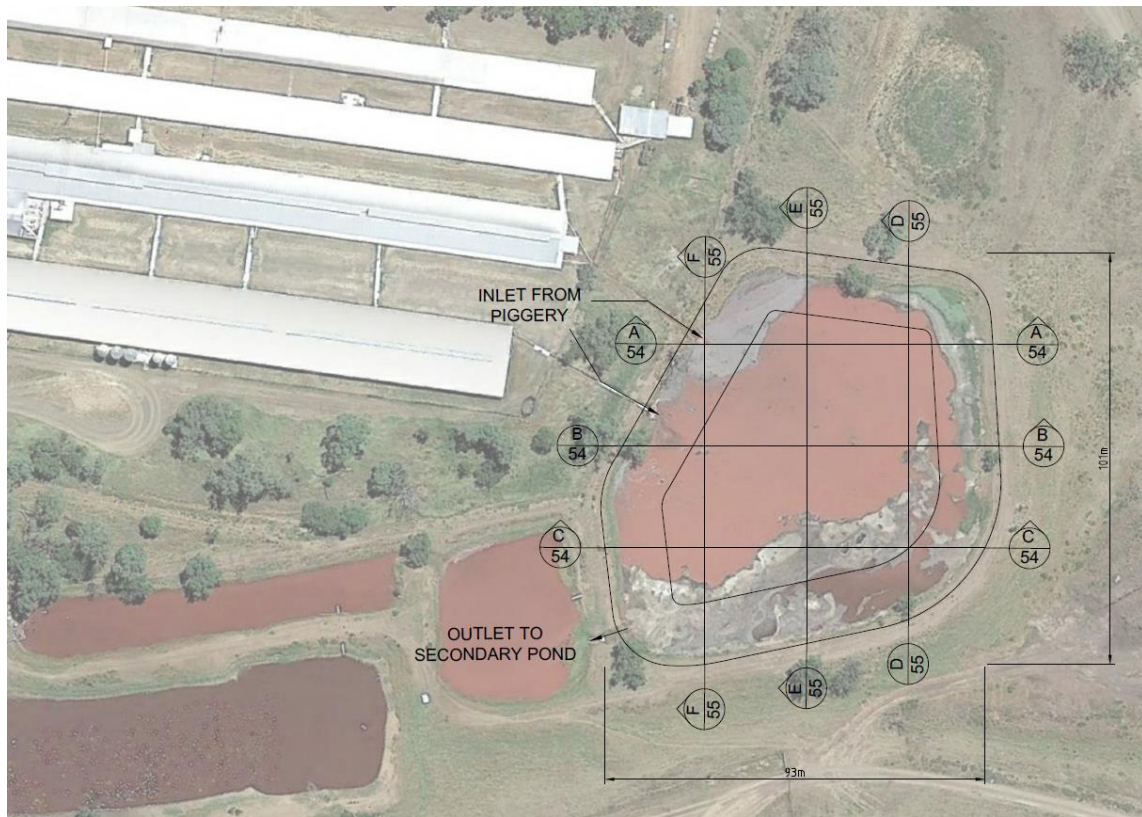


Figure 33 Aerial photograph of Piggery I, Pond 14.

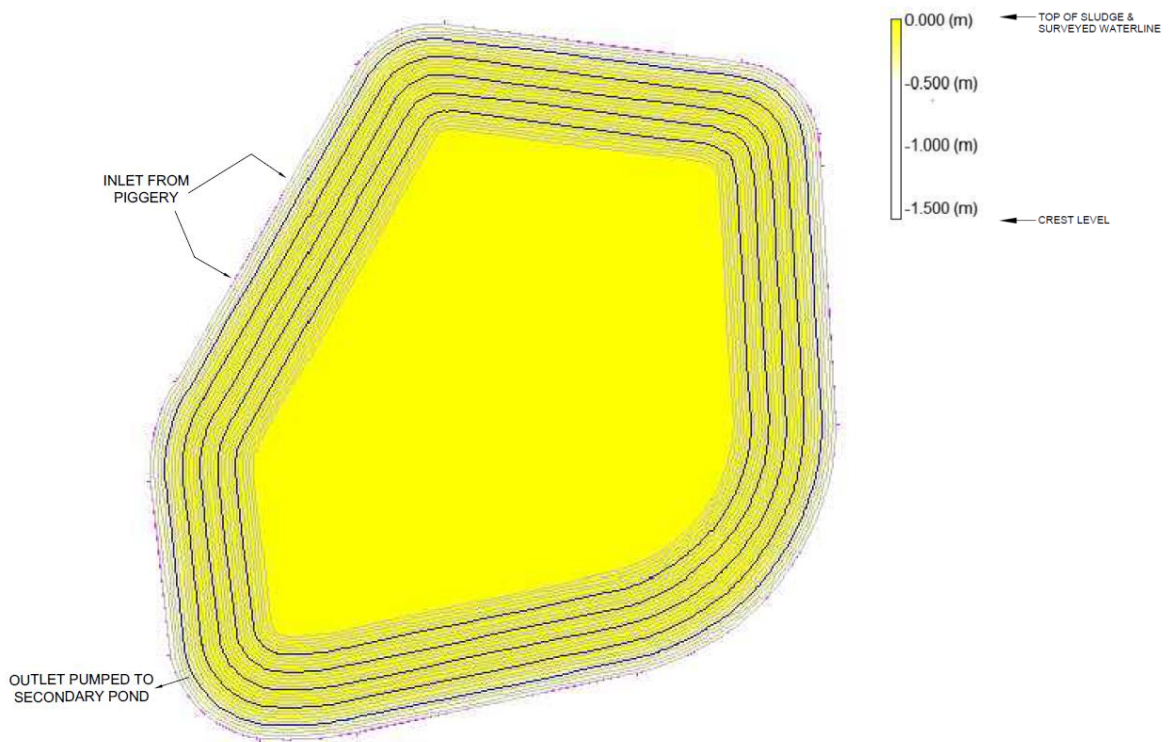


Figure 34 Sludge contour plan for Piggery I, Pond 14.

5.1.15 Pond 15, Piggery J (Primary pond: grower-finisher unit - 21,168 SPU)

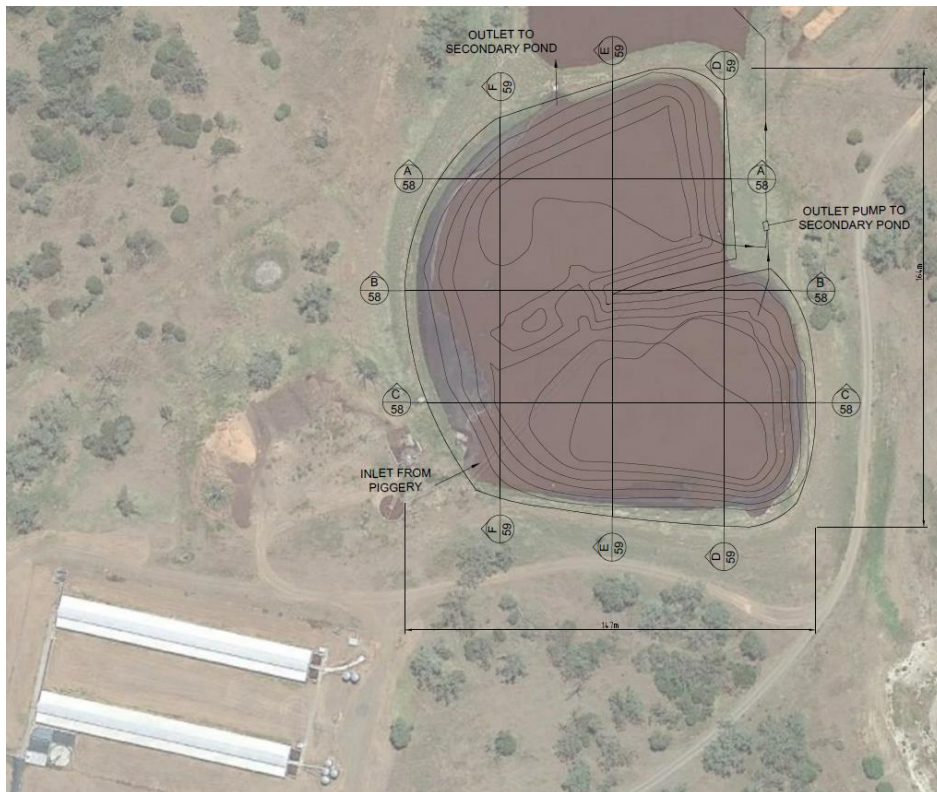


Figure 35 Aerial photograph of Piggery J, Pond 15.

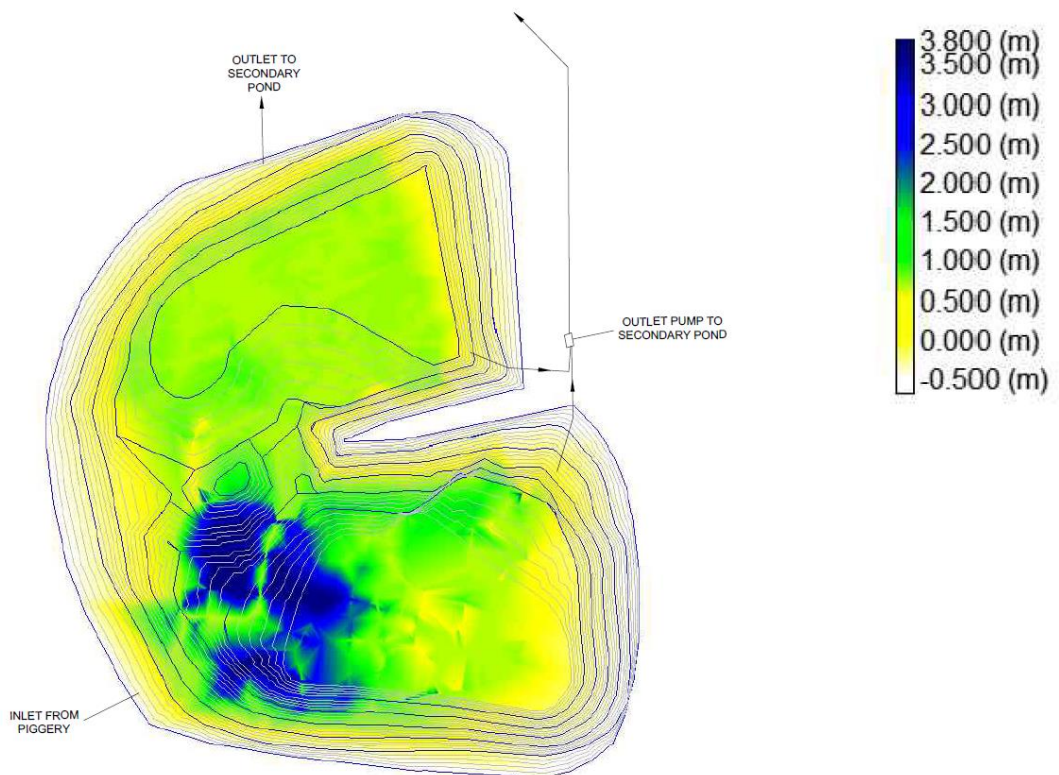


Figure 36 Sludge contour plan for Piggery J, Pond 15.





## 5.2 Sludge accumulation rate estimation

Details of the piggeries and individual ponds where the sludge surveys were carried out are provided in Tables 3 and 4. These details include the pond TS and VS loading rates estimated using the PigBal 4 model, hydraulic retention times and sludge accumulation times. The resulting sludge accumulation rates estimated for each of the eleven primary anaerobic ponds surveyed for this study are also plotted in Figure 37.

These estimated sludge accumulation rates ranged from 0.00054 to 0.00324 m<sup>3</sup>/kg TS, with a mean value of 0.00228 ± 0.00053 m<sup>3</sup>/kg TS (95% confidence intervals). This mean value is approximately equal to the mean of the previous design standard 0.00303 m<sup>3</sup>/kg TS (Barth, 1995) and the current design standard 0.00137 m<sup>3</sup>/kg TS (ASABE, 2011). The variability in the sludge accumulation rate estimates probably reflects the uncertainty regarding pond desludging dates and volumes of sludge removed, and possibly some unreported changes in pig herd, diet and management practices, particularly as the ownership of some of the piggeries has changed over long operational periods.

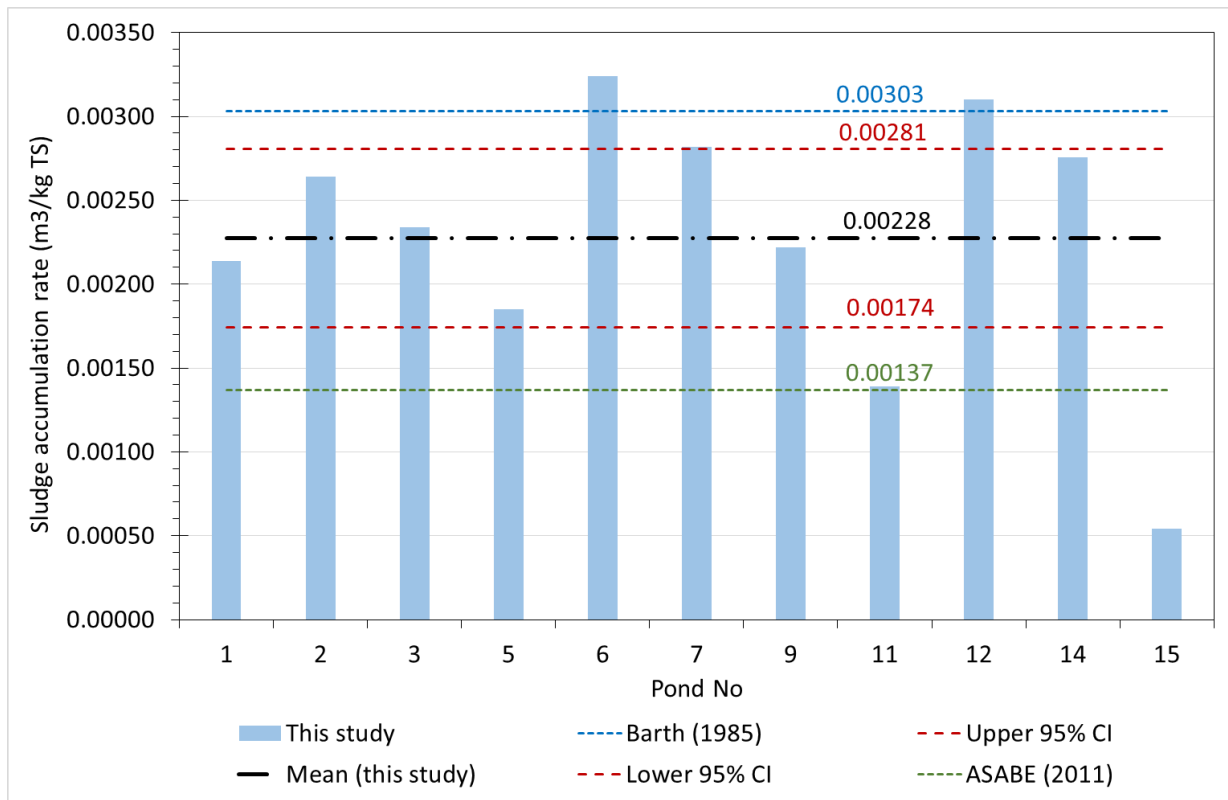


Figure 37 Estimated sludge accumulation rates in the eleven primary anaerobic ponds surveyed in this study. The mean and 95% confidence limits are shown on the graph along with the previous (Barth, 1985) and current (ASABE, 2011) standard values.

Another factor which may have influenced the sludge accumulation rate calculations is the possible increased carryover of sludge from primary anaerobic ponds to secondary ponds, as sludge levels in the primary ponds approached the full pond capacity. For example, the sludge level in pond 15 is noted as 72% (Tables 3 and 4); however, at the time of the survey, the pond overflow weir was set 0.4 m below the top water level, resulting in a sludge level of 82% of the effective pond capacity (up to the overflow weir level). While this pond had the lowest estimated sludge accumulation rate of

0.00054 m<sup>3</sup>/kg TS, this value may not have accounted for relatively high rates of sludge carryover into the secondary pond at the high sludge storage levels which have prevailed over recent years.

As noted in Section 3.2 of this report, Hamilton (2010) found that sludge accumulated more rapidly in a piggery effluent pond where some sludge was removed by effluent irrigation, compared to another unit where the sludge was left undisturbed. Most of the primary ponds included in this study overflowed by gravity into secondary ponds and effluent irrigation water was pumped from the secondary ponds. Pond 2 was an exception to this mode of operation. Effluent stored in this pond was transferred to a secondary pond by pumping from an approximately centrally located pontoon (Figure 38). While no precise measurements were taken, the pump suction line was probably drawing effluent from a depth of approximately 0.5 m below the effluent surface. At the time of the sludge survey, it was determined that this pond was 94% full of sludge and that the top of the sludge was practically at the effluent surface. This suggests that some sludge was being exported from the primary pond by the pumping operation; however, the degree of disturbance of the sludge layer would have been relatively minor compared to the disturbed pond studied by Hamilton (2010) where an agitator was sometimes used during effluent irrigation pumping operations to purposefully remove sludge from the pond. The sludge accumulation rate determined for pond 2 in the current study was 0.00264 m<sup>3</sup>/kg TS which is slightly higher than the average recorded for the eleven primary ponds.



*Figure 38 Pond 2 (Piggery A) showing the pontoon mounted pump used to transfer effluent to a secondary pond.*

Hamilton (2010) found that the sludge accumulation rate escalated when sludge accumulation approached 30% of the pond drawdown volume and following encroachment within 1.00 and 1.25 m

from the maximum drawdown level. In the current study, ten of the eleven primary ponds surveyed had sludge levels higher than 30% and several had sludge layers encroaching within 1 m from the effluent surface. The high sludge levels drastically increased the effective VS loading rates and decreased the HRTs. The resulting reduction in anaerobic treatment capacity is the most likely cause of higher sludge accumulation rates, although the carryover of sludge into secondary ponds may have moderated the measured sludge accumulation rates.

The current version of PigBal, which was used for estimating the TS entering the ponds, does not account for any TS in the recycled effluent used for shed flushing or recharging pull plug pits at some piggeries. This recycled effluent is typically drawn from a secondary effluent storage pond, having undergone anaerobic treatment in a primary pond, followed by further solids settling and facultative treatment in a secondary storage pond. Consequently, this recycled effluent is generally relatively stable, typically having a low TS concentration of approximately 0.5%. While the TS in the recycled flushing/recharge medium could theoretically contribute substantially to the TS loading entering a primary anaerobic pond (particularly in high flush piggeries), in reality it is likely to be relatively inert or unreactive, passing through the pond system without contributing substantially to sludge formation and deposition. Because sludge accumulation rates are expressed as a volume of sludge deposited per unit mass of TS entering the pond, the calculated sludge accumulation rates would be lower if the TS in the recycled flushing medium was included in the calculation. Consequently, it is considered to be more helpful to ignore the contribution to pond influent TS from recycled flushing medium, particularly for the design of new piggery ponds where flushing practices (volume/frequency) may change over time and the concentration of TS in the recycled effluent is unknown.

Table 3 Summary of piggery pond characteristics including the total solids (TS) loading rates and sludge accumulation times used to estimate the sludge accumulation rates.

Pond	Piggery ID	Unit description	Piggery capacity			Pond type	Total capacity (ML)	Sludge volume (ML)	Sludge % (%)	Accum. period (yr)	TS loading rate (kg TS/d)	Sludge accum. rate (m <sup>3</sup> . kg TS <sup>-1</sup> )
			(Sows)	(Pigs)	(SPU)							
1	A	Farrow to Finish	1,000	11,005	11,350	Primary	72.0	48.9	68%	15.0	4,170	0.00214
2	A	Gilts	0	980	1,679	Primary	7.2	6.8	95%	15.0	471	0.00264
3	A	Breeder	5,000	20,739	14,705	Primary	103.1	55.0	53%	15.0	4,293	0.00234
4	A	Grower/Finisher	0	38,239	48,064	Secondary	298.1	145.1	49%	15.0	19,210	0.00138
5	B	Grower/Finisher	0	4,704	6,350	Primary	43.4	20.8	48%	13.4	2,303	0.00185
6	C	Nursery (Weaners)	0	7,225	3,387	Primary	43.9	20.4	46%	19.0	908	0.00324
7	D	Farrow to Finish	1,500		16,000	Primary	67.6	57.1	84%	10.0	5,535	0.00282
8	D	Farrow to Finish	1,500		16,000	Secondary	9.5	7.5	79%	10.0	5,535	0.00037
9	E	Breeder	3,600	9,021	7,241	Primary	67.6	52.1	77%	20.0	3,216	0.00222
10	E	Breeder	3,600	9,021	7,241	Secondary	11.0	2.7	25%	20.0	3,216	0.00011
11	F	Farrow to Finish	1,200	12,246	12,054	Primary	50.8	35.9	71%	17.0	4,160	0.00139
12	G	Breeder	600	1,649	1,245	Primary	32.6	7.1	22%	14.0	448	0.00310
13	H	Breeder + Grower	3,100	19,810	18,546	Secondary	23.1	19.9	86%	6.5	6,111	0.00137
14	I	Breeder	2,600	6,473	5,195	Primary	26.7	21.6	81%	11.0	1,951	0.00276
15	J	Grower/Finisher	0	19,882	21,168	Primary	48.3	34.6	72%	24.0	7,264	0.00054
16	K	Breeder	4,500	12,973	9,527	Primary	8.5	5.0	59%		3,363	

Table 4 Summary of piggery pond characteristics including volatile solids (VS) loading rates and hydraulic retention times.

Pond	Piggery ID	Unit description	Piggery capacity			Pond type	Total capacity (ML)	Sludge volume (ML)	Sludge % (%)	Storage depth (m)	Batters (h/v)	Sludge accum. rate (m <sup>3</sup> /kg TS)	VS loading rate (kg VS. m <sup>-3</sup> . day <sup>-1</sup> )		Hydraulic retention time (days)	
			(Sows)	(Pigs)	(SPU)								Min <sup>a</sup>	Max <sup>b</sup>	Min <sup>c</sup>	Max <sup>d</sup>
1	A	Farrow to Finish	1,000	11,005	11,350	Primary	72.0	48.9	68%	8.0	4.0	0.00214	0.048	0.149	51	159
2	A	Gilts	0	980	1,679	Primary	7.2	6.8	94%	8.0	3.8 / 1.2	0.00264	0.054	1.018	6	117
3	A	Breeder	5,000	20,739	14,705	Primary	103.1	54.9	53%	8.0	4.0	0.00234	0.034	0.073	224	480
4	A	Grower/Finisher	0	38,239	48,064	Secondary	298.1	145.2	49%	10.0	4.0	0.00138				
5	B	Grower/Finisher	0	4,704	6,350	Primary	43.4	20.8	48%	6.7	4.0	0.00185	0.044	0.084	279	537
6	C	Nursery (Weaners)	0	7,225	3,387	Primary	43.9	20.4	46%	11.4	3.0	0.00324	0.017	0.032	54	102
7	D	Farrow to Finish	1,500		16,000	Primary	67.6	57.1	84%	5.5	4.0	0.00282	0.069	0.438	38	244
8	D	Farrow to Finish	1,500		16,000	Secondary	9.5	7.5	79%	3.5	4.0	0.00037				
9	E	Breeder	3,600	9,021	7,241	Primary	67.6	52.1	77%	5.5	4.0	0.00222	0.039	0.171	45	198
10	E	Breeder	3,600	9,021	7,241	Secondary	11.0	2.7	25%	4.0	3.6	0.00011				
11	F	Farrow to Finish	1,200	12,246	12,054	Primary	50.8	35.9	71%	6.0	3.0	0.00139	0.066	0.226	63	214
12	G	Breeder	600	1,649	1,245	Primary	32.6	7.1	22%	5.5	3.0	0.00310	0.011	0.014	1,542	1,972
13	H	Breeder + Grower	3,100	19,810	18,546	Secondary	23.1	19.8	86%	5.3	3.0	0.00137				
14	I	Breeder	2,600	6,473	5,195	Primary	26.7	21.6	81%	5.0	3.0	0.00276	0.058	0.223	17	65
15	J	Grower/Finisher	0	19,882	21,168	Primary	48.3	34.6	72%	5.4	varies	0.00054	0.127	0.442	22	76
16	K	Breeder	4,500	12,973	9,527	CAP	8.5	5.0	59%	3.0	2.5		0.319	0.784	3	7

<sup>a</sup> The minimum VS loading rates are based on the full pond capacities, prior to any sludge accumulation.

<sup>b</sup> The maximum VS loading rates are based on the reduced pond active capacities, estimated at the time of the sludge surveys.

<sup>c</sup> The minimum hydraulic retention times are based on the reduced pond active capacities, estimated at the time of the sludge surveys.

<sup>d</sup> The maximum hydraulic retention times are based on the full pond capacities, prior to any sludge accumulation.

### 5.3 Sampled sludge, supernatant and effluent analysis results

Figures 39 to 53 summarise the results of the various analyses carried out on the sludge, supernatant and effluent samples collected from ponds 2, 5, 7 and 16.

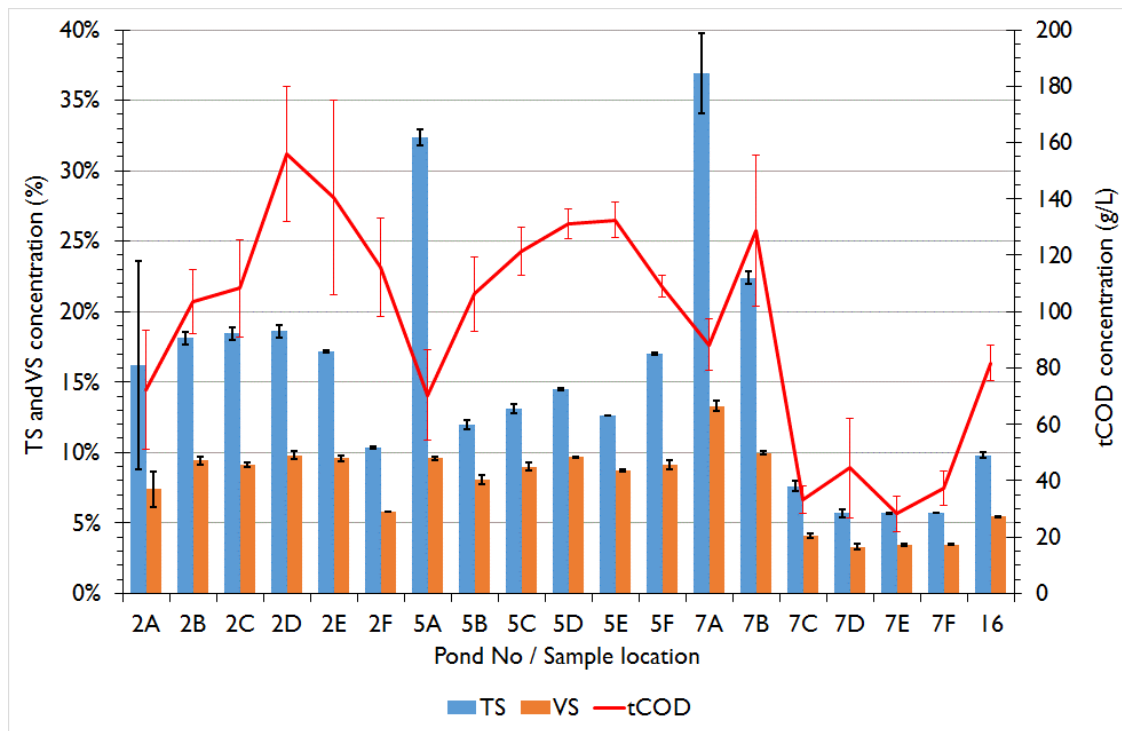


Figure 39 Sludge TS, VS and tCOD analysis results.

The sludge TS and VS values ranged from 6% to 37% and 3% to 13%, with mean  $\pm$  95% confidence interval (CI) values of  $15.5 \pm 4.0\%$  and  $7.8 \pm 1.3\%$ , respectively (Figure 39). The highest TS concentrations (32% and 37%) were recorded for samples 5A and 7A, respectively, which were collected near the shed effluent discharge points in ponds 5 and 7. These samples had a relatively 'gritty' texture, reflecting their high fixed solids (FS = TS – VS) or ash concentrations, apparently resulting from the settling of relatively heavy, inorganic solids, near the pond entry point. The COD values ranged from 28 to 156 g/L; the lower values being recorded for the samples collected near the pond inlets (2A, 5A and 7A). These low COD values are also consistent with the higher FS concentrations occurring near these sampling points.

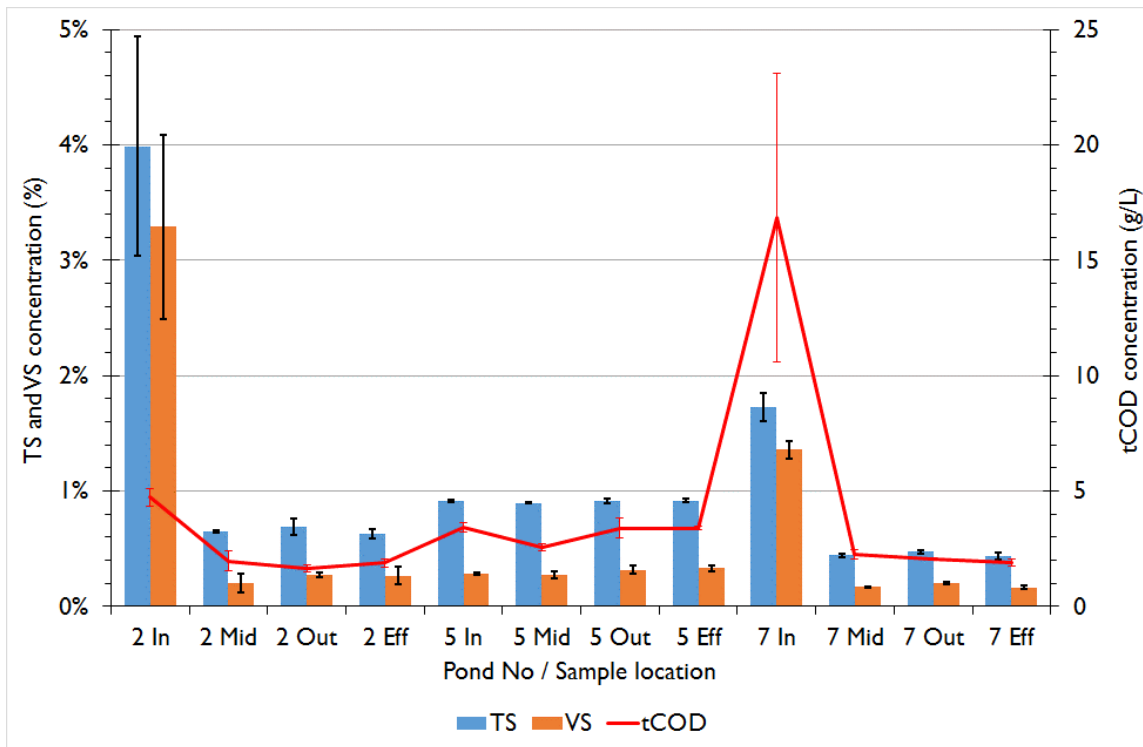


Figure 40 Supernatant and effluent TS, VS and tCOD analysis results.

The supernatant and pond effluent TS and VS values ranged from 0.44 to 3.99% and 0.17 to 3.29%, with mean  $\pm$  95% CI values of  $1.1 \pm 0.6\%$  and  $0.6 \pm 0.6\%$ , respectively (Figure 40). The highest values were observed for samples collected near the pond 2 and 7 inlets. This reflects the relatively raw nature of the pond supernatant at these points, before it undergoes effective mixing and anaerobic decomposition/treatment. The highest COD value was observed for the sample collected near the pond 7 inlet, once again demonstrating limited mixing and treatment at this sampling point. There appears to be little difference between the TS, VS and COD values recorded for the supernatant samples collected near the middle of the pond and near the pond outlet and the pond effluent samples, for each of the three ponds. This suggests that the shed effluent has undergone effective mixing and treatment at these sampling points and that supernatant is relatively homogenous (at least in terms of its TS, VS and COD composition) over the majority of the pond area.



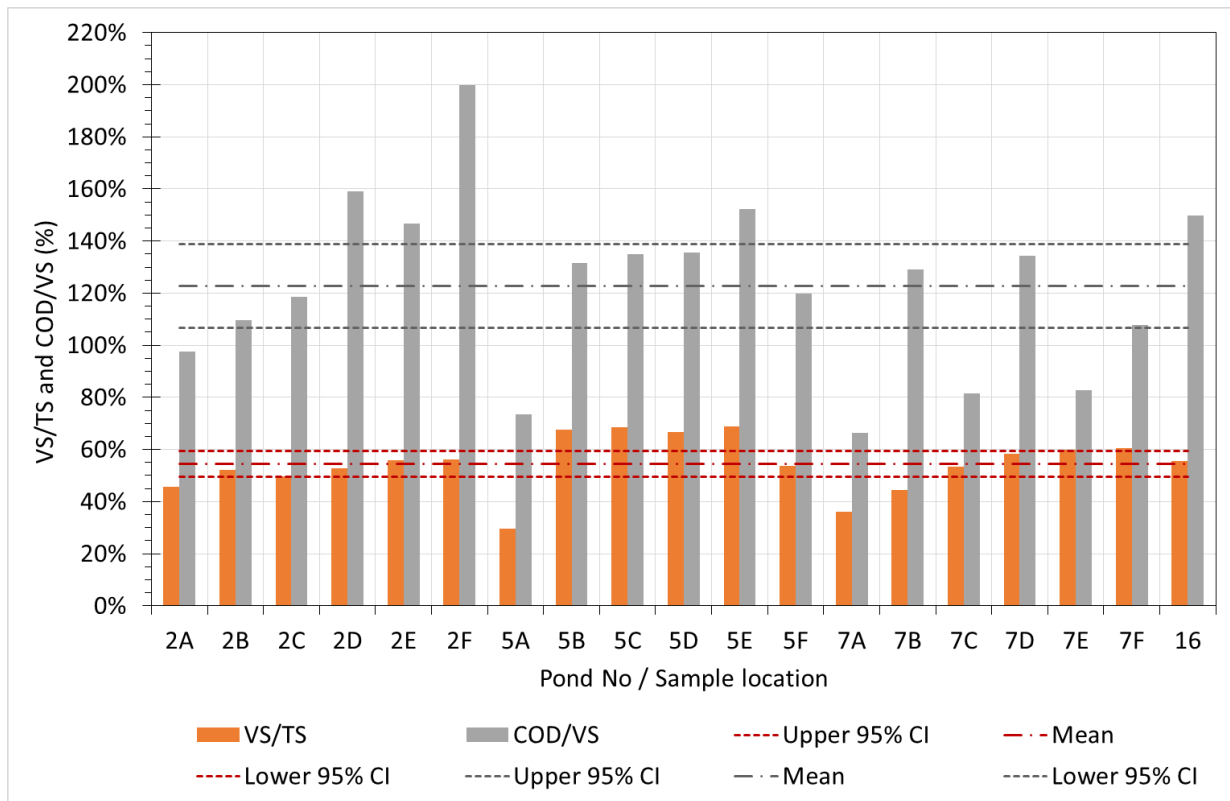


Figure 41 Sludge VS/TS and COD/VS analysis results.

The sludge VS/TS results ranged from 30% to 69%, with a mean  $\pm$  95% CI value of  $54 \pm 5\%$  (Figure 41). Excluding the results for samples 2A, 5A and 7A, which were collected near the pond inlets, the mean VS/TS ratio increased to  $58 \pm 4\%$ . These results are consistent with the findings of O’Keefe et al. (2013) and DAF (unpublished) who reported mean sludge VS/TS results of 60% for four Australian piggeries, and 55% for nine primary and single piggery ponds in southern Queensland, respectively.

VS/TS ratios of the piggery sludge provide an indication of the breakdown of VS that has occurred in the sludge. Assuming a VS/TS ratio of 0.85 for raw manure entering the pond and that the majority of the FS component of the manure settled in the sludge, the amount of VS degradation can be estimated (O’Keefe et al., 2013). For the range of sludge VS/TS ratios measured in the current study (30 to 69%), the estimated range of VS degradation is 61% to 92%. This indicates that the sludge samples were well degraded with only the highly indigestible lignin and similar components of the VS remaining in the sludge samples (O’Keefe et al., 2013).

The COD/VS ratios ranged from 66% to 200% with a mean  $\pm$  95% CI value of  $123 \pm 16\%$ . Relatively low values were recorded for the sludge samples collected near the pond inlets (samples 2A, 5A and 7A). As a general rule, high COD/VS ratios indicate higher concentrations of higher-energy organic compounds such as proteins, fats or at least “longer” chain fatty acids. Lower COD/VS ratios generally indicate higher concentrations of lower energy carbohydrates.

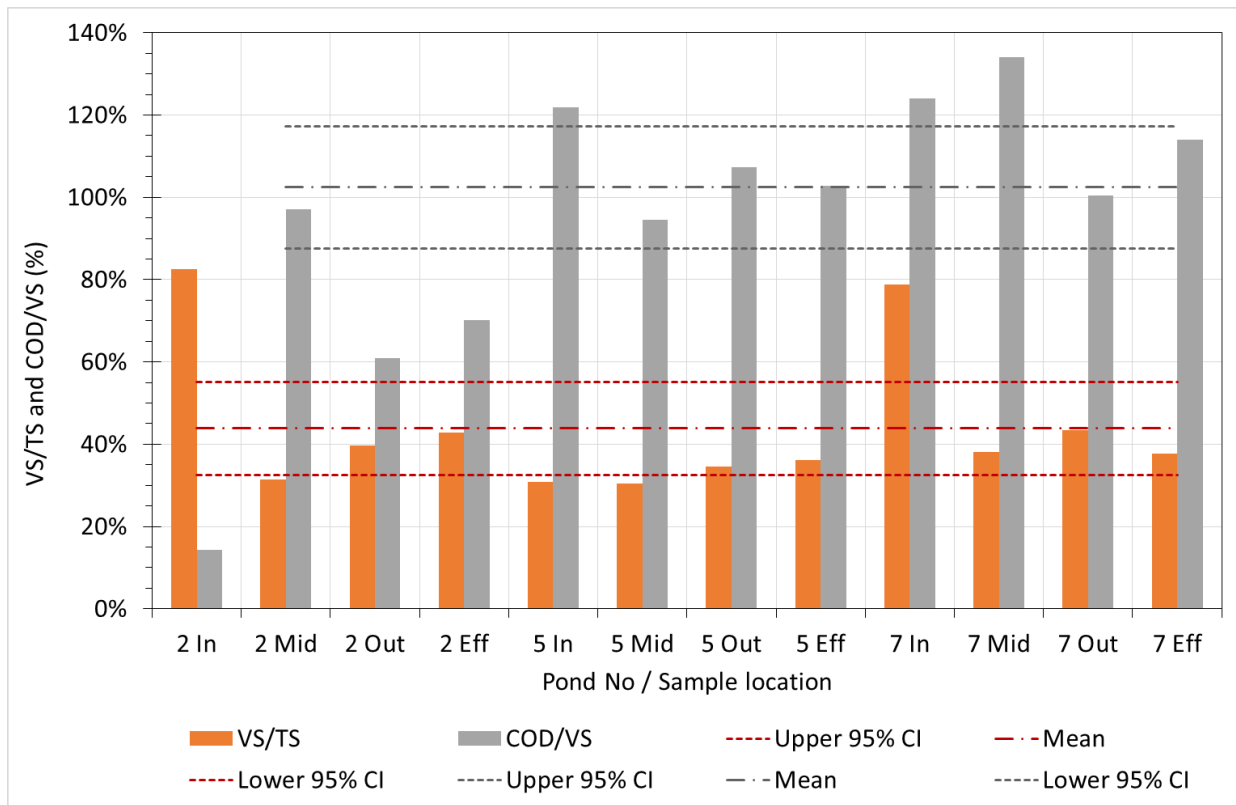


Figure 42 Supernatant and effluent VS/TS and COD/VS analysis results. (The COD/VS result for '2 In' (14%) appears to be an anomaly and has been omitted from the mean and CI calculations).

The supernatant and pond effluent VS/TS ratios ranged from 30% to 82%, with a mean  $\pm$  95% CI value of  $44 \pm 11\%$  (Figure 42). The highest values were recorded for samples collected near the inlets of ponds 2 and 7. These high values indicated ineffective mixing and treatment of the incoming solids at these locations. The average VS/TS ratio for the other samples was 36% which indicates a relatively high level of VS breakdown.

The COD/VS ratio recorded for the sample collected near the pond 2 inlet appeared to be an anomaly and was not included in subsequent data analyses. The range of COD/VS ratios recorded for all other samples was 61% to 134%, with a mean  $\pm$  95% CI value of  $102 \pm 15\%$ .

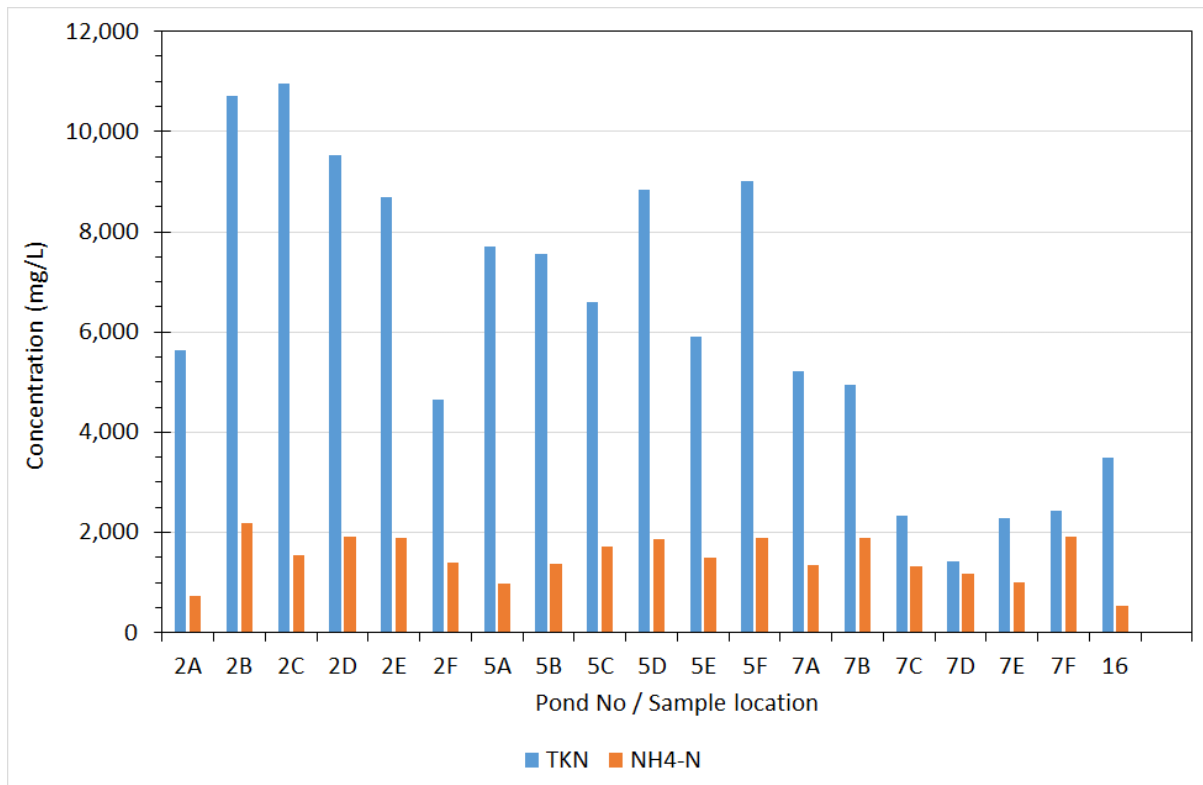


Figure 43 Sludge TKN and NH<sub>4</sub>-N analyses results.

The sludge TKN results ranged from 1,417 to 10,960 mg/L with a mean  $\pm$  95% CI value of  $6,206 \pm 1434$  mg/L. These results are lower than the DAF (unpublished) results reported by Tucker (2018) which had a mean value of 34,311 mg/L. The sludge NH<sub>4</sub>-N values ranged from 535 to 2,184 mg/L with a mean  $\pm$  95% CI value of  $1,485 \pm 217$  mg/L. This value was also lower than the DAF mean value of 2,532 mg/L. On average, the NH<sub>4</sub>-N accounted for  $31 \pm 10\%$  of the TKN. The remaining portion of the TKN would have been organic-N, with negligible nitrate or nitrite-N.

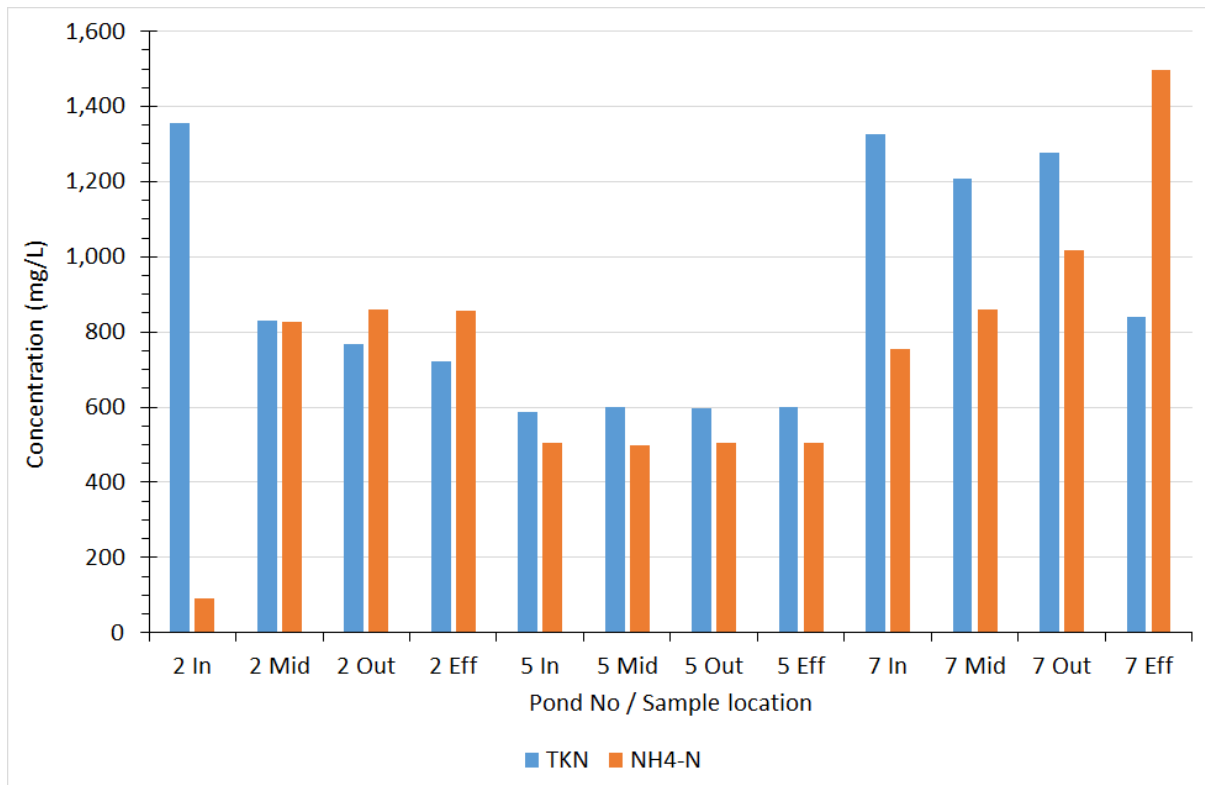


Figure 44 Supernatant and effluent TKN and NH<sub>4</sub>-N analyses results.

Some inaccuracies are evident in the supernatant and effluent TKN and NH<sub>4</sub>-N analysis results which indicate higher NH<sub>4</sub>-N concentrations than the TKN concentrations for some samples (2 Out, 2 Eff and 7 Eff). This is clearly not practically possible. The most likely explanation for these discrepancies is the considerable dilution required for the FIA analyses carried out at the AVMC laboratory which is primarily set up for analysing more dilute municipal wastewater.

The supernatant and effluent TKN values ranged from 587 to 1,357 mg/L with a mean value of  $893 \pm 197$  mg/L. These values are comparable to the DAF data published by Tucker (2018). The supernatant and effluent NH<sub>4</sub>-N values ranged from 91 to 1,496 mg/L with a mean value of  $731 \pm 222$  mg/L. These values are considerably higher than the DAF data which had a mean value of 144 mg/L. Differences in diets or ammonia volatilisation may account for the observed variations.

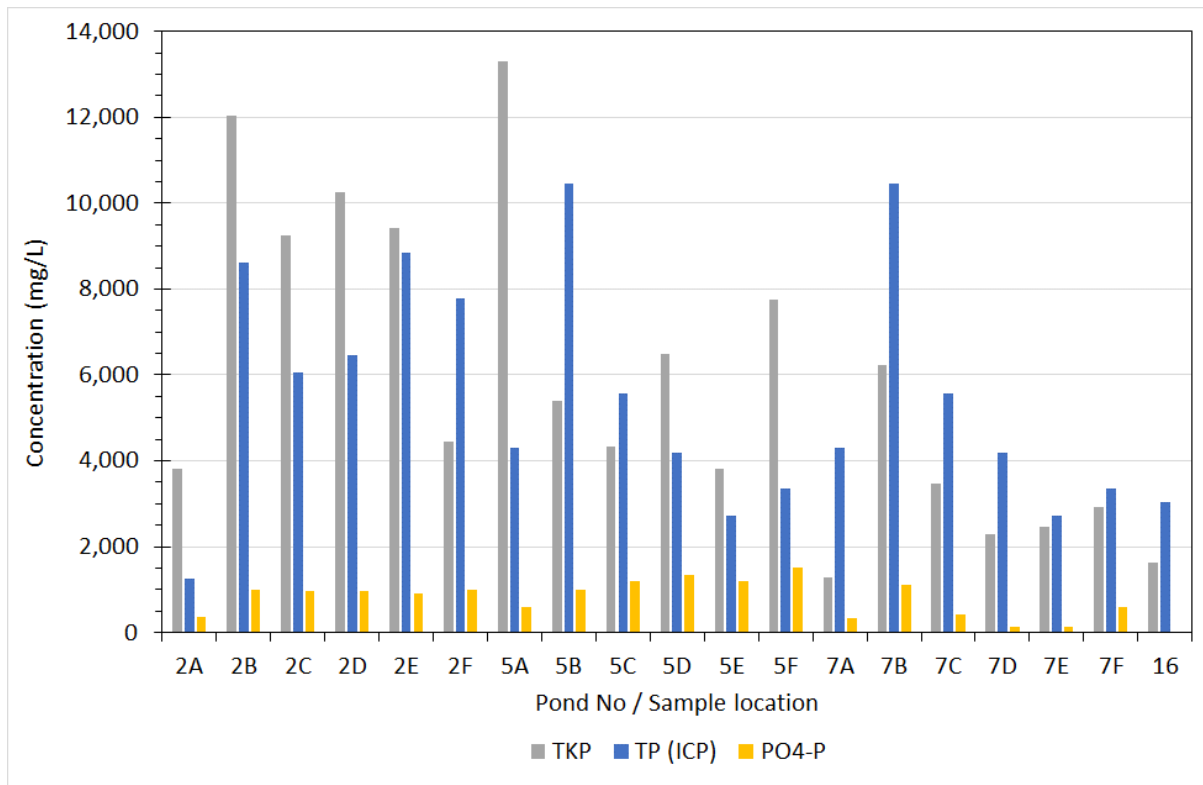


Figure 45 Sludge TKP, TP (ICP) and PO<sub>4</sub>-P analysis results.

There are some obvious inaccuracies in the sludge TKP and TP (ICP) analysis results (Figure 45) which should be approximately equal but differ considerably for some samples (e.g. 5A, 5B, 5F and 7B). As noted previously, the most likely explanation for these discrepancies is the considerable dilution required for the TKP (FIA) analyses carried out at the AVMC laboratory which is primarily set up for analysing more dilute municipal wastewater. For this reason, it is hypothesised that the TP (ICP) analyses are likely to be more accurate.

The TP (ICP) values range from 1,267 to 10,499 mg/L, with an average value of  $5,430 \pm 1,303$  mg/L. These values are generally lower than the DAF data reported by Tucker (2018) which had a mean value of 47,000 mg/L. On average, PO<sub>4</sub>-P accounted for  $16 \pm 6\%$  of the TP (ICP).

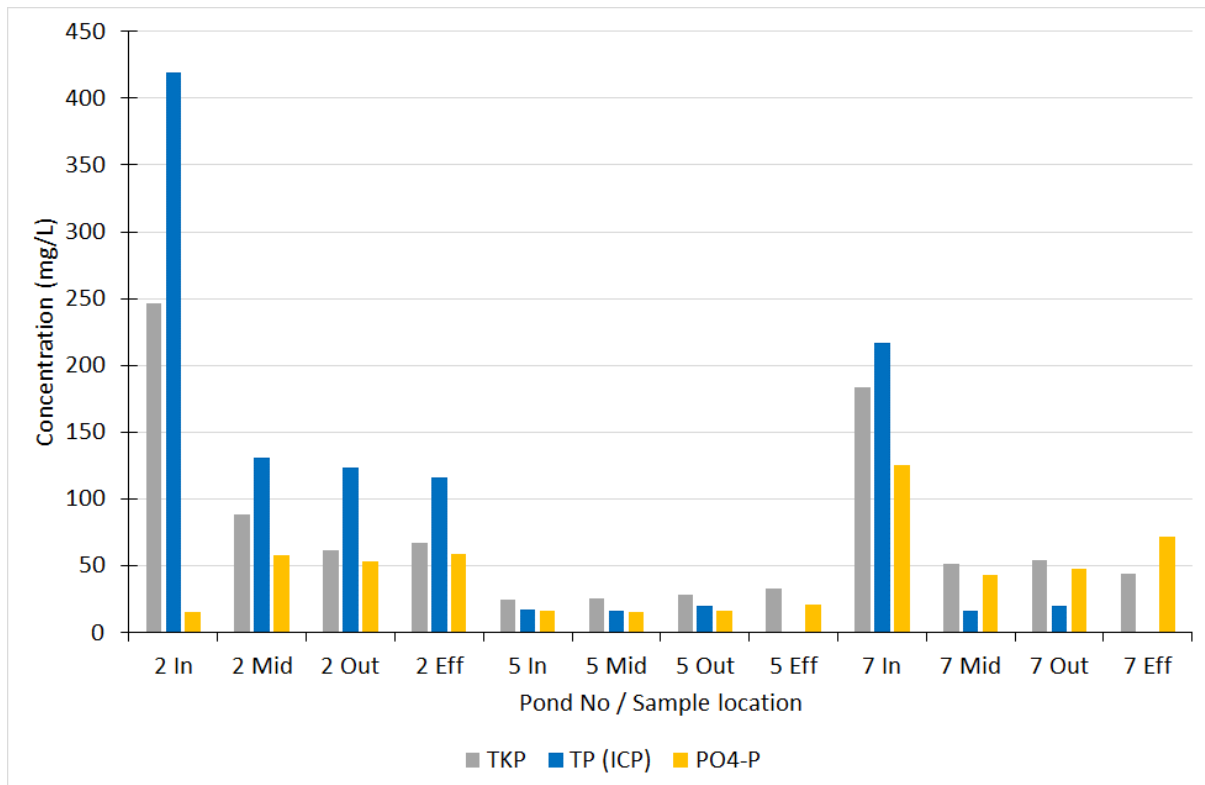


Figure 46 Supernatant and effluent TKP, TP (ICP) and PO<sub>4</sub>-P analysis results.

As noted for the sludge analyses, similar discrepancies between the TKP and TP (ICP) results were observed for the supernatant and effluent analysis results. Further discrepancies were observed between the TP (ICP) and PO<sub>4</sub>-P results for the 5 Eff, 7 Mid, 7 Out and 7 Eff samples for which the reported PO<sub>4</sub>-P concentrations exceeded the TP (ICP) concentrations. In these cases, the TKP results appear to be more accurate.

The TP concentrations in the supernatant and effluent samples were substantially lower than the values recorded for the sludge. The supernatant and effluent TP (ICP) values ranged from 0 to 419 mg/L, with a mean value of  $91 \pm 79$  mg/L. This mean value is approximately one sixtieth of the mean TP (ICP) value recorded for the sludge.

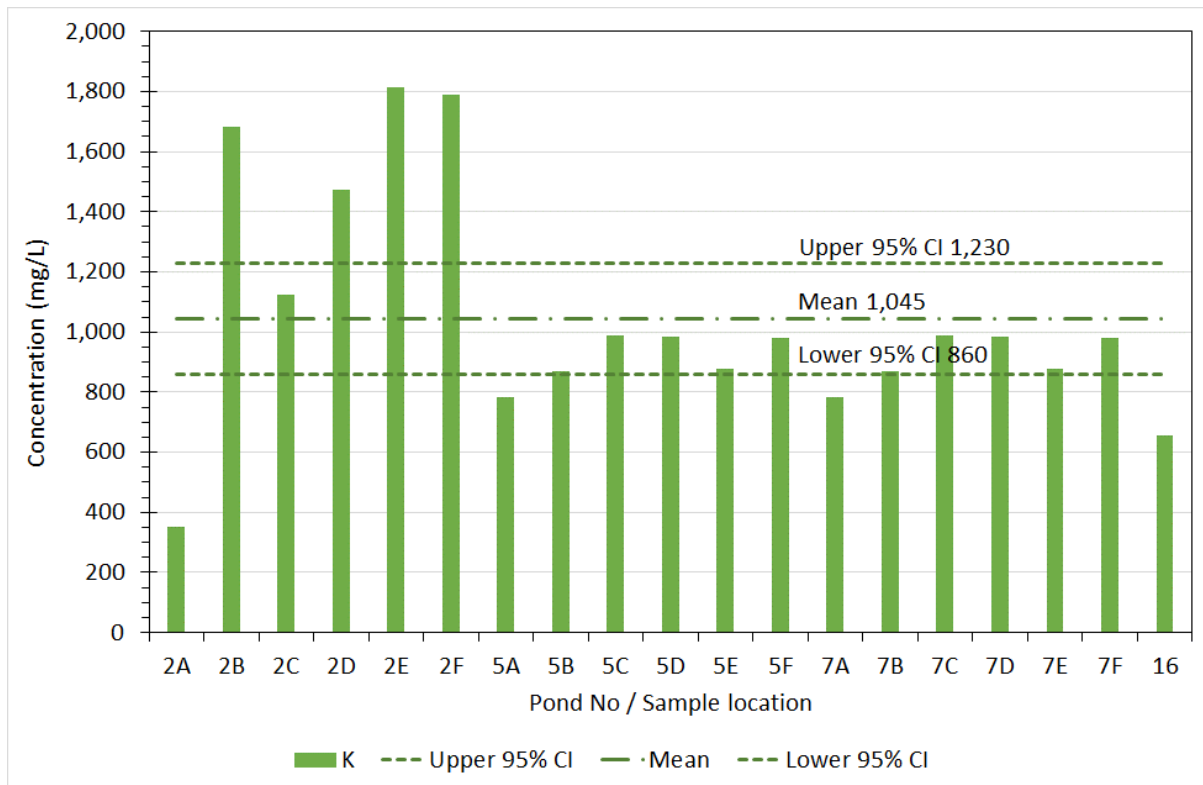


Figure 47 Sludge K (ICP) analysis results.

The sludge potassium (K) concentrations ranged from 352 to 1,816 mg/L, with a mean value of 1,045 ± 185 mg/L (Figure 47). This is considerably lower than the mean value recorded by DAF (7,478 mg/L), as reported by Tucker (2018). The sludge K concentrations recorded for pond 2 were substantially higher than the values recorded for ponds 5, 7 and 16, which were all relatively similar. These differences between ponds could possibly be attributed to different piggery drinking and flushing water sources and/or dietary variations.

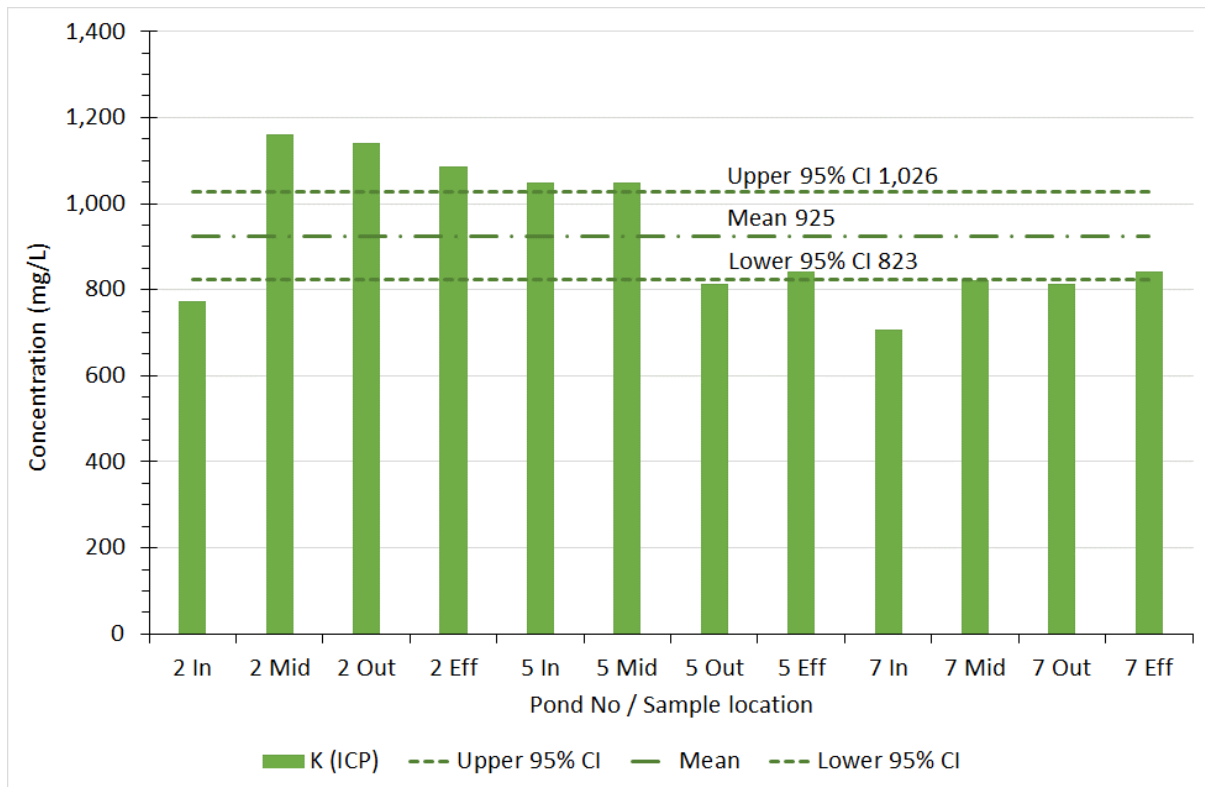


Figure 48 Supernatant and effluent K (ICP) analysis results.

The supernatant and effluent K concentrations were reasonably uniform for the three ponds, having a range from 772 to 1,161 mg/L, with a mean value of  $925 \pm 101$  mg/L. Similarly to the sludge samples, pond 2 recorded generally higher effluent K concentrations.



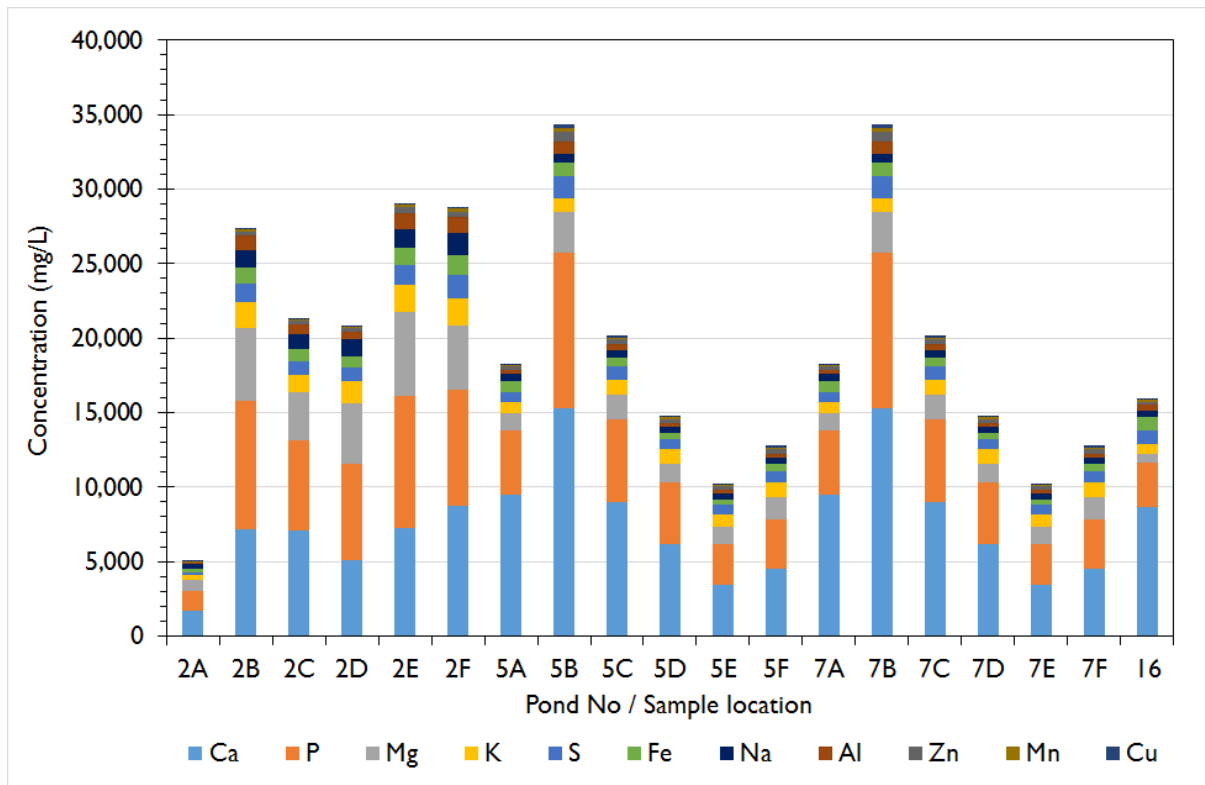


Figure 49 Stacked bar graph showing the concentrations of the eleven most abundant cations determined by ICP analysis for the sludge samples.

Figure 49 shows the concentrations of the eleven most abundant cations determined by the ICP analyses for the sludge samples. The cations concentrations are shown in decreasing order of abundance, with the most abundant cation (Ca) plotted closest to the x-axis for each of the stacked bars.

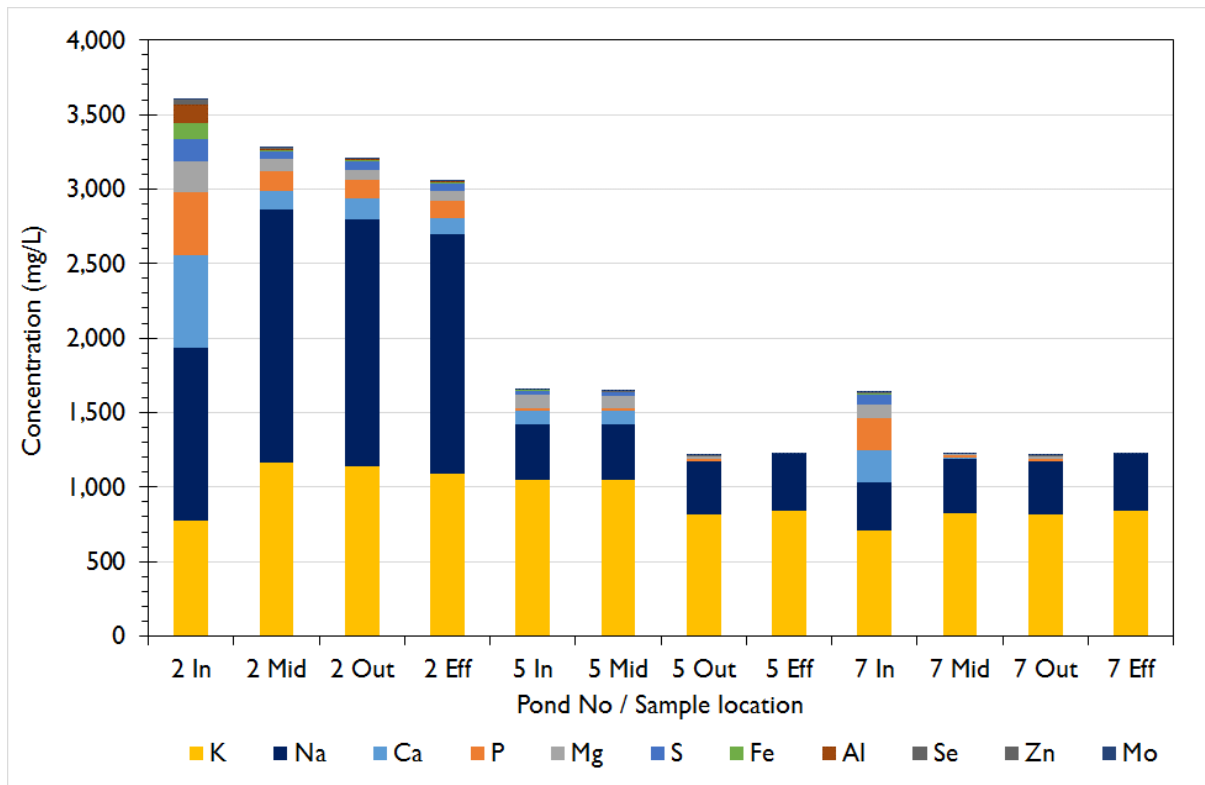


Figure 50 Stacked bar graph showing the concentrations of the eleven most abundant cations in the supernatant and effluent samples, determined by ICP analysis.

Figure 50 shows the concentrations of the eleven most abundant cations determined by the ICP analyses for the supernatant and effluent samples. The cations concentrations are shown in decreasing order of abundance, with the most abundant cation (K) plotted closest to the x-axis for each of the stacked bars. While the K concentrations are relatively uniform across all samples, the Na concentrations are consistently higher for the pond 2 samples. The total and individual cation concentrations in the supernatant and effluent are substantially lower than the values recorded for the sludge.

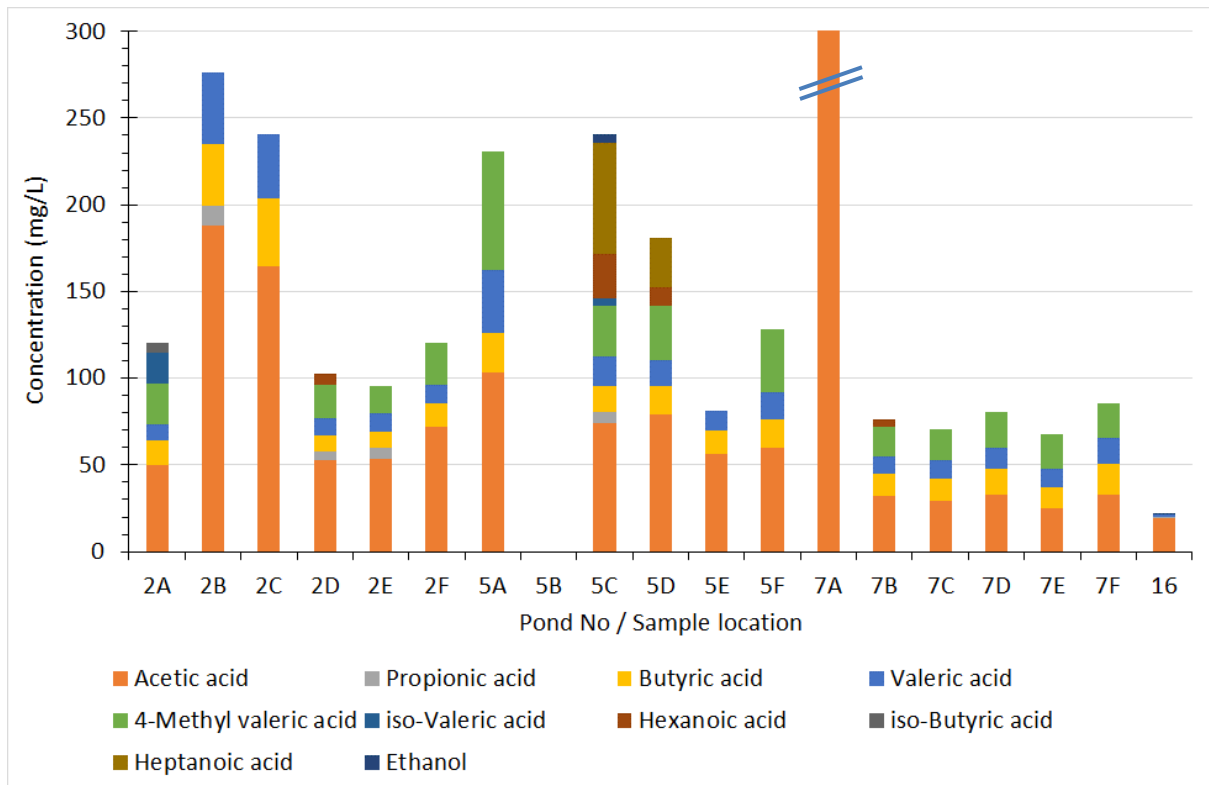


Figure 51 Stacked bar graph showing concentrations of various VFAs in the sludge samples. The bar representing sample '7A' has been truncated for scaling reasons (Total VFAs = 12,320 mg/L).

Figure 51 is a stacked bar graph showing the concentrations of VFAs in the sludge samples. Acetic acid is by far the most abundant VFA measured in these analyses. The concentration of VFAs in sample 7A, collected near the pond inlet, is extremely high in comparison to all other samples. This reflects the incomplete anaerobic digestion of the organic material in the sludge at this point.

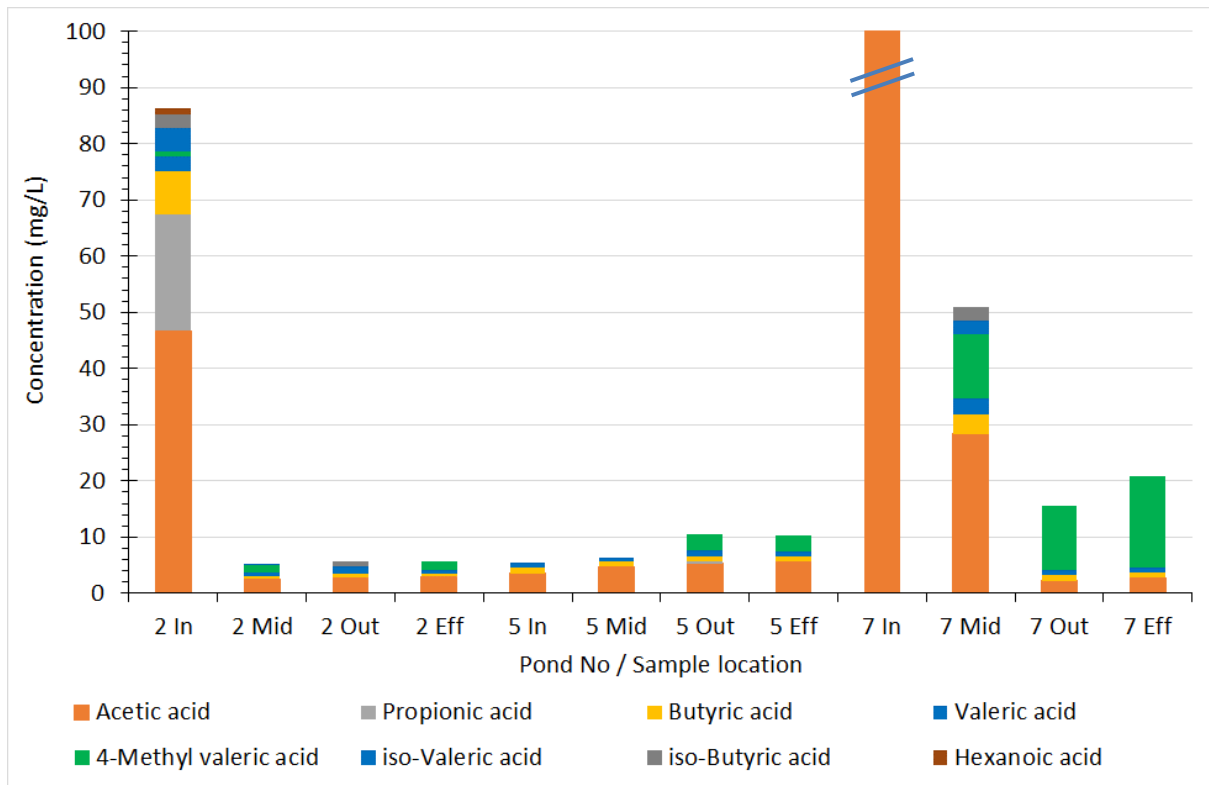


Figure 52 Stacked bar graph showing concentrations of various VFAs in the supernatant and effluent samples. The bar for sample '7 In' has been truncated for scaling reasons (Total VFAs = 2173 mg/L).

Figure 52 is a stacked bar graph showing the concentrations of VFAs in the supernatant and effluent samples. Similarly to the sludge samples, acetic acid is by far the most abundant VFA measured in these analyses and the concentration of VFAs in sample 7In, collected near the pond inlet, is also extremely high in comparison to all other samples.

Figure 53 is an example of the cumulative  $\text{CH}_4$  production data, plotted against time, derived from the triplicate AMPTS II analyses carried out on sludge sample 2F. The simple first-order kinetic curves (Equation 1) fitted to the AMPTS data are also plotted on this graph for each of the three replicate analyses. The average values of  $B_o$  (methane yield) and  $k_{\text{hyd}}$  (rate coefficient) (refer to Section 4.6) are shown in Table 5 for each of the ten sludge samples. These results show a high degree of variability between the  $B_o$  and  $k_{\text{hyd}}$  values for several of the triplicate samples. This variability is likely to be due to the low magnitudes of the sludge  $B_o$  values in comparison to substrates such as the raw piggery shed effluent which typically has  $B_o$  values from 300 to 400  $\text{NmL CH}_4/\text{g VS}$ .

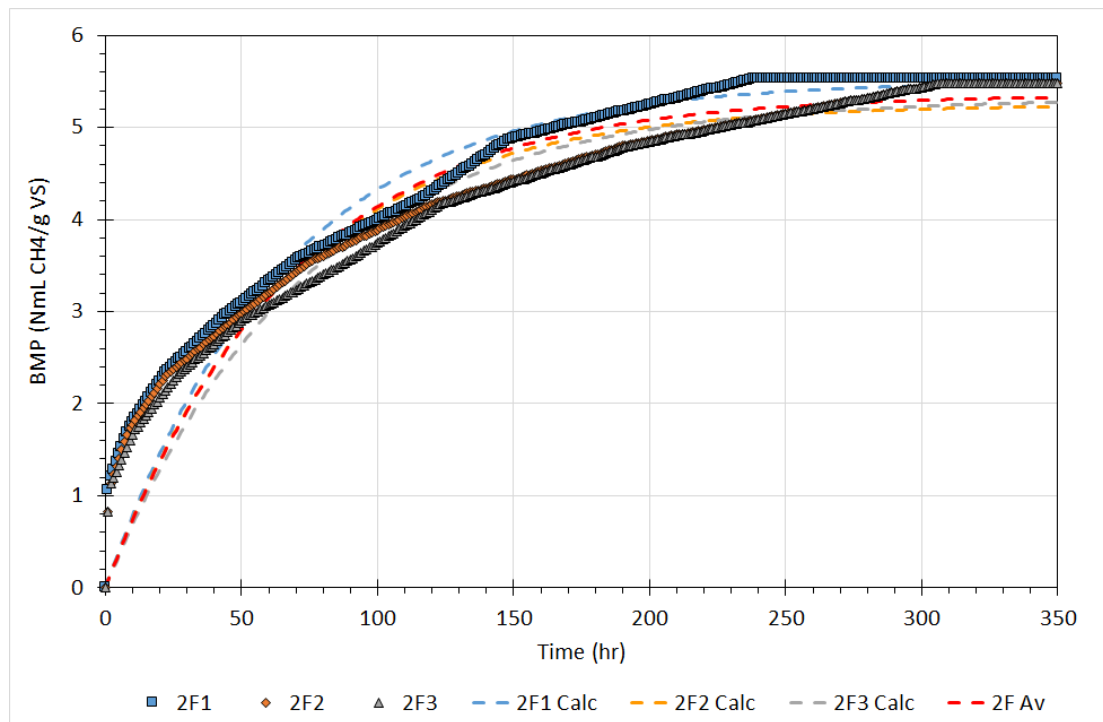


Figure 53 Cumulative  $\text{CH}_4$  production data plotted against time, derived from the triplicate AMPTS II analyses carried out on sludge samples collected from sampling location F on pond 2.

Table 5 Mean  $B_o$  and  $k_{\text{hyd}}$  values and 95% confidence intervals determined by fitting curves to the BMP analysis results.

Pond No / Sampling location	$B_o(\text{NmL CH}_4/\text{g VS})$	$k_{\text{hyd}}(\text{day}^{-1})$
2A	70.382 ± 62.574	0.141 ± 0.075
2D	3.177 ± 1.897	3.643 ± 8.612
2F	5.357 ± 0.330	0.356 ± 0.054
5A	1.663 ± 0.025	4.683 ± 0.103
5D	5.173 ± 1.846	0.234 ± 0.113
5F	3.427 ± 2.286	0.335 ± 0.346
7A	121.076 ± 22.452	0.100 ± 0.000
7D	12.298 ± 6.628	0.217 ± 0.355
7F	12.567 ± 10.175	0.174 ± 0.355
16	16.392 ± 11.906	0.125 ± 0.131

## 5.4 Hydrodynamic modelling results

### 5.4.1 2D Flow Simulation

Streamlines for 2D simulations for each of the four cases are shown in Figure 54. Streamlines represent the high probability dominant flow directions in which the fluid typically travels at a steady state. Images represent a two-dimensional horizontal cross-section (top view) of each pond at inlet height. The inlet positions are set at 10 m along the y-axis (0, 10) and outlets are in the lower right corner ( $x_{\max}$ , 0). The 2D simulations show the behaviour of a slow-moving vortex in which the bulk of the fluid circulates anticlockwise around a central dead zone (i.e. inactive zone with stagnant fluid), located in the centre of the pond structure in all cases except Pond 5. Pond 5 also shows a much larger central dead zone spanning roughly 1600 m<sup>2</sup> area. Furthermore, each pond shows a separate, much smaller vortex occurring in the immediate post-inlet area. This zone is representative of a post-inlet recirculation zone, in which high-velocity fluid from the inlet impacts into the otherwise low-velocity bulk volume, causing turbulence and back-mixing within a small area.

The same flow patterns are seen in the non-dimensional velocity contours in Figure 55. Velocities are at maximum in the stream from inlet and remain higher than 50% of maximum throughout the recirculation vortex. Similarly, the main vortexes in each pond show increased velocities, but not as high as those at recirculation. The minimum velocity areas match closely to the dead zones shown in Figure 54, either in the vortex centre or in areas not populated with streamlines.

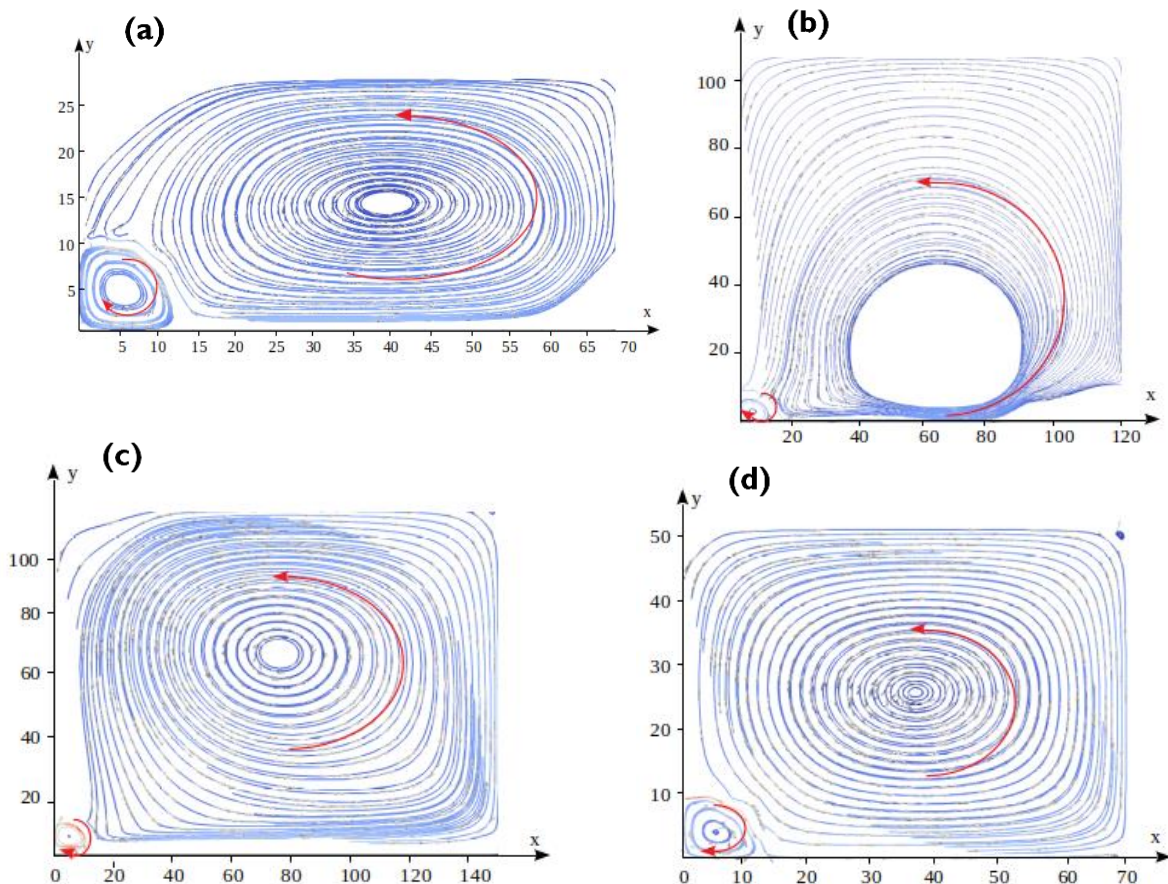


Figure 54 Top-view (i.e. x-y plane) of the streamlines for 2D single-phase models of Pond (a) 2, (b) 5, (c) 7 and (d) 16. Note that the unit of the x and y axis' are in m.

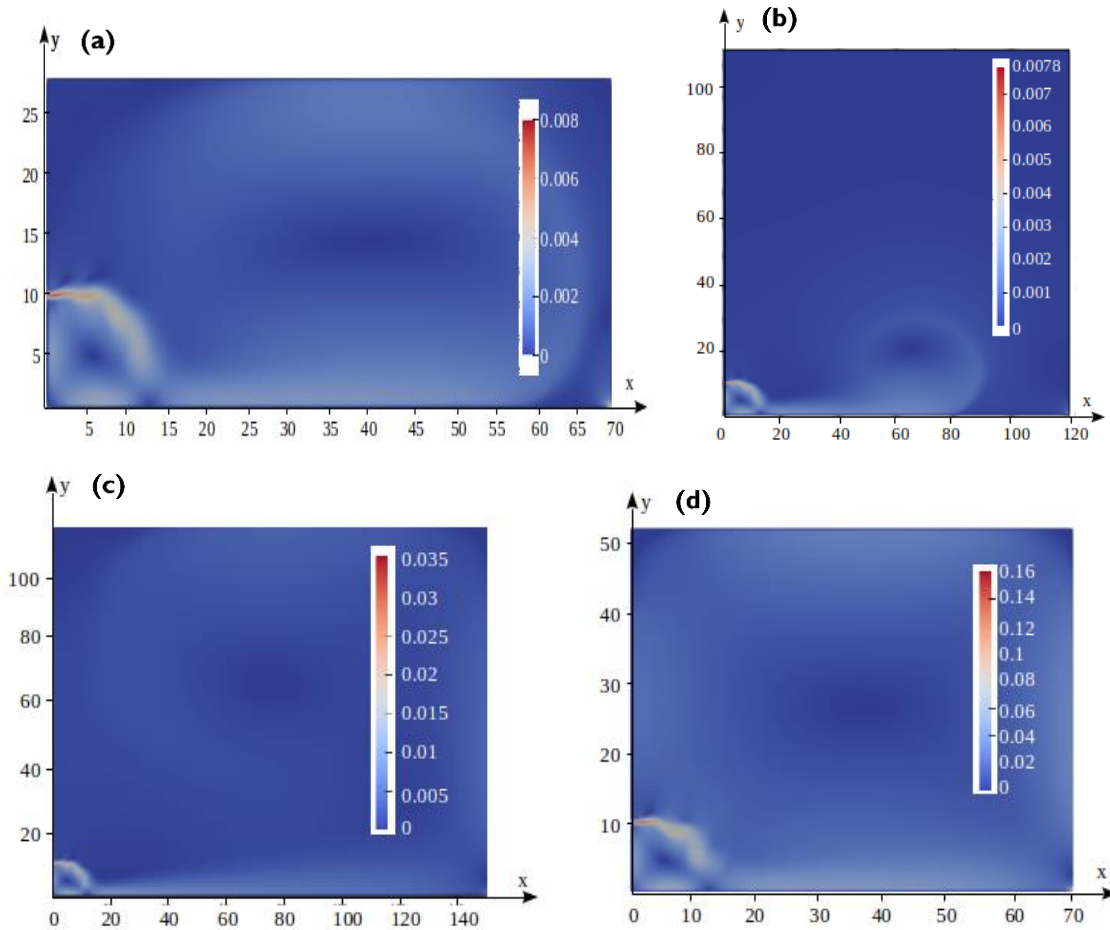


Figure 55 Non-dimensional velocity contours for 2D single-phase models of Pond (a) 2, (b) 5, (c) 7 and (d) 16. Note that the unit of the velocity magnitude is in m/s whereas the x- and y-axis are in m.

#### 5.4.2 3D Single-Phase Flow Simulation

The streamlines and the velocity contours at the surface of each pond, i.e. x-y plane, simulated in the 3D model are shown in Figures 56 and 57, respectively; whereas, the velocity contours at the longitudinal view, i.e. x-z plane, are shown in Figure 58. Note that the origin of the axis, i.e.  $x = y = z = 0$ , is taken at the bottom of the ponds due to better numerical representation of the results. In addition, it is worth mentioning that, unless otherwise stated, the results of the streamlines as well as the velocity contours are visualised at the horizontal (x-y plane) and longitudinal (x-z) planes since these give the overall three-dimensional evaluation of the flows. The streamlines show similar behaviour to the 2D cases, with a large vortex comprising the majority of the pond volume and a smaller vortex in the post-inlet area. Furthermore, pond 16 shows a third small vortex in the outlet vicinity. The 3D top-view velocity contours show noticeably lower velocities throughout each pond in contrast to their 2D counterparts (see Figure 54). The expanded volume with the inclusion of depth causes much of the fluid flow to dissipate and fill the larger volume. However, the faint outlines of higher velocities can still be seen in the shape of the vortices demonstrated in Figure 57. The side-view contours show how the fluid flows along the length of each pond. As expected, the fluid enters at maximal velocity, then dissipates to lower velocities in the immediate reaches beyond inlet. The velocity scales are very different, with Ponds 2 and 5 being comparable, Pond 7 being an order of magnitude higher, and Pond 16 being an order of magnitude higher than this. Therefore, the deeper pond has a reduced surface velocity for a given HRT. The long HRT pond, Pond 5, has the largest

stagnant zone. The bulk of each pond is at low velocity, indicating good velocity dissipation. However, Pond 5 shows higher velocity flow until about one third of the length of the pond (~40m) as a result of the much higher HRT.

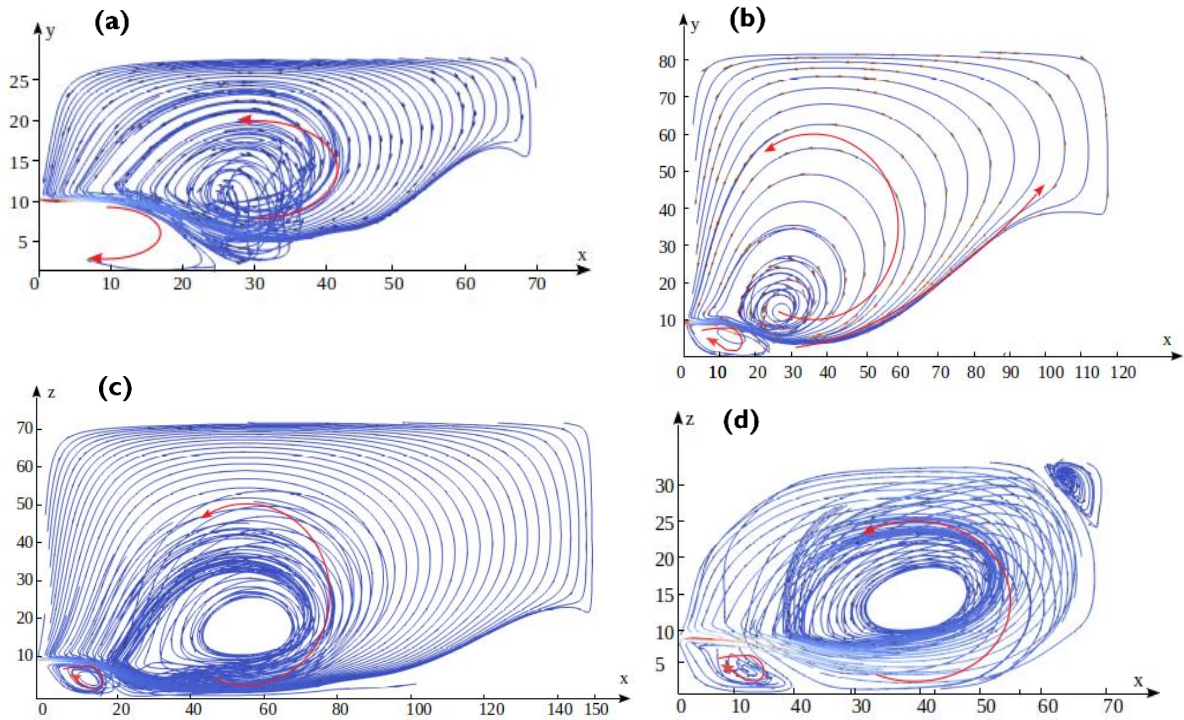


Figure 56 Top-view (i.e. x-y plane) of the streamlines for 3D single-phase models of Pond (a) 2, (b) 5, (c) 7 and (d) 16. Note that the origin of the axis,  $x = y = z = 0$ , is taken at the bottom of the ponds. Here, x-y planes correspond to the top-surfaces of the ponds.

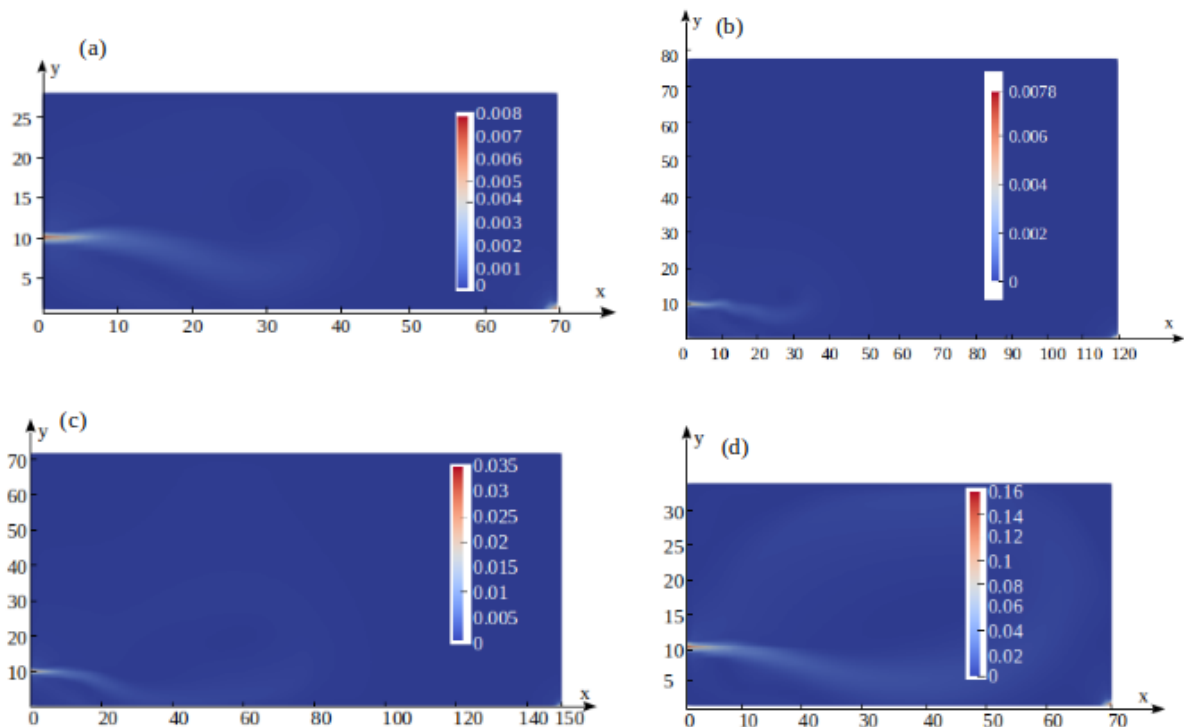


Figure 57 Top-view (i.e. x-y plane) of the non-dimensional velocity contours for 3D single-phase models of Pond (a) 2, (b) 5, (c) 7 and (d) 16. Note that the origin of the axis,  $x = y = z = 0$ , is taken at the bottom of the ponds. Here, x-y plane corresponds to the top-surfaces of the ponds.



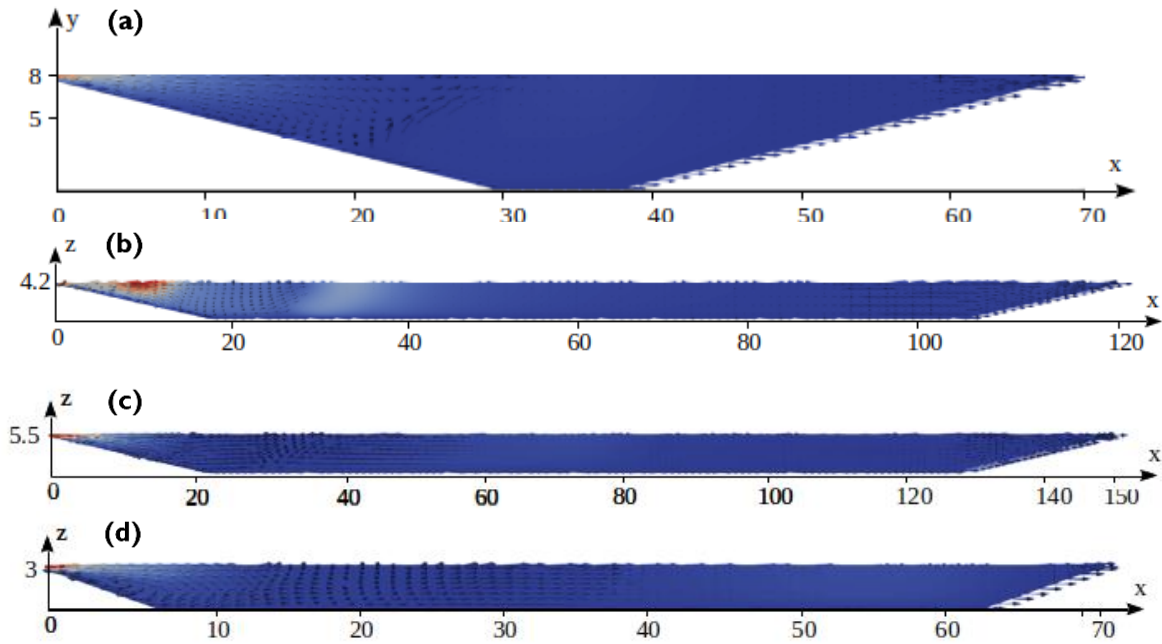


Figure 58 Side-view (i.e. x-z plane) of the non-dimensional velocity contours for 3D single-phase models of Pond (a) 2, (b) 5, (c) 7 and (d) 16. Note that the sections are taken through the stream-wise directions, i.e. through the inlet, of the ponds. Here, the legends of the velocity contours are same as the previous figures, i.e. Figure 57, and the arrows represent the glyph of the velocity vectors.

#### 5.4.3 3D Two-Phase Flow Simulation

An inlet solids concentration of  $3 \text{ kg/m}^3$  was used to determine general behaviour of sludge within the system and its impact on the hydraulics. This concentration was used in order to develop profiles and shorten simulation times in comparison with the actual inlet concentrations of  $\sim 3\%$ . The current solids models cannot effectively simulate concentrations above  $6\%$ , and this is an area of active research. In this case, the solids simulations are used to determine qualitative impact of input solids. Quantitative impact is further assessed through the compartmental based modelling which is also used to evaluate long-term performance.

It is clear that the introduction of solids into the framework drastically modifies the fluids behaviour from the single-phase models as is shown by the streamline plots (Figure 59) and top-view (Figure 60) and side-view (Figure 61) velocity contours for each pond under the two-phase model.

For Ponds 5, 7 and 16, the streamlines still show a large vortex constituting a large fraction of the pond, with the inlet flow entering straight into the vortex. Additionally, a separate flow pattern is observed near the outlet – the flow here could be envisioned as a vortex, but it mostly resembles turbulent, chaotic flow. The inactive zone in the centre of the vortex is more prominent in Pond 16. On the other hand, Pond 2 shows largely chaotic, high-velocity flow without ordered patterns throughout the pond. All ponds now show a large fraction of inactive space, which was mostly non-existent in the single-phase models. In particular, Pond 5 shows large amounts of inactive space throughout what appears to constitute half of the pond volume.

Unlike the single-phase cases, the top-view velocity contours do not necessarily match the patterns shown in streamlines. The chaotic flow patterns of Figure 59(a) appear as high-velocity sections in Figure 60(a) (Pond 2). This translates to a high degree of turbulence in the active treatment volume of

Pond 2, indicating a large mixing capacity and effective treatment throughput. On the other hand, Ponds 5, 7 and 16 do not show similar flow patterns across streamlines and velocity contours.

The main finding of the top view contours is the difference in top-layer velocity behaviour of Pond 2 as compared to Ponds 5, 7 and 16. Pond 2 maintains high-velocity, turbulent flow within its x-axis centre all along the y-direction, with low-velocity or stagnant flow at both x-boundaries along the y-axis (apart from the inlet region). Ponds 5, 7 and 16 show opposite behaviour – higher velocities occur along the y-direction at the x-axis boundaries, while the centres and bulk volume are largely stagnant. The primary factor causing the large difference is pond depth – Pond 2 has a greater depth than other ponds (8.0m for Pond 2 as compared to 4.2, 5.5 and 3.0m for Ponds 5, 7 and 16, respectively). The greater depth allows more potential for solids settling and greater prevalence of settling forces, which increases the liquid displacement and overall velocity in the top layers above the deepest region of the pond. In contrast, without a heavy dependence on solids behaviour, Ponds 5, 7 and 16 are more affected by superficial fluid velocity (i.e. velocity of fluid phase only), which dictates that the single-phase fluid is expected to flow faster downwards from the top of steep declines.

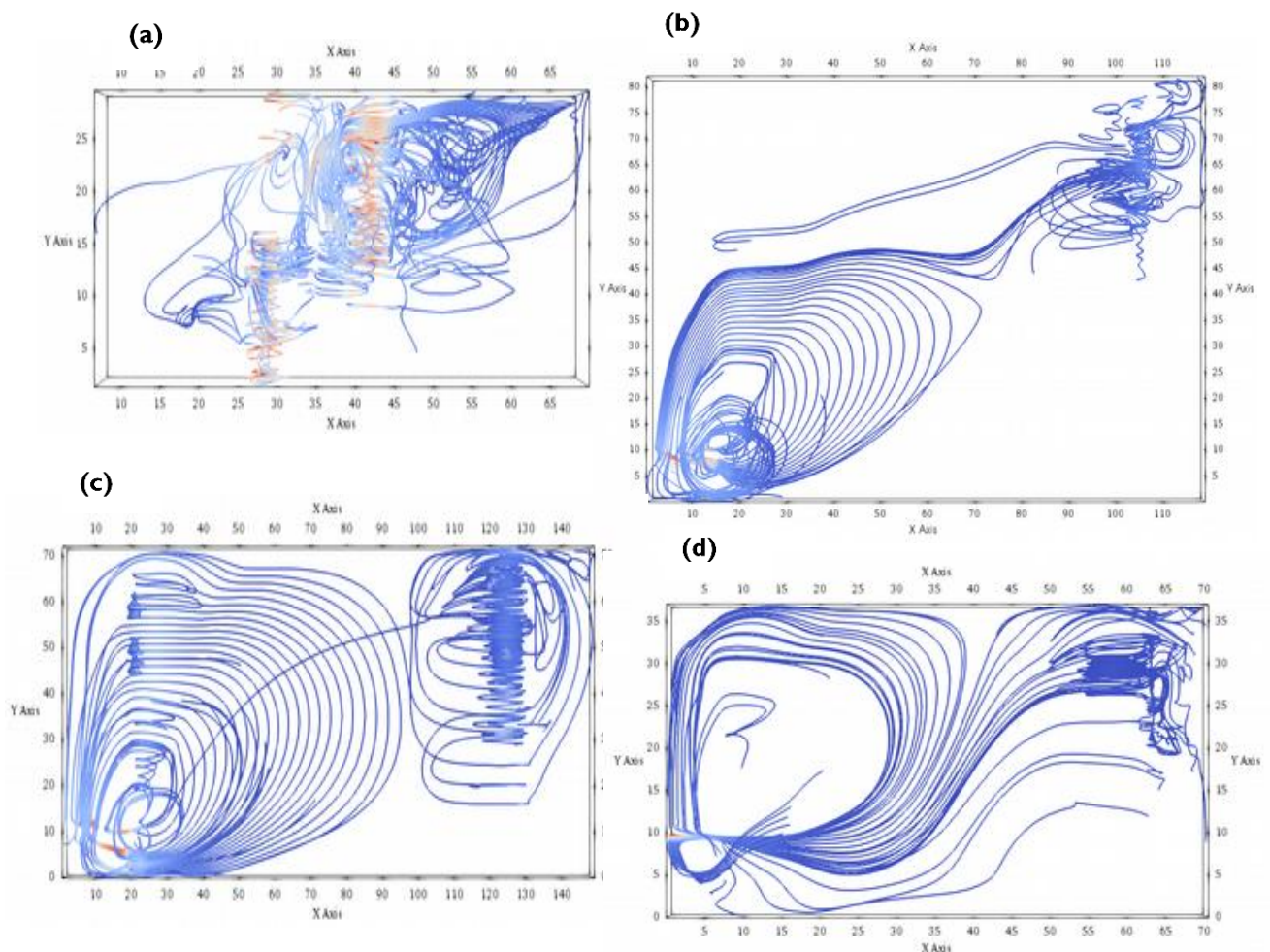


Figure 59 Top-view (i.e. x-y plane) of the streamlines for 3D two-phase models of Pond (a) 2, (b) 5, (c) 7 and (d) 16. Note that the origin of the axis,  $x = y = z = 0$ , is taken at the bottom of the ponds. Here, x-y plane corresponds to the top-surfaces of the ponds.

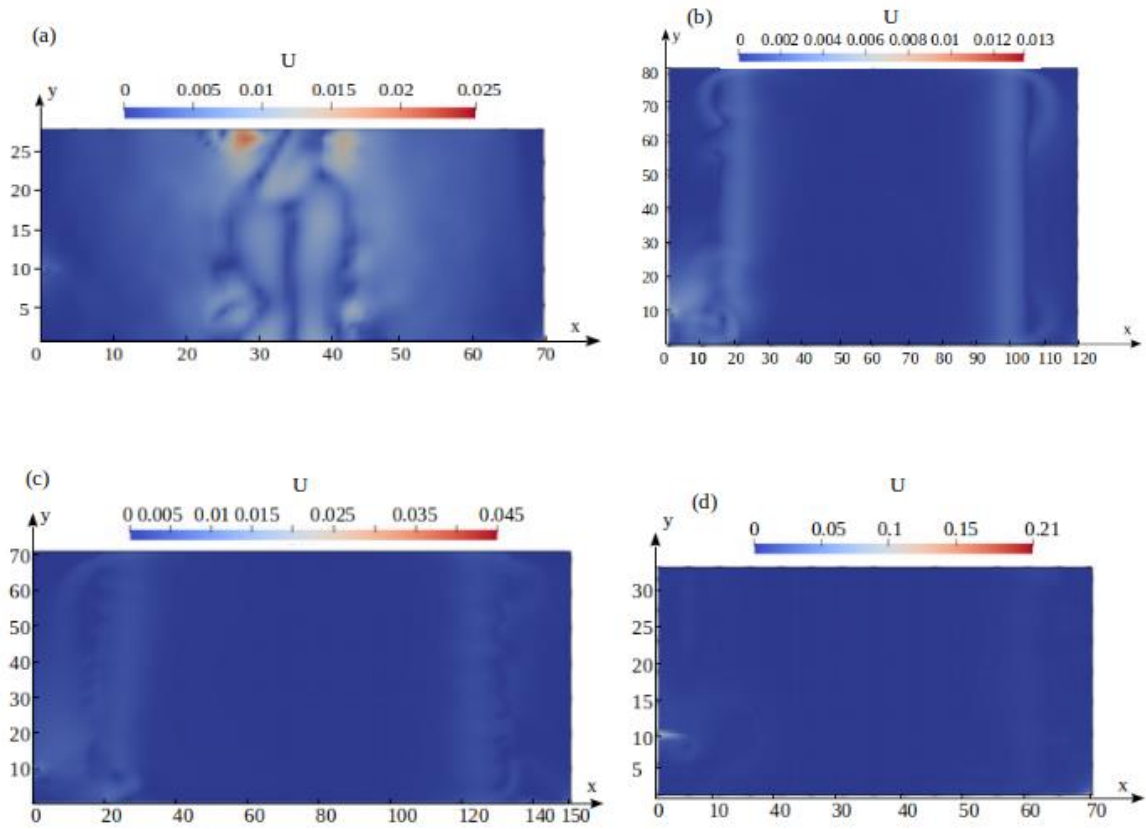


Figure 60 Top-view (i.e.  $x$ - $y$  plane) of the non-dimensional velocity contours for 3D two-phase models of Pond (a) 2, (b) 5, (c) 7 and (d) 16. Note that the origin of the axis,  $x = y = z = 0$ , is taken at the bottom of the ponds. Here,  $x$ - $y$  plane corresponds to the top-surfaces of the ponds.

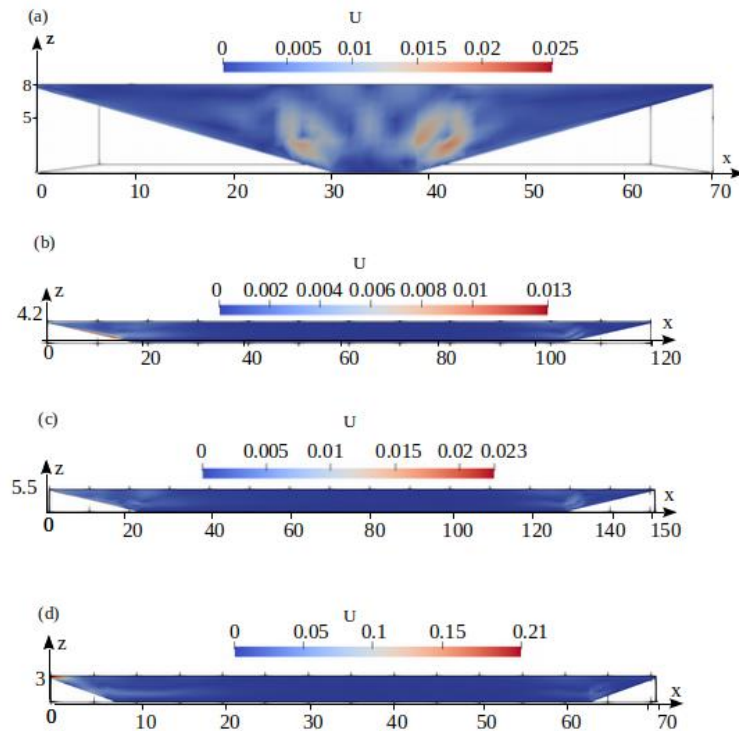


Figure 61 Side-view (i.e.  $x$ - $z$  plane) of the non-dimensional velocity contours for 3D two-phase models of Pond (a) 2, (b) 5, (c) 7 and (d) 16. Note that the sections are taken through the stream-wise directions, i.e. through the inlet, of the ponds.

#### 5.4.4 Solids Behaviour

The side-view concentration contours of Figure 62 determine sludge accumulation behaviour. Another view of the sludge concentration contours for each pond, in which the longitudinal axis is parallel to the inlet-to-outlet direction, is shown in Figure 63. Inlet region areas are magnified to highlight the minor inlet plumes. Figure 64 shows the sludge concentration profiles according to depth for each pond. It is important to note that inlet TS concentration for each simulation is set at 3000 mg/L ( $3 \text{ kg/m}^3 = 0.3\%$ ) and kept constant throughout. This is far lower than the actual inlet concentration (Section 5.3) to allow for numerical compatibility with certain simulations (the compartmental based model - CBM is used to simulate very high solids – see section 5.4.5). Note that, unless otherwise stated, the simulation results for Ponds 2, 5, 7, and 16 are demonstrated at simulation times of 74, 72, 66, and 16 days, respectively. The theoretical retention time (TRT) of these ponds are extremely long, which eventually constrains the numerical simulation to be run up to the TRT. With this in mind, the simulation results were taken at times, i.e. 74, 72, 66, and 16 days for the Pond 2, 5, 7, and 16, respectively, where the flow pattern does not change significantly and gives an indication of the overall nature of the flow for the long-term simulations. Having the flow variables as well as the solid accumulations from the CFD simulations at the mentioned times, the characteristic solids behaviour from the two-phase modelling work was taken to further develop the CBM and answer the primary research question, namely, how does the sludge bed accumulate long-term within the system and impact capacity.

Each pond shows typical settling behaviour with relatively high concentrations of sludge forming even, graded layers at the base of each pond, which has been observed in similar studies (Papadopoulos et al., 2003). This is due to the hindered nature of settling. (In this context, hindered means that individual solids particles interact, and ideal settling, according to Stokes law, no longer occurs.) Pond 16, which has steeper embankments, shows less concentrated deposits forming at the edge of the sludge bed along the embankment. Similarly, Pond 2, with a relatively low volume and proportionately low basin area, also shows some of the sludge deposits forming on the sludge embankment. Ponds 5 and 7 show a dilute sludge bed formed at around 72 and 66 days of simulation time, respectively, indicating that sludge accumulation is less prominent in these ponds. The rotated views of Figure 63 reveal that the sludge bed remains even across the entire surface area. This is related to the fact that solids are represented as a fluid. Fluids (no matter how viscous) will generally redistribute evenly due to gravity. To properly represent phenomena such as mounding, the mound must have mechanical cohesion and mechanical properties, which requires that a variable interface be simulated. This has not been done so far in the modelling literature and requires a substantial advancement in the state of the art (but is required to properly simulate short term solids accumulation behaviour). It is well beyond the scope of the current project.

Interestingly, the sludge forms beds up to similar heights across each pond, with the concentration profile showing an interface concentration at around 25% of the maximum height of each pond. However, the concentrations of the sludge beds are significantly higher in Ponds 2 and 16, even after taking into account the variations in scale. This is likely a result of HRT variation, which is lower in Ponds 2 and 16. While Pond 16 has a HRT an order of magnitude lower than Pond 2, the simulation time is similarly lower, restricting the amount of time for sludge to accumulate, which explains why concentrations are not proportionately higher as might be expected. Additionally, the geometry of Pond 2 likely affects the sludge bed concentration – the high depth, steep embankment inclines and small basin surface area allow for higher volumes of sludge to form concentrated beds within a small area.

We are not able to verify quantitatively against the field observation in Section 5.1; the field sludge profiling was conducted after a long period since the last desludging, and thus cannot be used to compare to the present concentration contours of 16 – 74 days. However, the shape of the sludge maps in the sludge profiling report do show some similarities to the present simulation results. This likely reveals what the simulations might show if performed for similar periods. Sludge maps of Ponds 2 and 7 show gradual increase of sludge bed depth (i.e. distance between pond surface to sludge surface) towards the deep centre region of the ponds, which is to be expected for a pond with sludge funnelled towards the basin as is shown by the present simulation results. Pond 5 shows the same graded sludge depths around the pond boundaries with some variations throughout the central region.

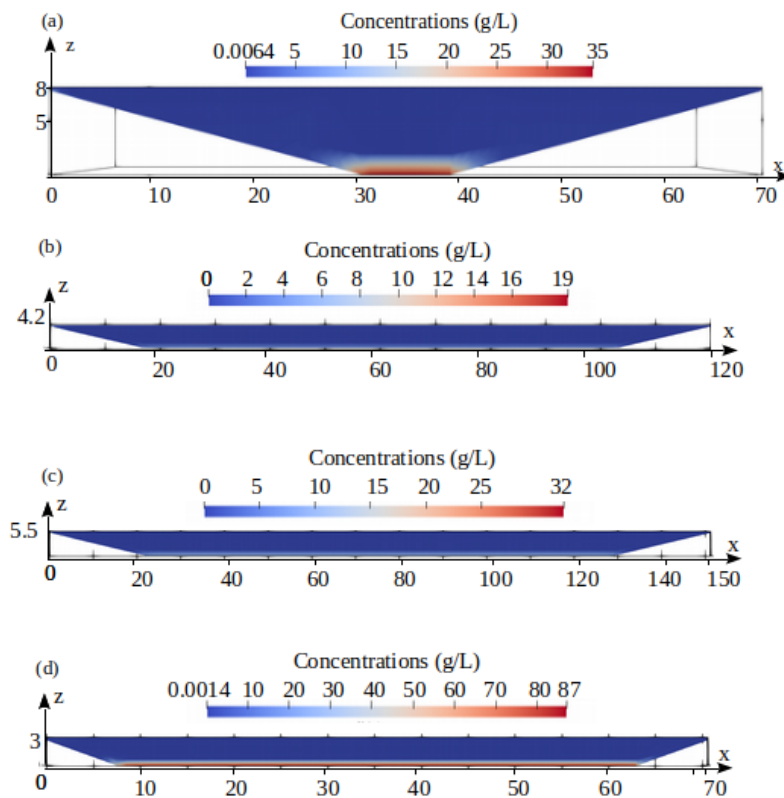


Figure 62 Side view (i.e.  $x$ - $z$  plane) of concentration contours for 3D two-phase models of Pond (a) 2, (b) 5, (c) 7 and (d) 16. Note that the sections are taken through the stream-wise directions, i.e. through the inlet, of the ponds.

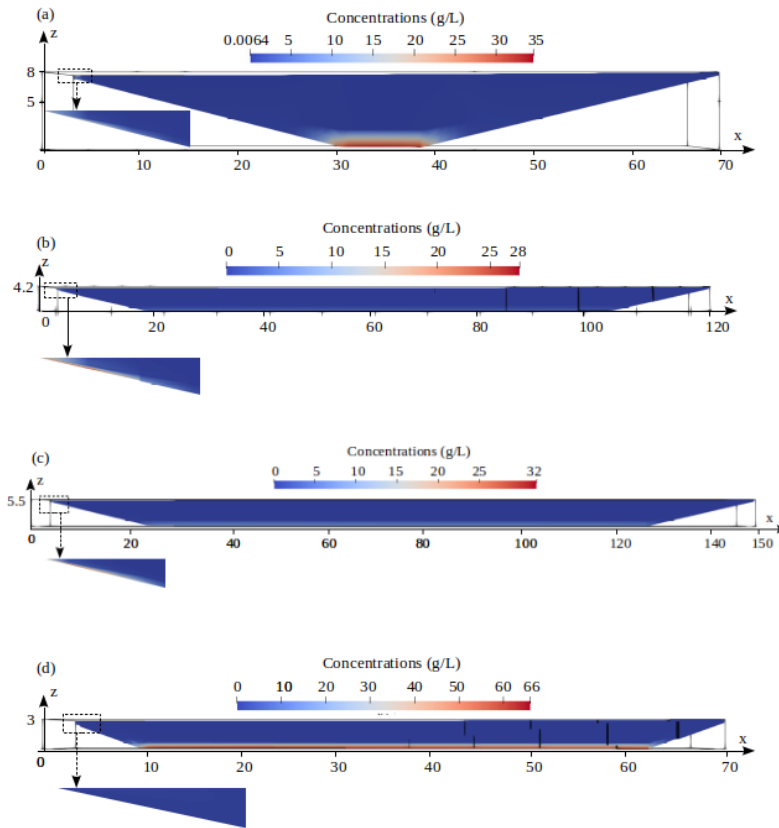


Figure 63 Orthographic view (i.e. longitudinal axis is parallel with inlet-outlet plane) of concentration contours for 3D two-phase models of Pond (a) 2, (b) 5, (c) 7 and (d) 16. Here, the black-dotted rectangle represents the enlarged section of the inlet plume.

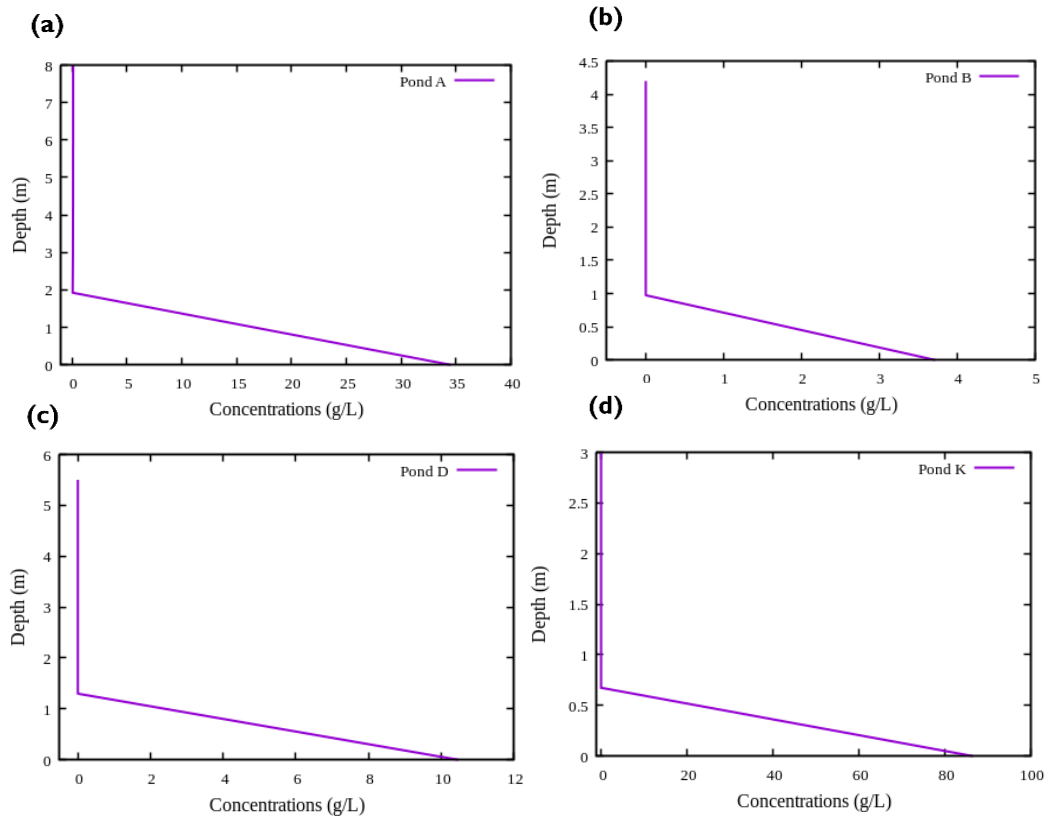


Figure 64 Concentration profiles for 3D two-phase models of Pond (a) 2, (b) 5, (c) 7 and (d) 16.

### 5.4.5 Compartmental Based Model Simulation

Virtual tracer tests are done to identify characteristic hydraulics behaviour during CFD analysis. A virtual tracer is introduced in a pulse at time zero, and its outlet concentration is simulated over time (residence time distribution – RTD). A perfectly mixed reactor would have a simple exponential decay, while a perfect plug flow reactor (with diffusion) would follow a Gaussian (normal distribution) profile.

The RTDs for the initial tracer tests performed through CFD are shown in Figure 65. Concentrations are normalised against initial concentrations, and time is normalised against the HRT for each case. The tracer injection occurs at  $t = 0$ .

Ponds 2 and 7 show very narrow initial peaks with a sharp decline following the sharp incline of the tracer input before steadying to a more gradual response. This is representative of a significant fraction of the flow bypassing the dominant streamlines and flowing directly to outlet. Each pond also shows a notable response delay with the first peak beginning sometime after the initial injection, representing the time taken for detectable concentrations to first reach the outlet. This delay is noticeably smaller in Pond 16, and is to be expected in a pond with smaller volume and HRT. This delay is due mainly to inlet effects and inlet plumbing. Pond 16 shows heavy oscillations after the first peak before reaching a steady decline. This is represented by large fractions of tracer concentrated flow exiting and recirculating into the outlet flow path. Thus, the oscillations can be emulated by a significant recycle component with re-entry relatively close to the outlet – this is discussed in the following paragraphs.

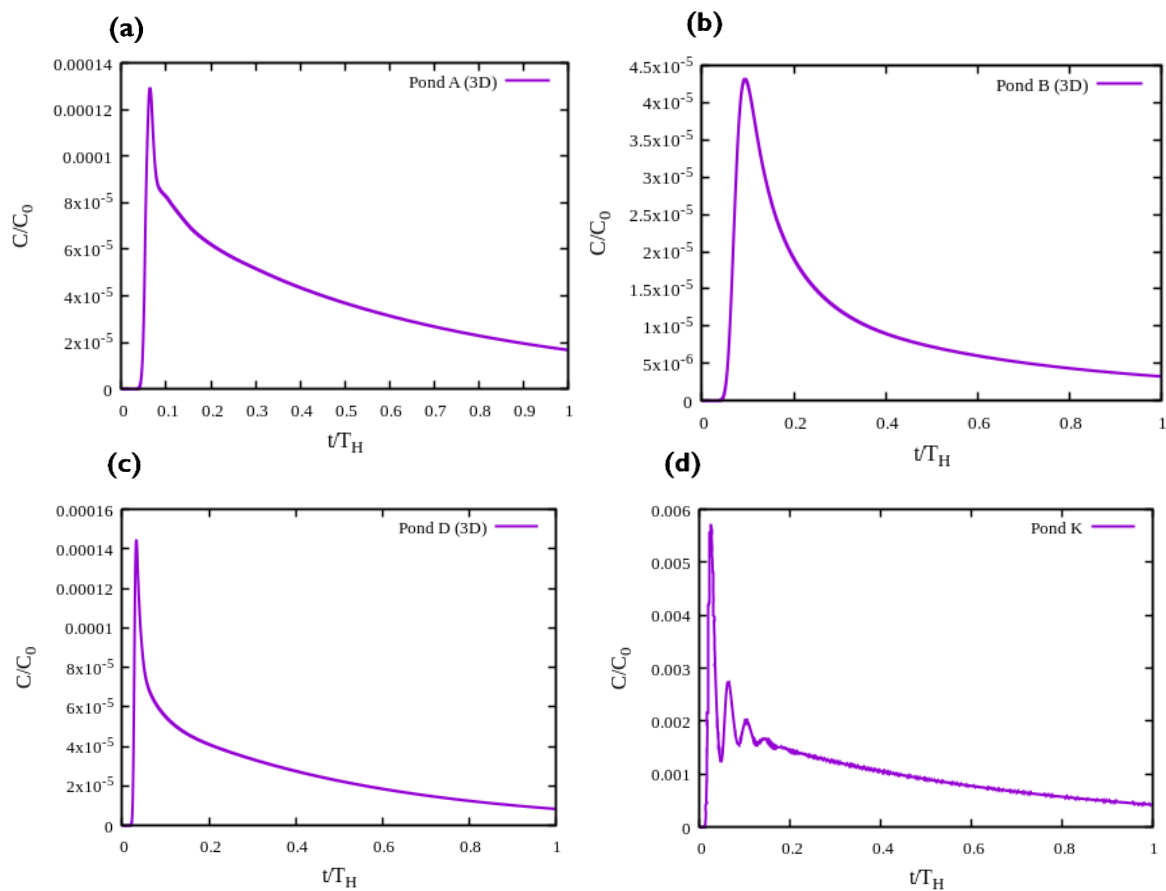


Figure 65 Residence time distribution curves of 3D single-phase models of Pond (a) 2, (b) 5, (c) 7 and (d) 16. Note that the concentration and the times are non-dimensionalised using the widely used relations as  $C/C_0$ , and  $t/T_H$ , respectively. Here,  $C$  is the concentration  $C(t)$ ,  $C_0$  is the initial concentration, which is inlet concentration during the pulse-width in this case,  $t$  is the time, and  $T_H$  is the theoretical retention time of the ponds.

The cases were simulated using the compartmental based model (CBM) and the results provided in Table 6. The four cases obtained very different results. Ponds 2 and 7 are comparable in HRT, with Pond 2 being deep and Pond 5 being shallow. Apparent active fraction varied substantially, with long HRT and shallow depth causing a lower active fraction. The deep depth in Pond 2 resulted in essentially stirred tank behaviour, with limited recycle and bypass. The high initial peak was caused by a limited bypass, but with a relatively long tail and very limited recycle. The shallow depth in Pond 7 caused an increase in apparent recycle, which also likely resulted in the increase in apparent bypass. This slightly decreases the effectiveness of the main volume overall, resulting in an increased fraction having a limited retention time in the pond (pushing more out to the end of the tail).

Table 6 Compartmental based model optimised parameters.

	<b>Pond 2</b>	<b>Pond 5</b>	<b>Pond 7</b>	<b>Pond 16</b>
Theoretical V (m <sup>3</sup> )	7200	43371	67600	8500
Modelled V (m <sup>3</sup> )	8164	24605	48744	6963
Active fraction	113%	57%	72%	82%
Input Flow (m <sup>3</sup> /d)	62	61	276	1248
Theoretical HRT (d)	117	708	244	6.81
Actual HRT (d)	131	402	177	6
Delay (d)	11.2	54	10.2	0.11
V <sub>main</sub> (m <sup>3</sup> )	8341	23867	25357	4626
V <sub>recycle</sub> (m <sup>3</sup> )	599	nil	23364	2254
Q <sub>recycle</sub> (m <sup>3</sup> /d)	20	N/A	1268	3238
V <sub>bypass</sub> (m <sup>3</sup> )	4	738	23	83
Q <sub>bypass</sub> (m <sup>3</sup> /d)	2	13	17	253
Fraction bypassed	3%	21%	6%	20%

Pond 5 had a very long retention time. Recycle was virtually eliminated, and there was a substantial bypass, with a large volume. Bypass appears to be induced more by shallow depths rather than short retention time, which is reasonable, since the deeper ponds allow lateral dispersion due to vertical turbulence. The high bypass volume was caused by increased dispersion of the bypass flow into the main hydraulic volume. It also had the lowest active fraction. Overall, Pond 5 does not effectively utilise its large volume.

Pond 16 had oscillating behaviour captured in the short-term dynamics, which could not be effectively captured by the model (a multi-stage recycle also could not capture the oscillations effectively). The delay was minimal and reduced in proportion to the HRT – essentially negligible, probably caused by rapid dissipation of inlet plumes caused by the high flows. Overall, the system was dominated by recycle, with a high bypass, and could not be effectively simulated by the CBM. A plug flow recycle stage could be included, but a better approach would be to simplify the CFD model for application to biochemical process modelling.



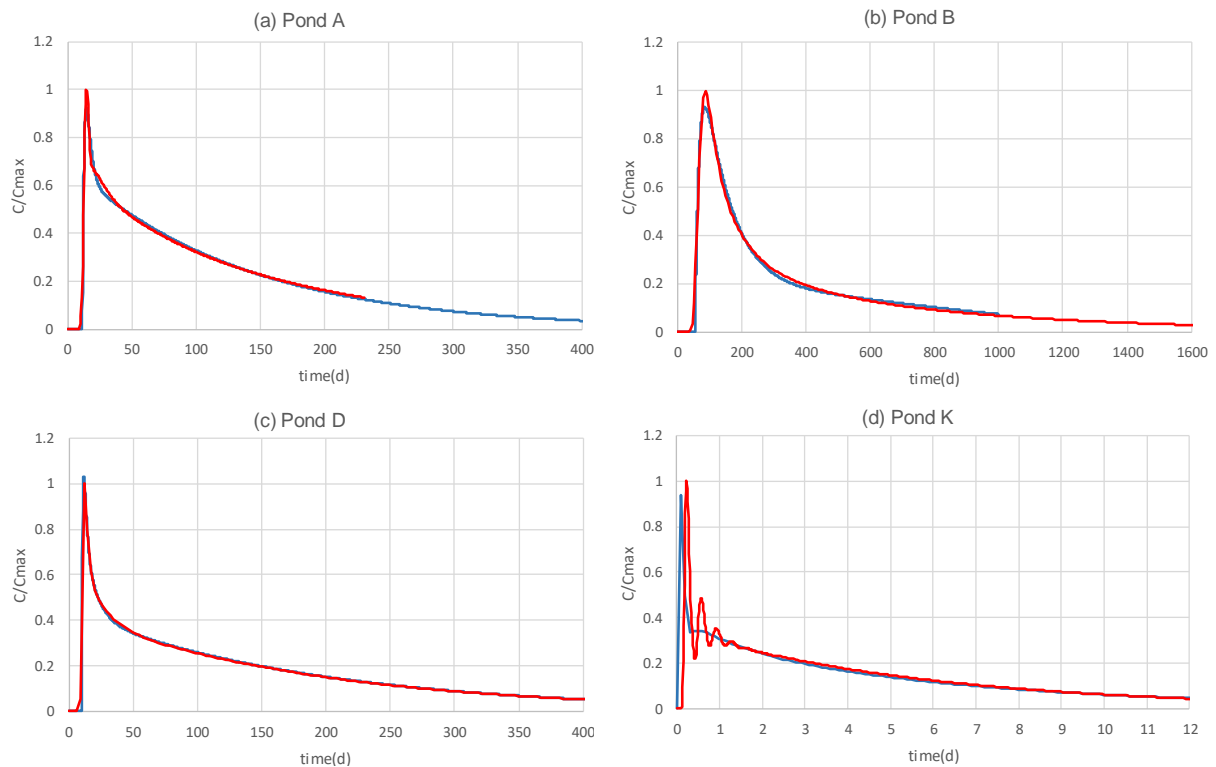


Figure 66 Comparison of residence time distribution between models of Pond (a) 2, (b) 5, (c) 7 and (d) 16. Optimised compartmental based model is shown in blue, and the CFD model is shown in red.

#### 5.4.6 Biochemical Model Simulation

Results of long-term simulations for unoccupied volume (pond volume not occupied by sludge) are shown in Figure 67. This shows predicted pond lifetime varying between 38 days (Pond 16), and 7.9 years (Pond 5). Pond lifetime has been set to the fully sludged state (it will need desludging prior to this state), though presumably pond 16 was operating in a fully sludged condition when the survey was carried out. The ponds are largely driven by solids loading rate, and total hydraulic volume. The reason that pond 16 is non-linear is due to a lack of biochemical degradation initially. Once a substantial inventory has built up, biochemical degradation mitigates accumulation rate. Modelled accumulation rates are shown in Table 7. These are approximately double the observed accumulation rates (see Section 5.4.2) but much closer than those determined by the hydrodynamic solids analysis of Section 3.4. This is likely due to either (a) additional solids degradation beyond what would be expected from the biochemical degradation (i.e., more than 60% is degrading), due to the very long retention times, or (b) differential separation of organic and mineral solids. The analysis of pond lifetime shown below assume the lower degradation extent as found by biochemical modelling. If further degradation occurs (as field observations would indicate), pond lifetime would naturally further extend.

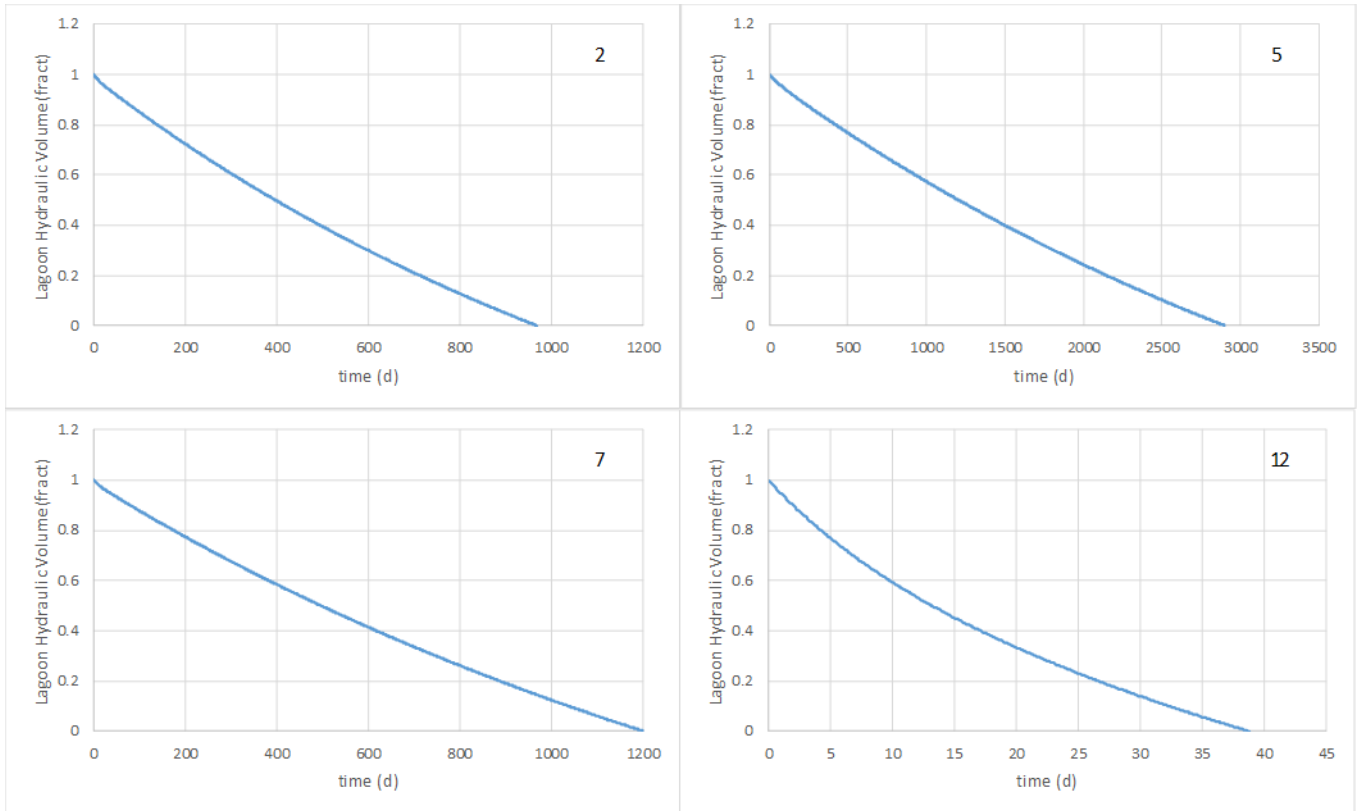


Figure 67 Comparison of occupied volume over the pond life.

Table 7 Summary of results from biochemical model simulations.

<b>Pond</b>	<b>2</b>	<b>5</b>	<b>7</b>	<b>16</b>
Lifetime	2.6y	7.9y	3.3y	38.3d
Effluent TS conc (EOL)*	1.10%	1.28%	1.10%	1.40%
Sludge VS/TS (EOL)	62%	62%	62%	68%
Modelled accumulation rate (m <sup>3</sup> / kg TS)	0.00500	0.00424	0.00490	0.00616
Observed accumulation rate <sup>c</sup> (m <sup>3</sup> / kg TS)	0.00264	0.00185	0.00282	/

EOL - Result at end of life

Pond 16 is the clear outlier, with a very short effective life, and otherwise poorer performance, in terms of both solids destruction (high sludge VS/TS), and poor outlet solids. This indicates that such a short HRT is not suitable for a piggery pond where solids accumulation is a significant mechanism. The model does not account for decreased solids retention at very short HRTs, which would further decrease the performance, and not substantially increase the pond lifetime.

Pond 5 is also different from 2 and 7 (which are comparable). This is due to the relatively high bypass, which was identified as being due to the very long retention time, and relatively shallow depth. The results reinforce the conclusion that this combination is not an effective use of pond volume.

As shown in Figure 68, it takes a substantial amount of time for the sludge in the pond to stabilise (indeed, pond 16 is never stable). While it is not necessary to wait until the end of the pond lifetime, in-situ harvesting of sludge can happen from approximately 100d (or 1 HRT if the pond has a HRT on the order of 150d).

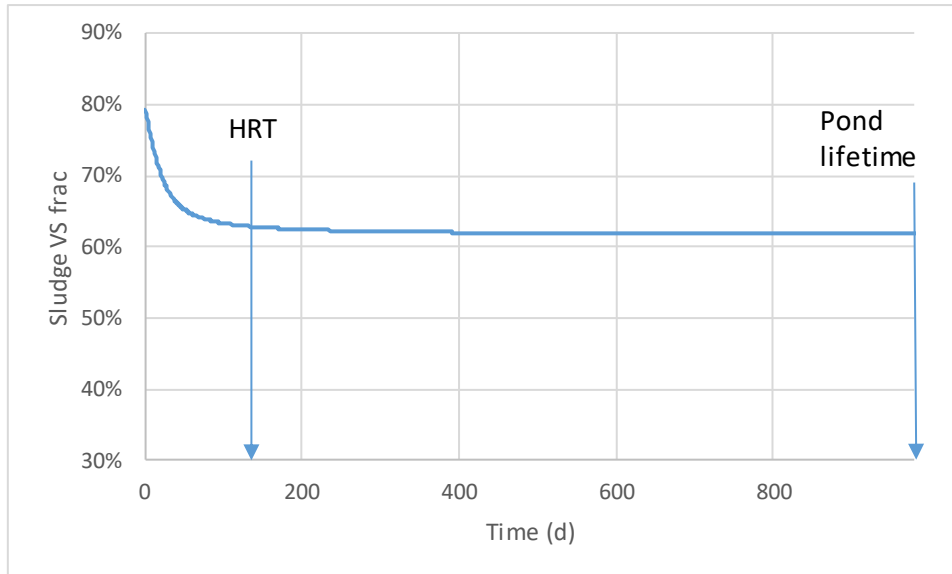


Figure 68 Sludge vs. fraction (indicating stability) over time for Pond 2

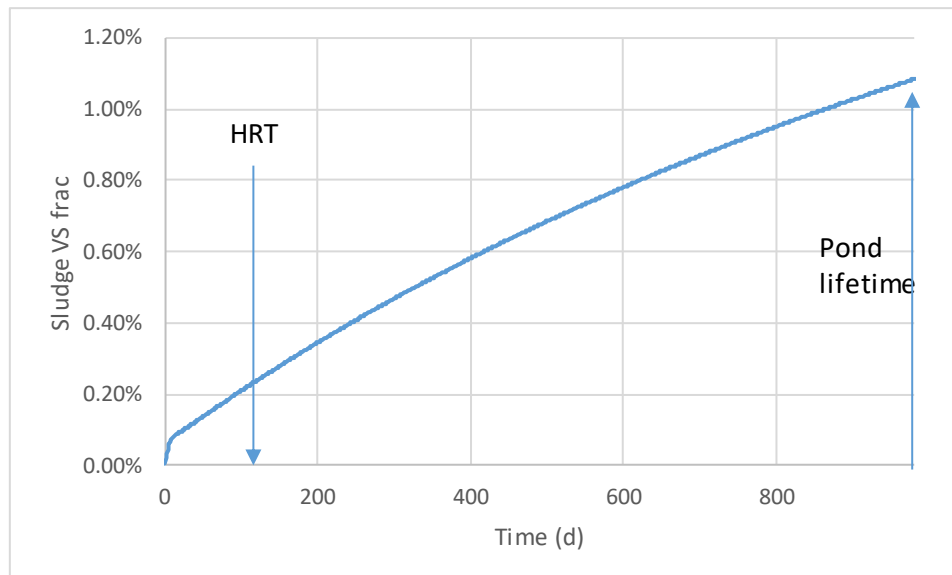


Figure 69 Outlet solids concentration from Pond 2

Outlet solids concentration is shown in Figure 69 and indicates that (from a clear water initial condition), there is an initial rapid increase, mainly driven by the bypass solids, followed by a steady increase as solids accumulate in the pond. The level to which the solids initially increases drives the longer-term performance. Where more solids are bypassed, the baseline is higher, but accumulation rate is lower.

## **6. Discussion**

### ***6.1 Sludge profiling***

The sludge profiling method used in this project proved to be effective. However, it involved considerable labour and the use of relatively specialised equipment and computer software. These requirements may limit its application for regular sludge monitoring in commercial piggery ponds. Future improvements could include developing a remote-controlled raft to convey the sonar and GPS units over the pond surface. This would further improve the safety and convenience of sludge profiling operations while reducing the labour investment. Once an initial pond survey is completed, regular sludge monitoring, at one to two yearly intervals, may be more economically feasible using a remote-controlled raft to collect the required sonar and GPS data, for subsequent post-processing by a commercial service provider, such as Premise Agriculture.

### ***6.2 Sludge accumulation rate***

The variability in the estimated sludge accumulation rates probably reflects the variation in pond design characteristics, uncertainty regarding pond desludging dates and volumes of sludge removed. There is also the possibility of unreported changes in pig herd, diet and management practices, particularly as the ownership of some of the piggeries changed over long operational periods. The results demonstrate that the current design standard is within the measured range of sludge accumulation rates. There appears to be insufficient evidence to suggest any major changes to the current standard, based on the results of this study.

### ***6.3 Hydrodynamic modelling***

#### ***6.3.1 Model Performance***

##### ***2D vs 3D Single-Phase Cases***

The 2D models only simulate the flow travelling along a horizontal plane at the surface level. While not able to provide a detailed description of solids-filled three-dimensional ponds, it does identify broad geometric factors and flow patterns, including; dead zones, recirculation extent, and the impact of bypass (which had a variable extent here). However, given the depth variation between ponds, along with an embankment that reduces horizontal boundaries as depth increases, the 2D models cannot accurately represent the actual flow behaviour. 2D models may be more suitable for simple rectangular or square pond geometries with negligible vertical flow effects and forces, or for simulations in which computational power is limited.

The mesh elements of the 3D models have narrower horizontal boundaries to offset their large boundary size caused by the extra sizing dimension. The result is smaller, finer mesh elements that more accurately capture the finer details of fluid flow throughout the pond. On the other hand, without the depth to consider, the 2D models can afford much wider boundaries while still retaining a reasonable simulation with regards to computational requirements. The 3D single-phase models represent pond hydrodynamics better than the 2D cases through flow path predictions, velocity distribution contours and residence time behaviour. However, they are unlikely to give a complete and realistic portrayal of a piggery pond with high solids inflow.

### *3D Two-Phase Cases*

Incorporating solids and sludge mechanics into the models result in much more useful analysis of the pond hydraulics. The first point to note is that solids introduce variations in velocity patterns in each pond. While the 2D and 3D single-phase cases show only mild velocities outside of the inlet and outlet, the two-phase velocity contours show largely varying flow regimes throughout the bulk of each pond, as well as distinct velocity patterns across ponds. It is expected that instead of the inlet and outlet velocities, the solids settling forces and momentum become the primary drivers of fluid flow. This is indeed representative of actual conditions, indicating high accuracy in this model.

After analysing the solids behaviour results, substantial variations exist between the modelled and experimental results. It is expected that short-term simulations are insufficient to find a realistic picture of accumulation. It is more useful to determine general solids behaviour and partitioning. It is likely that there is an initial stabilisation, or warm-up period, immediately after commissioning the pond. The sludge bed must then develop to a height where it approaches an equilibrium between sludge depositing onto the bed and sludge exiting the pond. This can also be thought of as a critical bed depth. Until then, accumulation rates will likely vary to levels not representative of long-term operation. The length of this theoretical period is unclear. In any case, long-term simulations will be beneficial for determining sludge behaviour among other outcomes.

After a review of literature, only one article appears to have studied sludge accumulation in wastewater stabilisation ponds through computational hydrodynamic models (Alvarado, Sanchez, et al. 2012). A primary finding among this study, as well as other studies using non-computational models of sludge accumulation (Nelson et al., 2004; Abis and Mara 2005; Picot et al., 2005), is that sludge deposits accumulate rapidly in tall mounds at a location relatively near the inlet as a result of high settling velocities and downward fluid velocities. In contrast, each pond of the current study has its inlet surrounded by embankments which, rather than allowing build-up of sludge mounds, direct sludge towards the flat basin into graded beds. This is a substantial advantage of a graded pond, and very important to pond longevity. Another finding in Alvarado, et al. (2012) is that sludge accumulation had noticeable effects on hydrodynamic flow, and that the growing topology of sludge over 10 years contributes to major changes in flow patterns and RTDs. Unfortunately, while the CBM reveals some findings of the holistic long-term flow behaviour, the current CFD simulation times were not long enough to examine the long-term effect of sludge accumulation on specific flow behaviour. However, it is expected that this effect can be reduced by employing pond geometries similar to Pond 2 – high depth, steep inclines and small central basin areas imitating a “V-shape” such that sludge is stored at a depth out of reach of the dominant flow region. The current report appears to be the first study examining sludge behaviour through a two-phase hydrodynamic model coupled with a computational biochemical model.

### *Compartmental Based Model*

The CBM could reasonably represent tracer results from the CFD analysis and expand the simulation timeframe from months to years. Importantly, the analysis identified that as pond HRT increased from smaller ponds (days) to moderate sized ponds (months) the hydraulics conformed more to ideal hydraulics, with decreased short-term dynamics due to internal recycles. As the system extended to very long HRTs (years), bypass became more important, probably due to insufficient turbulent dissipation. The effective volume variation with pond depth and HRT further confirmed the critical design HRT of ~150d, and depth of >6m. CBM can be used for simplifying CFD simulations and coupling with biochemical models. In this case, the CBM could accurately reproduce the holistic flow

outcomes of three of the four ponds. Chaotic flow patterns, such as recycles, bypasses or inactive zones, cause disruptions to the compartmental configuration and are difficult to model. We conclude that the CBM is more suitable for laminar flow regimes with moderate HRTs. Very short HRT ponds may need to be simulated using a CFD approach only due to their complexity, but this is the most computationally intensive case to simulate, particularly with a two-phase 3D model.

#### *Biochemical Model*

The biochemical model allows translation of short-term sludge behaviour results by CFD (and CBM) into long-term behaviour and provides a more accurate prediction of sludge accumulation rates. The related sludge accumulation rates are significantly closer to the experimental values than those of the CFD model, but still vary by a factor of at least 2. With extended development, the platform used for biochemical modelling can also be used for prediction of additional biochemically related performance statistics, such as methane production rates or nutrient recovery potential. The main issue is determining long-term parameters (including apparent degradability) from short term tests such as a methane potential test. The results here tend to indicate that short term tests are very conservative.

### 6.3.2 *Pond design considerations*

#### *Pond depth*

Depth appears to be the primary design factor affecting solid settling and sludge accumulation. Higher depth enables a higher inventory while enabling clear water separation, allowing the solids to either react in the active treatment volume or enter the exiting currents to outlet before settling. It also causes significant variations in the flow behaviour of both single- and two-phase fluid. In this study, higher depth ponds showed reduced prevalence of chaotic flow patterns such as backmixing and short circuiting (while HRT was kept similar). While higher mixing may improve sludge contact, it is believed that this is outweighed by the unpredictability in necessary operational parameters and difficulty in predicting long-term pond behaviour caused by turbulent backmixing. The field results indicate no substantial difference in stability (as determined by VS frac) between deep and shallow ponds. It should also be noted that superficially increasing depth allows for storage of sludge between desludging intervals. Not only will depth increase the storage capacity, it will allow sludge to be stored without having significant effects on the hydrodynamics of the active zones.

While studies of the effect of pond depth for wastewater stabilisation ponds are rare, Sutherland, et al. (2014) and Richmond and Grobbelaar (1986) have both reported that deeper algae raceway ponds with identical pond areas had consistently higher areal productivities than shallow ponds, albeit without identifying the mechanism. Although the flow mechanics in raceway ponds differ to stabilisation ponds, the treatment mechanism is the same (i.e. solids are treated in higher layers of the pond), which may translate this depth-productivity correlation to stabilisation ponds. A critical depth – a value at which higher depths begin to show drastically reduced sludge accumulation rates – would be valuable to pond designers and could likely be determined with further study.

#### *Inlet / outlet positioning*

Overall, this factor had a lower impact than expected, with metric geometry (depth, HRT etc.) having a stronger impact. The two-phase streamlines reveal findings about the effect of horizontal positioning on hydrodynamics. Essentially, while the inlet and outlet are on opposing boundaries, keeping them on the same width position causes straight streamlines with less mixing. As an example, for a 100 x 100 m pond, if the inlet is at (0, 10), placing the outlet at (100, 10) will allow for straight streamline between inlet and outlet. Placing the outlet at (100, 100) will increase the presence of vortexes and

mixing regimes. Too strong of a vortex may cause undesirable turbulence or funnel solids towards the basin but may also redistribute accumulated sludge into the active treatment layers. On the other hand, perfectly straight streamlines may increase the inactive fractions. It would be interesting to examine the hydrodynamics of models with inlets and outlets on perpendicular boundaries.

Based on intuition, increasing the depth of (lowering) the outlet will result in more sludge being captured in the outflow and less sludge accumulation onto the pond basin. Lower outlet positioning may also cause higher fluid velocities throughout the pond because of gravity affecting the exiting streams. On the other hand, too low of a position will cause premature sludge build-up in the outlet pipe during the early stages of sludge bed formation. Vertical positioning will also induce various flow patterns as would horizontal positioning. Future models should contain varying inlet and outlet depths to study the effect on both hydrodynamics and solids behaviour.

#### *Embankment incline*

The steeper embankments in the present models induce turbulence in the lower layers. This is likely a result of counteractive force as two-phase liquid impacts onto the embankment. If the turbulence occurs low enough to contact the sludge beds, this will induce remixing of the sludge into the active treatment, effectively reducing sludge accumulation and increasing treated throughput. On the other hand, steep enough embankment inclines may cause funnelling of solids towards the basin, allowing for selective zoning of sludge settling (and easier desludging) but possibly higher accumulation rates. A critical incline value at which embankments induce optimal turbulence would be valuable to pond designers. Such a value will likely vary according to the sizing dimensions and will need to be calculated for individual ponds.

It would be interesting to examine the effect of variation of incline between perpendicular embankments (i.e. embankment pairs along the x and y axes) or even opposite parallel embankments (i.e. individual embankments along one axis) on the flow behaviour. While Pond 2 has varying inclines between perpendicular embankments, the effect was not made clear in this study.

### *6.3.3 Operational considerations*

#### *Hydraulic Retention Time*

The optimal HRT for the given ponds was estimated at 150 days. The results suggest this as the period to maximise the pond performance and lifetime in consideration of the potential costs incurred by unpredictable flow dynamics. The CBM and CFD analysis showed that exceeding this causes backmixing, short circuiting and/or increased presence of low velocity and inactive regions. Furthermore, the results reinforce the expectation that lower HRTs result in higher solids accumulation. Other factors that affect accumulation rate, such as pond geometries, will compound with the accumulation rate effect of HRT. The high VS/TS ratios and accumulation rates in Pond 16 suggest that a low HRT pond is not suitable for the high solids concentration of piggery effluent. If sludge is actively recycled, it will effectively act as a solids digester and remove organic solids, but in this case, the design should incorporate this (as a high-rate solids lagoon), and include downstream treatment to achieve the same performance as long retention time lagoons.

#### *Desludging Intervals*

Larger sludge deposits disrupt the natural hydrodynamic flow behaviour and introduce undesirable flow patterns, such as bypass and remixing. Accumulation of sludge at a certain limit will cause overflows and prevent continued operation. On the other hand, increasing the storage time of sludge

increases its potential for treatment and capture of methane. Thus, when selecting a desludging interval, operators should aim to strike a balance between allowing maximum extraction of methane from sludge while minimising the interference to standard operation (by altering hydrodynamic behaviour or reducing lifetime). The biochemical simulation revealed that, for the long-term, each pond (excepting Pond 16) accumulates sludge at an approximately linear rate with time, allowing for easy selection of desludging intervals. Pond operators can use the biochemical sludge accumulation results to make more informed decisions when selecting desludging intervals, along with consideration of the logistics of desludging. However, the results suggest that an interval of at least 100 days is necessary to effectively remove degradable components of the sludge. Since accumulation rates vary according to a number of factors, desludging intervals should be individually considered for each pond using both qualitative and quantitative decision making.

Overall, a number of desirable features compete. If solids are to be removed from the influent, they are either degraded, or accumulate in the system. Therefore, good solids removal performance is balanced by a more rapid accumulation in the system. A long retention time is required to both increase pond lifetime, as well as enable biological degradation of the solids. The non-ideal nature of the hydraulics increases the level at which these factors compete, since the bypass reduces solids removal performance but decreases accumulation rate. In-situ solids removal allows for an improvement in overall pond lifetime, but should be done intermittently, in relatively large amounts and at high solids concentrations.



## 7. Implications & Recommendations

Regular sludge profiling would greatly assist with the ongoing management of commercial piggery ponds. Given the relatively high labour component and specialised equipment and computer software requirements associated with the sludge profiling method used in this project, there appears to be scope for one or more commercial service providers to offer sludge profiling services to producers. The development of a remote-controlled raft to convey the sonar and GPS units over the pond surface would further improve the safety and convenience of sludge profiling operations while reducing the labour investment.

The current standard sludge accumulation rate used in the design of piggery ponds in Australia is within the range determined during this project. Although the current standard is less than the mean of the estimated values, there is insufficient evidence to suggest any major changes to the standard value, without further long-term monitoring of sludge accumulation in a variety of ponds.

Based on the current results, the following conclusions can be drawn from the hydrodynamic modelling component of the project:

- Computational fluid dynamics (CFD) models for wastewater stabilisation ponds should include a minimum two-phase (solid-liquid) basis for accurate depiction of realistic hydrodynamic and sludge behaviour. A compartmental-based model (CBM) may be appropriate, depending on pond characteristics like laminar flow and reasonable hydraulic retention times (HRT). A numerical biochemical model can supplement short-term CFD simulations that are too computationally expensive for long-term simulation of sludge behaviour.
- Greater pond depths result in better active fractions and improved ability to manage and accumulate solids without detrimental performance on the main process.
- HRTs should be maintained within 100 – 300 days to retain active fraction, minimise short circuiting, and maintain effective lifetime. Short HRT ponds are not suitable as a stand-alone treatment method for piggery ponds (with a high solids feed), as the high solids concentration from piggery effluent causes rapid sludge accumulation.
- Where covered anaerobic lagoons are used (which are necessarily short HRT), solids load should be minimised, and solids management considered carefully, possibly by active withdrawal. The latter should recognise that stabilisation may be limited given the short solids retention time.
- Steep embankments up to a certain angle allow for remixing and retreatment of settled sludge and selective placement of sludge deposits for automatic desludging.
- Desludging intervals should be selected according to individual pond performance results, such as long-term accumulation rates, but should be higher than 100 days in order to maximise methane potential of the pond. The higher than expected solids destruction at very long retention times (as compared to the methane potential testing) increases pond lifetime but does not substantially change this conclusion.
- CFD based on short-term pond behaviour (up to 100 days) can provide guiding predictions about the fluid dynamics and preliminary solids behaviour, particularly suitable as input to the compartmental based model (CBM) but longer periods are required for overall sludge accumulation behaviour and operational outcomes.

We recommend for future work:

- Modelling on additional pond designs (existing, planned or otherwise) to verify the present conclusions and determine applicability to generic ponds. Other universal conclusions, such as a critical depth or a method for determining critical depth, could be found.
- Expansion of the hydrodynamic model into a three-phase system, particularly for very short HRT lagoons;
- Inclusion of environmental factors, such as thermal stratification, wind effects or evaporation, into the hydrodynamic model, along with a study of their effects on the operation of each pond;
- Improving the usability of current and future models for wastewater engineers, by integrating hydrodynamic, compartmental and biochemical modelling platforms into a combined approach suitable for pond design. This may require further targeted field validation.

## **8. Intellectual Property**

The majority of the intellectual property associated with the sludge profiling, PigBal modelling and sludge accumulation rate estimation components of this project is either published elsewhere in the public domain or not suitable for further commercial development. Consequently, it is in the industry's interest to widely disseminate and promote the project methods and outcomes.

The majority of the integrated hydrodynamic-biochemical modelling platform is contained in the form of written documentation and programming scripts designed for open sourced software and is thus suitable to be shared and understood with relative ease. The platform is valuable for interested professionals, such as pond designers and operators, wastewater engineers or biochemical researchers. Until further discussion, the platform will not be shared to external parties without the permission of all associated parties.

## 9. Literature cited

- Abis, K. and Mara, D. (2005). Research on Waste Stabilization Ponds in the United Kingdom: Sludge Accumulation in Pilot-scale Primary Facultative Ponds. *Environmental Technology*, 26(4), p.449-458.
- Alvarado, A., Sanchez, E., Durazno, G., Vesvikar, M. and Nopens, I. (2012). CFD analysis of sludge accumulation and hydraulic performance of a waste stabilization pond. *Water Science and Technology*, 66(11), p.2370-2377.
- Alvarado, A., Vedantam, S., Goethals, P. and Nopens, I. (2012). A compartmental model to describe hydraulics in a full-scale waste stabilization pond. *Water Research*, 46(2), p.521-530.
- Barth, C.L. and Kroes, J. (1985) 'Livestock waste lagoon sludge characterisation', in *Agricultural Waste Utilization and Management. Proceedings of the 5th International Symposium on Agricultural Waste*, 16-17 December, Chicago, IL, ASABE.
- Barth, C.L. (1985). 'The rational design standard for anaerobic livestock waste lagoons', in *Proceedings of the 5th International Symposium on Agricultural Wastes*, St Joseph, MI, USA, American Society of Agricultural Engineers, p.638-647.
- Batstone, D., Keller, J., Angelidaki, I., Kalyuzhnyi, S., Pavlostathis, S., Rozzi, A., Sanders, W., Siegrist, H. and Vavilin, V. (2002). The IWA Anaerobic Digestion Model No 1 (ADM1). *Water Science and Technology*, 45(10), p.65-73.
- Bellandi, G., De Mulder, C., Van Hoey, S., Rehman, U., Amerlinck, Y., Guo, L., Vanrolleghem, P., Weijers, S., Gori, R. and Nopens, I. (2019). Tanks in series versus compartmental model configuration: considering hydrodynamics helps in parameter estimation for an N<sub>2</sub>O model. *Water Science and Technology*, 79(1), p.73-83.
- Bioprocess Control (2016). 'AMPTS II and & AMPTS II Light - Automatic Methane Potential Test System', Operation and Maintenance Manual, Version 3.0, June 2016, Bioprocess Control Sweden.
- Brennan, D. (2001). 'The numerical simulation of two phase flows in settling tanks', Imperial College London (University of London).
- Brennen, C.E. (2005). 'Fundamentals of multiphase flow' (Cambridge university press).
- Chastain, J.P. (2006). 'Estimation sludge accumulation in lagoons', ASABE Paper No. 064114. St. Joseph, Michigan, ASABE.
- Craig, K., Nieuwoudt, M. and Niemand, L. (2013). CFD simulation of anaerobic digester with variable sewage sludge rheology. *Water Research*, 47(13), p.4485-4497.
- Duperouzel, D. (2005). 'Making waves in anaerobic pond treatment systems', Wasteline #13, Department of Primary Industries and Fisheries, Toowoomba, Qld.

Eshtiaghi, N., Markis, F., Yap, S., Baudez, J. and Slatter, P. (2013). Rheological characterisation of municipal sludge: A review. *Water Research*, 47(15), p.5493-5510.

Gernaey, K., Vanrolleghem, P. and Lessard, P. (2001). Modeling of a reactive primary clarifier. *Water Science and Technology*, 43(7), p.73-81.

Ho, L., Van Echelpoel, W. and Goethals, P. (2017). Design of waste stabilization pond systems: A review. *Water Research*, 123, p.236-248.

Jensen, P., Ge, H. and Batstone, D. (2011). Assessing the role of biochemical methane potential tests in determining anaerobic degradability rate and extent. *Water Science and Technology*, 64(4), p.880-886.

Lakehal, D., Krebs, P., Krijgsman, J. and Rodi, W. (1999). Computing Shear Flow and Sludge Blanket in Secondary Clarifiers. *Journal of Hydraulic Engineering*, 125(3), p.253-262.

Moukalled, F., Mangani, L., and Darwish, M. (2016). 'The finite volume method in computational fluid dynamics - An Advanced Introduction with OpenFOAM and Matlab'. Springer International Publishing Switzerland. DOI 10.1007/978-3-319-16874-6

Nelson, K., Cisneros, B., Tchobanoglous, G. and Darby, J. (2004). Sludge accumulation, characteristics, and pathogen inactivation in four primary waste stabilization ponds in central Mexico. *Water Research*, 38(1), p.111-127.

Papadopoulos, A., Parisopoulos, G., Papadopoulos, F. and Karteris, A. (2003). Sludge accumulation pattern in an anaerobic pond under Mediterranean climatic conditions. *Water Research*, 37(3), p.634-644.

Passos, R., Dias, D. and von Sperling, M. (2016). Review of practical aspects for modelling of stabilization ponds using Computational Fluid Dynamics. *Environmental Technology Reviews*, 5(1), p.78-102.

Peterson, E., Harris, J. and Wadhwa, L. (2000). CFD modelling pond dynamic processes. *Aquacultural Engineering*, 23(1-3), p.61-93.

Picot, B., Sambuco, J., Brouillet, J. and Riviere, Y. (2005). Wastewater stabilisation ponds: sludge accumulation, technical and financial study on desludging and sludge disposal case studies in France. *Water Science and Technology*, 51(12), p.227-234.

Richmond, A. and Grobbelaar, J. (1986). Factors affecting the output rate of *Spirulina platensis* with reference to mass cultivation. *Biomass*, 10(4), p.253-264.

Singh, K., Worley, J. and Risse, M. (2007) 'Sludge measurement using global positioning system (GPS) enabled sonar', in Proceedings of the International Symposium on Air Quality and Waste Management for Agriculture, ASABE.

Skerman, A., Collman, G., Duperouzel, D., Sohn, J., Atzeni, M. and Kelly, A. (2008). 'Improved piggery effluent management systems incorporating highly loaded primary ponds', Final report to Australian

Pork Limited (APL), Project 2108, Department of Primary Industries and Fisheries (DPI&F), Toowoomba, Queensland. <https://australianpork.infoservices.com.au/items/2006-2108-REPORT>

Skerman, A., Willis, S., Batstone, D., Yap, S. and Tait, S. (2017). Effect of feed wastage on piggery effluent characteristics. *Animal Production Science*, 57(12), p.2481.

Skerman, A.G., Willis, S., McGahan E.J. and Marquardt, B. (2013). 'PigBal 4 - A model for estimating piggery waste production', Department of Agriculture, Fisheries and Forestry, Queensland, and Australian Pork Limited. Available for download from APL website: <http://australianpork.com.au/industry-focus/environment/waste-management-pigbal/>

Sutherland, D., Turnbull, M. and Craggs, R. (2014). Increased pond depth improves algal productivity and nutrient removal in wastewater treatment high rate algal ponds. *Water Research*, 53, p.271-281.

Takács, I., Patry, G.G., and Nolasco, D. (1991). 'A dynamic model of the clarification-thickening process', *Water Research*, 25, p.1263-71.

Weiss, M., Plósz, B., Essemiani, K. and Meinhold, J. (2007). Suction-lift sludge removal and non-Newtonian flow behaviour in circular secondary clarifiers: Numerical modelling and measurements. *Chemical Engineering Journal*, 132(1-3), p.241-255.

Westerman, P., Shaffer, K.A. and Rice, J.M. (2008). 'Sludge survey methods of anaerobic lagoons', Northern Carolina State University, Published by North Carolina Cooperative Extension, Raleigh, NC. [http://www.ncagr.gov/SWc/tech/documents/sludge\\_survey.pdf](http://www.ncagr.gov/SWc/tech/documents/sludge_survey.pdf)

Yang, F., Bick, A., Shandalov, S., Brenner, A. and Oron, G. (2009). Yield stress and rheological characteristics of activated sludge in an airlift membrane bioreactor. *Journal of Membrane Science*, 334(1-2), p.83-90.

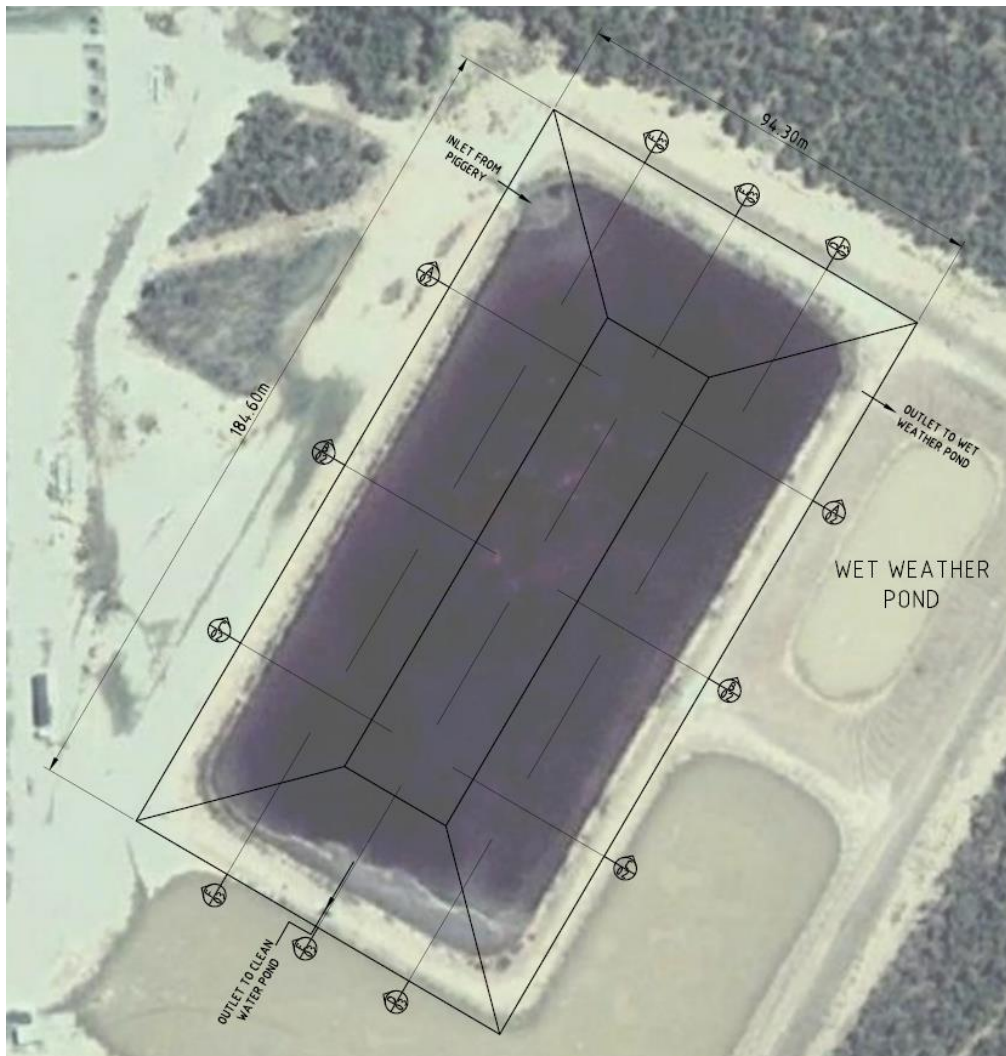
## **10. Publications Arising**

Much of this hydrodynamic modelling content of this report has been repurposed for a conference proceeding the upcoming 10th International Water Association Symposium on Modelling and Integrated Assessment (Watermatex, 2019) to be held in Copenhagen, Denmark, September 2019. The paper is tentatively titled: “A numerical study on evaluating the depth effect on the flow characteristics of the waste stabilisation ponds,” and an abstract has been submitted for review. The final paper may include any of the results contained in this report. Potentially sensitive intellectual property relating to the APL piggery ponds, such as pond dimensions, operational parameters and experimental results may be included to provide context. No submissions or publications will proceed without permission from all associated parties.

The AWMC is also preparing an article to be submitted for publication in a peer-reviewed scientific journal. The article is intended for the journal *Water Research* (ISSN: 0043-1354). While still in formulating stages, the article is intended to provide novel modifications to existing modelling techniques and highlight the effects of unique pond design on flow characteristics, solids behaviour and operational outcomes. Similarly, the article will likely use many of the results contained in this report and may include potentially sensitive intellectual property to provide context. No submissions or publications will proceed without permission from all associated parties.

**Appendix A - Pond cross-sections produced by the Premise Agriculture sludge surveys.**

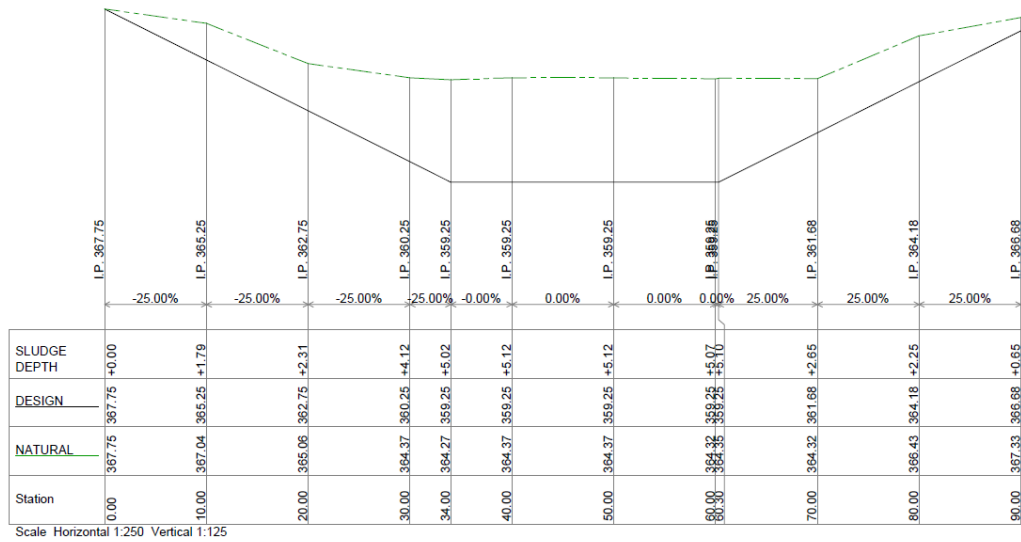
**A1. Piggery A, Pond 1.**







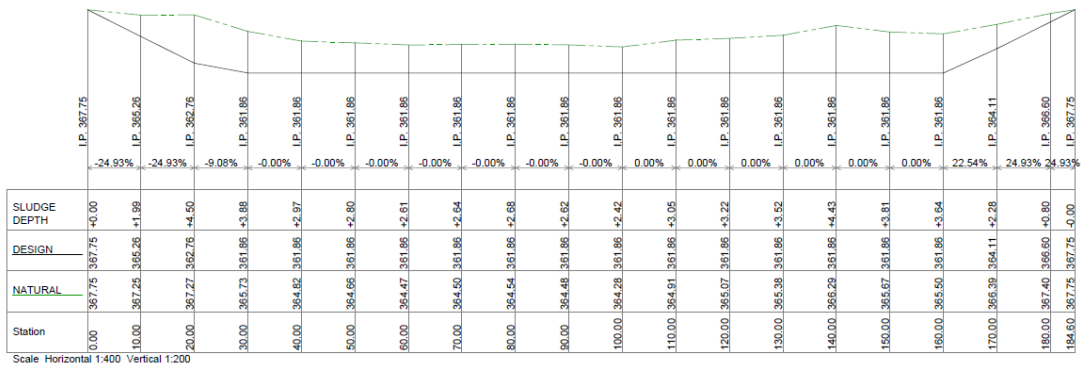
SECTION A  
01



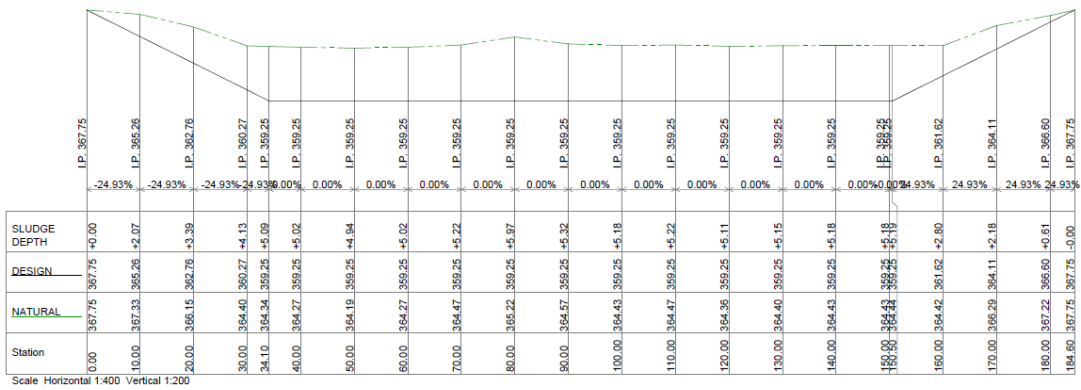
SECTION B  
01



SECTION C  
01



SECTION D  
01



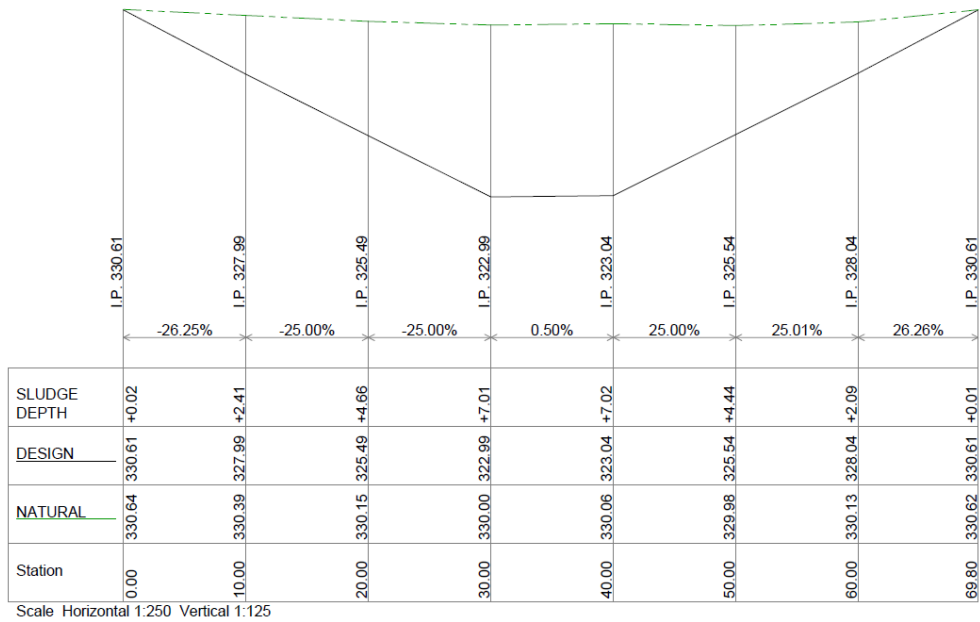
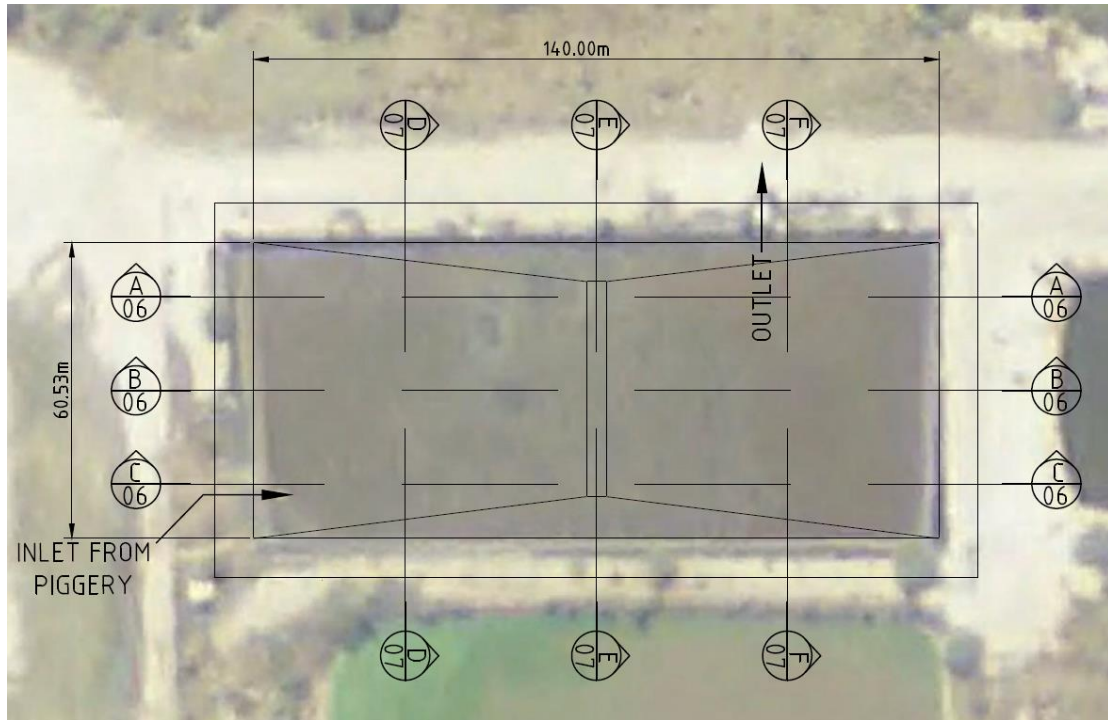
SECTION E  
01



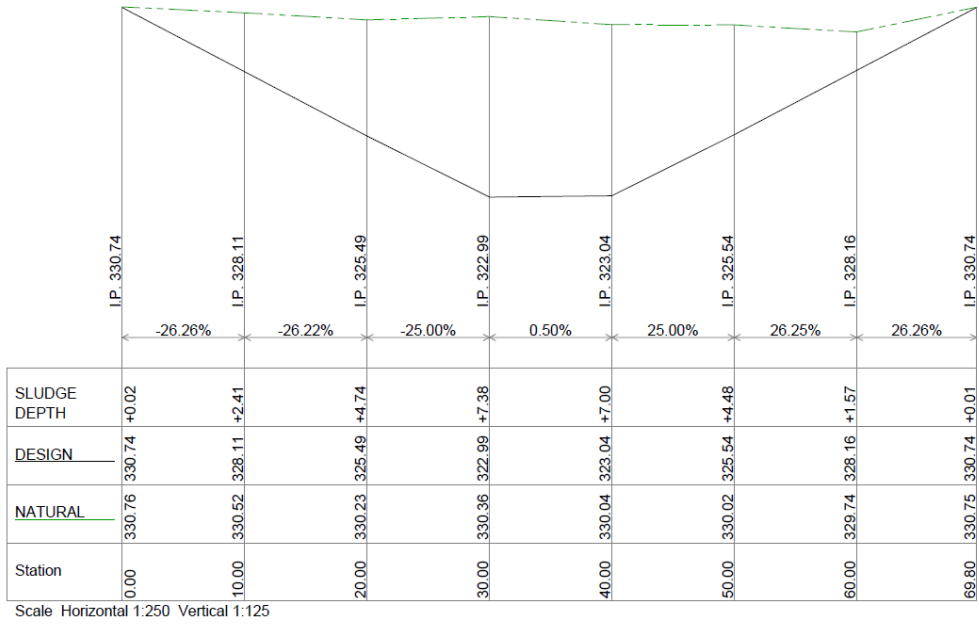
Scale Horizontal 1:400 Vertical 1:200

SECTION F  
01

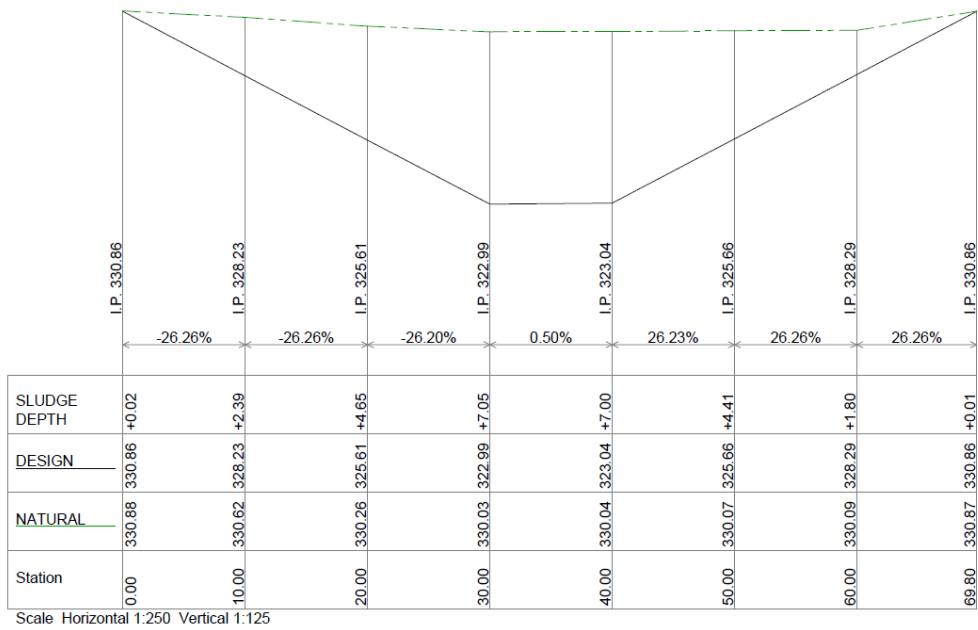
**A2. Piggery A, Pond 2**



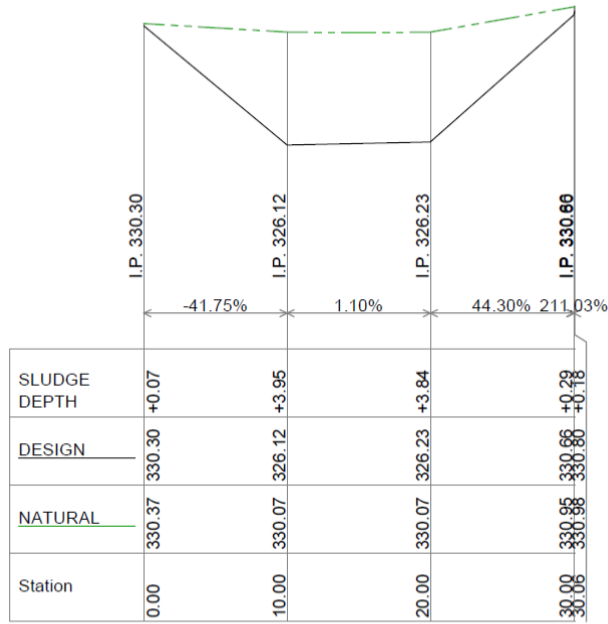
**SECTION A**  
**05**



SECTION **B**  
05

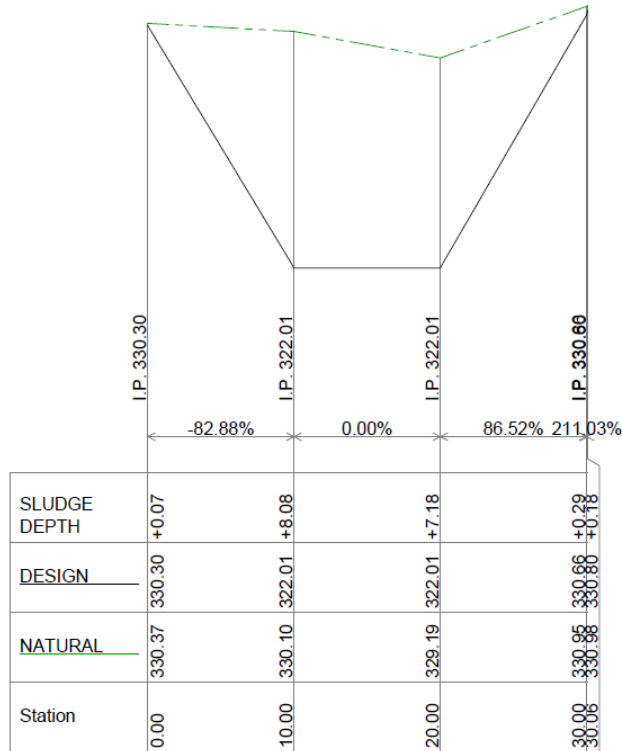


SECTION **C**  
05



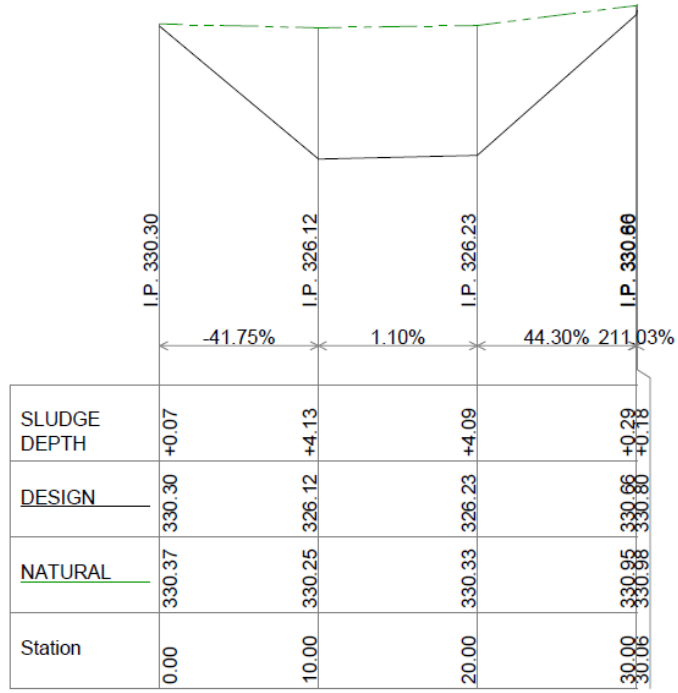
Scale Horizontal 1:250 Vertical 1:125

SECTION **D**  
05



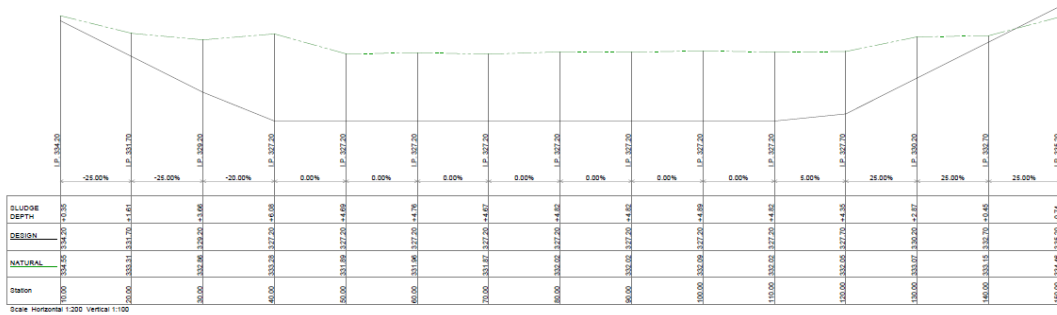
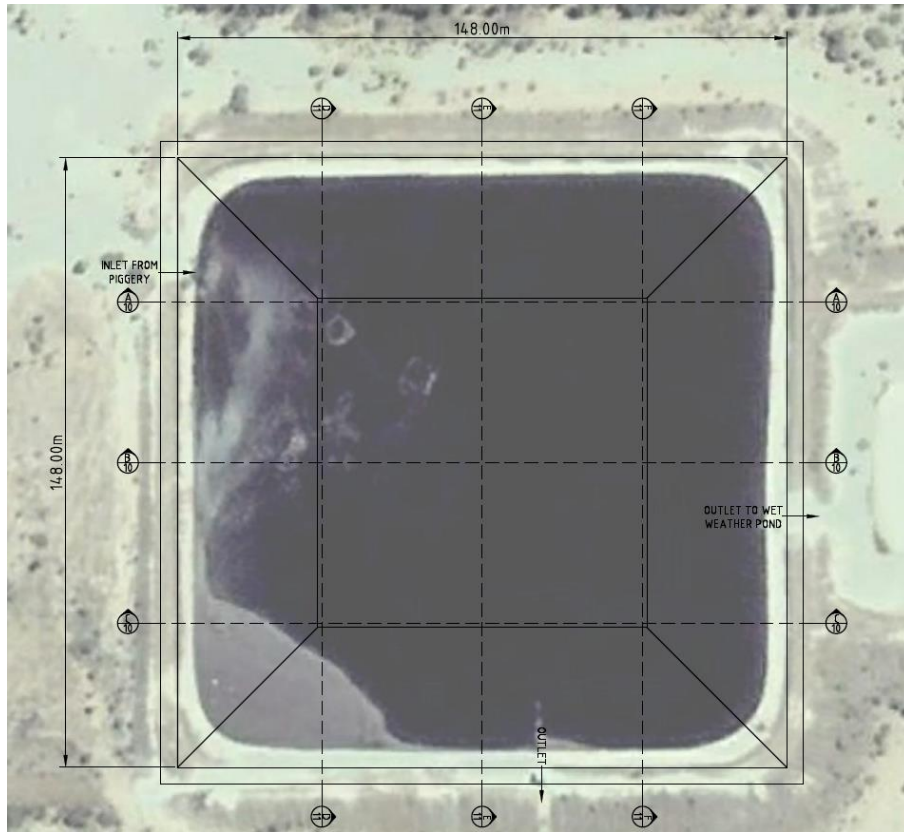
Scale Horizontal 1:250 Vertical 1:125

SECTION **E**  
05

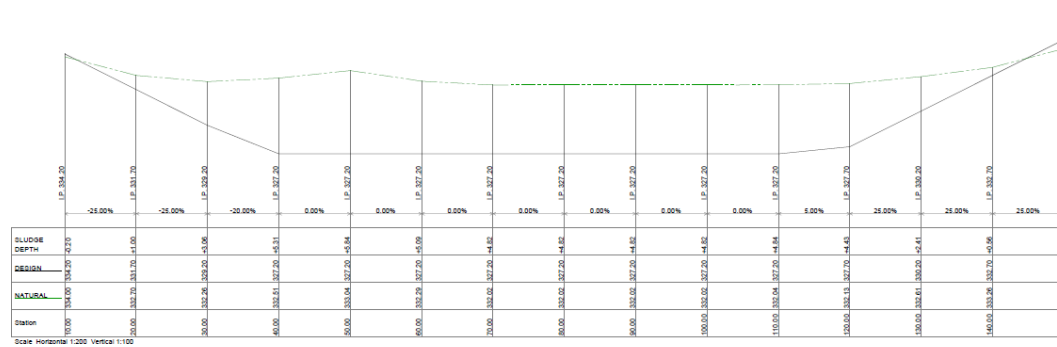


SECTION **F**  
05

### A3. Piggery A, Pond 3

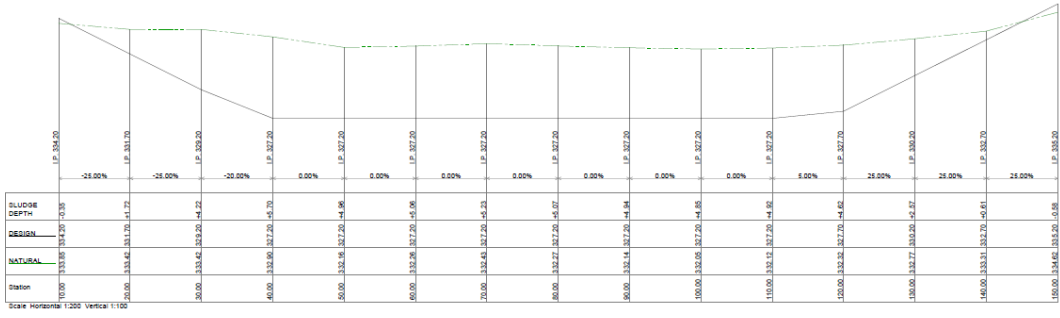


SECTION A-A

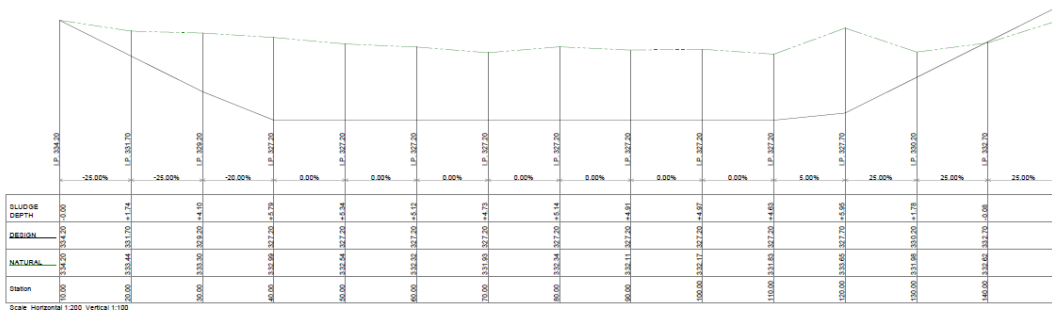


SECTION B-B

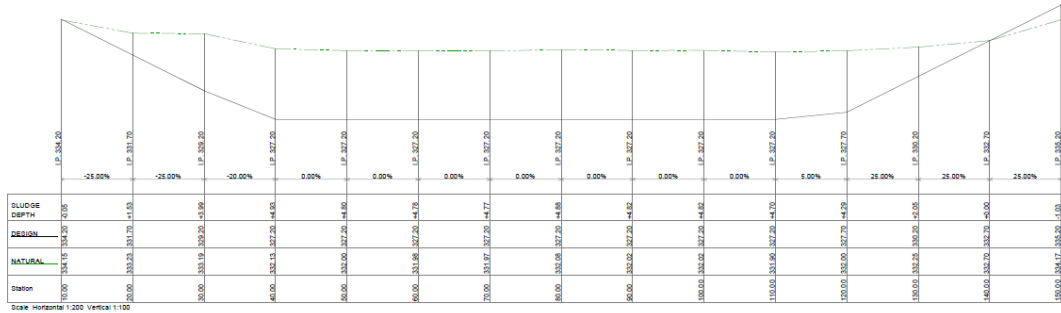




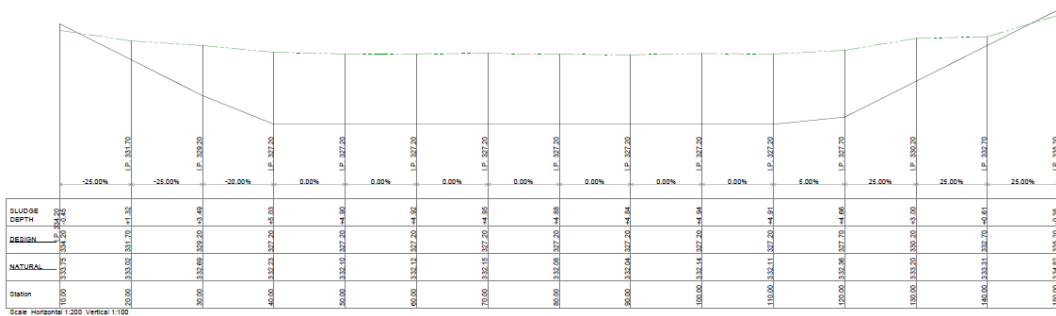
SECTION C  
09



SECTION D  
09

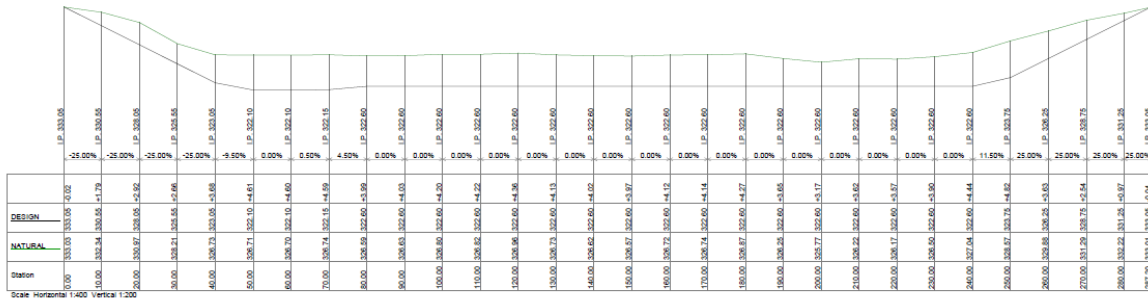
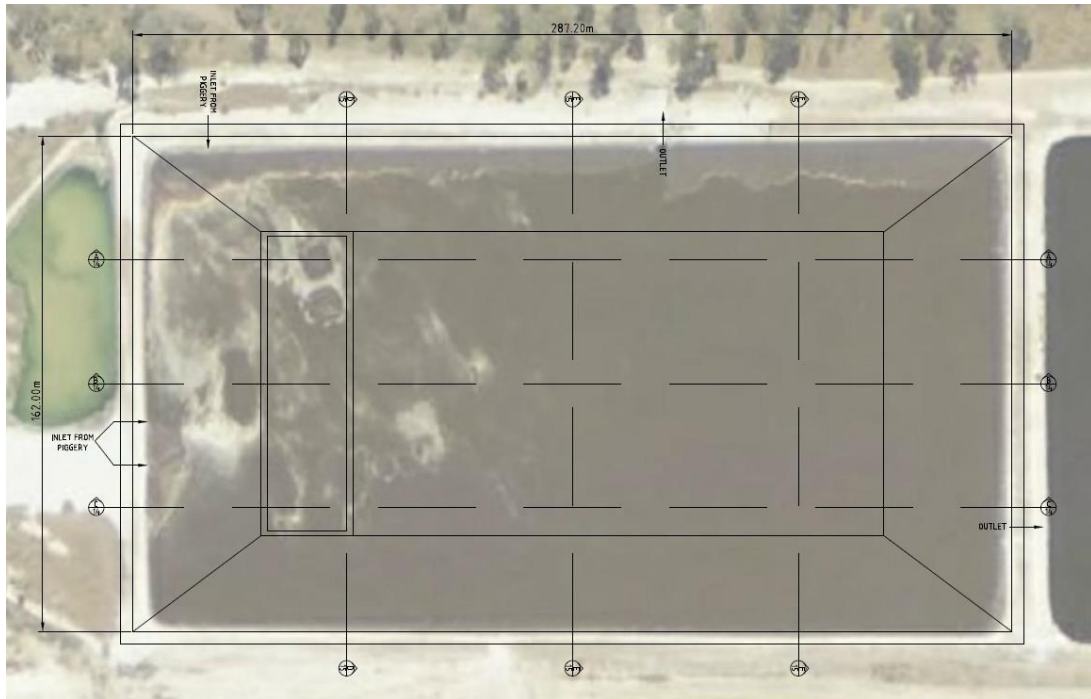


SECTION E  
09

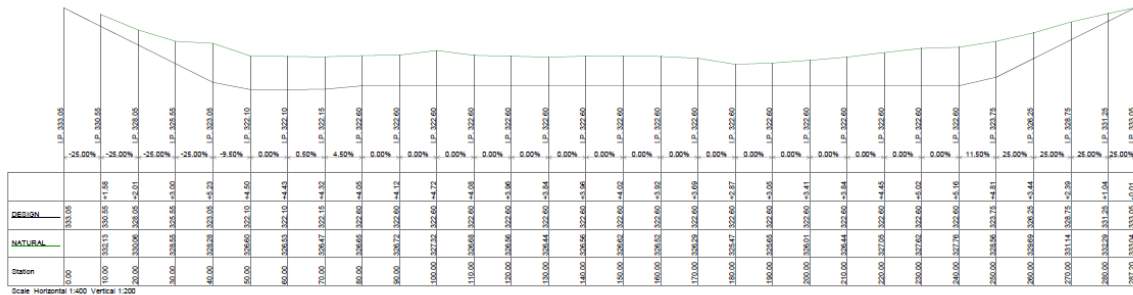


SECTION F  
09

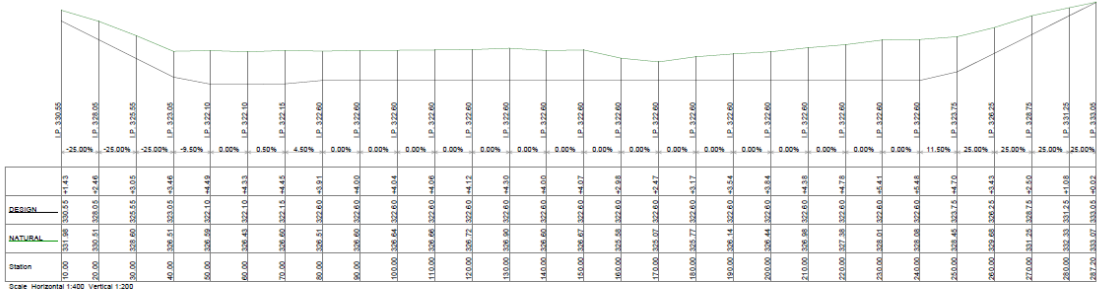
# A4. Piggery A, Pond 4



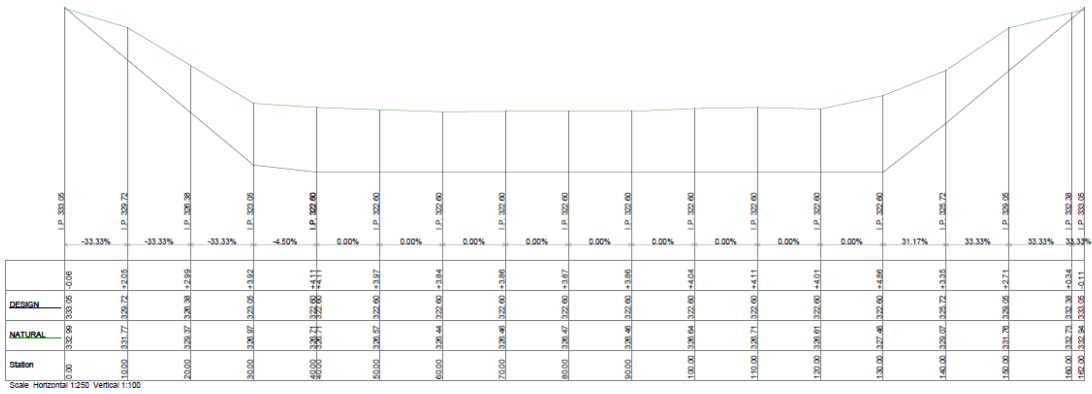
SECTION A-A



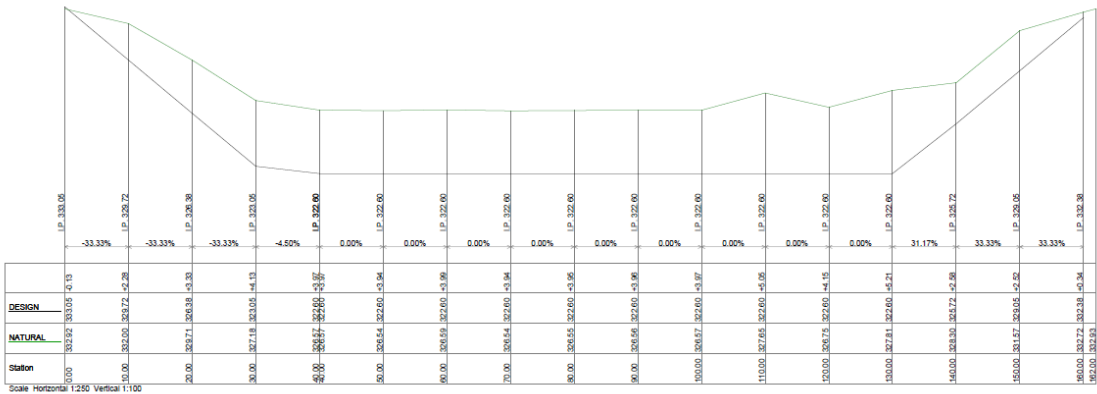
SECTION B-B



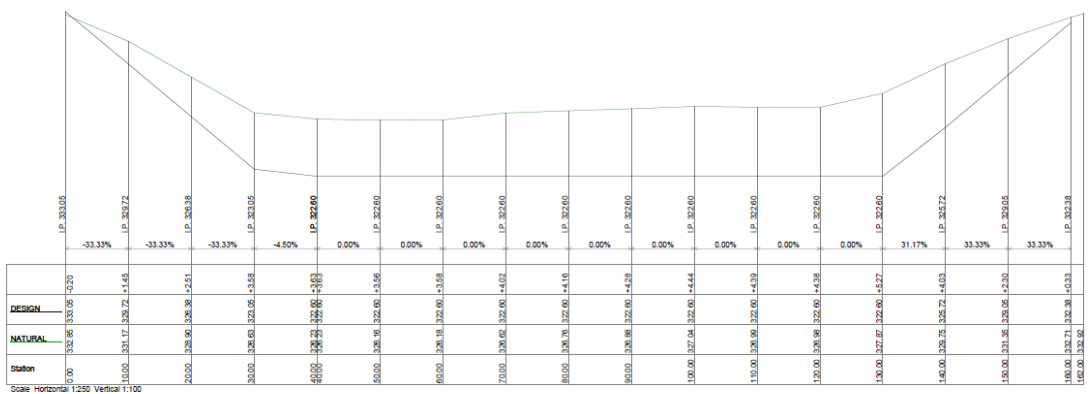
SECTION C



SECTION D

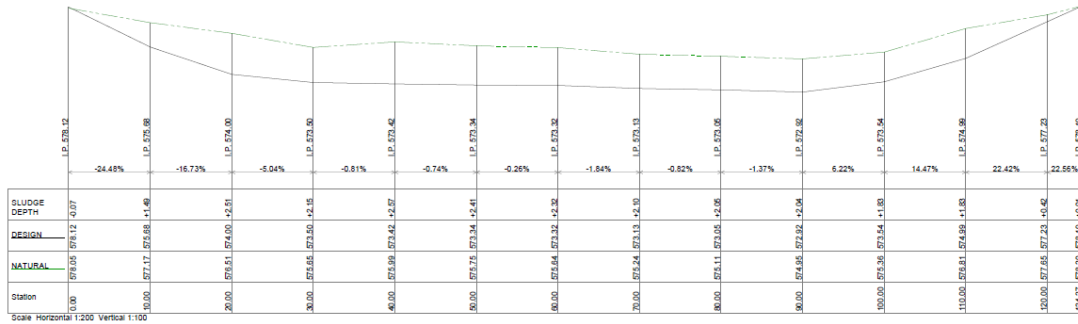
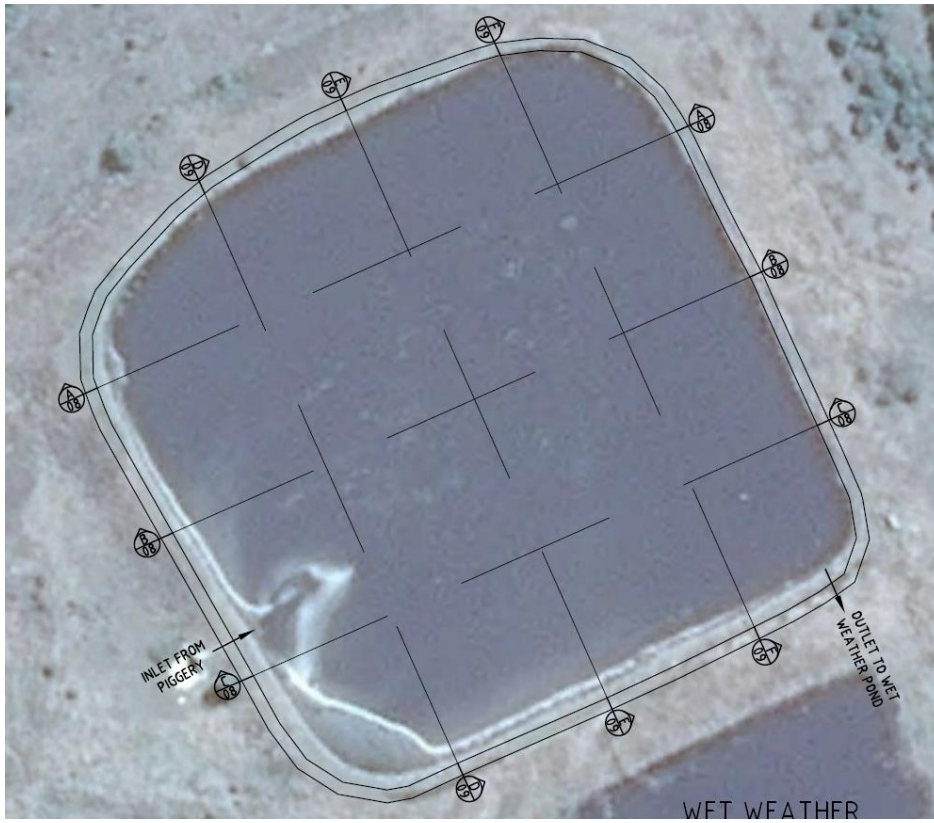


SECTION E

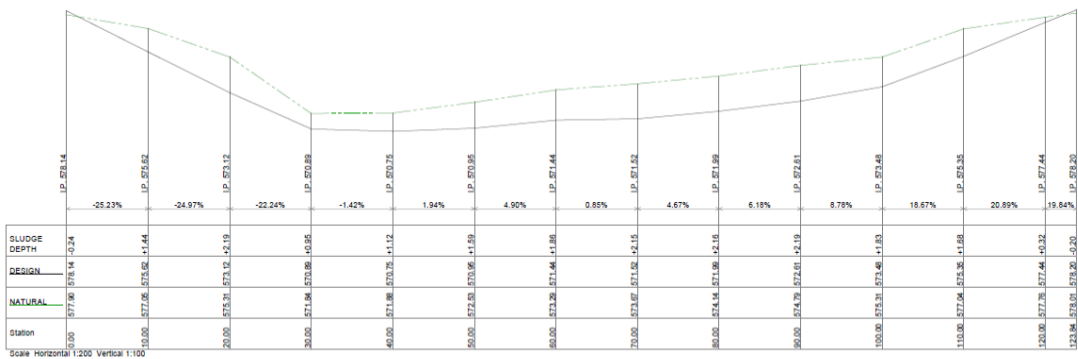


SECTION F

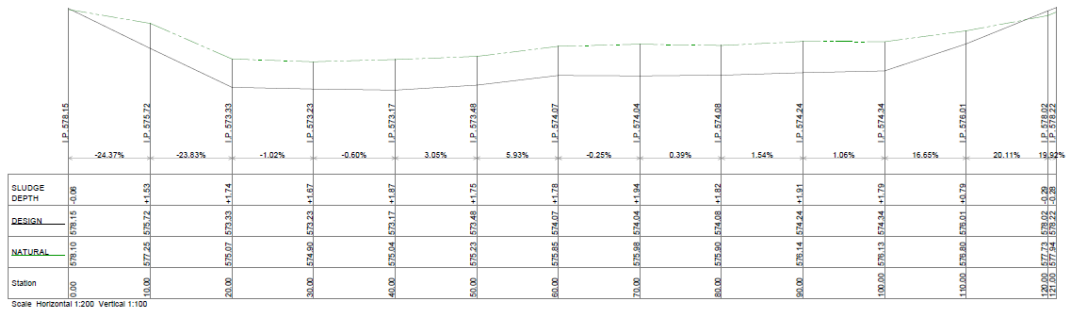
# A5. Piggery B, Pond 5



SECTION A-A



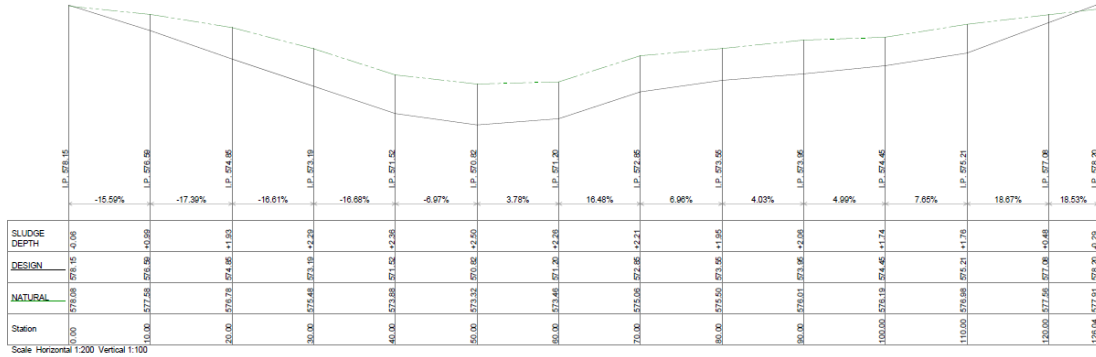
SECTION B-B



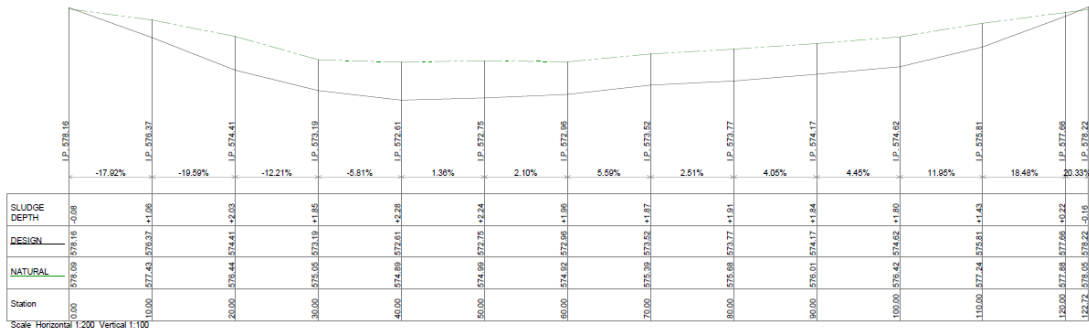
SECTION C  
37



SECTION D  
37

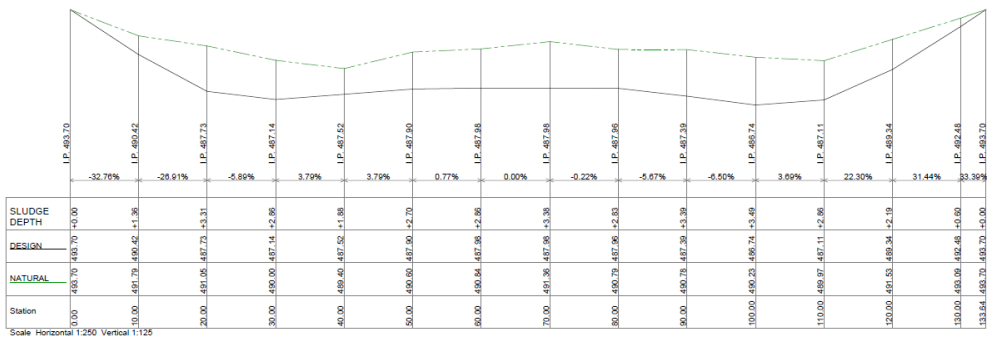


SECTION E  
37

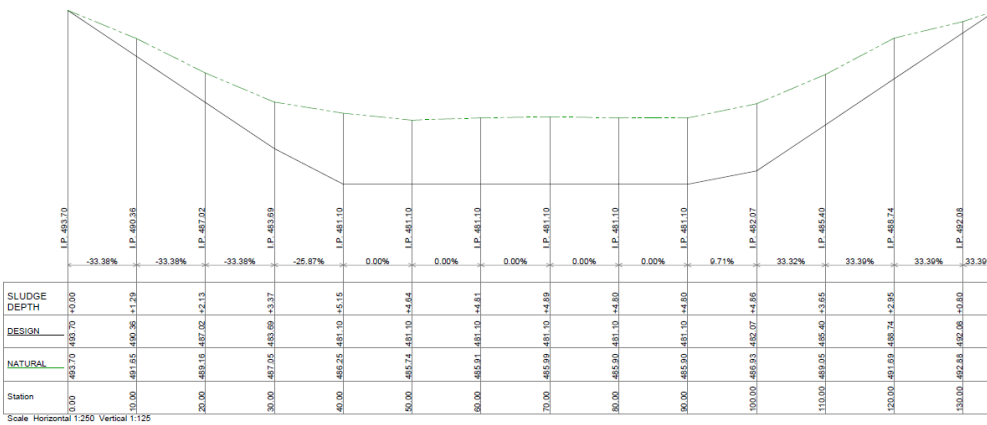


SECTION F  
37

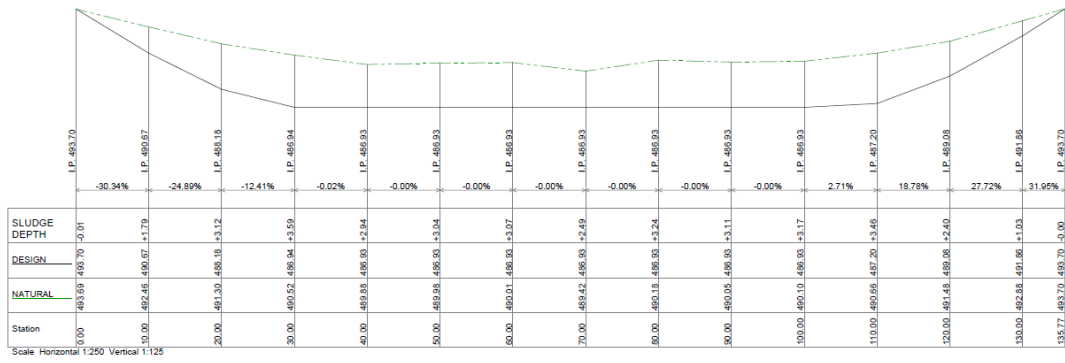
# A6. Piggery C, Pond 6



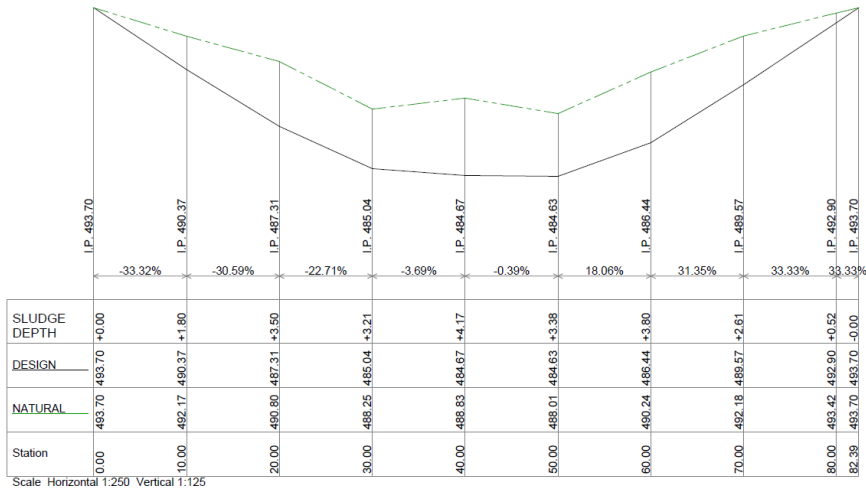
SECTION A  
17



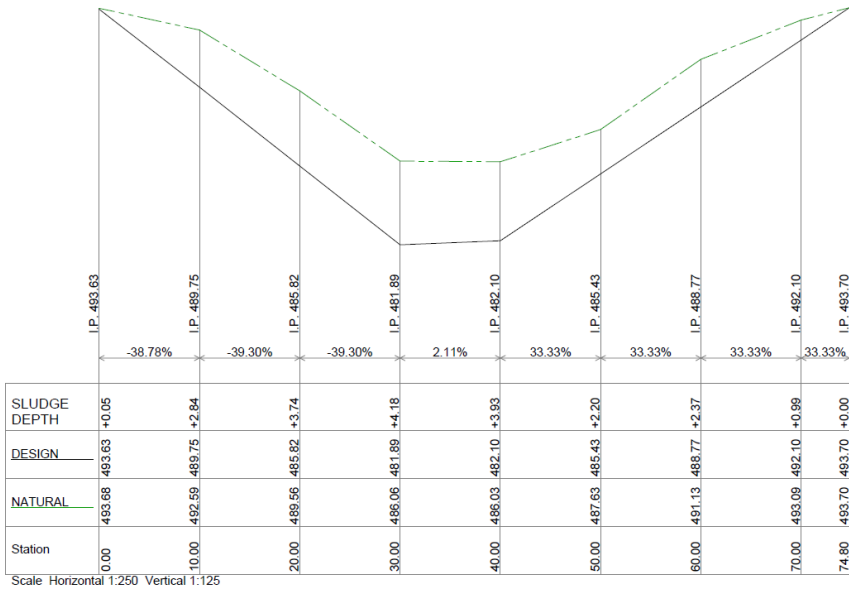
SECTION B  
17



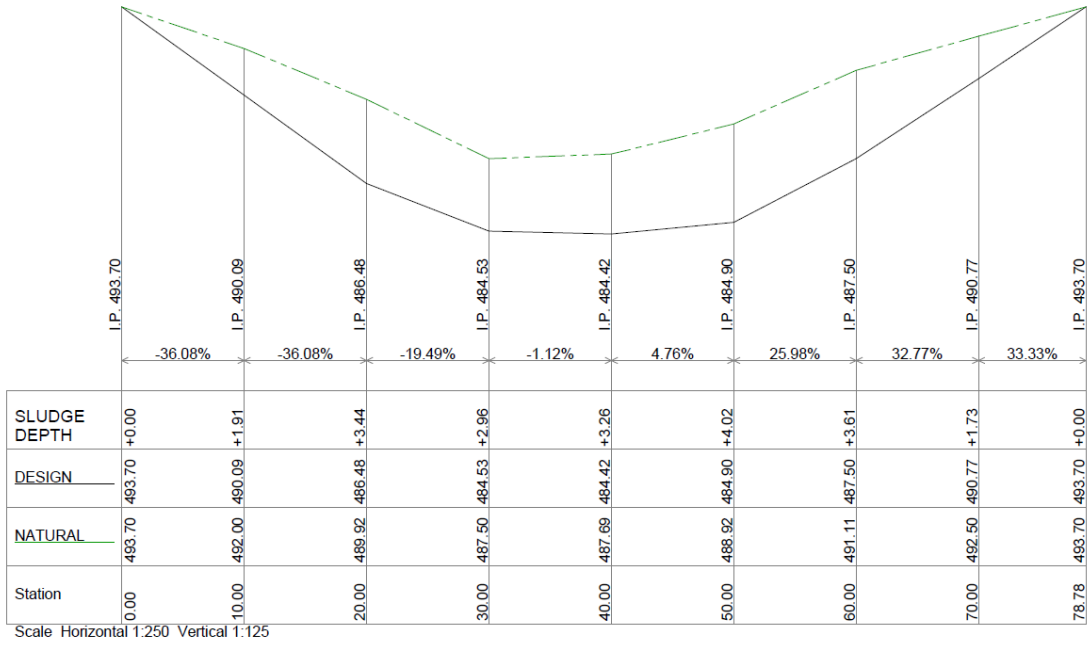
SECTION C  
17



SECTION D  
17



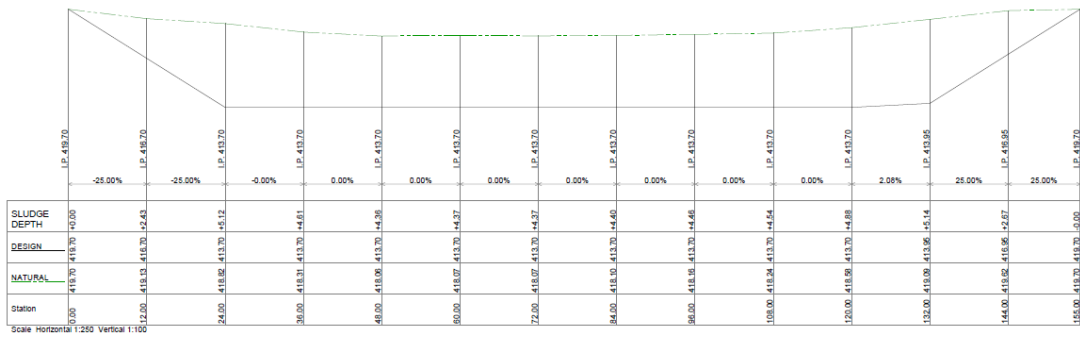
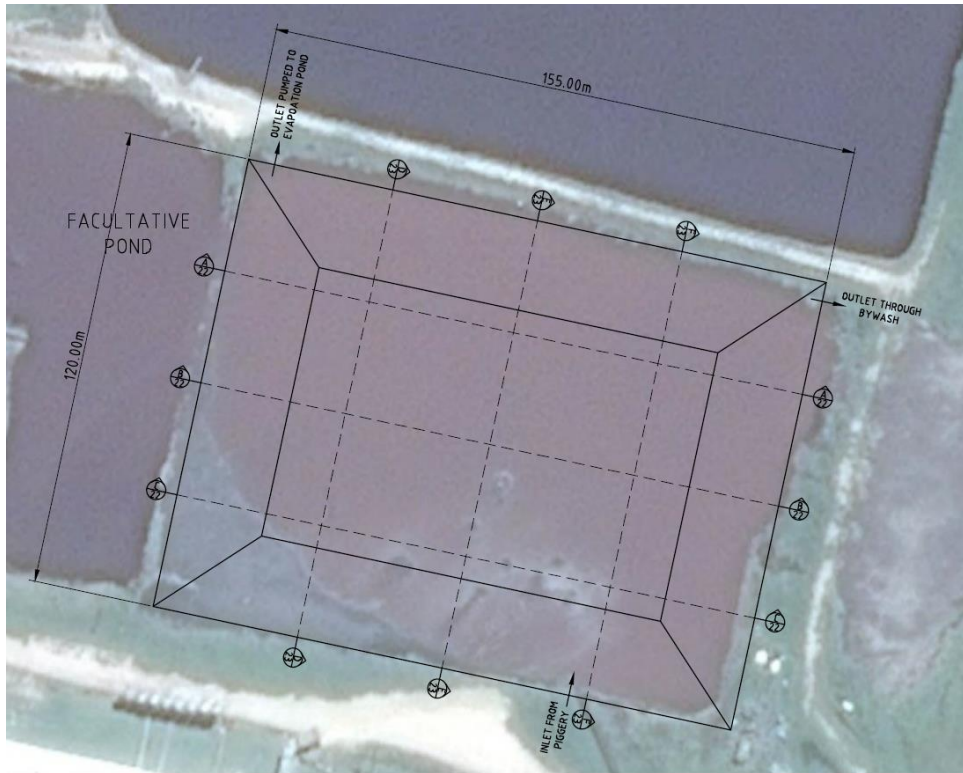
SECTION E  
17



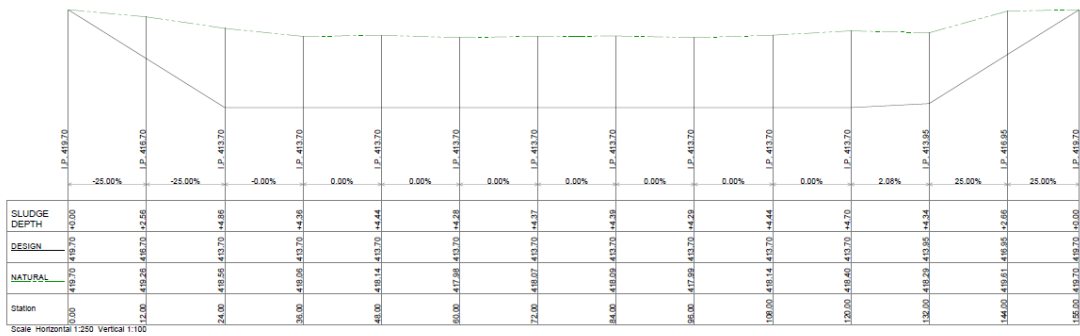
SECTION **F**  
17



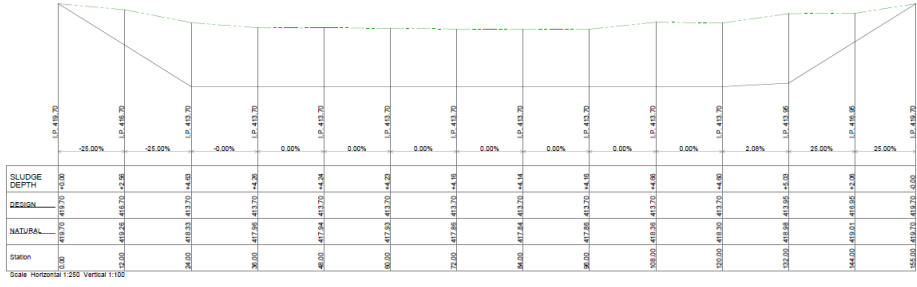
# A7. Piggery D, Pond 7



SECTION A-A



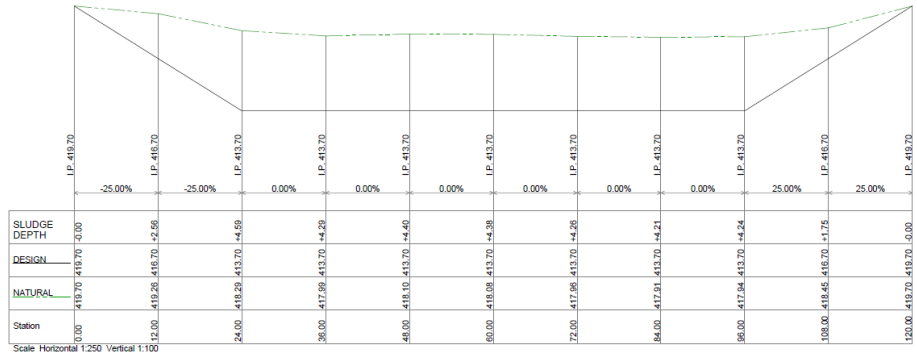
SECTION B-B



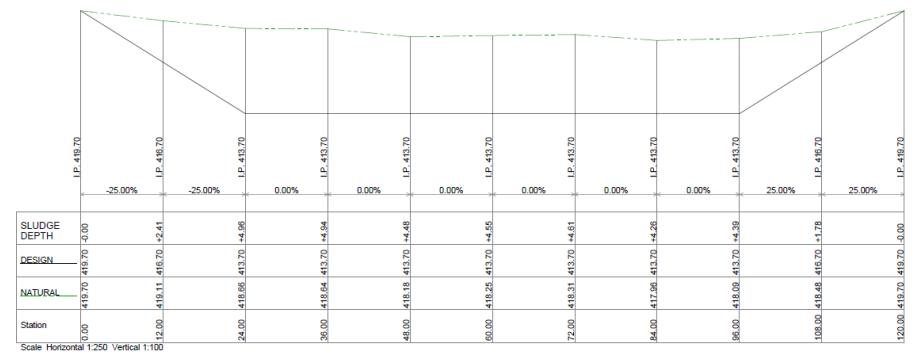
SECTION C/21



SECTION D/21

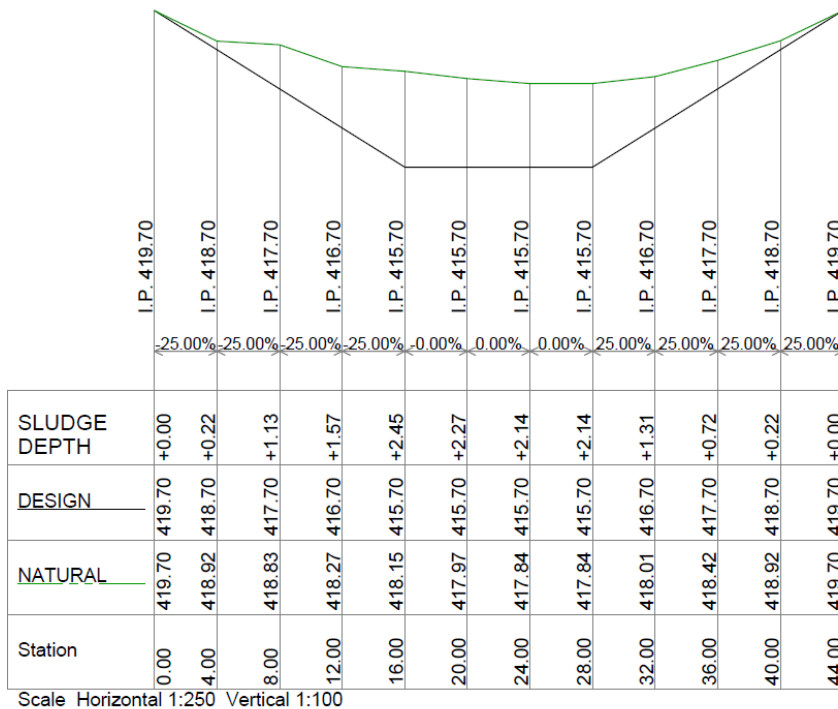
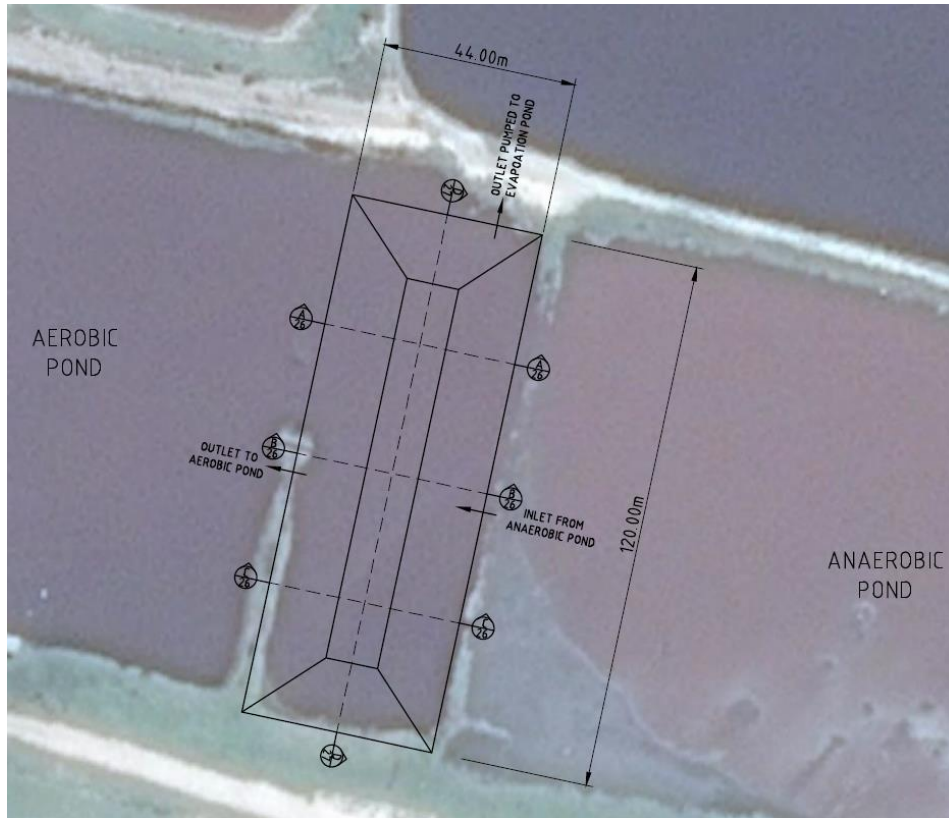


SECTION E/21



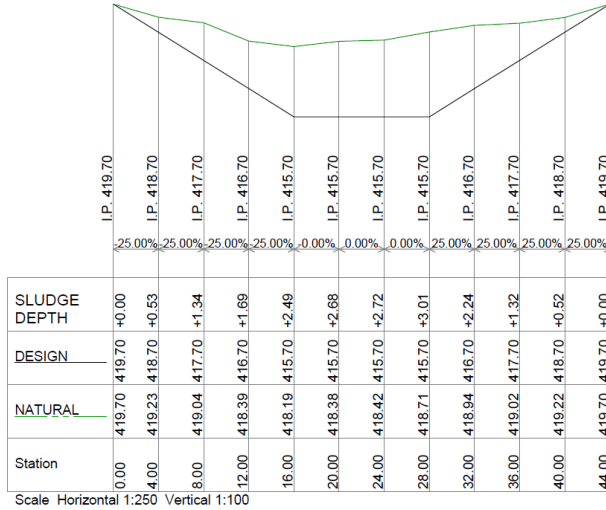
SECTION F/21

**A8. Piggery D, Pond 8**

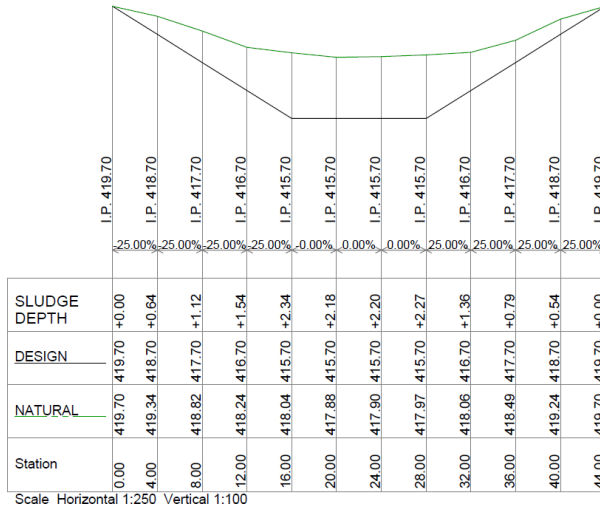


**SECTION A**





SECTION B  
25

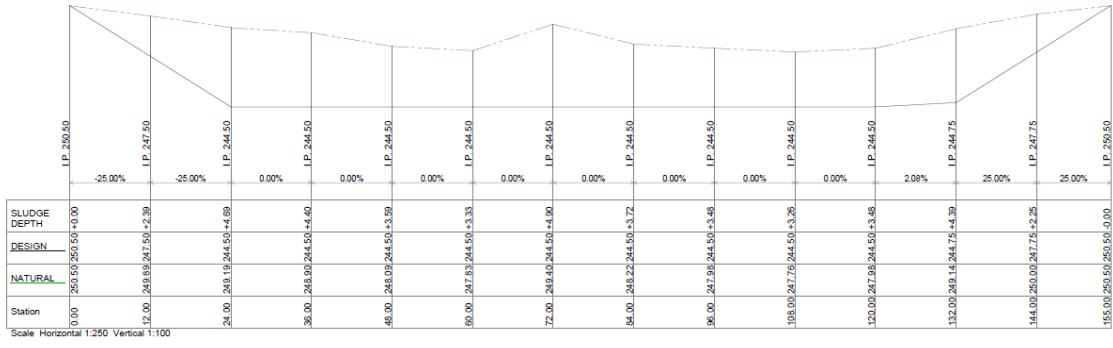
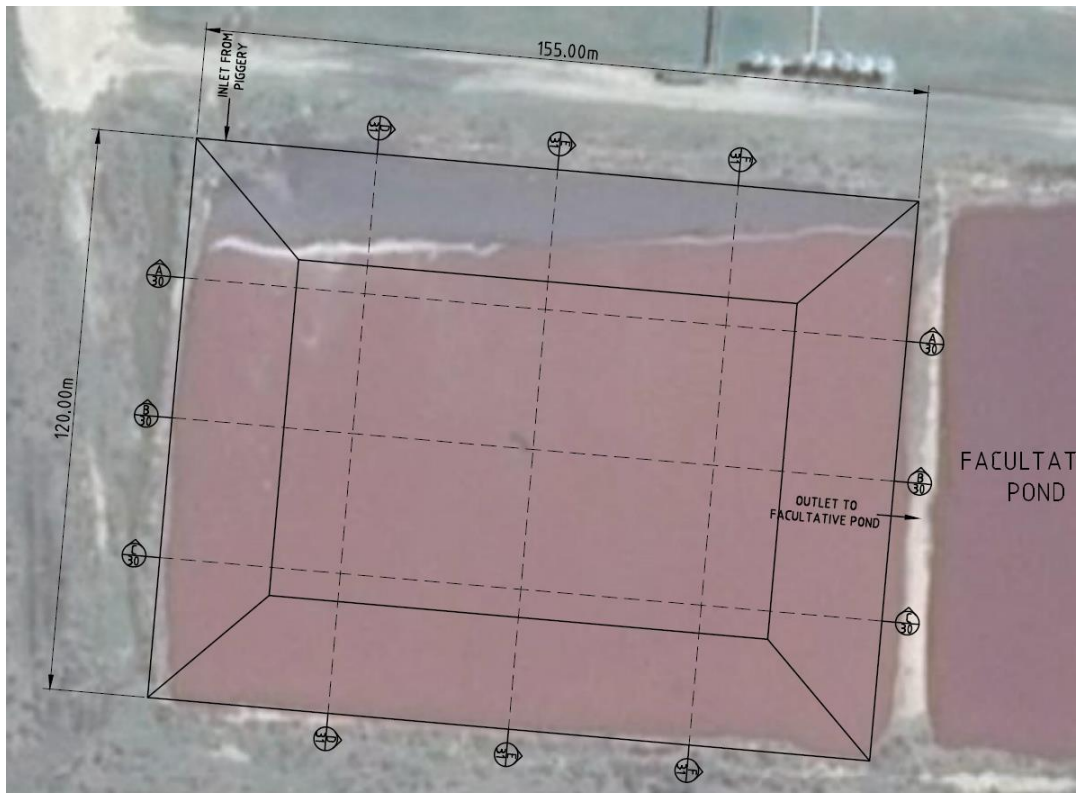


SECTION C  
25

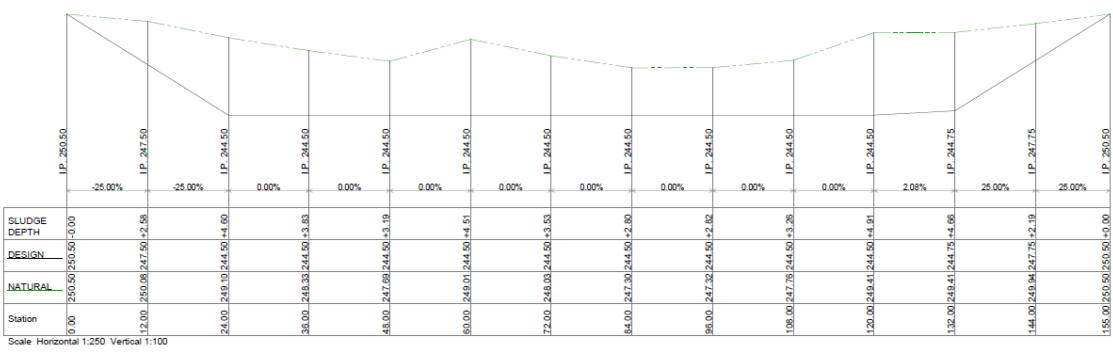


SECTION D  
25

# A9. Piggery E, Pond 9



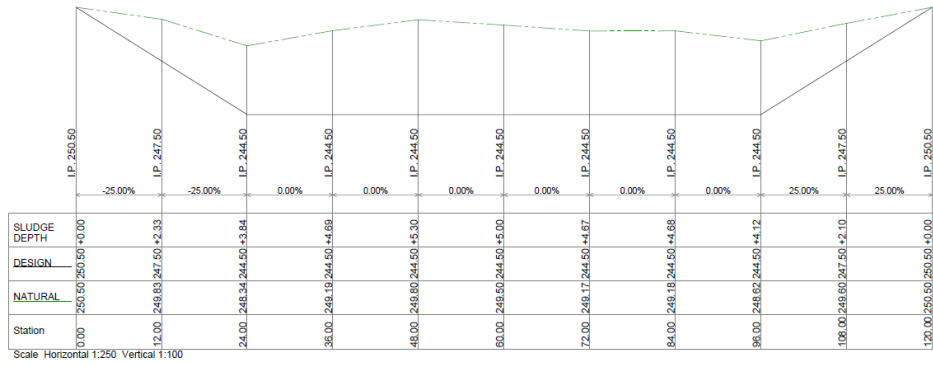
SECTION A-A



SECTION B-B



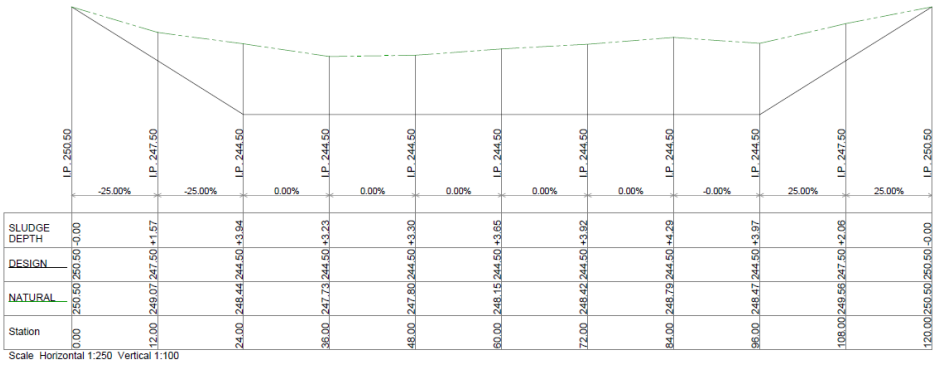
SECTION C



SECTION D

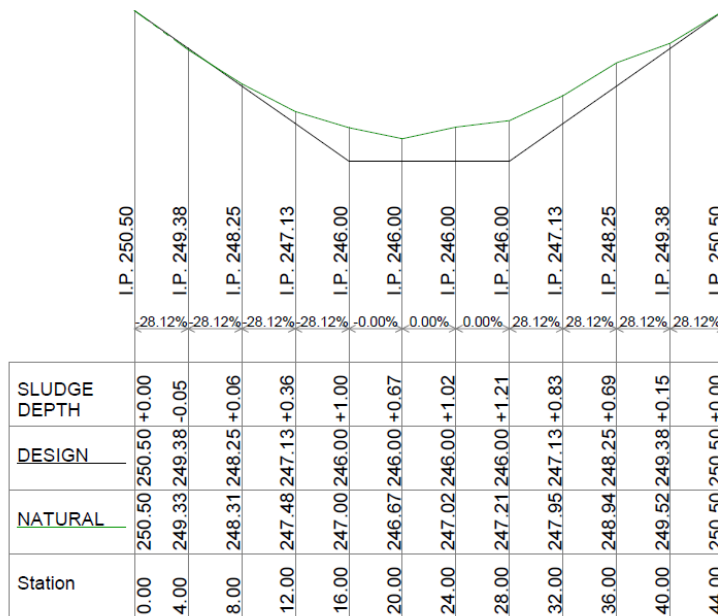
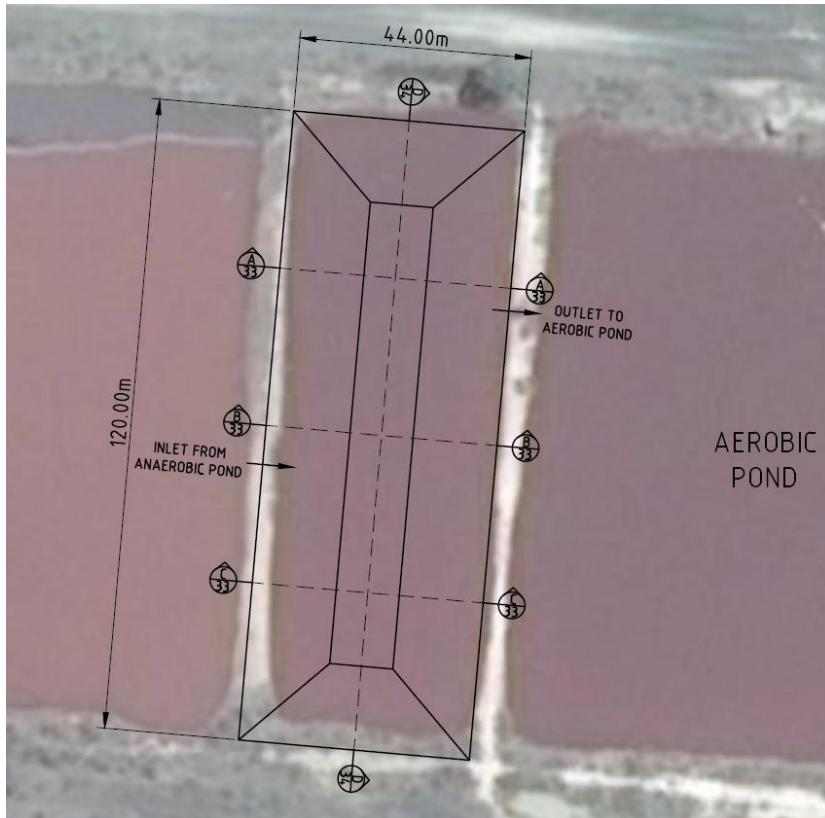


SECTION E



SECTION F

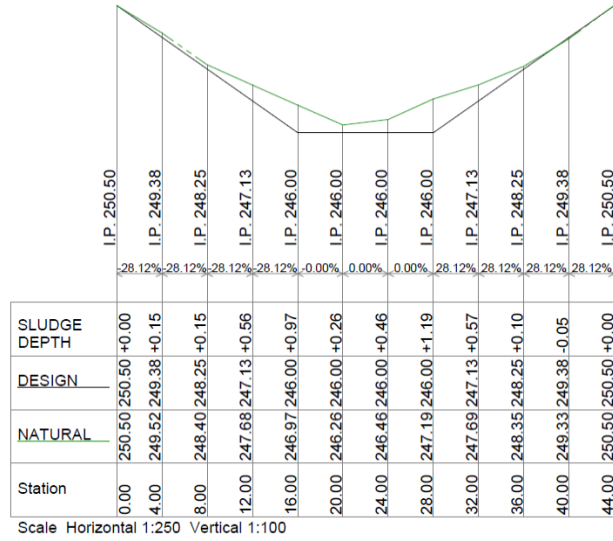
**A10. Piggery E, Pond 10**



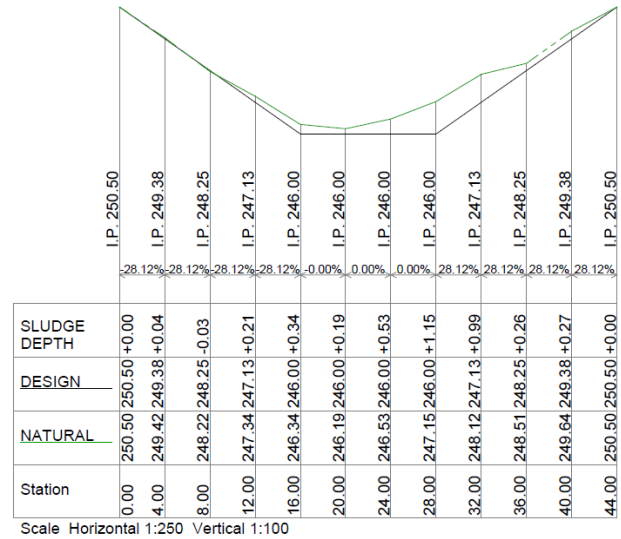
Scale Horizontal 1:250 Vertical 1:100

**SECTION A**

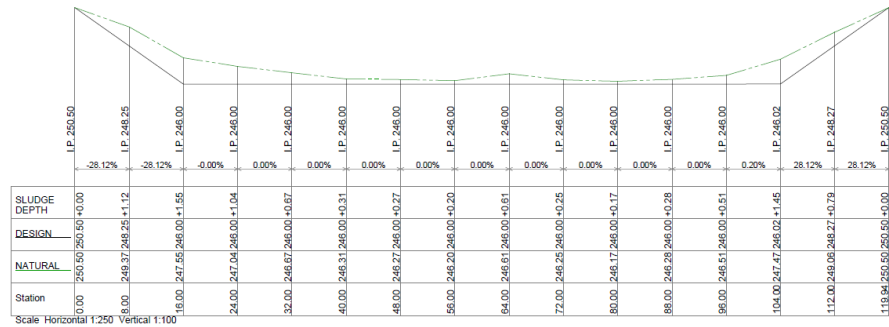
33



SECTION B  
33



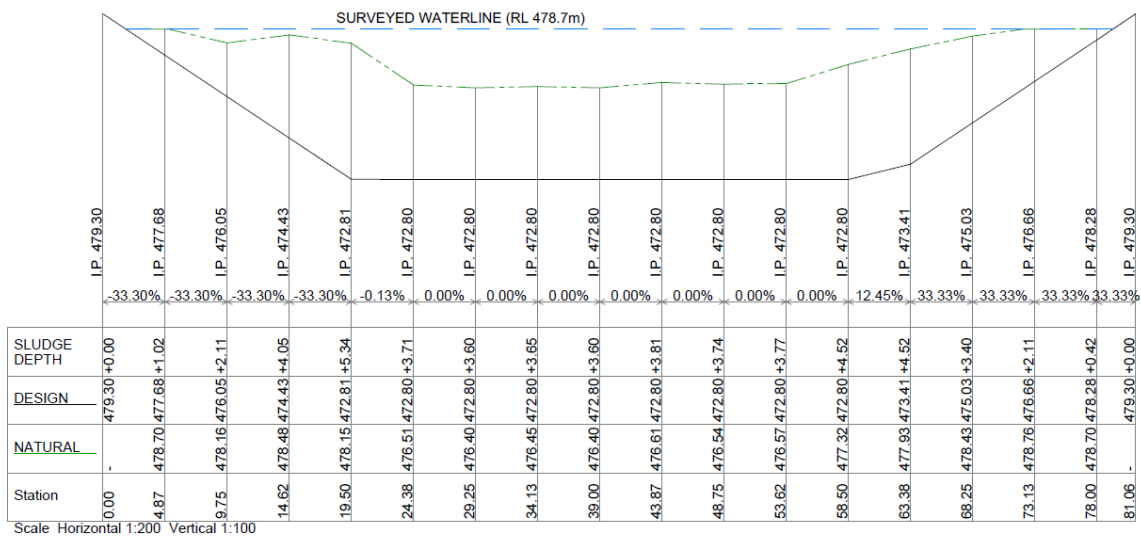
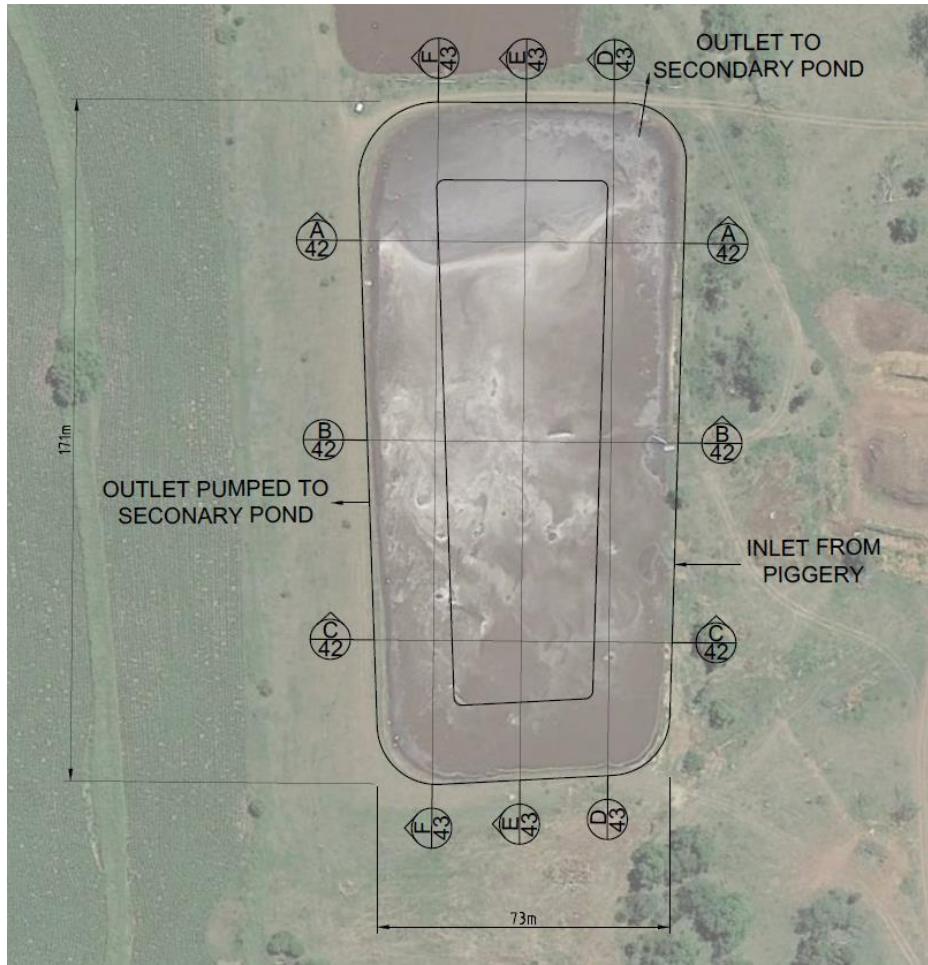
SECTION C  
33



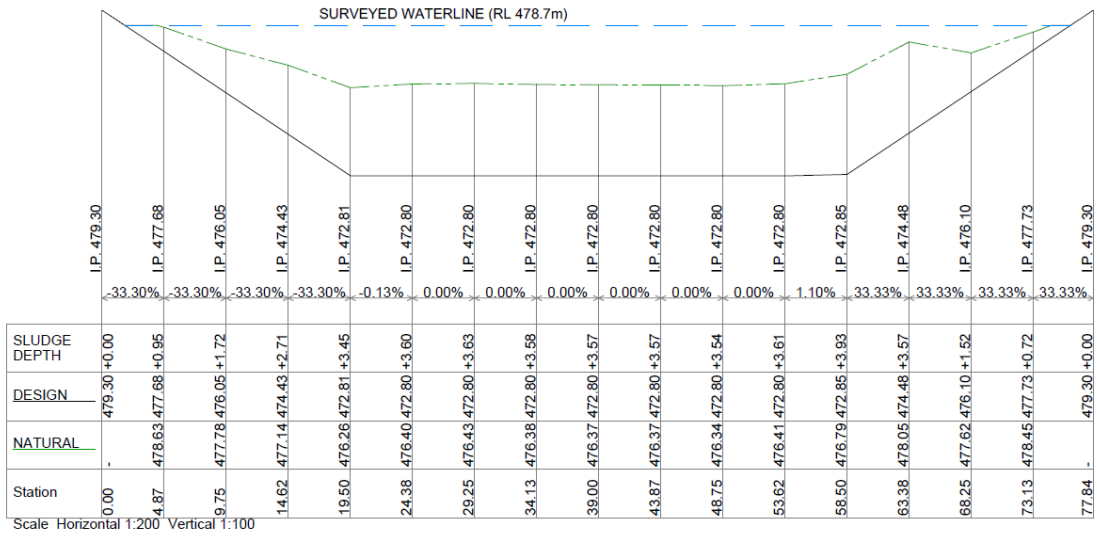
SECTION D  
33



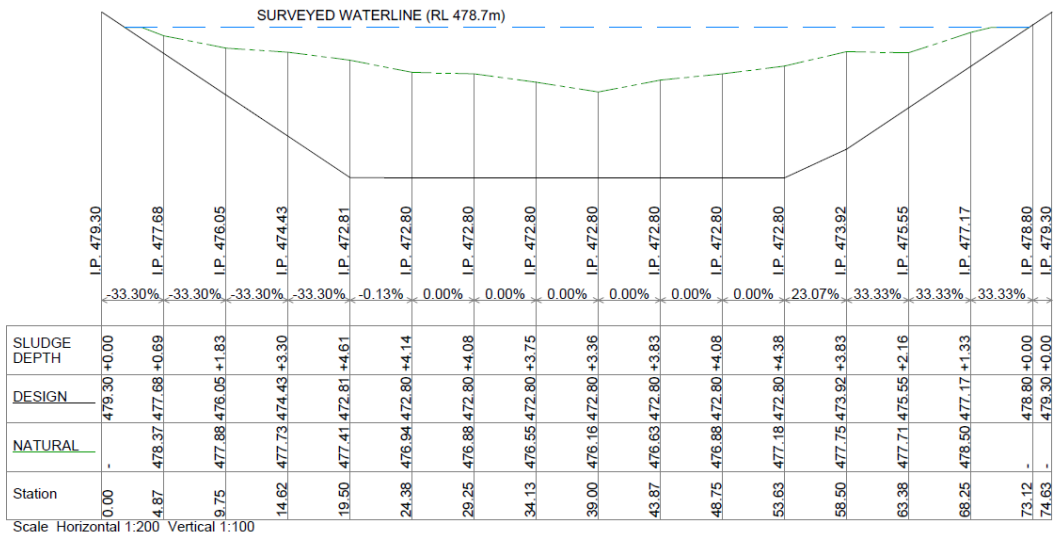
# A11. Piggery F, Pond 11



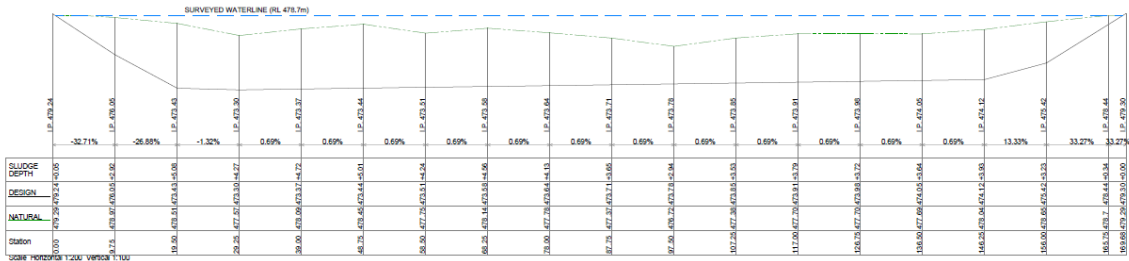
SECTION A  
41



SECTION B  
41



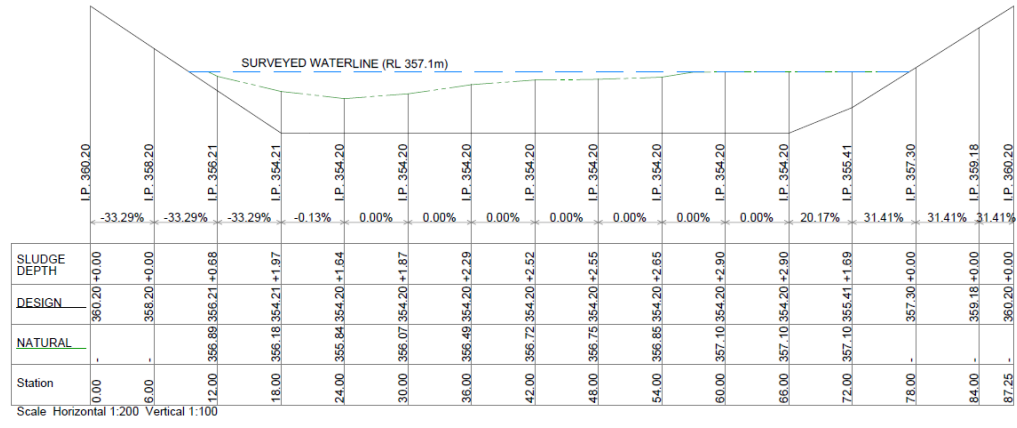
SECTION C  
41



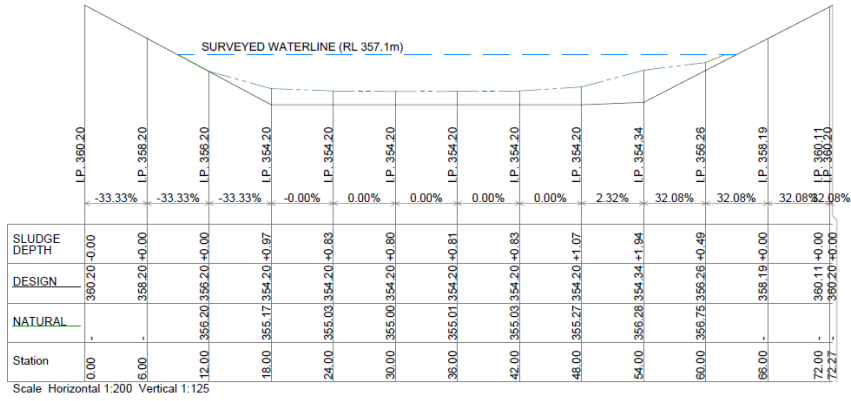
SECTION D  
41



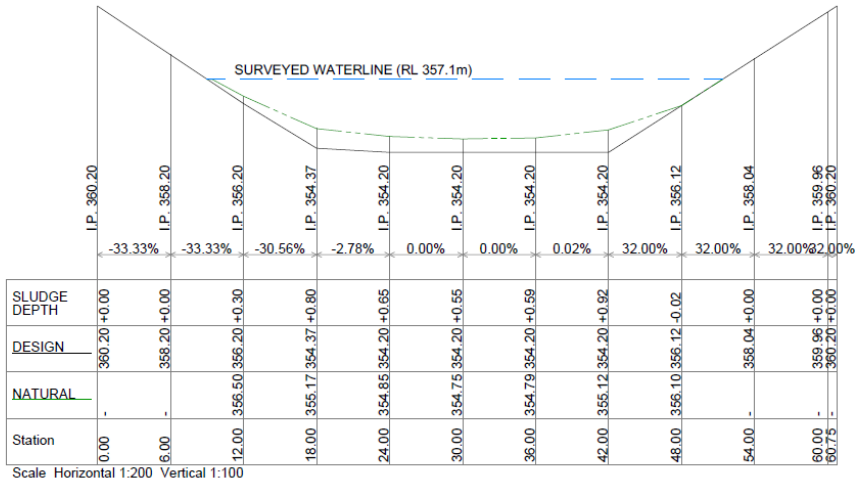
**A12. Piggery G, Pond 12**



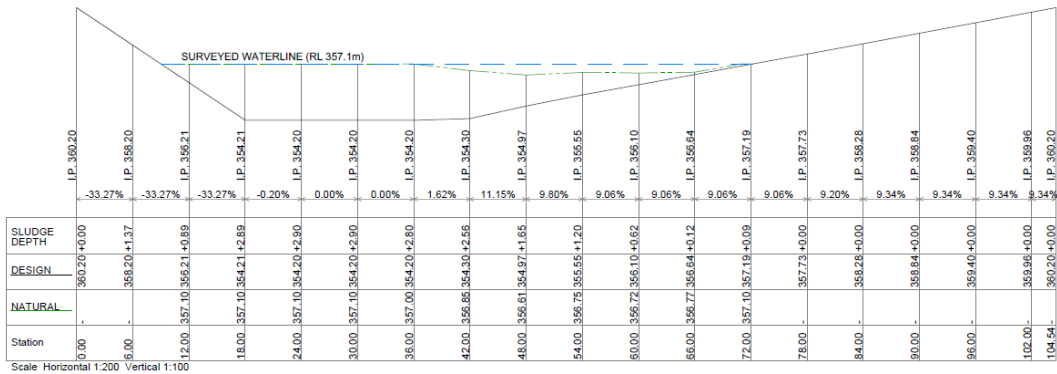
SECTION **A**  
45



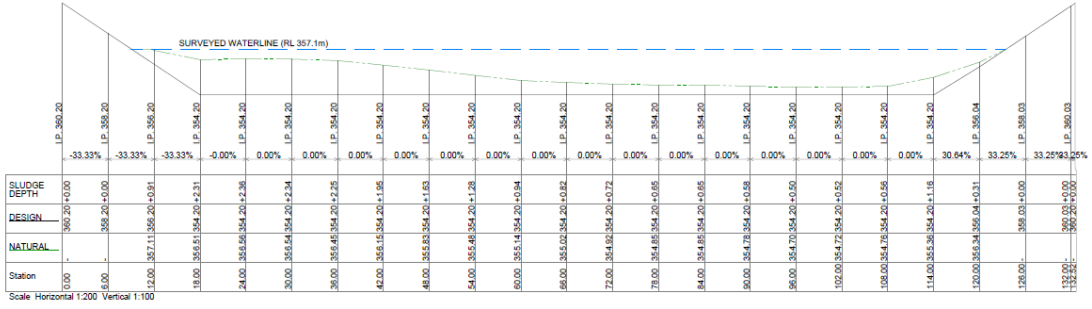
SECTION B  
45



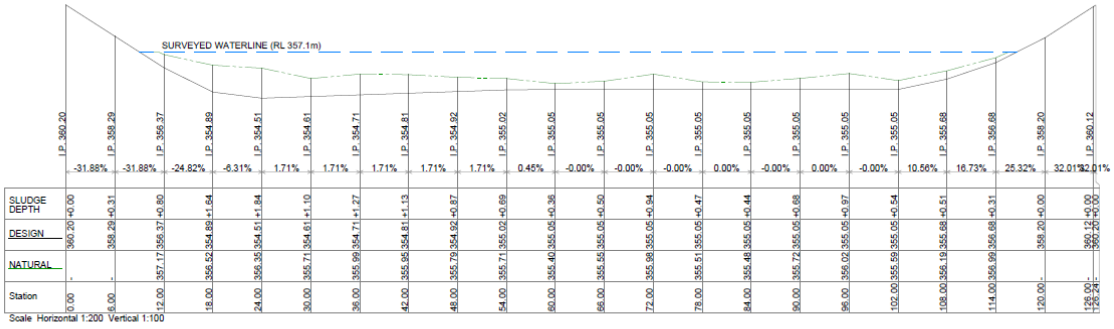
SECTION C  
45



SECTION D  
45

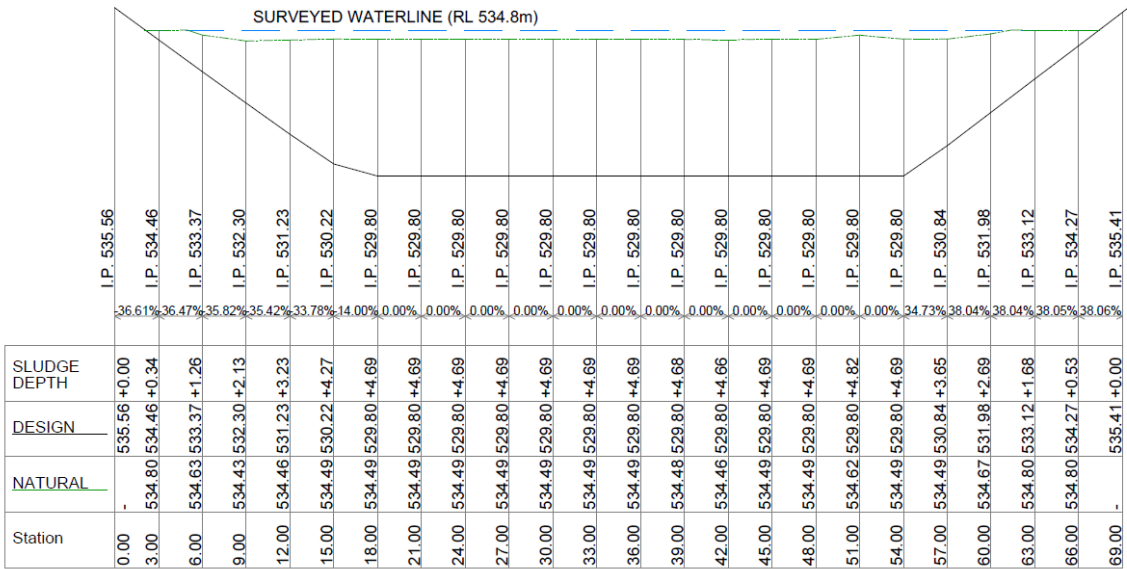
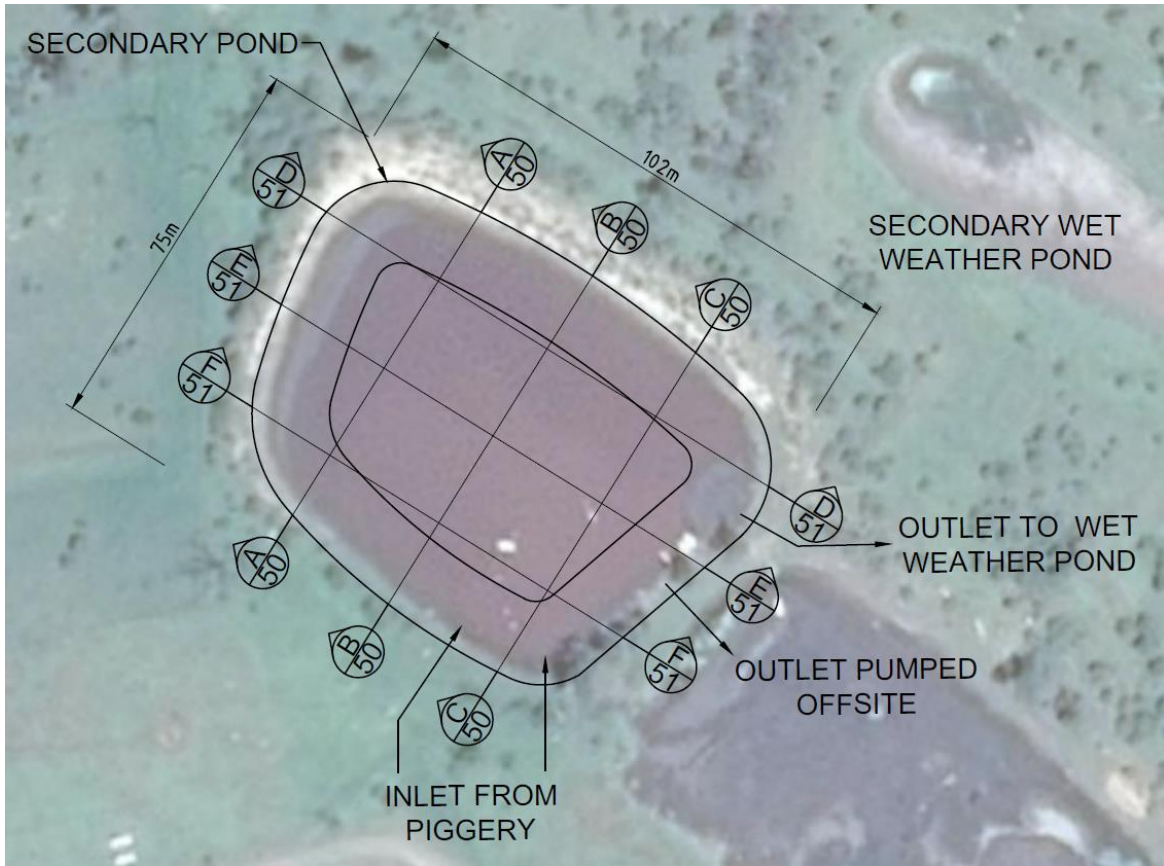


SECTION  $\frac{F}{45}$



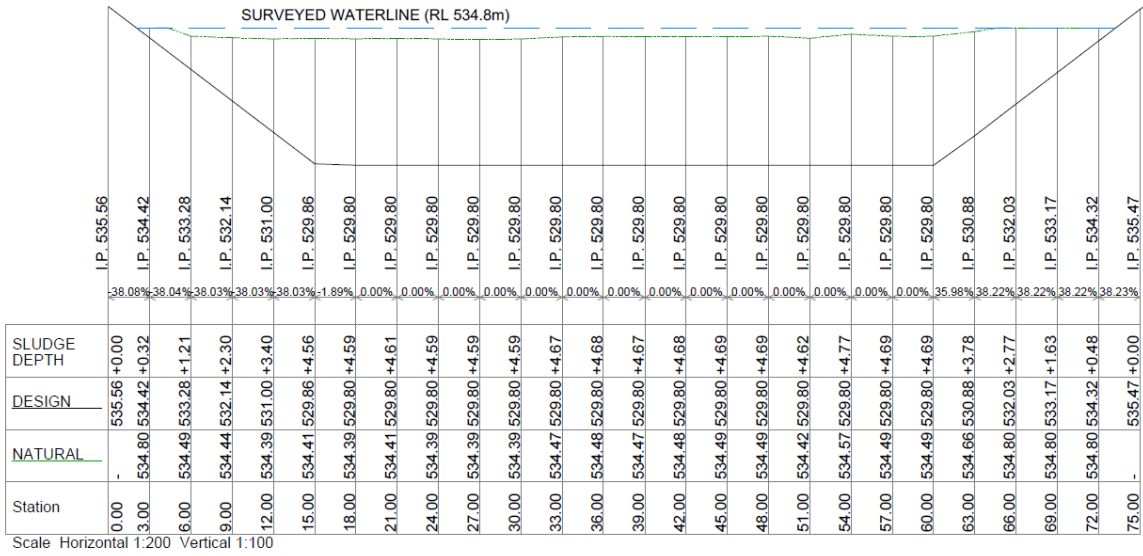
SECTION  $\frac{F}{45}$

**A13. Piggery H, Pond 13**

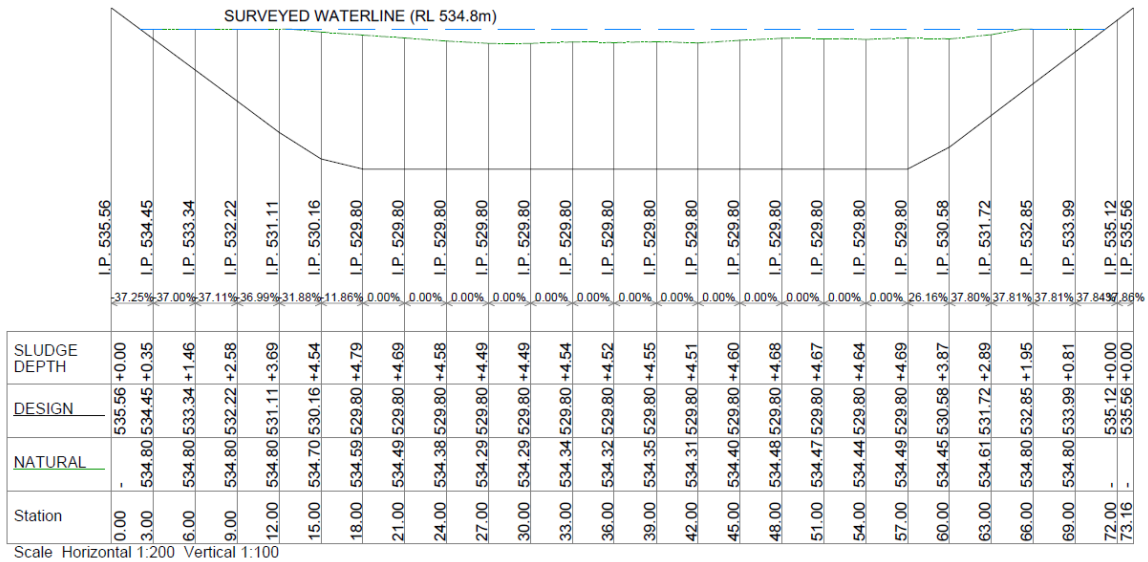


Scale Horizontal 1:200 Vertical 1:100

SECTION **A**  
49

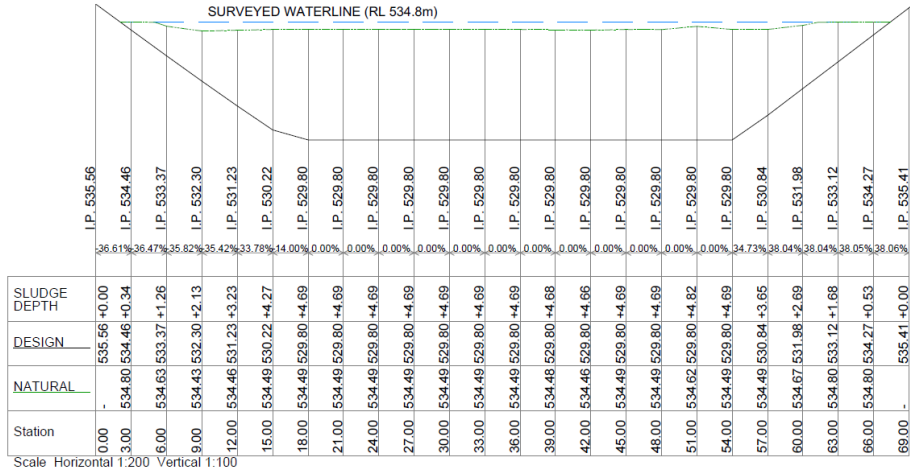


SECTION B  
49

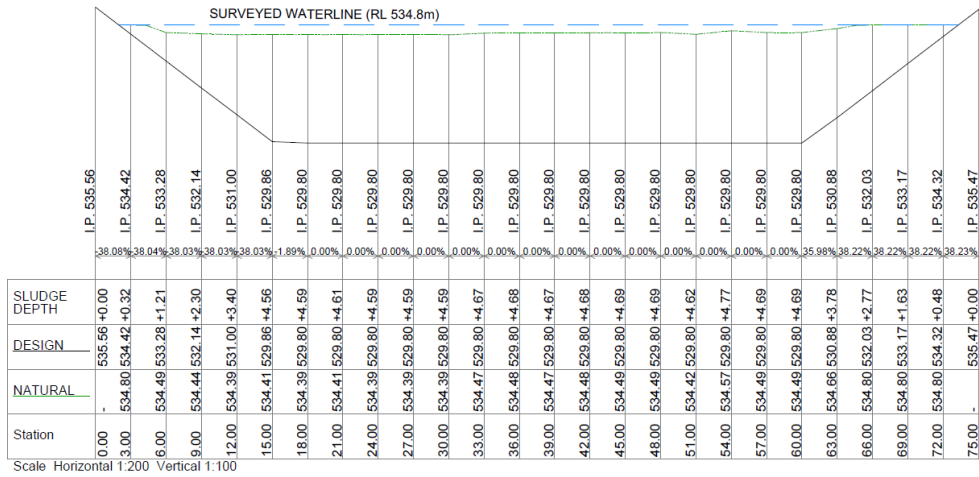


SECTION C  
49

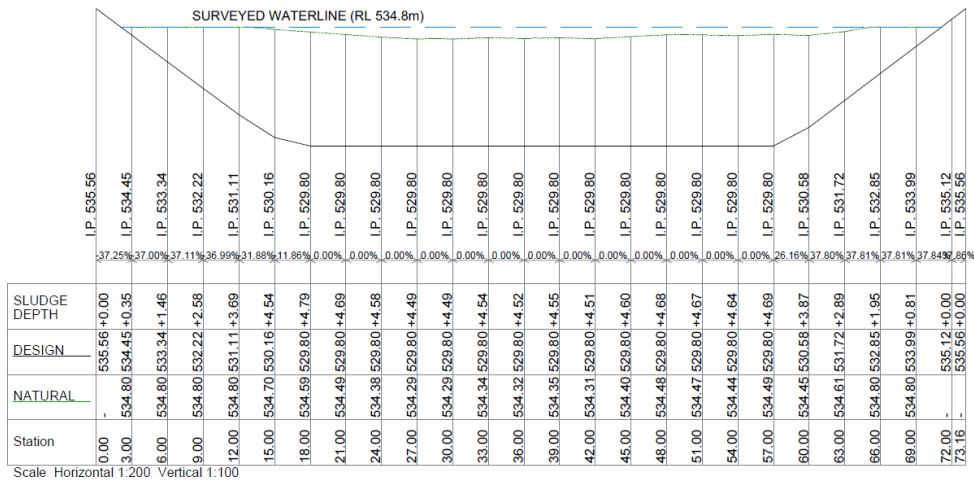




SECTION D  
49

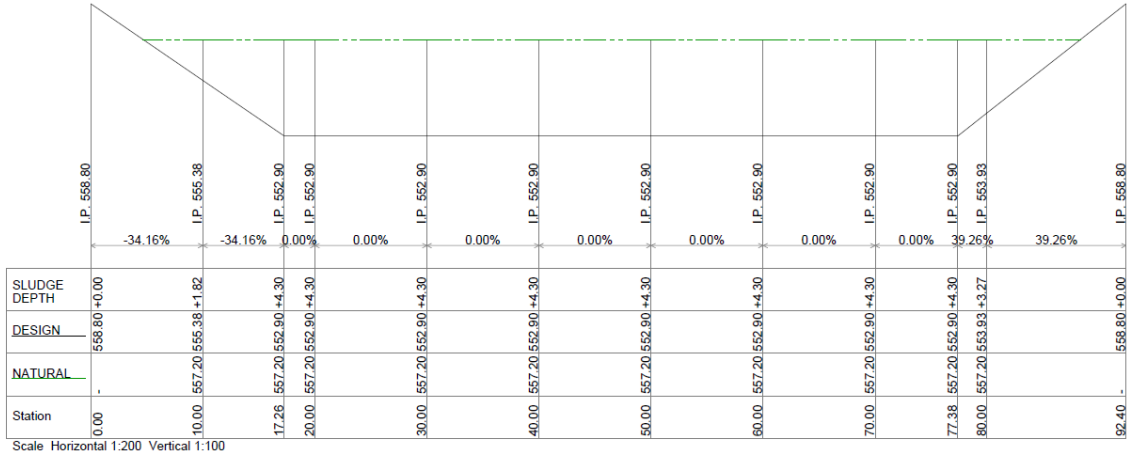


SECTION E  
49

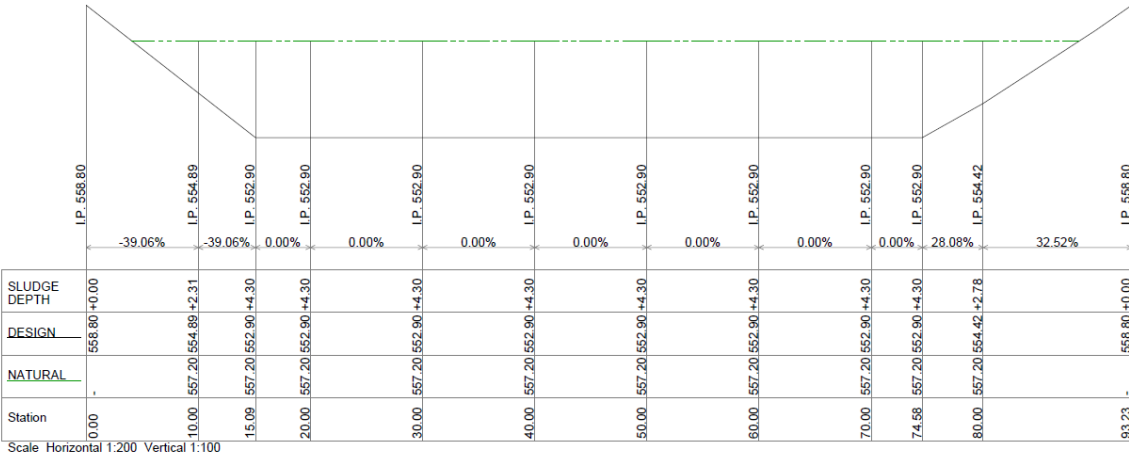


SECTION F  
49

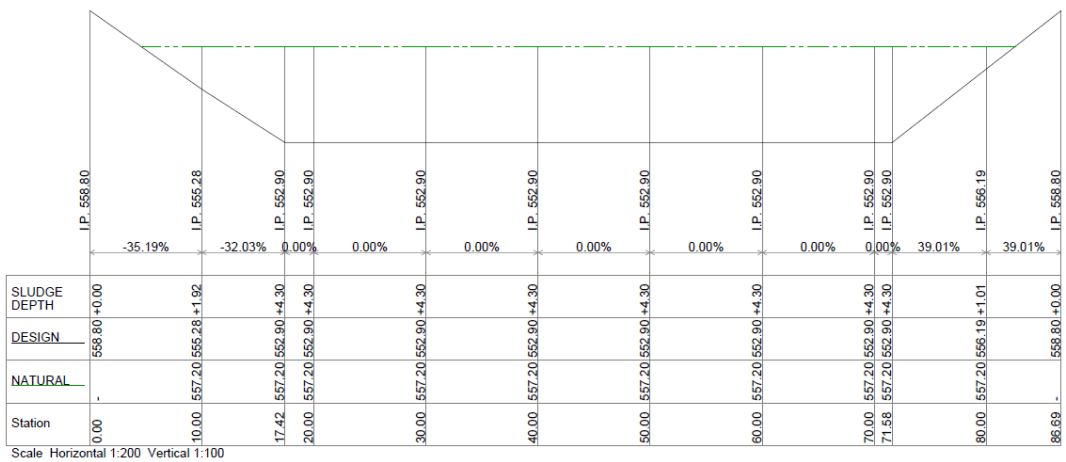




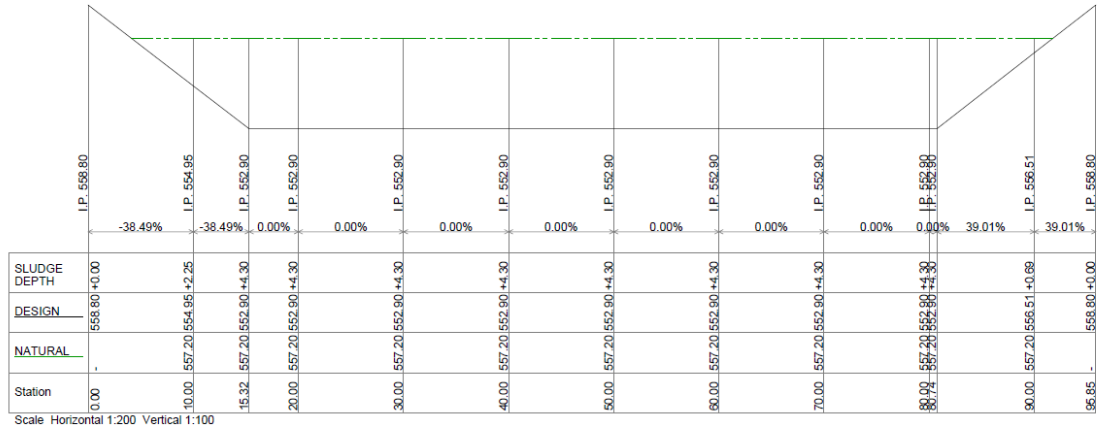
SECTION **B**  
53



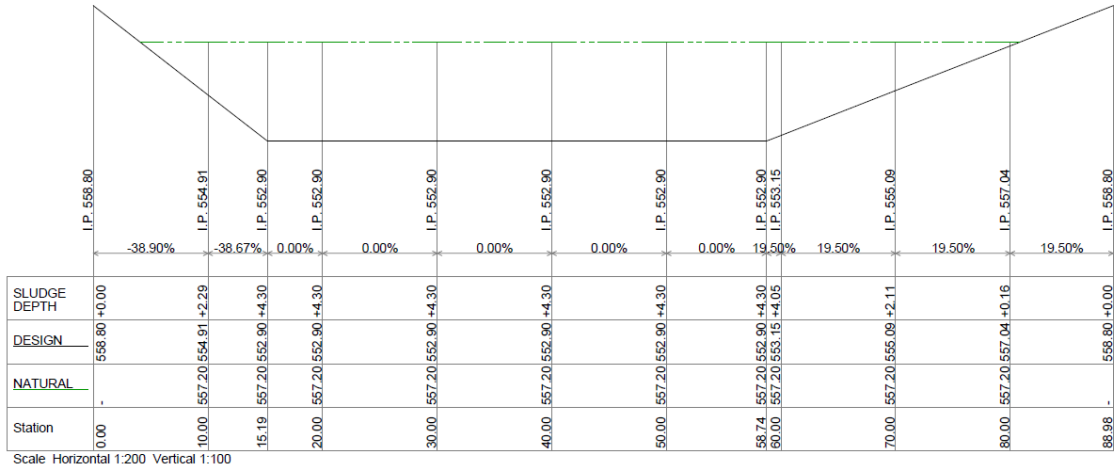
SECTION **C**  
53



SECTION **D**  
53

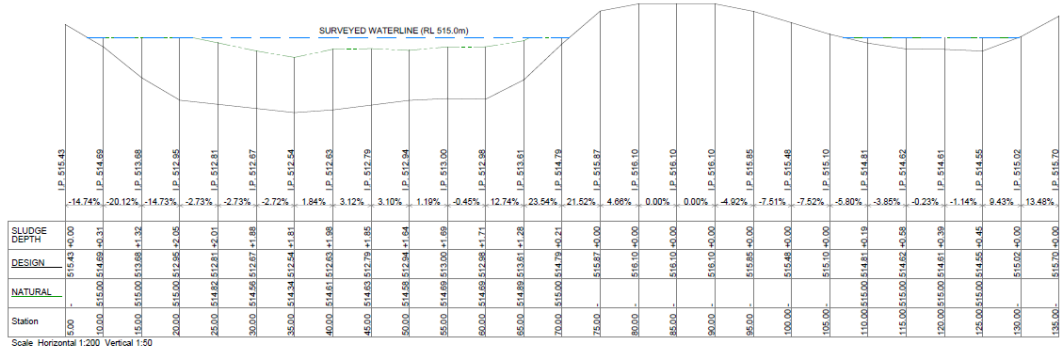


SECTION E  
53

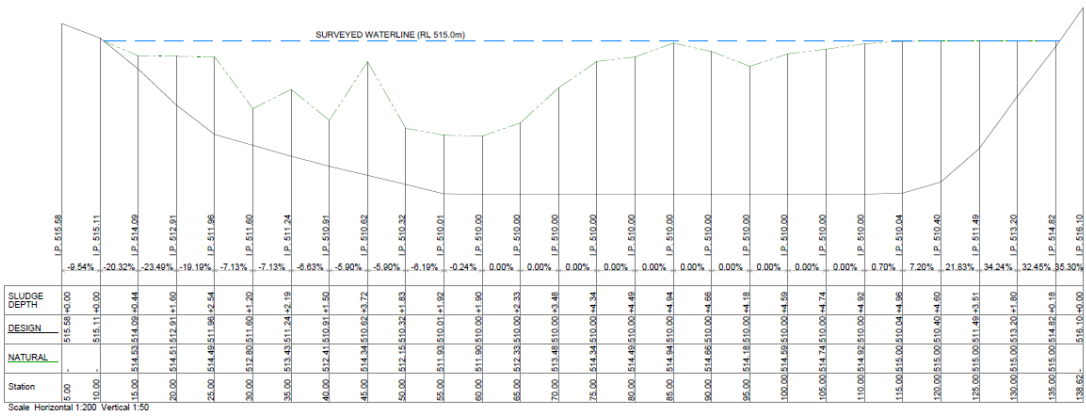


SECTION F  
53

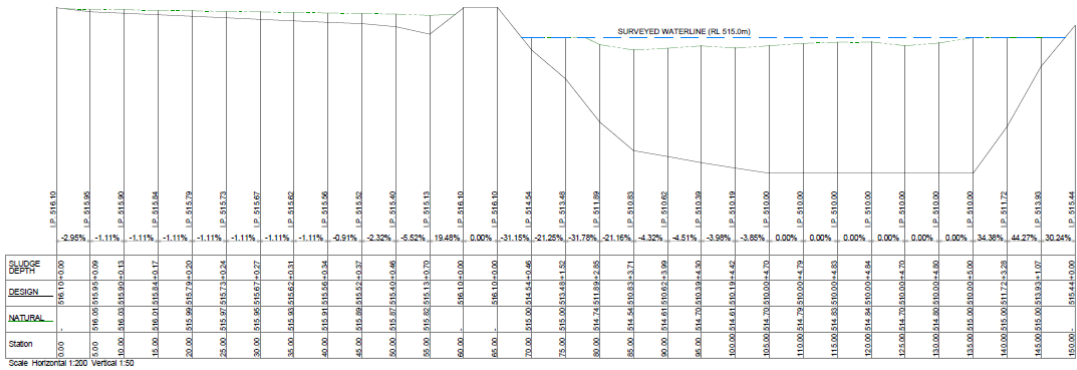




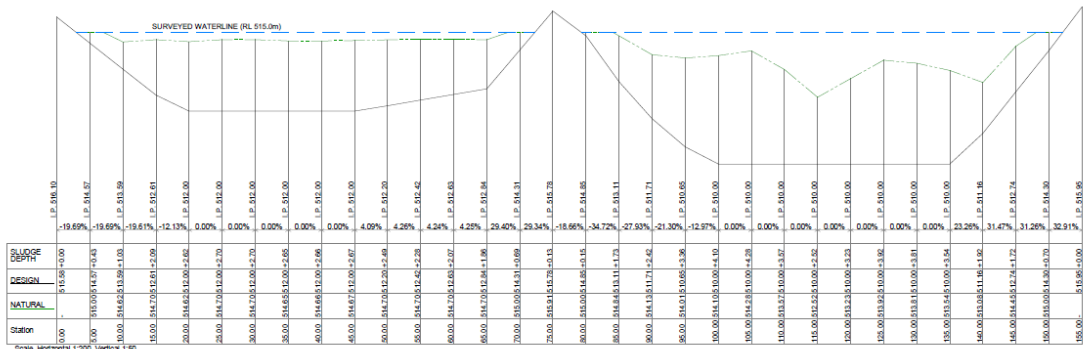
SECTION B  
57



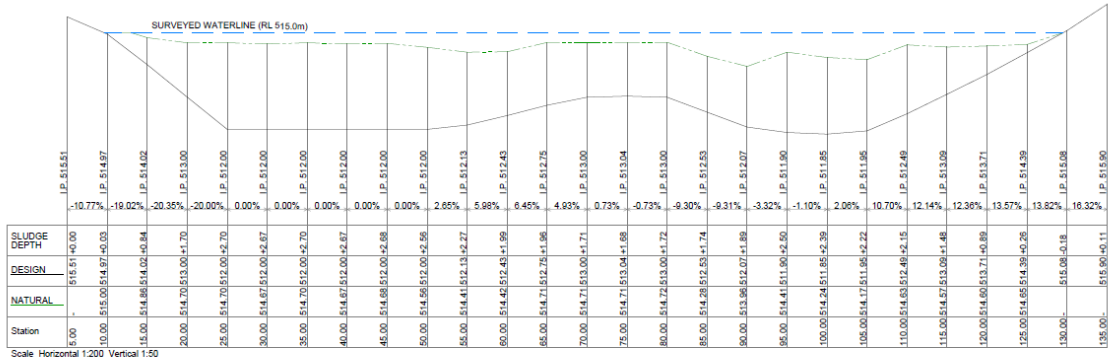
SECTION C  
57



SECTION D  
57



SECTION E  
57



Station	NATURAL	DESIGN	SLUDGE DEPTH	
5+00		515.51+0.00		P. 515.51
10+00	515.00	514.97+0.03		P. 514.97
15+00	514.86	514.02+0.84		P. 514.02
20+00	514.70	513.00+1.70		P. 513.00
25+00	514.70	512.00+2.70		P. 512.00
30+00	514.67	512.00+2.67		P. 512.00
35+00	514.70	512.00+2.70		P. 512.00
40+00	514.67	512.00+2.67		P. 512.00
45+00	514.68	512.00+2.68		P. 512.00
50+00	514.66	512.00+2.66		P. 512.00
55+00	514.41	512.13+2.27		P. 512.13
60+00	514.47	512.48+1.99		P. 512.43
65+00	514.71	512.75+1.96		P. 512.75
70+00	514.71	513.00+1.71		P. 513.00
75+00	514.71	513.04+1.66		P. 513.04
80+00	514.72	513.00+1.72		P. 513.00
85+00	514.28	512.53+1.74		P. 512.53
90+00	513.96	512.07+1.89		P. 512.07
95+00	514.41	511.90+2.50		P. 511.90
100+00	514.24	511.85+2.39		P. 511.85
105+00	514.17	511.95+2.22		P. 511.95
110+00	514.63	512.46+2.15		P. 512.46
115+00	514.57	513.05+1.48		P. 513.05
120+00	514.60	513.71+0.89		P. 513.71
125+00	514.65	514.36+0.26		P. 514.36
130+00		515.00+0.18		P. 515.00
135+00		515.90+0.11		P. 515.90

Scale Horizontal 1:200 Vertical 1:50

SECTION F  
57

## **Appendix B**

### ***Standard Operating Procedure (SOP)***

#### ***Sampling sludge from uncovered effluent ponds, Version: [2]***

##### ***B1. Purpose***

The purpose of this procedure is to describe the actions and practices to be taken by DAF and University of Queensland (UQ) employees to collect samples of sludge from an uncovered effluent pond operating at a commercial piggery, as required for Milestone 3 of APL Project No. 2016/085: Anaerobic pond sludge profiling and trigger point determination. The sludge samples will be collected from a range of depths in the sludge profile, at various locations across the pond surface. The sludge samples will be analysed in DAF and UQ laboratories to determine a range of physical, chemical and energy potential characteristics and to inform further development of a hydrodynamic-biochemical model to predict sludge behaviour.

##### ***B2. Application/scope***

This procedure applies to both DAF and University of Queensland (UQ) employees engaged in the collection of sludge samples for the collaborative research project described above.

The sludge may be collected from existing uncovered effluent ponds operating at commercial piggeries located in various Australian states. Uncovered effluent ponds are commonly used to treat and store effluent discharged from sheds used to house pigs in intensive piggeries.

Personnel undertaking the sludge sampling will require training in the safe use of the sampling apparatus and to ensure that they are aware of the potential hazards.

##### ***B3. Resources***

The following apparatus are required to complete the task:

- DAF 3.0 m flat-bottomed punt fitted with the steel structure, extending beyond the bow of the punt, specifically designed for holding 2 x 10 L sampling buckets.
- Transom-mounted outboard electric motor (Watersnake Slither SLW 54/42) powered by a minimum 100 Ah deep cycle battery.
- 20 m long emergency retrieval rope (200 kg breaking strain) attached to floating hand grip (e.g. ski tow rope or similar).
- Sampling pole of appropriate length to access sludge.
- Sample collection buckets with lids (typically 10 L polypropylene).
- 1 L wide-mouthed PP (polypropylene) sampling bottles with screw-on lids.
- Cooler box for sample storage and transport.

##### ***B4. Warnings***

- Biological hazard relating to the potential presence of pathogens in the pond effluent and sludge.
- Potential trip hazards around the pond embankment.



### **B5. Abbreviations, acronyms and definitions**

Explains a word, statement or acronym which has a specific interpretation or application within the procedure, or which is not readily understood by the reader.

<b>Term/acronym</b>	<b>Definition</b>
PPE	Personal Protective Equipment
PP	Polypropylene

### **B6. Procedure**

- Ensure that the minimum 100 Ah deep cycle battery used to power the electric motor is fully charged.
- Load DAF 3.0 m flat-bottomed punt and other sampling equipment onto the trailer and/or utility, using at least 2 physically-able people for lifting the boat, to avoid injury risk.
- Purchase ice required for sample preservation enroute to the piggery property.
- Continue to the piggery property and unless otherwise pre-arranged, call at the site office to sign any relevant entry, biosecurity or site induction documentation.
- Proceed to the pond site and locate the safest, most convenient site to launch the boat.
- Unload the punt, electric motor, battery and sampling equipment as close as possible to the selected launching position on the pond bank.
- Attach the electric motor to the punt transom, place the battery in the punt, connect the battery to the motor and place the sampling equipment (sampling pole and sample collection buckets) in the punt. Two x 10 L sample collection buckets should be placed in the holding rings provided in the steel extension structure attached to the bow of the punt.
- Check electric motor operation. Carry replacement 50 A fuses on the boat at all times during sampling.
- The sampler and assistant should then put on the following personal protective equipment (PPE):
  - ✓ Overalls (optional).
  - ✓ Rubber gloves to minimise exposure to biological hazards.
  - ✓ Life jacket – in case of punt capsizing or sampler falling into the pond.
- Generally, the sampling assistant drives the punt to and from the various sampling locations and uses the motor to maintain the boat's position during sampling.
- Once the sampling assistant is seated in the punt, the sampler launches the punt, bow-first, onto the surface of the effluent pond. The assistant then adjusts the propeller shaft angle and depth to effectively propel the punt to the first sampling site.
- The sampler and assistant should remain seated whenever the punt is moving.
- Once the punt arrives at the sampling site, the sampling pole is inserted through the punt sampling port to collect a sludge sample from the required depth. The sludge enters the sampling pole through a slot in the lower end of the pole. This slot may be opened and closed using the handles attached to the inner and outer tubes, near the upper end of the sampling pole. Before insertion, the slot in the sampling pole should be closed. After the pole is inserted into the sludge to the required depth, the slot should be opened for a few seconds, to allow the adjacent sludge to flow into the tube. The slot should then be closed, and the pole withdrawn from the sampling port.
- The lower end of the pole should be placed over the top of the sample collection bucket secured in the retaining ring, so that the slot is positioned over the bucket opening. The slot

should then be opened and the pole gently tapped against the rim of the bucket so that the sludge drains into the bucket. Depending on the volume of sample required (and its viscosity), this process may need to be repeated several times at each sampling site.

- The assistant is responsible for using the motor to hold the punt's position during sampling. This task becomes more crucial when strong winds are blowing.
- Once the required sludge sample volume has been deposited in the sampling bucket, the sampler and assistant should be seated before the assistant drives the punt to the next sampling location or back to the pond bank to change sample collection buckets.
- Each sludge sample should then be thoroughly mixed before sub-sampling into sample delivery bottles (typically 1 L wide-mouthed polypropylene bottles) which are then placed on ice in a cooler box for transport to the laboratory.
- Once the required samples have been obtained, the punt and sampling equipment may be loaded back onto the trailer and/or utility for transport back to the Tor Street, Toowoomba complex.
- Unless the samples are going to be immediately processed in the laboratory, they should be transferred from the cooler box to the cold room or refrigerator.
- The punt, motor and sampling equipment should then be thoroughly washed down using a pressure cleaner.
- After removal of any residual sludge, effluent or plant material inadvertently picked up at the previous farm, the punt, motor and sampling equipment should be sprayed with a commercial-grade disinfectant and left in the sun for a minimum period of 72 hours prior to use on another piggery effluent pond.

### ***B7. Responsibilities and accountabilities***

The research project leader has overall responsibility for ensuring that the sludge sampling is carried out safely and efficiently. The sampler and sampling assistant are responsible for following the procedures outlined in this document.

### ***B8. Related and reference documents***

Details other internal and external documents which have relevance or bearing on the activities within the procedure.

Policy	CHA/2014/1045 Managing Risks to Health and Safety v1.00 <a href="http://portal:6004/sites/PR/Register/Corporate/DAF%20DTEsb/managing-risks-to-hs-procedure.pdf">http://portal:6004/sites/PR/Register/Corporate/DAF%20DTEsb/managing-risks-to-hs-procedure.pdf</a>
	CHA/2014/1026 HSMS User Guide v1.0 <a href="http://portal:6004/sites/PR/Register/Corporate/DAF%20DTEsb/hsms-user-guide.pdf">http://portal:6004/sites/PR/Register/Corporate/DAF%20DTEsb/hsms-user-guide.pdf</a>
	Work Health and Safety Responsibilities – Performance Principles and Criteria <a href="http://portal:6004/sites/PR/Register/Corporate/DAF%20DTEsb/whs-responsibilities-performance-principles.pdf">http://portal:6004/sites/PR/Register/Corporate/DAF%20DTEsb/whs-responsibilities-performance-principles.pdf</a>

## ***B9. Appendices***

Appendices containing information supportive to the documented procedure may be included, such as tables, graphs, flow charts, forms and photographs (hard copy and electronic/hyperlinks are acceptable).

Appendix I                      Photographs showing the sampling pole details and the DAF 3.0 m punt identification plate and sampling port.



*Figure B1      Sampling pole.*



*Figure B2      Slot in sampling pole.*



Figure B3 Sampling pole handles used to open and close the slot.

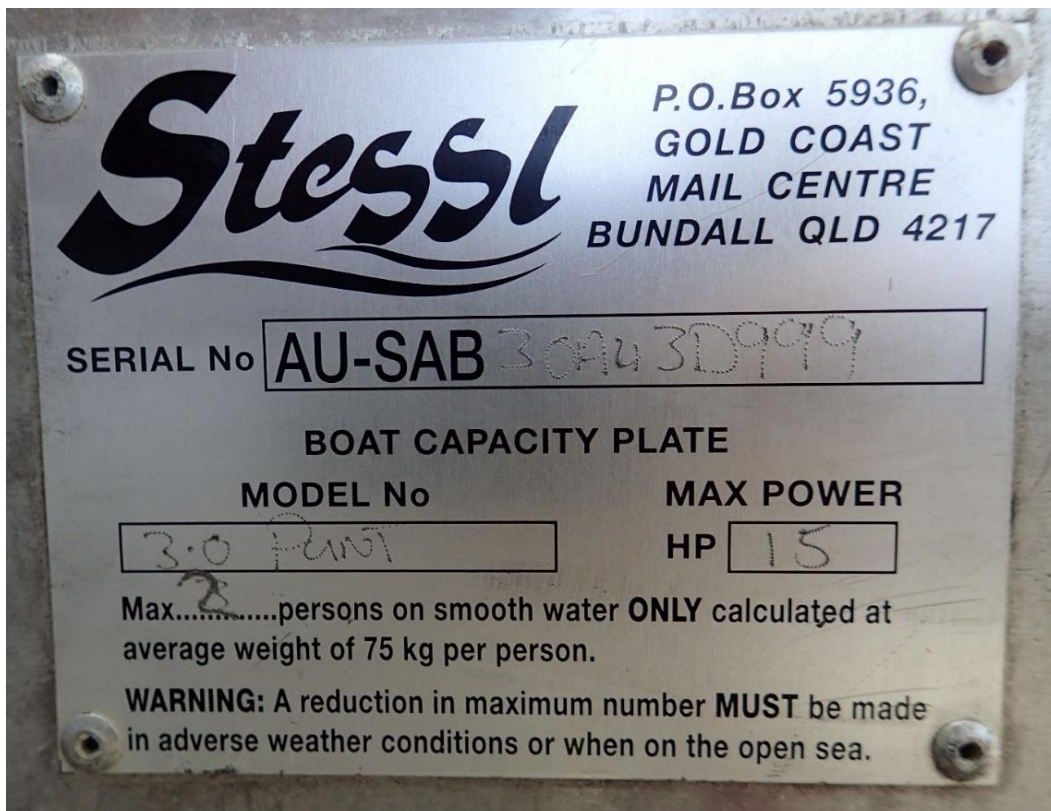


Figure B4 DAF 3.0 m flat-bottomed punt identification plate.



Figure B5 Punt mid-hull sampling port.